

## ABSTRACT

Title of dissertation:                   **CHARACTERIZING RICE RESIDUE BURNING  
AND ASSOCIATED EMISSIONS IN VIETNAM  
USING A REMOTE SENSING AND FIELD-  
BASED APPROACH**

Kristofer Lasko, Doctor of Philosophy, 2018

Dissertation directed by:           **Christopher Justice, Chair and Professor,  
Department of Geographical Sciences**

Agricultural residue burning, practiced in croplands throughout the world, adversely impacts public health and regional air quality. Monitoring and quantifying agricultural residue burning with remote sensing alone is difficult due to lack of field data, hazy conditions obstructing satellite remote sensing imagery, small field sizes, and active field management. This dissertation highlights the uncertainties, discrepancies, and underestimation of agricultural residue burning emissions in a small-holder agriculturalist region, while also developing methods for improved bottom-up quantification of residue burning and associated emissions impacts, by employing a field and remote sensing-based approach. The underestimation in biomass burning emissions from rice residue, the fibrous plant material left in the field after harvest and subjected to burning, represents the starting point for this research, which is conducted in a small-holder agricultural landscape of Vietnam. This dissertation quantifies improved bottom-up air pollution emissions estimates through refinements to each component of the fine-particulate matter emissions equation, including the use of synthetic aperture radar timeseries to explore rice land area variation between different datasets and for date of burn estimates,

development of a new field method to estimate both rice straw and stubble biomass, and also improvements to emissions quantification through the use of burning practice specific emission factors and combustion factors. Moreover, the relative contribution of residue burning emissions to combustion sources was quantified, demonstrating emissions are higher than previously estimated, increasing the importance for mitigation. The dissertation further explored air pollution impacts from rice residue burning in Hanoi, Vietnam through trajectory modelling and synoptic meteorology patterns, as well as timeseries of satellite air pollution and reanalysis datasets. The results highlight the inherent difficulty to capture air pollution impacts in the region, especially attributed to cloud cover obstructing optical satellite observations of episodic biomass burning. Overall, this dissertation found that a prominent satellite-based emissions dataset vastly underestimates emissions from rice residue burning. Recommendations for future work highlight the importance for these datasets to account for crop and burning practice specific emission factors for improved emissions estimates, which are useful to more accurately highlight the importance of reducing emissions from residue burning to alleviate air quality issues.

CHARACTERIZING RICE RESIDUE BURNING AND ASSOCIATED EMISSIONS  
IN VIETNAM USING A REMOTE SENSING AND FIELD-BASED APPROACH

by

Kristofer Lasko

Dissertation submitted to the Faculty of the Graduate School of the  
University of Maryland, College Park in partial fulfillment  
Of the requirements for the degree of  
Doctor of Philosophy  
2018

Advisory Committee:

Professor Christopher Justice, Chair  
Professor Krishna Vadrevu, Co-Chair  
Professor Ivan Csiszar  
Professor Louis Giglio  
Professor Michael Gollner  
Professor Matthew Hansen

© Copyright by  
Kristofer Lasko  
2018



## **Foreword**

Chapters 2-5 contain jointly authored work in which Kristofer Lasko is the primary author. Conceptualization, methods development, processing, analysis, and manuscript writing was led by Kristofer Lasko with contributions from the other co-authors named in each corresponding chapter.

## **Acknowledgements**

I first thank my Co-Advisor Dr. Krishna Vadrevu. Thanks for taking me on initially as an intern during my undergraduate degree where I got my first research experience. At that time, I did not realize I would continue on to a master's degree, let alone a PhD! Thanks for providing me the opportunity to have a great research experience to jump-start my graduate education, coupled with guidance on how to work effectively towards a goal and career. I also thank my advisor, Dr. Christopher Justice, for providing support, networking connections, and broad guidance on my PhD topic, as well as helping me stay on track by focusing on the most important parts of my research.

I am grateful for the mentorship, guidance, and critical analysis provided by my remaining committee members, each of whom is a leading expert in their sub-discipline: Ivan Csizsar, Louis Giglio, Matthew Hansen, and Michael Gollner.

I am thankful for the chance to work with the NASA Land Cover / Land Use Change program as a research assistant and meeting coordinator under leadership from Dr. Garik Gutman. I'm also grateful for the opportunities to travel abroad to conduct research, give training sessions, and network –a result of funding from UMD, START, NAS LCLUC, and the SMART scholarship program. I also thank William Salas and Nathan Torbick of Applied Geosolutions LLC for taking time to teach me about SAR in relation to rice mapping. Lastly, the support of scientists from Vietnam National University was critical, especially for field logistics, I specifically thank Thanh Thi Nhat Nguyen, Hung Quang Bui, Vinh Tuan Tran, Chuc Duc Man, and Ha Pham Van, and Pham Van Cu.

I am thankful to my office colleagues and 2014 PhD cohort for assistance, advice, troubleshooting as well as camaraderie helping to alleviate the stress of the PhD program.

I will miss you all very much!

Lastly, I am eternally thankful to my family, including my parents for their support during this stressful, but incredibly rewarding PhD journey. Lastly, thank you to my wife, Nicole, for all that you've done.

# Table of Contents

<b>Foreword</b> .....	ii
<b>Acknowledgements</b> .....	iii
<b>Table of Contents</b> .....	v
<b>Chapter 1: Introduction</b> .....	1
1.1 Background and motivation of the study .....	1
1.2 Purpose of the study.....	4
1.3 Research questions and design.....	5
1.3.1 <i>Design of the study</i> .....	5
1.3.2 <i>Research objectives</i> .....	6
1.4 Significance of study area.....	8
1.5 Organization of the study.....	10
1.6 References.....	12
<b>Chapter 2: Mapping and characterizing paddy rice with Sentinel-1A at varying spatial scales and polarizations in Hanoi, Vietnam</b> .....	15
2.1 Abstract.....	15
2.2 Introduction.....	16
2.3 Study area and datasets .....	19
2.3.1 <i>Study area</i> .....	19
2.3.2 <i>Satellite data</i> .....	20
2.3.3 <i>Training and validation data</i> .....	22
2.3 Methodology.....	23
2.3.1 <i>Double and single crop rice mapping</i> .....	24
2.3.2 <i>Accuracy Assessment</i> .....	25
2.3.3 <i>Spatial Analysis</i> .....	26
2.3.4 <i>Rice phenology</i> .....	28
2.4 Results.....	28
2.4.1 <i>Mapped area variation</i> .....	28
2.4.2 <i>Accuracy assessment and areal adjustment</i> .....	29
2.4.3 <i>Pixel-level rice variation</i> .....	33
2.4.4 <i>Province-level rice variation</i> .....	33
2.4.5 <i>Commune-level rice variation</i> .....	34
2.4.6 <i>Rice phenology</i> .....	36
2.4.7 <i>Rice landscape metrics</i> .....	37
2.4.8 <i>Input band importance</i> .....	38
2.5 Discussion.....	39
2.6 Conclusion .....	44
2.7 Acknowledgement .....	45
2.8 References.....	46
<b>Chapter 3: Satellite data may underestimate rice residue and associated burning emissions in Vietnam</b> .....	54
3.1 Abstract.....	54
3.2 Introduction.....	55
3.3. Datasets and methods.....	59
3.3.1 <i>SAR data</i> .....	59
3.3.2 <i>Rice residue and emissions estimation</i> .....	61
3.4 Results.....	65
3.4.1 <i>Fuel-loading factors</i> .....	65

3.4.2 Emissions estimates .....	69
3.4.3 SAR data and biomass relationship .....	74
3.5 Discussion .....	74
3.6 Conclusion .....	77
3.7 Acknowledgements .....	78
3.8 References .....	78
<b>Chapter 4: Improved rice residue burning emissions estimates: Accounting for practice-specific emission factors in air pollution assessments of Vietnam .....</b>	<b>84</b>
4.1 Abstract .....	84
4.2 Introduction .....	86
4.3 Study area .....	91
4.4 Methods .....	92
4.4.1 Emission factors .....	92
4.4.2 Rice area for Hanoi Capital Region .....	96
4.4.3 Rice area for the entirety of Vietnam .....	96
4.4.4 Emissions estimation and scenarios .....	97
4.4.5 Date of burning and pollutant transport .....	99
4.5 Results .....	101
4.5.1 Rice area estimates .....	101
4.5.2 Burning practice specific emission factors .....	104
4.5.3 PM <sub>2.5</sub> emission Scenarios .....	105
4.5.4 Emissions transport .....	107
4.6 Perspectives and conclusions .....	111
4.7 Acknowledgements .....	114
4.8 References .....	114
<b>Chapter 5: Current status of air pollution over Hanoi, Vietnam using reanalysis data, satellite-based data, and synoptic-scale patterns .....</b>	<b>124</b>
5.1 Abstract .....	124
5.2 Introduction .....	125
5.2.2 Study area .....	128
5.3 Data and Methods .....	129
5.3.1 Merra-2 Reanalysis data .....	129
5.3.2 Rainfall data .....	130
5.3.3 Active Fires data .....	130
5.3.4 Ultraviolet Aerosol Index (UVAI) data .....	130
5.3.5 Cloud cover data .....	131
5.4 Methods .....	131
5.5 Results .....	134
5.5.1 Cloud conditions over Hanoi .....	134
5.5.2 UVAI and number of clear observations .....	135
5.5.3 MERRA-2 BC patterns and de-trending .....	140
5.5.4 Wind and active fires .....	149
5.5.5 Rain .....	151
5.6 Discussion .....	154
5.7 Conclusion .....	157
5.8 References .....	158
<b>Chapter 6: Summary findings and conclusion .....</b>	<b>166</b>
6.1 Summary .....	166
6.2 Key Findings and implications from Chapter 2 .....	167

6.3 Findings and implications from Chapter 3.....	170
6.4. Findings and implications from Chapter 4.....	172
6.5 Findings and implications from chapter 5.....	174
6.6 Recommendations for future work .....	176
6.7 References.....	179
<b>Appendix</b> .....	<b>181</b>
Unbiased areal estimates in accuracy assessment.....	181
<b>Bibliography</b> .....	<b>185</b>

## **Chapter 1: Introduction**

### **1.1 Background and motivation of the study**

Agricultural residue burning in croplands throughout the world adversely impacts public health, Greenhouse Gas Emissions (GHGs) and emits aerosols affecting regional air quality (Streets et al 2003; Korontzi et al 2006). The effects from biomass burning episodes in agricultural lands can persist for weeks to months with impacts on atmospheric chemistry, weather, biogeochemical cycles, ecology, as well as the potential for long-distance transport into remote regions (Yan et al. 2006; Badarinath et al. 2009; Vadrevu et al. 2012; Cristofanelli et al. 2014; Ponette-Gonzalez et al. 2016; Sanderfoot 2017). The underestimation and uncertainty in biomass burning emissions from rice residue burning represent the starting point for this research. Rice residue, defined as the inedible and fibrous plant material left in the field after harvest, is commonly burned in order to clear fields for the next growing season (Hong Van et al. 2014; Duong and Yoshiro 2015). Global studies estimate that biomass burning accounts for about 41% of total black carbon emissions as compared with residential, industrial, energy, and transportation sectors (Streets et al. 2004). However, in Southeast Asia the relative contribution has been reported lower, around 35% (Streets et al. 2004). Further, agricultural waste burning emissions in Southeast Asia were reported to be as low as about 9% of total biomass burning emissions including savanna, boreal forest, temperate forest, tropical forest, peat, and agriculture; whereas in other regions such as Europe, the agricultural emissions account for around 59% (van der Werf et al. 2017). However, these and previous studies could be basing the estimates on non-region specific data or generalized methods. Thus, agricultural emissions contribution may be higher than

previously thought when estimates are based on the region-specific data and novel methods integrating both satellite and ground-based methods, as undertaken in this dissertation.

To quantify emissions, studies often rely upon grain-to-straw ratios for crops obtained from the literature and based upon crop production statistical databases. However, these ratios may not be regionally-representative, or could underestimate the amount of residue as they may not include the standing, uncut stubble component. Moreover, global and regional agricultural biomass burning studies also rely on generalized crop emission factors (i.e. not crop specific), and broad land cover categories which may not be representative of the observed biomass estimates and resulting emissions. For example, in regions where there is one dominant crop such as rice in Vietnam (Vietnam Office of Statistics 2016), the emissions estimated by global or regional studies could be significantly different than studies using crop-specific factors. In addition, the specific burning practice (figure 1.1) may impact the resulting emissions, a factor not typically accounted in regional or global biomass burning studies (van der Werf et al. 2010; Heinsch et al. 2016; Holder et al 2017; van der Werf et al. 2017). Because studies rely upon remote sensing alone to quantify the burning, this effect is further amplified by the difficulty to detect agricultural fires with remote sensing datasets. This is especially attributed to the ephemeral nature and small size of these fires compounded by cloud cover hampering active fire detections (Justice et al 2002; Schroeder et al. 2008; Giglio et al. 2013). Remote sensing is often employed to estimate some of the important factors for biomass burning emissions such as crop area, crop type, and fire location. However, different methods such as using SAR, optical imagery, multitemporal imagery vs single



data imagery, different spatial resolutions, and disparate classification methods all lead to differing results as shown in chapter 2. Thus, it's important to develop effective land cover mapping methods not only for operational monitoring of crops and production, but also for spatially-explicit applications such as biomass burning, emissions, and air quality impacts. Due to the use of generalized emission factors as well as small, low temperature, and often cloud-obscured satellite fire observations in small-holder agricultural fields, alternative approaches are needed to quantify the rice residue burning emissions and compare with satellite burned area based, bottom-up approaches to evaluate the current status of existing fire emission databases, and to quantify the relative contribution of rice residue burning to all emission sources of PM<sub>2.5</sub> by integrating with a top-down (national scale data disaggregated at subnational scale) emission inventory. PM<sub>2.5</sub> is dangerous to human health and is linked to millions of premature deaths annually (Pope et al. 2002; Dennis et al. 2005; Apte et al. 2015) with agricultural fires emitting a relatively high amount. Because of this, estimating PM<sub>2.5</sub> emissions from rice residue burning is important not only for human health, but also for air quality and the environment.

**Figure 1.1 The different rice residue burning practices found in Vietnam**



## 1.2 Purpose of the study

This dissertation explores how rice residue burning emissions vary based on the different inputs of the PM<sub>2.5</sub> emissions equation including rice planted area (objective 1), rice fuel-loading factors relating to the amount of residue in the field (objective 2), emission factors relating to the amount of pollutant released per unit of residue burned (objectives 2 and 3), and combustion factors relating to the completeness of the burning (equation 1.1). The dissertation objective is to: 1) develop improved bottom-up emissions estimates using novel techniques including improved field methods for residue estimation, 2) employ crop-specific and novel burning practice-specific emission factors, 3) and integrate remote sensing datasets for rice area mapping and to obtain important ancillary information related to residue burning in a cloud-prone region. The resulting emission estimates are compared with existing global and regional fire emissions databases, including the Global Fire Emissions Database (GFED), to determine if and by how much these global databases differ from the bottom-up estimates quantified in this dissertation. Moreover, while previously unknown, the relative contribution of rice residue burning in Vietnam to all PM<sub>2.5</sub> combustion emissions is also quantified by comparing with the Regional Emissions Inventory in Southeast Asia (REAS) all-combustion sources inventory.

The findings from this research are intended to shed light on the current status of crop residue burning emissions using paddy rice as an example, while also demonstrating the

### Equation 1.1 Generalized emission equation

#### PM<sub>2.5</sub> Emissions Equation

*RiceArea* x *FuelLoad* x *PercentBurned* x *EmissionFactor* x *CombustionFactor*

 Variation explored for this variable

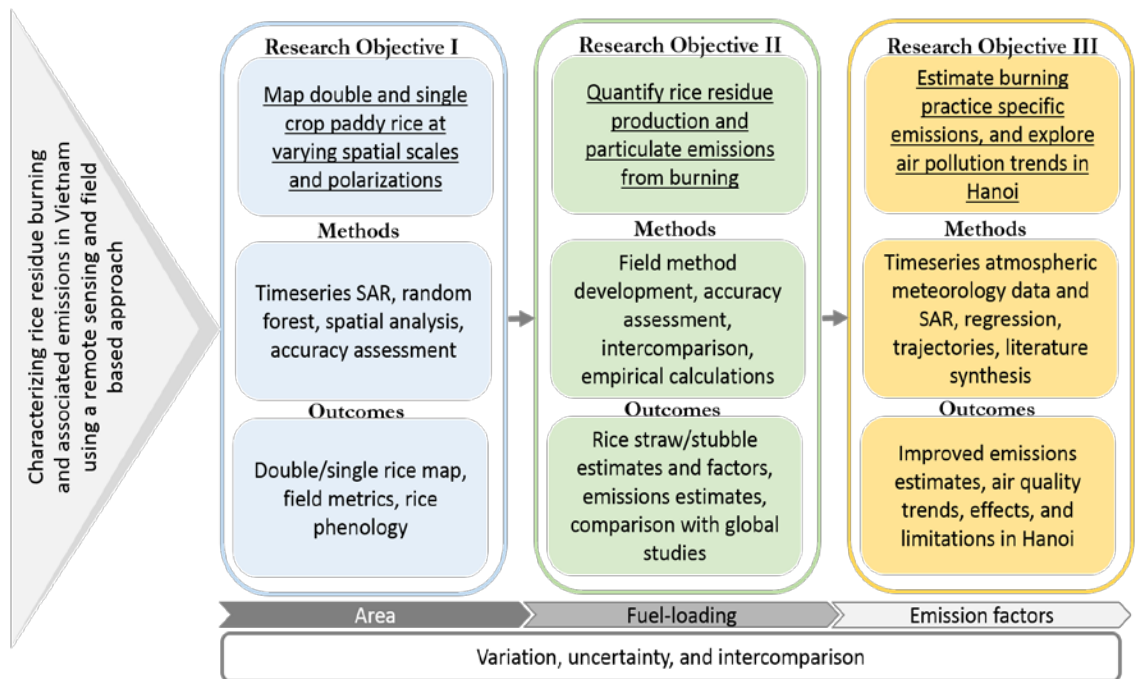
importance of accurate remote sensing based methods useful in cloud-prone regions. In this dissertation, rice in Vietnam is studied within the Red River Delta where the emissions contribute to an already degraded atmospheric environment. Integrating field work, time-series remote sensing, modelling, and literature review, the three specific chapters and objectives are addressed in the proceeding sections.

### 1.3 Research questions and design

#### 1.3.1 Design of the study

This dissertation is built around three main research objectives and follows an integrated approach using remote sensing, field methods and data, and comprehensive analysis of existing data (figure 1.2). The three main research chapters are closely intertwined. The first objective uses a time-series of SAR data to estimate rice paddy area and phenology useful as a basis for subsequent emissions estimation. The second objective involves

**Figure 1.2: Overview of dissertation objectives**



development of a novel method to estimate rice residues in the field and quantify emissions from burning based on a commonly-applied approach used in global studies. The third objective further improves upon the emissions quantification by developing burning practice specific emission factors and estimates, while also analyzing the air pollution and air quality in Hanoi resulting from rice residue burning, and documenting the current difficulties and limitations in monitoring air quality in the Hanoi region.

### *1.3.2 Research objectives*

*Objective 1: Map paddy rice area extent and variation based on different SAR polarizations and spatial resolutions, and characterize the paddy rice landscape and phenology.*

Objective 1 emphasizes the need for effective paddy rice mapping datasets and methods important not only as the basis for rice residue burning emissions in this dissertation, but also for operational monitoring of paddy rice. Objective 1 maps single and double crop paddy rice using six different input SAR datasets with different polarizations and different spatial resolutions. It also explores SAR-based rice phenology monitoring.

*Objective 2: Quantify post-harvest rice residue production through a field study and calculate resulting particulate matter emissions from burning using an approach employed in global studies.*

Objective 2 involves developing a novel field technique to estimate not only the amount of rice straw, but also the amount of standing, uncut stubble. These field estimates were compared with residue estimates calculated using a popular crop

production statistics-based approach and discrepancies are identified. Emissions from burning were then quantified based on the field data and using general agricultural emission factors similar to those used in global biomass burning studies. The field data are also compared with the SAR signal to explore the potential for residue mapping just prior to rice harvest season, which would be useful for forecasting applications.

*Objective 3: Estimate burning practice specific emissions from rice residue burning, and explore resulting air pollution and air quality effects in Hanoi, Vietnam.*

Objective 3 contains the majority of the research findings from this study as it combines results and input from objective 1 and objective 2. The first part of this objective analyzes the existing emission factors in the literature and the residue estimates from objective 2 to quantify burning practice specific emission factors and emissions for rice residue burning. The emission estimates are compared with total combustion sources from the Regional Emission inventory in Asia (REAS). The rice residue burning emission estimates are also compared with satellite-derived estimates from the Global Fire Emissions Database (GFED) in order to evaluate satellite-based emission estimates in a small-holder agricultural region such as Vietnam. Emission factors from the literature are synthesized to generate burning-practice specific factors for the two prominent burning styles, pile burning and non-pile burning. Resulting emissions for Vietnam are compared and demonstrate potential to significantly alleviate residue burning emissions.

#### **1.4 Significance of study area**

Rice is a staple crop for economic and cultural livelihood throughout much of Southeast Asia including Vietnam. Paddy rice production in Vietnam has consistently grown with 32.5million metric tons in 2000 to 45.2million metric tons in 2015 (Vietnam Office of Statistics). Concurrently, the area under cultivation has slightly increased with 7.67 million ha in 2000 and 7.83 million ha in 2015, suggesting notable agricultural intensification. Intensification is critical in areas of the Red River Delta around Hanoi, where population pressure and a robust economy are driving peri-urban expansion into some agricultural areas and thus reducing the area under cultivation (Pham et al. 2015).

The Hanoi Capital Region (HCR) was recently established by the Government of Vietnam in 2008. The area includes a population of over 12 million people and growing as of 2015 (Vietnam Office of Statistics, 2016). The region is home to Hanoi City, the capital of Vietnam, which outside of the immediate downtown area, exhibits a mosaic landscape dominated by small-holder paddy rice, farms, and plantations all intermixed amongst a growing peri-urban area (Pham et al 2015). Thus, in Hanoi many residential and commercial areas are impacted not only by urban-related emissions, but also by smoke from rice residue burning. Hanoi is at the core of the HCR and it is surrounded by Vinh Phuc Province to the North, Bac Ninh and Hung Yen to the East, and Ha Nam to the South (figure 1.3). The HCR also includes the following provinces: Hai Duong, Hoa Binh, Bac Giang, Phuc Tho, and Thai Nguyen. Of the different provinces, Bac Ninh (44.2%) has the highest proportion of rice area, followed by Hung Yen (43.7%), Ha Nam (39.3%), Hai Duong (38.4%), Hanoi (32.8%), and Vinh Phuc (22.5%). The remaining

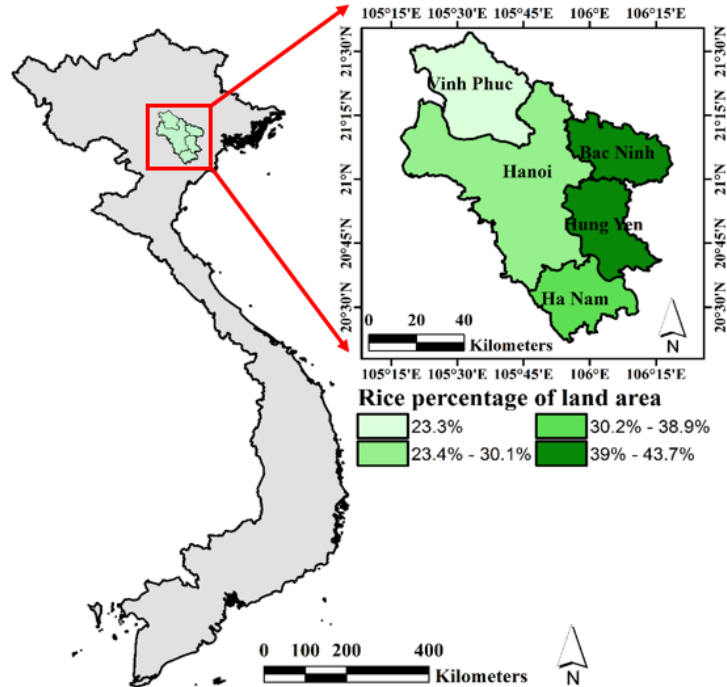
provinces have less rice, under 20% and are more than 50km from Hanoi City, and are thus excluded from the study area.

The HCR is located within the heart of the Red River Delta, Vietnam's oldest and most dense rice producing hub with about 15% of the country's total production (Vietnam Office of Statistics, 2016).

Accordingly, rice is the most prevalent crop, often double-

rotated and irrigated with two main seasons: a winter crop planted around February usually after the Tet holiday, and a Spring/Summer crop planted in late-June or July. The average field size is about 800m<sup>2</sup> ( $\sigma=625m^2$ ) with individual fields typically ranging from 150m<sup>2</sup> – more than 3000m<sup>2</sup> (Lasko et al. 2017) with other studies suggesting slightly larger fields averaging 2800m<sup>2</sup> in more rural areas away from Hanoi (Patanothai 1996). However, the paddy rice fields are typically planted in large groups ranging from about 3.5 to 8 fields, referred to as collectives. This grouping facilitates agricultural activities such as irrigation, access to roads, and more. After the harvest, a large volume of rice straw is left in narrow rows or piles on the field, along with uncut standing stubble. In order to prepare the field for the next harvest, farmers routinely burn the residues. While

**Figure 1.3: Primary study area with proportion of rice land area obtained from Vietnam Office of Statistics**



most of the straw is burned, it also has other uses such as: reincorporation into the soil, mushroom cultivation, composting, cattle feed, and bioenergy (Trach 1998; Nguyen 2012; Hong Van et al. 2014; Duong and Yoshiro 2015; Oritate et al. 2015).

In comparison to rural areas, suburban and peri-urban areas such as within Hanoi, typically burn a higher proportion of the rice straw as these areas have fewer cattle relying on it for food (Duong and Yoshiro 2015). Thus, with the higher proportion of rice residue burned, there is an amplified emissions impact. Accurate paddy rice mapping is crucial in the small-holder agricultural lands where about 50% of the rice residues are subjected to burning in order to clear the field for the next harvest, however some is returned back to the soil, used as cattle feed, or for mushroom straw (Nguyen 2012; Tran et al. 2014; Hong Van et al. 2014; Duong and Yoshiro 2015).

The temperature and precipitation of the region are monsoon-influenced. Accordingly, the summertime from May-August is characterized by high temperatures and increasingly heavy rainfall. Whereas the autumn (Sep – Oct) and winter (Nov – Jan) experience slightly cooler temperatures and less rainfall with high humidity throughout the year. The region is also home to a vibrant economy including aquaculture, fisheries, mangrove forestry, construction, and other industrial and commercial services. The economy is driven by demand from its growing population with density averaging over 1,200 people per square km (Devienne 2006).

### **1.5 Organization of the study**

This dissertation is composed of six distinct chapters. Chapter 1: introduction, provides research background and relevance, study objectives, purpose, and details about the study area. Chapters 2-5 contain the three research objectives and are presented with the same



material as published or submitted in the journal. Chapter 2 corresponds to objective 1 and is published in *IEEE Journal of Selected Topics in Applied Earth Observation and Remote Sensing*. Chapter 3 corresponds to objective 2 and is published in *Environmental Research Letters*. Chapter 4 corresponds to the first part of objective 3 and is under review in *Environmental Pollution*. Chapter 5 corresponds to the second part of objective 3 and is under review in *PLoS One*. Each of the chapters are interrelated, but independent, as each one has a specific and relevant literature review, figures, tables, and a list of references.

Chapter 2: *Mapping of double and single crop paddy rice with Sentinel-1A at varying spatial scales and polarizations in Hanoi, Vietnam*, addresses objective 1 and provides not only rice area maps useful for emissions estimation, but also highlights regional variation.

Chapter 3: *Satellites may underestimate rice residue and associated burning emissions in Vietnam* addresses objective 2, and develops a novel field method to estimate rice residue as well as estimate contribution of rice residue emissions from burning, and relates field estimates to the SAR data.

Chapter 4: *Improved rice residue burning emissions estimates, Accounting for practice-specific emission factors in air pollution assessments* addresses objective 3, and quantifies further improved rice residue burning emissions based on burning practice specific factors, and demonstrates a method to indirectly estimate residue burning in cloud-covered regions using remote sensing.

Chapter 5: *Spatiotemporal trends of air pollution over Hanoi, Vietnam using Merra-2 reanalysis, satellite-based UVAI and ancillary atmospheric data* also addresses

objective 3, and explores the trends in black carbon levels within Hanoi, Vietnam and across the surrounding region using multiple datasets while factoring in synoptic meteorology and atmospheric transport systems. It also demonstrates the difficulty of monitoring air pollution in this region.

Chapter 6: *Summary of Research*, connects the different chapters together and provides a synopsis of all research findings, concluding remarks, as well as future directions for the research.

## 1.6 References

Apte, J.S., Marshall, J.D., Cohen, A.J. and Brauer, M., 2015. Addressing global mortality from ambient PM<sub>2.5</sub>. *Environmental science & technology*, 49(13), pp.8057-8066.

Badarinath, K.V.S., Kharol, S.K. and Sharma, A.R., 2009. Long-range transport of aerosols from agriculture crop residue burning in Indo-Gangetic Plains—a study using LIDAR, ground measurements and satellite data. *Journal of Atmospheric and Solar-Terrestrial Physics*, 71(1), pp.112-120.

Cristofanelli, P., Putero, D., Adhikary, B., Landi, T.C., Marinoni, A., Duchi, R., Calzolari, F., Laj, P., Stocchi, P., Verza, G. and Vuillermoz, E., 2014. Transport of short-lived climate forcers/pollutants (SLCF/P) to the Himalayas during the South Asian summer monsoon onset. *Environmental Research Letters*, 9(8), p.084005.

Devienne, S. 2006. Red River Delta: fifty years of change. *Moussons*, 9-10.

Duong, P.T. and Yoshiro, H., 2015. Current Situation and Possibilities of Rice Straw Management in Vietnam. Accessed from [http://www.jsrsai.jp/Annual\\_Meeting/PROG\\_52/ResumeC/C02-4.pdf](http://www.jsrsai.jp/Annual_Meeting/PROG_52/ResumeC/C02-4.pdf).

Giglio, L., Randerson, J.T. and Werf, G.R., 2013. Analysis of daily, monthly, and annual burned area using the fourth-generation global fire emissions database (GFED4). *Journal of Geophysical Research: Biogeosciences*, 118(1), pp.317-328.

Heinsch, F.A., McHugh, C.W. and Hardy, C.C., 2016. Fire, Fuel, and Smoke Science Program 2015 Research Accomplishments. Accessed from [https://198.61.190.25/sites/default/files/images/downloads/FFS\\_AnnualReport\\_FY2015.pdf](https://198.61.190.25/sites/default/files/images/downloads/FFS_AnnualReport_FY2015.pdf).

- Holder, A.L., Gullett, B.K., Urbanski, S.P., Elleman, R., O'Neill, S., Tabor, D., Mitchell, W. and Baker, K.R., 2017. Emissions from prescribed burning of agricultural fields in the Pacific Northwest. *Atmospheric Environment*, 166, pp.22-33.
- Hong Van, N.P., Nga, T.T., Arai, H., Hosen, Y., Chiem, N.H. and Inubushi, K., 2014. Rice Straw Management by Farmers in a Triple Rice Production System in the Mekong Delta, Viet Nam. *Tropical Agriculture and Development*, 58(4), pp.155-162.
- Justice, C.O., Giglio, L., Korontzi, S., Owens, J., Morisette, J.T., Roy, D., Descloitres, J., Alleaume, S., Petitcolin, F. and Kaufman, Y., 2002. The MODIS fire products. *Remote Sensing of Environment*, 83(1), pp.244-262.
- Korontzi, S., McCarty, J., Loboda, T., Kumar, S. and Justice, C., 2006. Global distribution of agricultural fires in croplands from 3 years of Moderate Resolution Imaging Spectroradiometer (MODIS) data. *Global Biogeochemical Cycles*, 20(2).
- Lasko, K., Vadrevu, K., Tran, V., Ellicott, E., Nguyen, T., Bui, H. and Justice, C., 2017. Satellites may underestimate rice residue and associated burning emissions in Vietnam. *Environmental Research Letters*, 12(8) 05006.
- Oritate, F., Yuyama, Y., Nakamura, M., Yamaoka, M., Nguyen, P.D., Dang, V.B.H., Mochidzuki, K. and Sakoda, A., 2015. Regional diagnosis of biomass use in suburban village in Southern Vietnam. *Journal of the Japan Institute of Energy*, 94(8), pp.805-829.
- Patanothai, A., 1996. *Soils under stress: nutrient recycling and agricultural sustainability in the Red River Delta of Northern Vietnam*. Honolulu: East-West Center.
- Pham, V.C., Pham, T.T.H., Tong, T.H.A., Nguyen, T.T.H. and Pham, N.H., 2015. The conversion of agricultural land in the peri-urban areas of Hanoi (Vietnam): patterns in space and time. *Journal of Land Use Science*, 10(2), pp.224-242.
- Ponette-González, A.G., Curran, L.M., Pittman, A.M., Carlson, K.M., Steele, B.G., Ratnasari, D. and Weathers, K.C., 2016. Biomass burning drives atmospheric nutrient redistribution within forested peatlands in Borneo. *Environmental Research Letters*, 11(8), p.085003.
- Pope III, C.A. and Dockery, D.W., 2006. Health effects of fine particulate air pollution: lines that connect. *Journal of the air & waste management association*, 56(6), pp.709-742.
- Sanderfoot, O.V. and Holloway, T., 2017. Air pollution impacts on avian species via inhalation exposure and associated outcomes. *Environmental Research Letters*, 12(8), 083002.
- Schroeder, W., Csiszar, I. and Morisette, J., 2008. Quantifying the impact of cloud obscuration on remote sensing of active fires in the Brazilian Amazon. *Remote Sensing of Environment*, 112(2), pp.456-470.

Streets, D.G., Bond, T.C., Carmichael, G.R., Fernandes, S.D., Fu, Q., He, D., Klimont, Z., Nelson, S.M., Tsai, N.Y., Wang, M.Q. and Woo, J.H., 2003. An inventory of gaseous and primary aerosol emissions in Asia in the year 2000. *Journal of Geophysical Research: Atmospheres*, 108(D21).

Streets, D.G., Bond, T.C., Lee, T. and Jang, C., 2004. On the future of carbonaceous aerosol emissions. *Journal of Geophysical Research: Atmospheres*, 109(D24).

Trach, N.X., 1998. The need for improved utilisation of rice straw as feed for ruminants in Vietnam: An overview. *Livestock Research for Rural Development*, 10(2), pp.1-14.

Vadrevu, K.P., Ellicott, E., Giglio, L., Badarinath, K.V.S., Vermote, E., Justice, C. and Lau, W.K., 2012. Vegetation fires in the himalayan region—Aerosol load, black carbon emissions and smoke plume heights. *Atmospheric Environment*, 47, pp.241-251.

Vietnam Office of Statistics, 2016. Agriculture, forestry, and fishery. Accessed from [http://www.gso.gov.vn/default\\_en.aspx?tabid=467&idmid=3](http://www.gso.gov.vn/default_en.aspx?tabid=467&idmid=3).

van der Werf, G.R., Randerson, J.T., Giglio, L., Collatz, G.J., Mu, M., Kasibhatla, P.S., Morton, D.C., DeFries, R.S., Jin, Y.V. and van Leeuwen, T.T., 2010. Global fire emissions and the contribution of deforestation, savanna, forest, agricultural, and peat fires (1997–2009). *Atmospheric Chemistry and Physics*, 10(23), pp.11707-11735.

van der Werf, G.R., Randerson, J.T., Giglio, L., Van Leeuwen, T.T., Chen, Y., Rogers, B.M., Mu, M., Van Marle, M.J., Morton, D.C., Collatz, G.J. and Yokelson, R.J., 2017. Global fire emissions estimates during 1997–2016. *Earth System Science Data*, 9(2), p.697.

Yan, X., Ohara, T. and Akimoto, H., 2006. Bottom-up estimate of biomass burning in mainland China. *Atmospheric Environment*, 40(27), pp.5262-5273.

## Chapter 2: Mapping and characterizing paddy rice with Sentinel-1A at varying spatial scales and polarizations in Hanoi, Vietnam<sup>1</sup>

### 2.1 Abstract

Paddy rice is the prevalent land cover in the mosaicked landscape of the Hanoi Capital Region, Vietnam. In this study, we map double and single crop rice in Hanoi using a random forest algorithm and a time-series of Sentinel-1 SAR imagery at 10 and 20m resolution using VV-only, VH-only, and both polarizations. We compare spatial and areal variation and quantify input band importance, estimate crop growth stages, estimate rice field/collective metrics using Fragstats with image segmentation, and highlight the importance of the results for land use and land cover. Results suggest double crop rice ranged from 208,000 to 220,000 ha with 20m resolution imagery accounting for the most area in all polarizations. Based on accuracy assessment, we found 10m data for VV/VH to have highest overall accuracy (93.5%,  $\pm 1.33\%$ ), while VV at 10m and 20m had lowest overall accuracies (90.9%  $\pm 1.57$ ; 91.0%  $\pm 2.75$ ). Mean decrease in accuracy suggests for all but VV at 10 m, data from harvest and flooding stages are most critical for classification. Results show 20 m data for both VV and VH overestimates rice land cover, however 20m data may be indicative of rice land use. Analysis of growing season shows average estimated length of 93–104 days for each season. Commune-level results suggest up to 20% coefficient of variation between VV10m and VH10m with significant spatial

---

<sup>1</sup> The presented material was previously published in Lasko K, Vadrevu K P, Tran V T, and Justice C 2018. Mapping double and single crop paddy rice with Sentinel-1A at varying spatial scales and polarizations in Hanoi, Vietnam. *IEEE Journal of Selected Topics in Applied Earth Observation and Remote Sensing* 11(2), 498-512. In reference to IEEE copyrighted material which is used with permission in this thesis, the IEEE does not endorse any of University of Maryland's products or services. Internal or personal use of this material is permitted. If interested in reprinting/republishing IEEE copyrighted material for advertising or promotional purposes or for creating new collective works for resale or redistribution, please go to [http://www.ieee.org/publications\\_standards/publications/rights/rights\\_link.html](http://www.ieee.org/publications_standards/publications/rights/rights_link.html) to learn how to obtain a License from RightsLink. © 2018 IEEE.

variation in rice area. Landscape metrics show rice fields are typically planted in groups of 3–4 fields with over 796,000 collectives and 2.69 million fields estimated in the study area.

## **2.2 Introduction**

Rice (*Oryza sativa*) is the staple crop for economic and cultural livelihood throughout much of Southeast Asia, including Vietnam. Production of paddy rice in Vietnam has been expanding consistently over time with 32.5 million metric tons produced in year 2000 to 45.2 million metric tons in the year 2015 (General Statistics Office of Vietnam, 2016). All the while, area under cultivation has only slightly increased with 7.67 million ha in 2000 and 7.83 million ha in 2015, suggesting notable agricultural intensification. Intensification is critical especially in areas of the Red River Delta such as the Hanoi Capital Region, where population pressure and a robust economy are driving peri-urban expansion into agricultural areas (Pham et al. 2015). Thus, reducing the amount of area under cultivation in some areas.

Accordingly, it is of increasing importance to develop efficient methods for mapping paddy rice in Vietnam. The two dominant rice-producing hubs in Vietnam are within the Red River Delta and the Mekong River Delta, together accounting for the majority of national rice production. Optical imagery such as from MODIS or Landsat are frequently cloud contaminated during key agricultural stages (i.e., planting and harvest); thus, hampering mapping efforts (Whitcraft et al. 2015). C-band Sentinel-1 imagery is capable of penetrating through cloud cover making it the obvious choice for timely mapping of paddy rice.

Efforts to map paddy rice using SAR originated in the 1990s with selected images from ERS-1 C-band imagery with approximately 12.5–30 m spatial resolution and a repeat pass of 35 days (Paudyal et al. 1993; Aschbacher et al. 1995; Takeuchi et al. 1996; Chakraborty et al. 1997; Le Toan et al. 1997; Liew et al. 1998), and also using C-band RADARSAT at spatial resolution of 10–100 m and a repeat pass of 24 days (Yun et al. 1997; Ribbes 1997; Panigrahy et al. 1999). These pioneering studies were often stymied by lack of quality ground-truth imagery, single polarization, or were limited to small spatial scale studies due to high data volumes. Subsequent studies began focusing on utilizing multitemporal SAR over larger land areas for improved rice mapping and testing various algorithms with ERS-1, ERS-2, and RADARSAT (Shao et al. 2001; Suga et al. 2000; Inoue et al. 2002; Lee and Lee 2003; Chen and McNairn 2006). Improvements in sensors and availability of ground-truth data led to further more extensive rice mapping studies using L-band SAR such as ALOS/PALSAR or JERS-1 (Salas et al. 2007; Zhang et al. 2009), EN- VISAT ASAR (Lam-Dao et al. 2007; Bouvet et al. 2009; Jia et al. 2012; Nguyen et al. 2015), TerraSAR-X and COSMO-SkyMed (Pei et al. 2011; Gebhardt et al. 2012; Inoue et al. 2014; Nelson et al. 2014). Recent studies include RADARSAT-2 data, object-oriented crop mapping (Jiao et al. 2014; Hoang et al. 2016), combined optical and SAR data (Asilo et al. 2014; Karila et al. 2014; Torbick et al. 2017), and Sentinel-1 C-band SAR (Nguyen et al. 2016; Mansaray et al. 2017; Son et al. 2017). More details are available in a recent review (Steele-Dunne et al. 2017).

While a variety of strong classification methods exist, a number of recent studies have employed random forests for SAR applications, including wetlands mapping (Whitcomb et al. 2009; White et al. 2015; Wang et al. 2017), general agriculture/land

cover (Shiraishi et al. 2014), and in paddy rice mapping with promising results (Torbick et al. 2017b; Waske and Braun 2009; Sonobe et al. 2014). Recent remote sensing studies have also included use of texture-based classification such as Gray Level Co-occurrence Matrix (GLCM) with promising results (Jia et al. 2012; Uhlmann et al. 2014; Zhang et al. 2017). In addition to mapping paddy rice areal extent, other studies have employed SAR for agricultural phenology estimation with multitemporal imagery (Lopez-Sanchez et al. 2012; Jiao et al. 2014), including studies with rice paddy fields and polarization variation, (Koppe et al. 2013; Erten et al. 2014; Erten et al. 2015; Lopez-Sanchez et al. 2014; Kucuk et al. 2016; de Bernardis et al. 2015; Xie et al. 2015; Yuzugullu et al. 2015). While some of these studies applied time-series filters to derive accurate phenology metrics, these are not always requisite due to the unique dynamic range of paddy rice signal from SAR (Torbick et al. 2017). The SAR signal seen in a time-series can accurately capture different stages of crop growth useful for monitoring biophysical variables as well as length of season, planting, and harvest dates. While local farmers and stakeholders have knowledge of the crop phenology, SAR-based information is useful for broader national or regional operational monitoring of crops (i.e., crop conditions, status, or health) which is a major goal of international initiatives such as Asia-Rice Crop Estimation and monitoring (Asia-RiCE) project or the Global Agricultural Monitoring (GEOGLAM) initiative (Oyoshi et al. 2016; Whitcraft et al. 2015). The SAR observations can survey the entire region, whereas optical data can often be obstructed by cloud. Thus, SAR data can be useful for crop mapping and monitoring at regular intervals.



## **2.3 Study area and datasets**

### *2.3.1 Study area*

The mosaic landscape of the Hanoi Capital Region includes a variety of land cover types dominated by rice agriculture, as well as other small-holder croplands, urban areas, small plantations, and aquaculture. The typical rice field size in the area is about 790m<sup>2</sup> with fields routinely planted in large collectives as necessary to facilitate irrigation. The field size is suitable for moderate-to-fine resolution mapping (Lasko et al. 2017). The Hanoi Capital Region is situated within the Red River Delta, Vietnam's oldest rice producing region, accounting for about 15% of the country's total rice production (General Statistics Office of Vietnam, 2016). Of all the different crops, rice is most prevalent and it is the dominant crop type in the region. It has two distinct seasons: Winter-Spring, and Spring-Summer. Rice has three distinct stages: sowing/transplanting, growth, and harvest/post-harvest, all of which can be identified using satellite data (Le Toan et al. 1997). In the study area, rice is sown or transplanted after the Tet holiday in February or early March. Subsequently, a significant green-up is observed as the rice matures in its vegetative stage, especially after heading in April (Xiao et al. 2005; Kontgis et al. 2015). During late May to June the rice is harvested, and rapidly prepared for the next season starting in late June or July. After the harvest in each season (June and October) the rice residues including straw and stubble, are regularly burned accounting for as much as 13% of PM2.5 emissions for Vietnam; thus, burning may constitute a significant air quality issue (Duong and Yoshiro 2015; Lasko et al. 2017).

The rice fields are supported by a vast network of irrigation and drainage canals and small access roads seen throughout the region. While most fields practice double cropping, some fields cultivate a single crop of rice. After the harvest, single rice fields

remain flooded to support the growing aquaculture industry Dey and Ahmed 2005; Ottinger et al. 2017). The study area has seen rapid expansion of aquaculture with 16,500 ha in year 2000, and 46,000 ha in year 2014, with the vast majority of growth occurring in Hanoi province (General Statistics Office of Vietnam, 2016).

### 2.3.2 Satellite data

The Sentinel-1 satellite from the European Space Agency provides C-band SAR imagery (5.4 GHz) near globally with a 12-day revisit time or 6-day revisit time depending on availability of Sentinel-1B imagery. The Sentinel-1 imagery is provided as dual-polarized

**Table 2.1 SAR average local incidence angle variation (degrees) for VVVH10m over the study area.**

Band	Date	Avg Angle (Double Rice)	Std Angle (Double Rice)	Avg angle (Single Rice)	Std Angle (Single Rice)	Avg angle (Not Rice)	Std Angle (Not Rice)
1	02/03/2016	38.630	3.343	39.304	3.328	39.547	6.414
2	02/15/2016	38.639	3.347	39.314	3.326	39.547	6.414
3	02/27/2016	38.640	3.349	39.316	3.327	39.543	6.414
4	03/10/2016	38.629	3.341	39.306	3.328	39.550	6.412
5	03/22/2016	38.640	3.350	39.326	3.322	39.539	6.411
6	04/03/2016	38.644	3.351	39.334	3.326	39.538	6.409
7	04/15/2016	38.640	3.343	39.325	3.322	39.545	6.411
8	04/27/2016	38.644	3.345	39.327	3.322	39.546	6.411
9	05/09/2016	38.637	3.344	39.322	3.325	39.543	6.410
10	05/21/2016	38.644	3.353	39.331	3.337	39.542	6.408
11	06/02/2016	38.624	3.337	39.306	3.327	39.547	6.412
12	06/14/2016	38.634	3.342	39.315	3.325	39.546	6.412
13	07/08/2016	38.632	3.347	39.303	3.327	39.547	6.410
14	07/20/2016	38.632	3.340	39.313	3.326	39.548	6.412
15	08/01/2016	38.620	3.336	39.302	3.327	39.547	6.412
16	08/13/2016	38.627	3.339	39.303	3.327	39.550	6.411
17	08/25/2016	38.627	3.339	39.304	3.327	39.550	6.412
18	09/06/2016	38.626	3.336	39.307	3.327	39.553	6.412
19	09/18/2016	38.629	3.340	39.307	3.327	39.548	6.412
20	09/30/2016	38.629	3.340	39.310	3.325	39.543	6.412
21	10/12/2016	38.638	3.346	39.325	3.327	39.542	6.410
22	10/24/2016	38.640	3.344	39.325	3.322	39.543	6.411

Interferometric Wide swath (IW) data with vertical transmit, vertical receive (VV), and vertical transmit, horizontal receive (VH) polarizations. Each polarization is at a nominal spatial resolution of 5m x 20m prior to preprocessing using an open-access operational baseline observation strategy. A full time-series stack of 22 Sentinel-1A images was acquired during the 2016 growing season (February– October) (table 2.1). No Sentinel-1B imagery was available over the study area. Level-1 ground-range detected, descending mode, IW imagery acquired from the Alaska Satellite Facility (a direct mirror of ESA’s Sci-hub) were processed using the free and open source Sentinel-1 toolbox. The ground-range detected images were processed following guidelines including applying restituted orbit files, multi-look azimuthal compressions to 20m, terrain correction using SRTM 30m version 4 DEM, radiometric calibration adjustments to correct for viewing geometry effects, and refined lee speckle filter to reduce constructive and destructive interference, all resulting in sigma-nought backscatter data logarithmically scaled in decibel (Zuhlke et al. 2015). Given the relatively small study region with generally flat terrain, incident angle artifacts and layover/shadow effects were relatively minimal. We display incident angle and SAR backscatter ranges across the study area in Table I. We

also highlight average SAR signal and the temporal dynamic across the different land cover types found in the study area (figure 2.1).

### 2.3.3 Training and validation data

We conducted fieldwork throughout the study area during May/June and September/October of 2016 as part of a related project on rice residue burning. The data included surveys on crop calendar, crop rotation, field conditions, and biomass data. Over 900 geolocated photos were taken of paddy fields and non-rice areas such as aquaculture, wetlands, and other land cover types found within the region. These field photos were used for training or validation along with fine-resolution imagery from Google Earth and the original Sentinel-1 imagery. No training data were included in the validation. We show a multitemporal composite of the SAR data with the training polygons overlaid (figure 2.2).

**Figure 2.1 timeseries SAR signal over different land cover types**

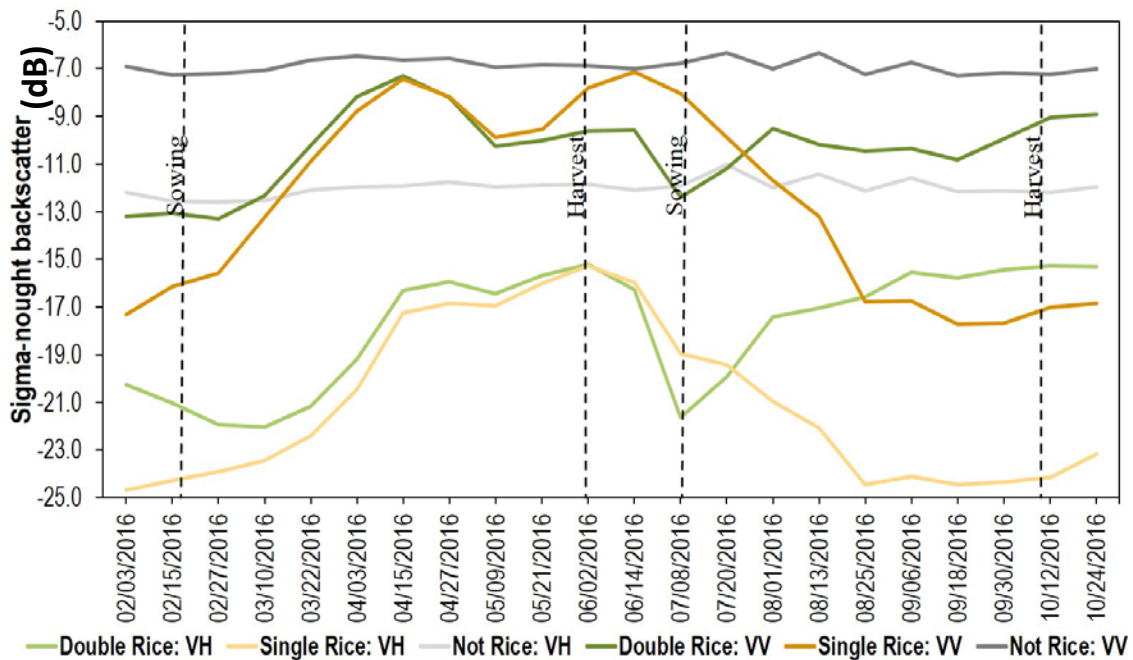
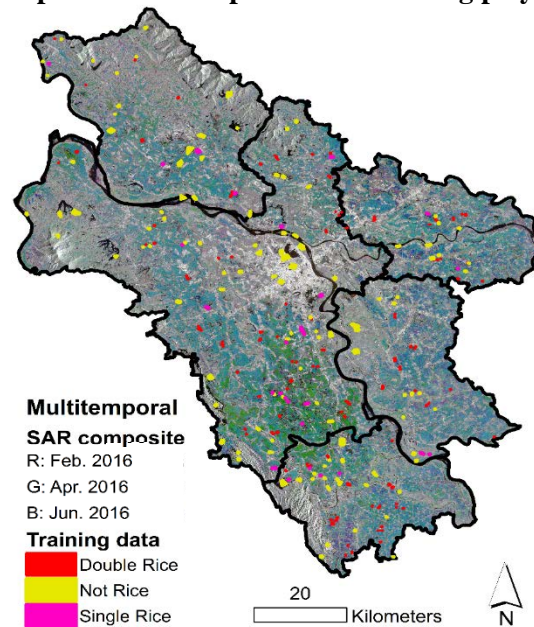


**Figure 2.2 multitemporal SAR composite with training polygons overlaid**



### **2.3 Methodology**

We classified the six different datasets (Table 2.2) using the random forest algorithm to obtain rice areal estimates and as a basis to compare the datasets. These resulting datasets were the basis for comparison of the different polarizations and spatial resolutions for mapping small-holder paddy rice. Accordingly, we selected nominal 10m resolution as it is the native resolution of Sentinel-1 and 20m resolution data for comparison. We addressed the following questions in our study: 1) Which dataset yields the highest overall and class specific accuracies and mapped areas, and are there notable differences between them? 2) What is the typical rice phenology including start/end of season and length of growing season? 3) How do the resulting mapped rice area estimates vary at the

province and commune level? 4) Based on landscape analysis, what are the spatial characteristics of paddy fields and approximately how many are in the study area?

### 2.3.1 Double and single crop rice mapping

We employed an ensemble, machine-learning random forest algorithm for mapping single and double crop paddy rice, as well as for evaluating the relative importance of specific input data for mapping (Breiman 2001). The machine-learning random forest algorithm implemented in Scikit-learn python package uses bootstrap aggregated

**Table 2.2 SAR dataset descriptions**

Dataset name	Description
VV10m	Vertical-vertical (VV) polarized bands at 10m spatial resolution
VH10m	Vertical-horizontal (VH) polarized bands at 10m spatial resolution
VVVH10m	Both VV and VH bands at 10m resolution
VV20m	VV bands at 20m spatial resolution
VH20m	VH bands at 20m spatial resolution
VVVH20m	Both VV and VH bands at 20m spatial resolution

sampling to build individual decision trees for classification. Each decision tree was built with a bootstrap sample from the training data, with the unsampled data used for out-of-bag sampling. Within the structure of a tree, a random sample of the square root of the number of predictors was chosen for each split as best candidates derived from the entire predictor set. Random forest is robust against outliers and over-fitting, nonparametric, has high classification accuracy, and can yield a measure of variable importance.

We implemented the random forest algorithm using all 22 (VV or VH) or 44 input bands (VV & VH) (Table 2.2) for each of the six datasets separately. We populated the

random forest with 1000 trees, where out-of-bag errors reach asymptotic values (Breiman 2001). The same classification technique was applied to each dataset. Out of bag samples, which are randomly withheld from classification training were used as an indicator of feature importance. From the 1000 trees populated in our random forest, the mean decrease in classification accuracy for the input bands was reported. This was useful as a measure of feature importance in mapping paddy rice and each input band can be linked to a general crop growth stage (i.e., sowing, vegetative growth, and harvest). Training polygons were digitized over the single rice, double rice, and non-rice areas within each province using field photos, Sentinel-1 data, survey information, and fine-resolution Google Earth imagery.

### *2.3.2 Accuracy Assessment*

We performed an accuracy assessment on the resulting rice maps. Random points across the study area were generated using a stratified random sampling scheme (Congalton and Green 2008). Based on the proportion of each resulting mapped class, a stratified random sample of 402 total polygons for double crop rice (125), single crop rice (41), and non-rice (236) classes were generated for the 10m data. For the 20m data, the same polygons were used for comparison consistency; however, there are fewer total pixels due to reduced spatial resolution. We specified a 600m minimum distance between polygons to prevent field overlap.

Following good practices in accuracy assessment, we adjusted the classification accuracies as well as the mapped rice area estimates based on the weighting from the proportion of land area for each class (Olofsson et al. 2014; Appendix I). This weighting results in unbiased areal estimates. Based on the same, we derived uncertainty estimates for the accuracy-adjusted areas using a 95% confidence interval for each of our resulting

mapped classes. The accuracy-adjusted area provides a more robust assessment of the area mapped for each class. We also computed the confidence intervals for adjusted class and overall accuracies to be used for comparison among the different maps.

### 2.3.3 Spatial Analysis

We compared the paddy rice maps through a number of metrics including average absolute deviation (AAD) (equation 2.1) and coefficient of variation (CV) (equation 2.2) to explore absolute and relative variation in mapped area for each of the six different datasets as follows:

**Equation 2.1**

$$AAD = \frac{\sum|x - \bar{x}|}{N}$$

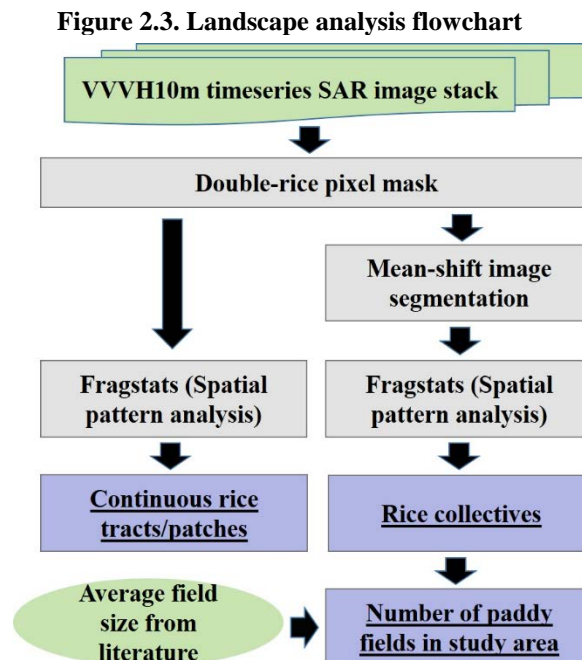
**Equation 2.2**

$$CV = \left(\frac{\sigma}{\bar{x}}\right) 100$$

Where  $x$  is the rice area in hectares for one of the six rice maps,  $\bar{x}$  is the mean rice area of all 6 datasets, and  $N$  is the number of datasets for (1). While for (2)  $\sigma$  is the standard deviation of all rice area for all six datasets, and  $\bar{x}$  is the mean rice area for all datasets. The final value is a percentage.



We compared the AAD and CV at the commune-level (third-level administrative subdivision) and study-area level to assess overall and spatial variability. In addition, we computed pixel-level thematic change for each dataset. We also employed Fragstats (Version 4.2) for landscape-scale analysis on the most accurate resulting dataset including number of patches (collections of connected/adjacent paddy rice pixels) and patch metrics useful for evaluating the size of large connected aggregations/collections of paddy rice fields. Further, we employed mean-shift image segmentation on the double-rice pixels of the time-series imagery stack to estimate rice collective size (groups of fields with similar crop phenology) and number of fields in the study area by including typical paddy field size of 790m<sup>2</sup> (Lasko et al. 2017). We show the general flowchart in figure 2.3. Mean-shift image segmentation is a non-parametric iterative algorithm fitting a neighborhood window around each pixel, calculating the data mean in the window, and shifting the neighborhood window to the mean (Fukunaga and Hostetler 1975;



Comaniciu and Meer 2002). The algorithm is useful for clustering pixels with similar signal and has been used in a variety of land cover remote sensing applications (Senthilnath et al. 2012; Su and Zhang 2017).

#### 2.3.4 Rice phenology

While some of the prior studies utilized spatiotemporal filtering to derive crop phenology metrics, we derived the metrics based on the unique rice dynamic range combined with general phenology timeframes. Sentinel-1 VH-polarized backscatter imagery were used to estimate sowing /transplanting and harvest dates for both seasons of rice. Based on the unique phenology of paddy rice measured by SAR and selecting a general timeframe based on a-priori knowledge, we found local planting date coincides with the local minimum value (indicative of flooding, constrained to February or March), and harvest date when the local maximum backscatter value is reached (indicative of peak maturity of rice just prior to harvest, constrained to May or June) as noted in previous studies (Le Toan et al. 1997; Choudhury and Chakraborty 2006; Koppe et al. 2013; Torbick et al. 2017). The estimated range is based on the overpass dates of the Sentinel-1 satellite. The approximate length of growing season is derived by differencing the median date within the planting range and the harvest date range.

## 2.4 Results

### 2.4.1 Mapped area variation

The six paddy rice maps generated from the random forest classifier and their spatial patterns are shown in figure 2.4. The pixel classification count for double rice is also shown in figure 2.4 zoomed to a hotspot of variation area in Bac Ninh, highlights that along edges and smaller fields some of the rice maps are not in agreement. Overall, 66%

of the pixels were in agreement (where pixel count = 6). On another note, when the absolute mapped rice areas are compared we notice more variation. For example, the total mapped double-rice area for each is: 208,276 ha (VV-10m), 212,465 ha (VH-10m), 214,565 ha (VV&VH-10m), 214,903 ha (VV-20m), 218,788 ha (VH-20m) and 220,356 ha (VV&VH-20m). This general pattern suggests 10m imagery systematically reports lower mapped area than 20m imagery, and VV reports less mapped area than VH with VV&VH combination accounting for the most area. This is attributed to VV signal attenuated by the vertical structure of rice. The same pattern is not clear for single rice. Whereas 10m datasets exhibited less area than 20m datasets, and reported areas varied between polarizations. In comparison to the official government rice areal statistics for 2016 of 232,700 ha paddy rice, our estimates reported about 12,000 – 24,000 ha less (General Statistics Office of Vietnam, 2016). In comparison to same statistics for the entire Red River Delta (546,950 ha), our study area has about 40% of the total rice area. The mapped areas for single rice can be seen in table 2.3.

#### *2.4.2 Accuracy assessment and areal adjustment*

We evaluated the accuracy of each dataset and present the confusion matrices with the total number of pixels for each class, as well as user, producer and overall accuracies adjusted using the unbiased areal estimates. We also provide 95% confidence intervals for each statistic for purposes of comparison. The dataset overall accuracies in descending order are VV&VH-10m (93.5%), VH-10m (93.1%), VV&VH-20m (92.5%), VH-20m (91.4%), followed by VV-20m (91.0%), and VV-10m (90.9%). We note the confidence interval ranges between VV&VH-20m and VV&VH-10m, and the same for the others, suggests they may not be significantly different overall. However, when

**Figure 2.4. Classified paddy rice maps.** Each SAR dataset's resulting rice map is shown, and a pixel classification count of double-rice agreement between the six datasets is shown on the far right side of the figure.

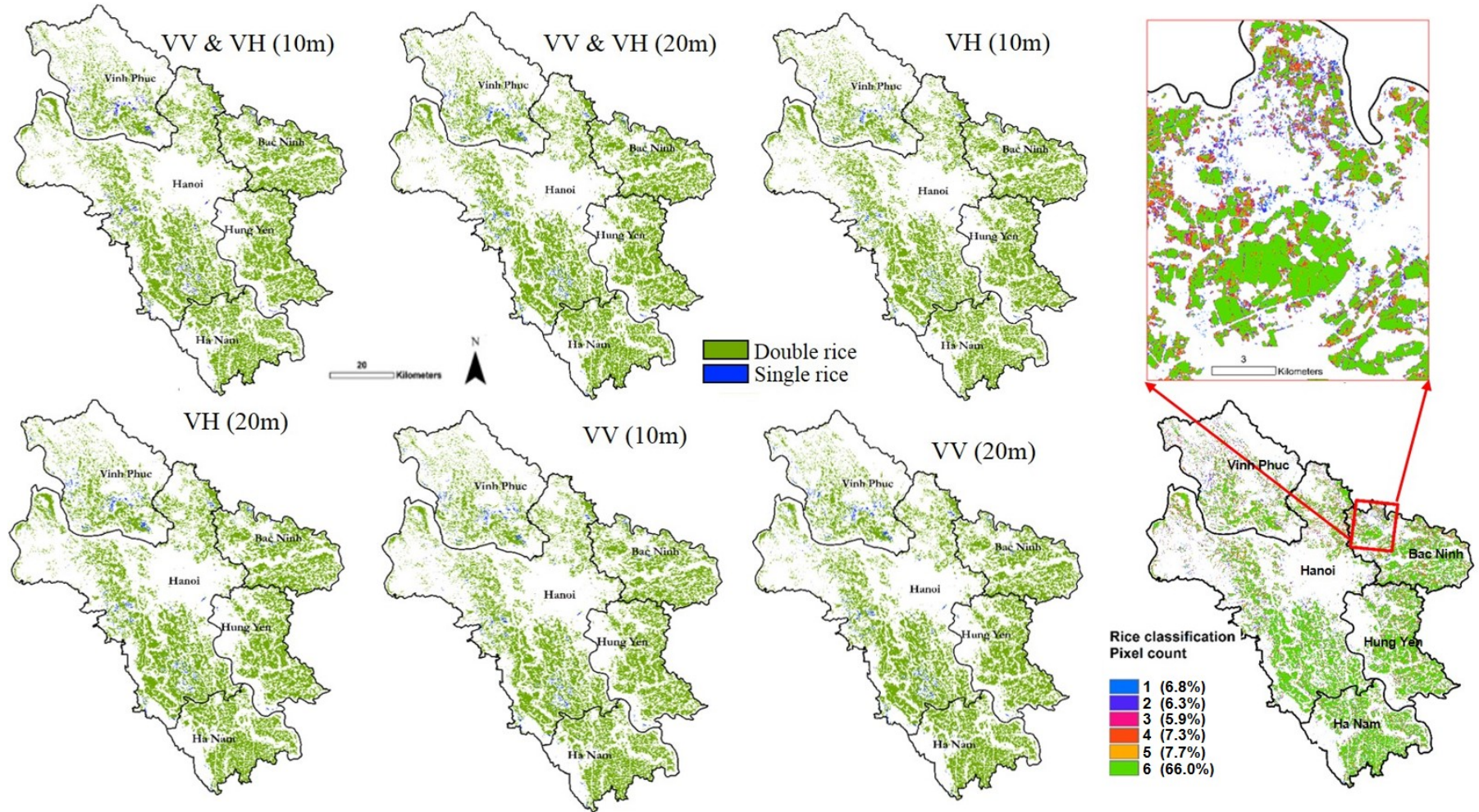


**Table 2.3. Confusion matrices.** 10m datasets are on the left, and 20m datasets are on the right. It contains associated pixels per class, mapped area per class, and adjusted accuracies with confidence intervals based on the calculated unbiased areal estimates.

REFERENCE						
VV and VH Class	Double rice	Single rice	Non-rice	Total	Adj. User's Acc.	Area (ha)
Double rice	420	2	17	439	95.7% (0.09%)	214,565
Single rice	0	160	1	161	99.4% (0.10%)	4,719
Non-rice	68	4	916	988	92.7% (0.05%)	588,449
<b>Total</b>	<b>488</b>	<b>166</b>	<b>934</b>	<b>1588</b>		<b>807,733</b>
Adj. Producer's Acc.	83.5% (0.15%)	58.3% (0.59%)	98.5% (0.03%)			
Overall Accuracy: 93.5% (1.33%)						

REFERENCE						
VH Class	Double rice	Single rice	Non-rice	Total	Adj. User's Acc. (C.I)	Area (ha)
Double rice	410	0	13	423	96.9% (0.08%)	212,465
Single rice	0	161	3	164	98.2% (0.16%)	4,319
Non-rice	78	5	918	1001	91.7% (0.05%)	590,950
<b>Total</b>	<b>488</b>	<b>166</b>	<b>934</b>	<b>1588</b>		<b>807,733</b>
Adj. Producer's Acc.	81.7% (0.16%)	59.0% (0.58%)	98.8% (0.02%)			
Overall Accuracy: 93.1% (1.38%)						

REFERENCE						
VV Class	Double rice	Single rice	Non-rice	Total	Adj. User's Acc. (C.I)	Area (ha)
Double rice	389	3	14	406	95.8% (0.10%)	208,276
Single rice	0	145	1	146	99.3% (0.11%)	4,908
Non-rice	99	13	919	1031	89.1% (0.06%)	594,549
<b>Total</b>	<b>488</b>	<b>161</b>	<b>934</b>	<b>1583</b>		<b>807,733</b>
Adj. Producer's Acc.	77.8% (0.17%)	35.0% (0.58%)	98.7% (0.02%)			
Overall Accuracy: 90.9% (1.57%)						

REFERENCE							
VV and VH Class	Double rice	Single rice	Non-rice	Total	Adj. User's Acc.	Mapped Area (ha)	
Double rice	120	1	6	127	94.5% (0.35%)	220,356	
Single rice	1	48	1	50	95.2% (1.02%)	5,533	
Non-rice	24	3	299	326	89.5% (0.18%)	581,839	
<b>Total</b>	<b>145</b>	<b>52</b>	<b>306</b>	<b>503</b>		<b>807,729</b>	
Adj. Producer's Acc.	82.9% (0.51%)	42.8% (1.90%)	98.1% (0.09%)				
Overall Accuracy: 92.5% (2.52%)							

REFERENCE							
VH Class	Double rice	Single rice	Non-rice	Total	Adj. User's Acc.	Mapped Area (ha)	
Double rice	117	0	7	124	94.4% (0.37%)	218,788	
Single rice	0	48	1	49	98.0% (0.58%)	5,227	
Non-rice	28	4	298	330	90.3% (0.18%)	583,713	
<b>Total</b>	<b>145</b>	<b>52</b>	<b>306</b>	<b>503</b>		<b>807,729</b>	
Adj. Producer's Acc.	80.7% (0.54%)	42.0% (1.90%)	97.7% (0.10%)				
Overall Accuracy: 91.4% (2.68%)							

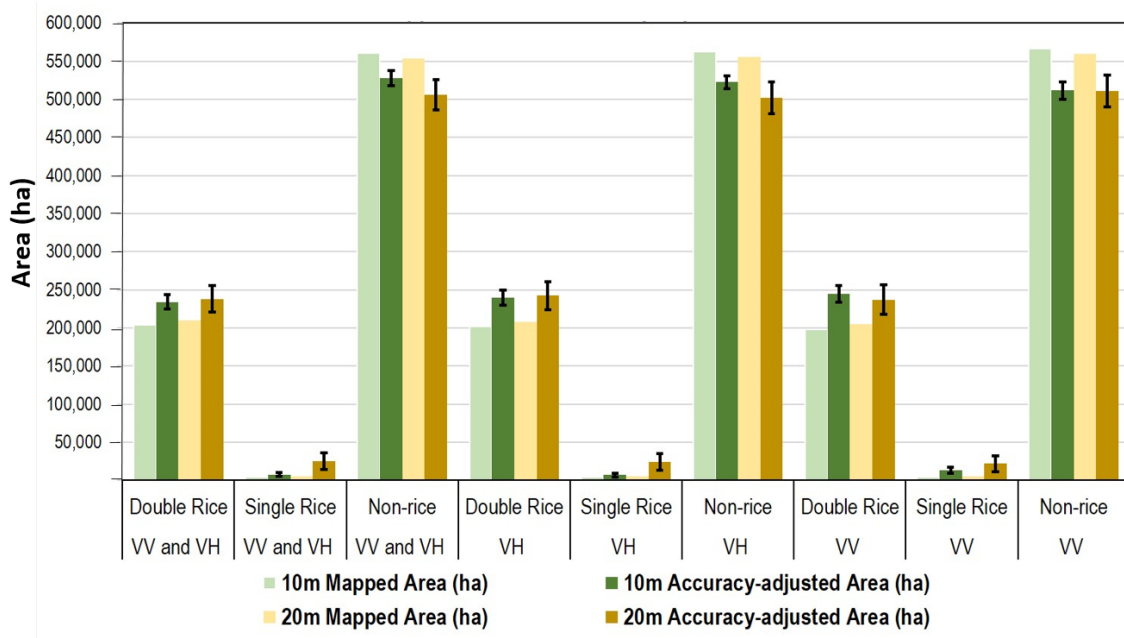
  

REFERENCE							
VV Class	Double rice	Single rice	Non-rice	Total	Adj. User's Acc.	Mapped Area (ha)	
Double rice	116	2	8	126	92.1% (0.42%)	214,903	
Single rice	0	48	0	48	100% (0.00%)	5,450	
Non-rice	29	2	298	329	90.6% (0.17%)	587,376	
<b>Total</b>	<b>145</b>	<b>52</b>	<b>306</b>	<b>503</b>		<b>807,729</b>	
Adj. Producer's Acc.	79.3% (0.55%)	43.8% (1.91%)	97.5% (0.10%)				
Overall Accuracy: 91.0% (2.75%)							

comparing class specific user and producer accuracies for double crop rice and single crop rice the differences are clear. The biggest difference is for single crop rice where the 10m datasets have higher user and producer accuracies (except VV). For double crop rice, the user and producer accuracies are higher in the 10m than the 20m datasets. Across all datasets, user accuracies for single and double crop rice are higher than producer accuracies suggesting a net-positive of rice omission errors. Further details on the confusion matrices are shown in table 2.3.

We adjusted the total mapped areas based on the accuracy assessment and resulting unbiased areal estimates for each dataset and compared the trends as shown in figure 2.5. Overall, we found that accuracy-adjusted areas for single and double rice were higher than the mapped areas. This is due to the rice omission errors found during the accuracy assessment. The accuracy-adjusted areas yield an improved areal estimate useful for studies requiring rice land area as a non-spatial input. The 95% confidence

**Figure 2.5. Mapped areas and accuracy-adjusted areas.**



intervals for each class are also shown with figure 2.5 highlighting uncertainty in the mapped areas.

#### *2.4.3 Pixel-level rice variation*

Analysis of pixel-level thematic variation between each dataset was conducted. For the 10m datasets we found the biggest difference between VV and VH where 48,372 ha of classified land area were different (6.29% difference) which is much higher than total rice area variation (214,565 ha VH10m vs 208,276ha VV10m). The main differences were attributed to double-rice pixels converted to non-rice pixels, non-rice converted to double rice, followed by non-rice into single rice. The smallest difference was between VH and VV&VH with 12,343 ha (1.60% difference). In descending order, the majority was attributed to non-rice to double rice, double rice to non-rice, and non-rice to single rice. The 20m datasets change was very similar with VV and VH (46,613 ha with 6.01% difference), VV and VV&VH (39,848 ha with 5.18% difference), and VH and VV&VH (10,288 ha with 1.34% difference). In all cases 20m datasets had about 0.2% less difference than the 10m datasets, with each following a similar pattern of variation.

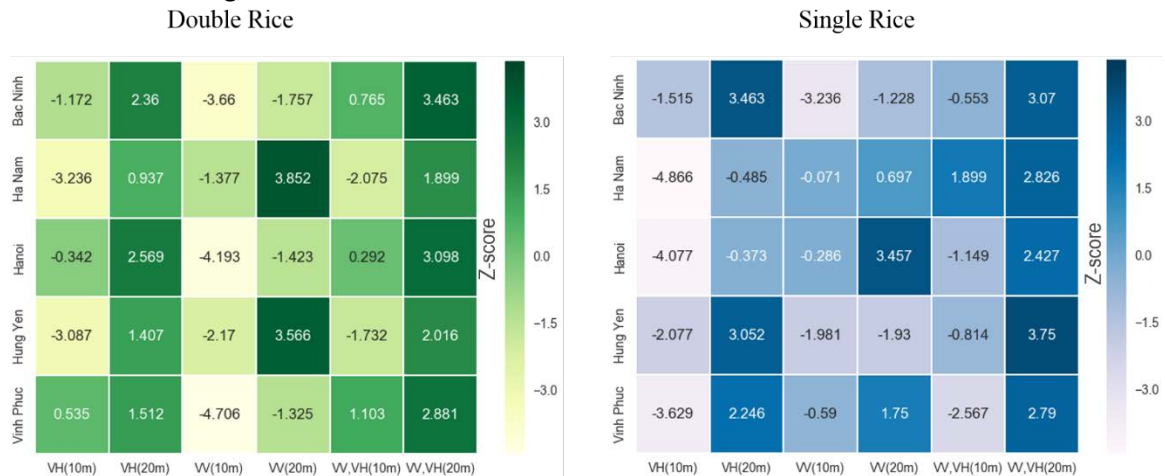
#### *2.4.4 Province-level rice variation*

We evaluated the province-level variation in mapped rice area between the different datasets through coefficient of variation and z-scores for double and single rice (figure 2.6). The CV results suggest relatively low and uniform variation in double rice across the provinces with highest variation in Bac Ninh (2.82%) and Hanoi (2.30%) followed by Ha Nam (2.02%), Vinh Phuc (1.92%), and Hung Yen (1.77%). For single rice the variation was wide ranging depending on the province, with Vinh Phuc exhibiting the



highest (11.57%) variation followed by Bac Ninh (8.90%), Hanoi (8.37%), Ha Nam (5.71%), and Hung Yen (4.17%). We attribute the highest variation in Vinh Phuc to small-holder agriculture and mosaicked landscape making classification difficult. The z-score results for double-rice suggested more insight into province-level variation. For VV20m Ha Nam and Hung Yen had the highest positive z-scores whereas all other provinces had negative Z-scores, and that VV had the most variation in z-score across the provinces. This suggests the VV may be more sensitive to different environmental parameters such as water and moist soil underlying much of these areas. We note similar Z-scores for VVVH20m with the least variation across provinces in single and double crop rice. The same also goes for VH20m with all z-scores for each dataset as positive. Generally, the 20m datasets tend to have more similar z-scores than the 10m datasets.

**Figure 2.6. Province-level rice variation.** Double and single rice province-level z-scores indicating deviation from the mean



#### 2.4.5 Commune-level rice variation

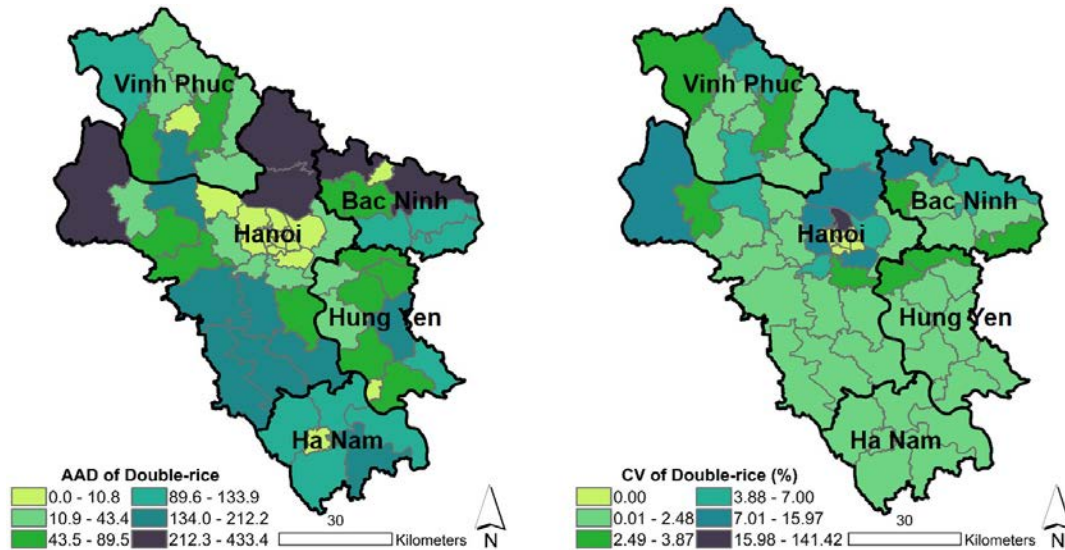
For the entire study area, the total mapped double rice area for each dataset is relatively similar ranging from: 208,276ha (VV10m) to 220,536ha (VVVH20m). However, results



at the commune level (third-level administrative subdivision) suggest more variation. We note that while VV10m had the overall lowest double-rice mapped area, the trend is not spatially universal as VV10m had 27 communes with more rice than VH10m. For example, VH10m in Loung Tai had 249ha less rice than VV10m with a percent difference of 4.60%. However, the biggest percent difference between the two was in Ba Vi where VV10m had 20% less rice than VH10m.

To better evaluate spatial variation at the commune level, we measured the AAD and CV. Across all communes for each dataset we found rice area did not vary uniformly across space, based on the AAD and CV results (figure 2.7). We found an average CV of 4.75% for each commune. The spatial pattern suggested that much of the variation proportionately occurred in the northern half of the study area (Vinh Phuc, northern Hanoi, and northern Bac Ninh provinces), whereas communes in Hung Yen and Ha Nam had variation between the datasets almost always less than 2.5%. We also note that the communes surrounding Hanoi City had relatively higher CV, but low AAD due to small amount of rice in these areas. We attribute the spatial clustering of variation to land cover and land use differences, and the difficulty of mapping in a small-holder mosaicked landscape. Accordingly, the northern areas dominated by more wetlands, hills, and especially smaller rice fields intermixed with small-holder non-rice crops are likely to have greater class confusion.

**Figure 2.7. Commune-level rice variation.** AAD and CV for double rice area per commune with province boundaries overlaid. Most AAD in communes with high rice mapped areas, while CV shows communes in the north tended to have higher percentage variation attributed to mapping difficulties in mosaicked landscapes.



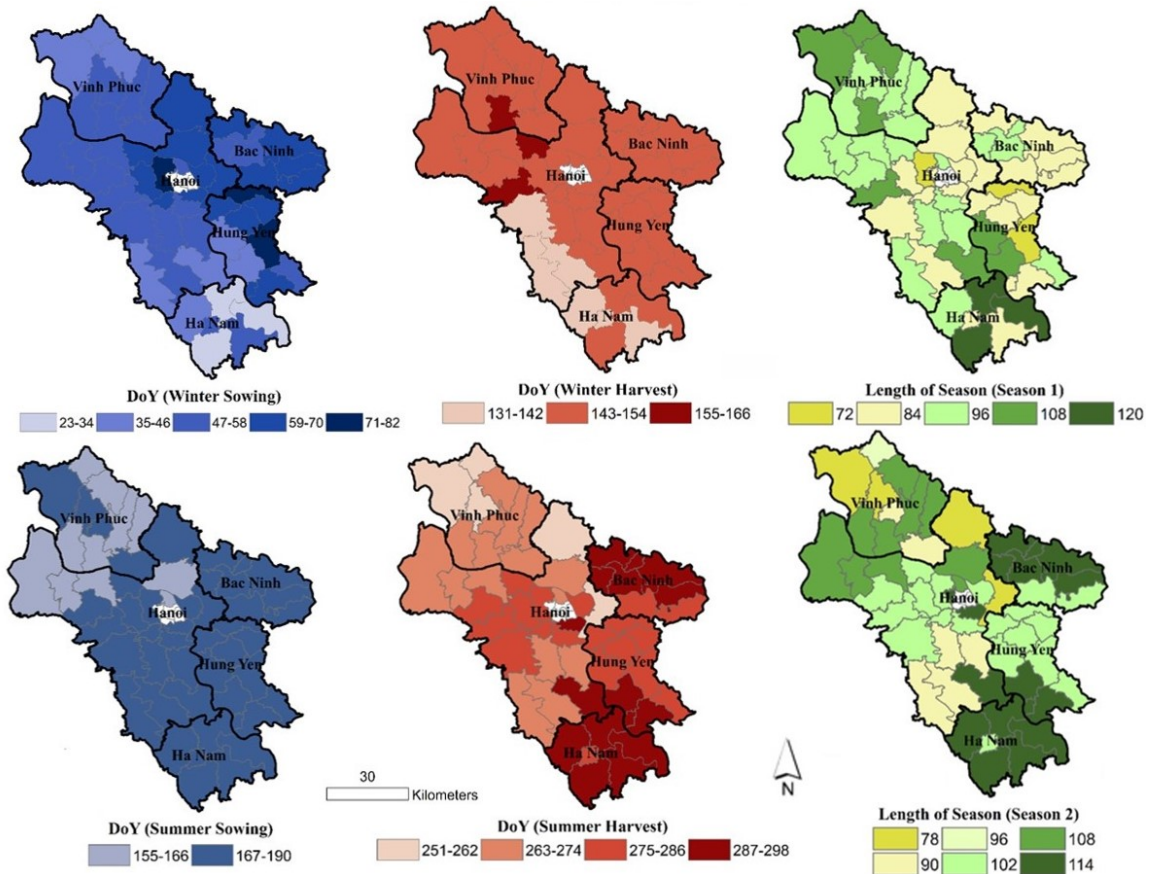
#### 2.4.6 Rice phenology

We estimated the length of growing season, start of season, and end of season for rice based on the SAR time-series and the unique dynamic range in SAR signal found for rice paddies (figure 2.8). The results were aggregated to commune level for comparison.

Across all communes we found an average length of the first rice season to be 93 days, while the second season was approximately 104 days. We attribute the relatively lower range in season 1 due to most fields remaining flooded for several months from the previous season harvest and missing SAR data for ~June 28th. In reality, the first season length is likely slightly underestimated. In addition, these are approximations dependent on the Sentinel-1 overpass dates (+/-11 days). The estimated average sowing date for the 2nd season is Day of Year (DoY) 175 (23rd of June) and DoY 55 (24th of February) for the first season. For the harvest we found an average DoY of 148 (27th of May) for

season 1. Whereas for season 2 we found estimated average harvest of DoY 279 (5th of October). These estimates are generally in line with our local knowledge and field experience. A more precise estimate of length of season, harvest, and sowing could be obtained by including both Sentinel-1A and Sentinel-1B, cutting the overpass time in half.

**Figure 2.8. Commune-level rice phenology.** Sowing and harvest day of year ranges based on Sentinel-1 signal. Minimum variation in summer sowing is due to missing data for 06/28.



#### 2.4.7 Rice landscape metrics

Fragstats analysis using the most accurate VVVH10m map produced a total of 31,934 large continuous tracts/patches of double-rice pixels with an average area of 6.72ha ( $\sigma=59.4$ ha) and large standard deviation. Mean-shift image segmentation combined with

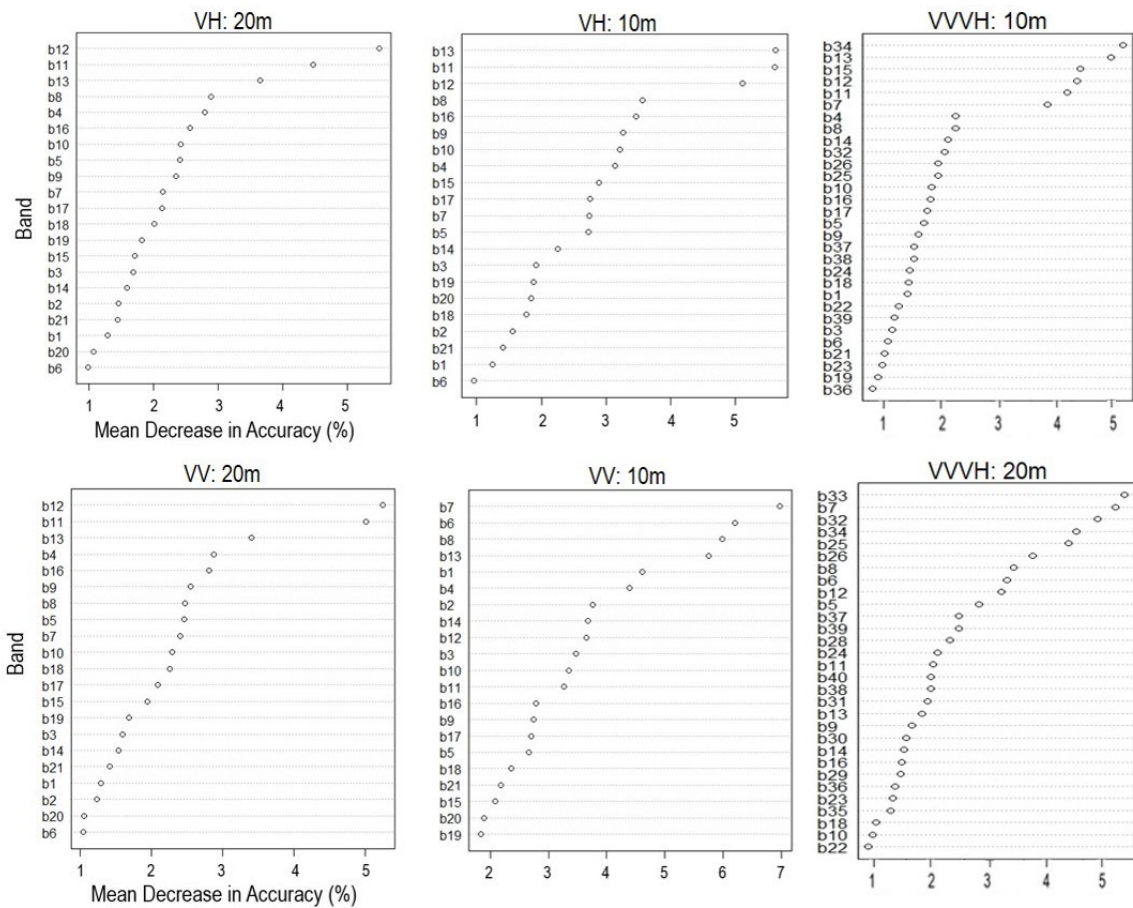
fragstats analysis on the time-series stack masked for double-rice pixels, suggests 796,720 rice collectives (small patches of rice with similar SAR signal) with an average area of 2668m<sup>2</sup> ( $\sigma=7250\text{m}^2$ ). The average field size is reported to be 790m<sup>2</sup> ( $\sigma =625\text{m}^2$ ) (Lasko et al. 2017), thus an average of 3.4 individual rice fields make up a typical rice collective which follow a similar rice phenology pattern including harvest and flooding dates, due to similarity in image segmentation. Based on the aforementioned average field size and total double-rice area from the VVVH10m scenario we estimate 2.69 million double-rice paddy fields within the HCR.

#### *2.4.8 Input band importance*

The feature importance of each input band for the paddy rice classification was assessed in the random forest classifier through mean decrease in accuracy (figure 2.9). We found that the top 3 most important bands for VH(10m and 20m), and VV(20m) were generally the same with bands 11, 12, and 13 (figure 2.9). These three bands were from June and early July (table 2.1) suggesting that imagery from spring harvest and summer planting season are most important as removing one of these bands results in a mean decrease in accuracy of 3-6% depending on the dataset. In addition, these bands are important for discriminating between single and double crop rice. Other bands obtained during planting, growth, and harvest, however, are also important as removing any one of them still reduces overall accuracy significantly. For VV (10m only) we found bands 7, 6, and 8 to be most important. These bands are from the main vegetative growth stage for winter rice (April). A relatively similar trend was observed in VVVH datasets. The average local incidence angle and standard deviation over rice areas suggests minimal variation in incidence angle ( $\mu = 38.63\text{degrees}$ ,  $\sigma = 3.34\text{degrees}$ ). Thus, it is not critical to account for

the incidence angle variation effects on backscatter in the study area (table 2.1) due to minimal variation. In addition, the time-series signal of double rice versus single rice shows it is possible to differentiate between the two with only the first season of data. Double rice areas have relatively higher backscatter throughout the first rice season (figure 2.1).

**Figure 2.9. Mean decrease in accuracy.** MDA (%) suggests bands from all rice growth stages are important, but bands from second season planting and first season harvest generally most important. Note for VVVH, bands 1-22 are VV and bands 23-44 are VH.



## 2.5 Discussion

Early rice mapping studies in Asia employing SAR have had varying degrees of success and accuracy. Some of the earliest studies using RADARSAT or ERS-1 found good

agreement between their rice maps and existing validation data, with the latter study reporting overall accuracy of 87% for a small study area and coarse resolution imagery (Aschbacher et al. 1995; Le Toan et al. 1997; Ribbes 1999). More recent studies employing C-band RADARSAT imagery have reported rice class accuracies as high as 98% and 90% using TerraSAR-X imagery (Choudhury and Chakraborty 2006; Asilo et al. 2014). Studies have also highlighted advantage of multi-date versus single-date imagery for rice mapping (Jiao et al. 2014). However, in Vietnam the case is different. In the Mekong River Delta using multi-temporal SAR including ENVISAT and Sentinel-1, studies have found overall accuracy for land cover or rice maps ranging from 80% - 92% (Lam-Dao et al. 2007; Bouvet et al. 2009; Nguyen et al. 2015; Karila et al. 2014; Chen et al. 2016; Nguyen et al. 2016; Son et al. 2017). In the Red River Delta, using multitemporal SAR such as RADARSAT-2 and ENVISAT, studies have found overall accuracy for rice maps ranging from 71-95% (Hoang et al. 2014; Nguyen et al. 2015; Hoang et al. 2016; Torbick et al. 2017); and overall accuracy of 89% in Vietnam with TerraSAR-X (Nelson et al. 2014).

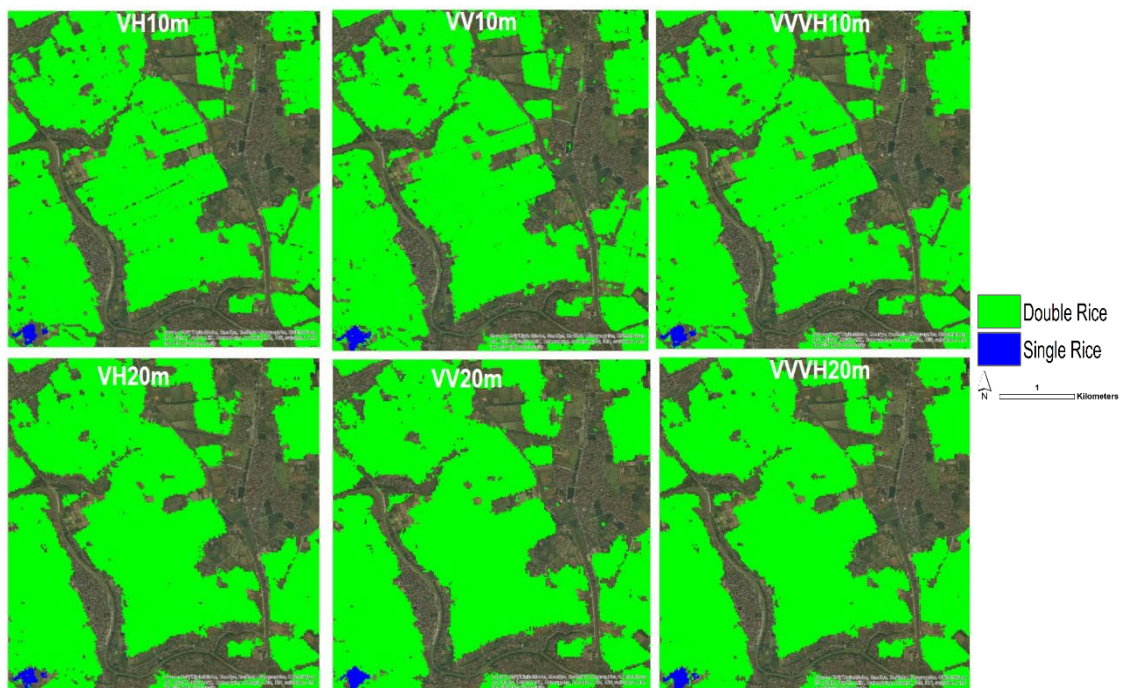
Our accuracy assessment found overall strong user's accuracies for most datasets and classes with double rice ranging from 92.1% - 96.9% and single rice (95.2% - 100%). Whereas, producer's accuracies were generally lower (77.8% - 83.5% double rice, and 35.0% - 59.0% single rice) with overall accuracies between 90.9% - 93.5%.

Our study findings are important in that the different spatial resolution or polarization combinations have significant impacts on mapped rice area. While these differences may not be high at the study area scale, the difference between the datasets is high at the commune and pixel level with CV averaging about 10% at the commune



scale. The most variation was found in communes in the northern half of the study area in Northern Hanoi, Vinh Phuc, and Bac Ninh where small-holder farms in mosaicked landscapes are dominant, making mapping difficult (Nguyen et al. 2015; Pham et al. 2015). These spatial differences are important for different rice mapping applications where spatial location is critical, such as rice straw burning emissions and air quality assessments. We highlight the importance of selecting the most accurate map which in this case is VVVH10m. We also demonstrate through comparison at different spatial scales that 10m data has more variation in rice area compared to 20m data. We find that 20m data may prove effective for land use mapping due to inclusion of a variety of classes such as irrigation canals, and adjacent dirt farm roads, whereas 10m may be best for specific thematic (rice in our case) mapping (figure 2.10). Our study also found that VH polarization were more accurate than VV polarizations for rice mapping. This has

**Figure 2.10. Rice land cover / land use example.** Close-up of each of the six datasets in Hanoi Province highlighting potentially better mapping of land use (20m) vs land cover (10m)



been attributed to VV more influenced by standing water in fields and the signal attenuated by vertical structure of rice (Bouvet et al. 2009; Son et al. 2017). Whereas VH is less affected and more representative of the actual rice growth and plant canopy structure (Nguyen et al. 2016). We also found our map had slightly more rice area than the official government data, and other rice mapping studies have found good agreement between maps and government data in Vietnam (Kontgis et al. 2015; Nguyen et al. 2015).

Using a simple method to replicate metrics on rice phenology, we demonstrate the utility of our phenology estimates for regional and global rice monitoring systems such as Asia-RiCE or GEOGLAM. Additional applications could improve upon existing SAR and MODIS disaster management strategies with improved phenology metrics (Boschetti et al. 2015). This is also demonstrated through random forest feature importance metrics that reducing some input data (i.e. near harvest) can yield slightly less accurate maps as they may not capture the wide backscatter range useful to distinguish paddy rice from other land cover classes. However, these maps are still useful for operational monitoring applications.

Combining our most accurate rice map with image segmentation, Fragstats landscape analysis and field data, we estimated the total number of paddy rice fields in the study area (2.69million). In addition, we found the average size of continuous rice area patches, as well as the estimate of the average size of a rice collective (2668m<sup>2</sup>, or 3.4 rice fields). As mentioned, the rice collectives are continuous rice areas undergoing similar rice phenology (i.e. managed in-sync).

While other classification methods could have been used we chose random forest as it is robust, widely applied, generally has similar results in agricultural applications



(Sonobe et al. 2014), is less of a black box, and computes faster than other algorithms such as support vector machines or artificial neural networks (Belgiu and Dragut 2016). Ensemble-mean classifiers such as random forest also outperform standard approaches such as single decision tree or maximum-likelihood classifier (Waske and Braun 2009). Random forest classifier is also used for reducing feature inputs to reduce data dimensionality, processing time, and redundancy (Loosvelt et al. 2012; Rodriguez-Galliano et al. 2012), whereas for this study we maintained all inputs as we already needed the full time-series of SAR for growing season estimates.

Our study was limited due to several factors. The availability of Sentinel-1A, but not 1B, limits data input to approximately 12-day time intervals. At this temporal frequency, it can be difficult to fully capture distinct crop periods of initial inundation or harvest due to very active field management. Increased availability of Sentinel-1B, however, will enhance phenology monitoring. The rice phenology estimates are limited by the same satellite overpass dates. In general our length of season estimates for season 1 seemed slightly lower than our local knowledge of about 100-115 days due to missing SAR data on June 28th (as some areas harvest around this time). However, it still highlights the utility of SAR for monitoring the length of season without the need to employ a complex algorithm or filtering.

We attribute relatively low single-rice producer's accuracy to the limited availability of training and validation data. This land cover class occupies less than 1% of the landscape and we could only obtain 41 polygons for validation. As such, when we adjusted the producer's accuracy to get unbiased areal estimates, the accuracy decreased significantly. For example, VH10m un-adjusted producer's accuracy for single rice is

97.0% with only 5 pixels out of 166 confused with other classes. However, after calculating the accuracy using unbiased areal estimates, the accuracy decreases to 59%. Whereas for double rice, the changes are less dramatic (i.e. just a few percentage points) due to appropriate sample size.

With further analysis, the results could be useful for land cover versus land use mapping. In addition, based on the SAR signal, it is possible to map single rice and double rice areas with only the first season of data. Results could be useful for aquaculture applications and land use planning. It may also be beneficial to integrate moderate resolution Sentinel-1 SAR imagery with high resolution UAV-obtained imagery for relating to monitoring and improving crop growth parameter estimation (Uto et al. 2013).

## **2.6 Conclusion**

Using a random forest classifier, we compared single and double crop paddy rice mapping using 6 different datasets based on varied polarizations (VV, VH, and both) as well as different spatial resolutions (10m and 20m). Local incidence angles for the complete SAR time-series dataset suggest that imagery can be obtained for the whole year with negligible variation reducing the need to account for angular influence on backscatter. The time-series Sentinel-1 SAR imagery was able to estimate start of season, end of season, and length of season for each rice crop at the commune level with promising results. Rice mapping estimates for the 6 datasets suggested the most accurate dataset to be VVVH10m (93.5% OA), whereas 20m datasets generally had lower overall, user's and producer's accuracies compared to the 10m datasets. Thematic change between the datasets suggested the least spatial variation in classes to be between VH and

VVVH (10m and 20m). The most common difference was between double crop rice and non-rice areas. 20m datasets overestimated rice land area more compared with 10m datasets, as pixels were too large to capture small roads and ditches within paddy fields. The 20m datasets, however, could be well-representative of not only rice land cover, but especially rice land use. Province-level variation in mapped rice areas suggested the most occurring with VV20m, and also more variation in single rice than double rice based on the coefficient of variation. Moderately-high spatial variation was found at the commune-level with the maximum variation in rice area as 20% with VV10m and VH10m. This spatial variation could be critical for spatially-explicit land cover mapping applications. Average absolute deviation and coefficient of variation results suggest communes in the northern portion of the study area and those immediately surrounding Hanoi City have the most proportional variation. This is important as these areas are subject to peri-urban expansion and important for air quality studies as areas closest to the city could have the highest impact on urban air quality.

Overall our study compared six different datasets (VV10m, VV20m, VH10m, VH20m, VVVH10m, and VVVH20m) for mapping paddy rice, evaluated importance of input bands from different dates for classification, estimated rice phenology and calculated rice landscape metrics. The results from our study provide useful insights for crop mapping/monitoring efforts using SAR datasets in general and particularly within the Red River Delta of Vietnam.

## **2.7 Acknowledgement**

This work was supported by the University of Maryland, Council on the Environment Green Fund Fellowship. K. Lasko was partially supported by the Science, Mathematics

and Research for Transformation (SMART) scholarship by the American Society for Engineering Education. The authors thank Thanh Nhat Thi Nguyen and Hung Quang Bui (Vietnam National University Hanoi) for field assistance, and William Salas and Nathan Torbick (Applied Geosolutions, LLC) for SAR expertise. K. Lasko thanks Michael Campbell (Geospatial Research Lab) for support and also thanks his PhD committee members including Christopher Justice, Krishna Vadrevu, Ivan Csiszar, Louis Giglio, and Matthew Hansen for support. Lastly, we thank the European Space Agency for the open data policy and Alaska Satellite Facility for hosting a mirror of the Sentinel-1 data.

## 2.8 References

- Aschbacher, J., Pongsrihadulchai, A., Karnchanasutham, S., Rodprom, C., Paudyal, D.R. and Le Toan, T., 1995. Assessment of ERS-1 SAR data for rice crop mapping and monitoring. In *Geoscience and Remote Sensing Symposium, 1995. IGARSS'95. 'Quantitative Remote Sensing for Science and Applications', International* Vol. 3, 2183-2185.
- Asilo, S., de Bie, K., Skidmore, A., Nelson, A., Barbieri, M. and Maunahan, A., 2014. Complementarity of two rice mapping approaches: Characterizing strata mapped by hypertemporal MODIS and rice paddy identification using multitemporal SAR. *Rem. Sens.*, 6(12), 12789-12814.
- Belgiu, M. and Drăguț, L., 2016. Random forest in remote sensing: A review of applications and future directions. *ISPRS J. Photogramm. Remote Sens.*, 114, pp.24-31.
- Boschetti, M., Nelson, A., Nutini, F., Manfron, G., Busetto, L., Barbieri, M., Laborte, A., Raviz, J., Holecz, F., Mabalay, M.R.O. and Bacong, A.P., 2015. Rapid assessment of crop status: An application of MODIS and SAR data to rice areas in Leyte, Philippines affected by Typhoon Haiyan. *Remote Sensing*, 7(6), pp.6535-6557.
- Bouvet, A., Le Toan, T. and Lam-Dao, N., 2009. Monitoring of the rice cropping system in the Mekong Delta using ENVISAT/ASAR dual polarization data. *IEEE Trans. on Geosci. Rem. Sens.*, 47(2), 517-526.
- Breiman, L., 2001. Random forests. *Machine learning*, 45(1), pp.5-32.
- Chakraborty, M., Panigrahy, E.S. and Sharma, S.A., 1997. Discrimination of rice crop grown under different cultural practices using temporal ERS-1 synthetic aperture radar data. *ISPRS J. Photogramm. Remote Sens.*, 52(4), 183-191.

- Chen, C. and McNairn, H., 2006. A neural network integrated approach for rice crop monitoring. *Int. J. Rem. Sens.*, 27(7), pp.1367-1393.
- Chen, C.F., Son, N.T., Chen, C.R., Chang, L.Y. and Chiang, S.H., 2016. Rice crop mapping using Sentinel-1A phenological metrics. *ISPRS-International Archives of the Photogrammetry, Remote Sensing and Spatial Information Sciences*, 41, p.B8
- Choudhury, I. and Chakraborty, M., 2006. SAR signature investigation of rice crop using RADARSAT data. *Int. J. Rem. Sens.*, 27(3), pp.519-534.
- Comaniciu, D. and Meer, P., 2002. Mean shift: A robust approach toward feature space analysis. *IEEE Transactions on pattern analysis and machine intelligence*, 24(5), pp.603-619.
- Congalton, R.G. and Green, K., 2008. *Assessing the accuracy of remotely sensed data: principles and practices*. CRC press.
- de Bernardis, C.G., Vicente-Guijalba, F., Martinez-Marin, T. and Lopez-Sanchez, J.M., 2015. Estimation of key dates and stages in rice crops using dual-polarization SAR time series and a particle filtering approach. *IEEE J-STARS*, 8(3), pp.1008-1018.
- Dey M.M. and Ahmed, M., 2005. Aquaculture—food and livelihoods for the poor in Asia: a brief overview of the issues. *Aquaculture Economics & Management*, 9(1-2), pp.1-10.
- Duong, P.T. and Yoshiro, H., 2015. Current Situation and Possibilities of Rice Straw Management in Vietnam. Accessed from: [http://www.jsrsai.jp/Annual\\_Meeting/PROG\\_52/ResumeC/C02-4.pdf](http://www.jsrsai.jp/Annual_Meeting/PROG_52/ResumeC/C02-4.pdf).
- Erten, E., Rossi, C. and Yüzügüllü, O., 2015. Polarization impact in TanDEM-X data over vertical-oriented vegetation: The paddy-rice case study. *IEEE Geosci. Rem. Sens. Lett.*, 12(7), 1501-1505.
- Erten, E., Rossi, C., Yüzügüllü, O. and Hajnsek, I., 2014, July. Phenological growth stages of paddy rice according to the BBCH scale and SAR images. In *Geosci. and Rem. Sens. Symp. (IGARSS), 2014 IEEE International* (pp. 1017-1020).
- Fukunaga, K. and Hostetler, L., 1975. The estimation of the gradient of a density function, with applications in pattern recognition. *IEEE Transactions on information theory*, 21(1), pp.32-40.
- Gebhardt, S., Huth, J., Nguyen, L.D., Roth, A. and Kuenzer, C., 2012. A comparison of TerraSAR-X Quadpol backscattering with RapidEye multispectral vegetation indices over rice fields in the Mekong Delta, Vietnam. *Int. j. rem. sens.*, 33(24), pp.7644-7661.
- General Statistics Office of Vietnam, 2016. Agriculture, Forestry, and Trade. Accessed from: [http://www.gso.gov.vn/Default\\_en.aspx?tabid=491](http://www.gso.gov.vn/Default_en.aspx?tabid=491).

- Hoang, H.K., Bernier, M., Duchesne, S. and Tran, Y.M., 2016. Rice Mapping Using RADARSAT-2 Dual-and Quad-Pol Data in a Complex Land-Use Watershed: Cau River Basin (Vietnam). *IEEE J-STARs*, 9(7), 3082-3096.
- Hoang, K.H., Bernier, M., Duchesne, S. and Tran, M.Y., 2014, July. Classification of rice fields in a complex land-use watershed in Northern Vietnam using RADARSAT-2 data. In *Geoscience and Remote Sensing Symposium (IGARSS), 2014 IEEE International* pp. 1501-1503.
- Inoue, Y., Kurosaki, T., Maeno, H., Uratsuka, S., Kozu, T., Dabrowska-Zielinska, K. and Qi, J., 2002. Season-long daily measurements of multifrequency (Ka, Ku, X, C, and L) and full-polarization backscatter signatures over paddy rice field and their relationship with biological variables. *Rem. Sens. of Enviro.*, 81(2), 194-204.
- Inoue, Y., Sakaiya, E. and Wang, C., 2014. Capability of C-band backscattering coefficients from high-resolution satellite SAR sensors to assess biophysical variables in paddy rice. *Rem. Sens. Enviro.*, 140, pp.257-266.
- Jia, K., Li, Q., Tian, Y., Wu, B., Zhang, F. and Meng, J., 2012. Crop classification using multi-configuration SAR data in the North China Plain. *Int.l J. Rem. Sens.*, 33(1), pp.170-183.
- Jiao, X., Kovacs, J.M., Shang, J., McNairn, H., Walters, D., Ma, B. and Geng, X., 2014. Object-oriented crop mapping and monitoring using multi-temporal polarimetric RADARSAT-2 data. *ISPRS J. Photogram. Rem. Sens.*, 96, pp.38-46.
- Jiao, X., Kovacs, J.M., Shang, J., McNairn, H., Walters, D., Ma, B. and Geng, X., 2014. Object-oriented crop mapping and monitoring using multi-temporal polarimetric RADARSAT-2 data. *ISPRS J. Photogram. Rem. Sens.*, 96, pp.38-46.
- Karila, K., Nevalainen, O., Krooks, A., Karjalainen, M. and Kaasalainen, S., 2014. Monitoring changes in rice cultivated area from SAR and optical satellite images in Ben Tre and Tra Vinh Provinces in Mekong Delta, Vietnam. *Rem. Sens.*, 6(5), pp.4090-4108.
- Kontgis, C., Schneider, A. and Ozdogan, M., 2015. Mapping rice paddy extent and intensification in the Vietnamese Mekong River Delta with dense time stacks of Landsat data. *Rem. Sens. Enviro.*, 169, 255-269.
- Koppe, W., Gnyp, M.L., Hütt, C., Yao, Y., Miao, Y., Chen, X. and Bareth, G., 2013. Rice monitoring with multi-temporal and dual-polarimetric TerraSAR-X data. *Int. J. Appl. Earth Obs. Geoinfo.*, 21, pp.568-576.
- Küçük, Ç., Taşkın, G. and Erten, E., 2016. Paddy-rice phenology classification based on machine-learning methods using multitemporal co-polar X-band SAR images. *IEEE J-STARs*, 9(6), pp.2509-2519.
- Lam-Do, N., Apan, A., Young, F.R., Le-Van, T., Le-Toan, T. and Bouvet, A., 2007, November. Rice monitoring using ENVISAT-ASAR data: preliminary results of a case

study in the Mekong River Delta, Vietnam. In *Proceedings of the 28th Asian Conference on Remote Sensing (ACRS 2007)*. Geoinformatics Center (Klong Luang).

Lasko, K., Vadrevu, K., Tran, V., Ellicott, E., Nguyen, T., Bui, H. and Justice, C., 2017. Satellites may underestimate rice residue and associated burning emissions in Vietnam. *Enviro. Res. Lett.*, 12(8), 085006.

Le Toan, T., Ribbes, F., Wang, L.F., Floury, N., Ding, K.H., Kong, J.A., Fujita, M. and Kurosu, T., 1997. Rice crop mapping and monitoring using ERS-1 data based on experiment and modeling results. *IEEE Transactions on Geoscience and Remote Sensing*, 35(1), 41-56.

Lee, K. S., and S. I. Lee. "Assessment of post-flooding conditions of rice fields with multi-temporal satellite SAR data." *Int. j. Rem. sens.* 24, no. 17 (2003): 3457-3465.

Liew, S.C., Kam, S.P., Tuong, T.P., Chen, P., Minh, V.Q. and Lim, H., 1998. Application of multitemporal ERS-2 synthetic aperture radar in delineating rice cropping systems in the Mekong River Delta, Vietnam. *IEEE Trans. Geosci. Rem. Sens.*, 36(5), 1412-1420.

Loosvelt, L., Peters, J., Skriver, H., De Baets, B. and Verhoest, N.E., 2012. Impact of reducing polarimetric SAR input on the uncertainty of crop classifications based on the random forests algorithm. *IEEE Transactions on Geoscience and Remote Sensing*, 50(10), pp.4185-4200.

Lopez-Sanchez, J.M., Cloude, S.R. and Ballester-Berman, J.D., 2012. Rice phenology monitoring by means of SAR polarimetry at X-band. *IEEE Trans. Geosci. Rem. Sens.*, 50(7), 2695-2709.

Lopez-Sanchez, J.M., Vicente-Guijalba, F., Ballester-Berman, J.D. and Cloude, S.R., 2014. Polarimetric response of rice fields at C-band: Analysis and phenology retrieval. *IEEE Trans. Geosci. Rem. Sens.*, 52(5), pp.2977-2993.

Mansaray, L.R., Zhang, D., Zhou, Z. and Huang, J., 2017. Evaluating the potential of temporal Sentinel-1A data for paddy rice discrimination at local scales. *Rem. Sens. Lett.*, 8(10), pp.967-976.

Nelson, A., Setiyono, T., Rala, A.B., Quicho, E.D., Raviz, J.V., Abonete, P.J., Maunahan, A.A., Garcia, C.A., Bhatti, H.Z.M., Villano, L.S. and Thongbai, P., 2014. Towards an operational SAR-based rice monitoring system in Asia: Examples from 13 demonstration sites across Asia in the RIICE project. *Rem. Sens.*, 6(11), pp.10773-10812.

Nguyen, D., Wagner, W., Naeimi, V. and Cao, S., 2015. Rice-planted area extraction by time series analysis of ENVISAT ASAR WS data using a phenology-based classification approach: A case study for Red River Delta, Vietnam. *The International Archives of Photogrammetry, Remote Sensing and Spatial Information Sciences*, 40(7), p.77.

- Nguyen, D.B., Clauss, K., Cao, S., Naeimi, V., Kuenzer, C. and Wagner, W., 2015. Mapping rice seasonality in the Mekong Delta with multi-year Envisat ASAR WSM data. *Rem. Sens.*, 7(12), pp.15868-15893.
- Nguyen, D.B., Gruber, A. and Wagner, W., 2016. Mapping rice extent and cropping scheme in the Mekong Delta using Sentinel-1A data. *Rem. Sens. Lett.*, 7(12), pp.1209-1218.
- Olofsson, P., Foody, G.M., Herold, M., Stehman, S.V., Woodcock, C.E. and Wulder, M.A., 2014. Good practices for estimating area and assessing accuracy of land change. *Rem. Sens. Environ.*, 148, 42-57
- Ottinger, M., Clauss, K. and Kuenzer, C., 2017. Large-Scale Assessment of Coastal Aquaculture Ponds with Sentinel-1 Time Series Data. *Rem. Sens.*, 9(5), p.440.
- Oyoshi, K., Tomiyama, N., Okumura, T., Sobue, S. and Sato, J., 2016. Mapping rice-planted areas using time-series synthetic aperture radar data for the Asia-RiCE activity. *Paddy and Water Environment*, 14(4), pp.463-472.
- Panigrahy, S., Manjunath, K.R., Chakraborty, M., Kundu, N. and Parihar, J.S., 1999. Evaluation of RADARSAT standard beam data for identification of potato and rice crops in India. *ISPRS J. Photogramm. Remote Sens.*, 54(4), 254-262.
- Paudyal, D.R. and Aschbacher, J., 1993. Land-cover separability studies of filtered ERS-1 SAR images in the tropics. In *Geoscience and Remote Sensing Symposium, IGARSS'93. Better Understanding of Earth Environment., International* 1216-1218.
- Pei, Z., Zhang, S., Guo, L., McNairn, H., Shang, J. and Jiao, X., 2011. Rice identification and change detection using TerraSAR-X data. *Canadian J. Rem. Sens.*, 37(1), 151-156.
- Pham, V.C., Pham, T.T.H., Tong, T.H.A., Nguyen, T.T.H. and Pham, N.H., 2015. The conversion of agricultural land in the peri-urban areas of Hanoi (Vietnam): patterns in space and time. *J. Land Use Sci.*, 10(2), pp.224-242.
- Ribbes, F., 1999. Rice field mapping and monitoring with RADARSAT data. *Int. J. Rem. Sens.*, 20(4), 745-765.
- Rodriguez-Galiano, V.F., Chica-Olmo, M., Abarca-Hernandez, F., Atkinson, P.M. and Jeganathan, C., 2012. Random Forest classification of Mediterranean land cover using multi-seasonal imagery and multi-seasonal texture. *Rem. Sens. Environ.*, 121, pp.93-107.
- Salas, W., Boles, S., Li, C., Yeluripati, J.B., Xiao, X., Frohling, S. and Green, P., 2007. Mapping and modelling of greenhouse gas emissions from rice paddies with satellite radar observations and the DNDC biogeochemical model. *Aquatic conservation: Marine and freshwater ecosystems*, 17(3), 319-329.
- Senthilnath, J., Omkar, S.N., Mani, V., Tejovanth, N., Diwakar, P.G. and Shenoy, A.B., 2012. Hierarchical clustering algorithm for land cover mapping using satellite images. *IEEE J-STARS*, 5(3), pp.762-768.



- Shao, Y., Fan, X., Liu, H., Xiao, J., Ross, S., Brisco, B., Brown, R. and Staples, G., 2001. Rice monitoring and production estimation using multitemporal RADARSAT. *Rem. Sens. Environ.*, 76(3), 310-325.
- Shiraishi, T., Motohka, T., Thapa, R.B., Watanabe, M. and Shimada, M., 2014. Comparative assessment of supervised classifiers for land use–land cover classification in a tropical region using time-series palsar mosaic data. *IEEE J-STARS*, 7(4), pp.1186-1199.
- Son, N.T., Chen, C.F., Chen, C.R. and Minh, V.Q., 2017. Assessment of Sentinel-1A data for rice crop classification using random forests and support vector machines. *Geocarto Int.*, pp.1-15.
- Sonobe, R., Tani, H., Wang, X., Kobayashi, N. and Shimamura, H., 2014. Random forest classification of crop type using multi-temporal TerraSAR-X dual-polarimetric data. *Rem. Sens. Lett.*, 5(2), 157-164.
- Steele-Dunne, S.C., McNairn, H., Monsivais-Huertero, A., Judge, J., Liu, P.W. and Papathanassiou, K., 2017. Radar remote sensing of agricultural canopies: A review. *IEEE J-STARS*, 10(5), pp.2249-2273.
- Su, T. and Zhang, S., 2017. Local and global evaluation for remote sensing image segmentation. *ISPRS Journal of Photogrammetry and Remote Sensing*, 130, pp.256-276.
- Suga, Y., Takeuchi, S., Oguro, Y. and Konishi, T., 2000. Monitoring of rice-planted areas using space-borne SAR data. *Int. Arch. of PHOTOGAM. and Rem. Sens.*, 33(B7/4; PART 7), pp.1480-1483.
- Takeuchi, S. and Suwanwerakamton, R., 1996. Monitoring of Land Cover Conditions in Paddy Fields Using Multitemporal SAR Data. *Int. Archives of Photogramm. And Rem. Sens.*, 31, 683-688.
- Torbick, N., Chowdhury, D., Salas, W. and Qi, J., 2017. Monitoring Rice Agriculture across Myanmar Using Time Series Sentinel-1 Assisted by Landsat-8 and PALSAR-2. *Rem. Sens.*, 9(2), p.119.
- Torbick, N., Salas, W., Chowdhury, D., Ingraham, P. and Trinh, M., 2017. Mapping rice greenhouse gas emissions in the Red River Delta, Vietnam. *Carbon Management*, 8(1), pp.99-108.
- Uhlmann, S. and Kiranyaz, S., 2014. Integrating color features in polarimetric SAR image classification. *IEEE Transactions on Geoscience and Remote Sensing*, 52(4), pp.2197-2216.
- Uto, K., Seki, H., Saito, G. and Kosugi, Y., 2013. Characterization of rice paddies by a UAV-mounted miniature hyperspectral sensor system. *IEEE J-STARS*, 6(2), pp.851-860.

- Wang, W., Yang, X., Li, X., Chen, K., Liu, G., Li, Z. and Gade, M., 2017. A Fully Polarimetric SAR Imagery Classification Scheme for Mud and Sand Flats in Intertidal Zones. *IEEE Trans. Geosci. Rem. Sens.*, 55(3), pp.1734-1742.
- Waske, B. and Braun, M., 2009. Classifier ensembles for land cover mapping using multitemporal SAR imagery. *ISPRS Journal of Photogrammetry and Remote Sensing*, 64(5), pp.450-457.
- Whitcomb, J., Moghaddam, M., McDonald, K., Kellndorfer, J. and Podest, E., 2009. Mapping vegetated wetlands of Alaska using L-band radar satellite imagery. *Canadian J. of Rem. Sens.*, 35(1), 54-72.
- Whitcraft, A.K., Becker-Reshef, I. and Justice, C.O., 2015. A framework for defining spatially explicit earth observation requirements for a global agricultural monitoring initiative (GEOGLAM). *Remote Sensing*, 7(2), pp.1461-1481.
- Whitcraft, A.K., Vermote, E.F., Becker-Reshef, I. and Justice, C.O., 2015. Cloud cover throughout the agricultural growing season: Impacts on passive optical earth observations. *Rem. Sens. Enviro.*, 156, 438-447.
- White, L., Brisco, B., Dabboor, M., Schmitt, A. and Pratt, A., 2015. A collection of SAR methodologies for monitoring wetlands. *Rem. sens.*, 7(6), pp.7615-7645.
- Xiao, X., Boles, S., Liu, J., Zhuang, D., Frohling, S., Li, C., Salas, W. and Moore, B., 2005. Mapping paddy rice agriculture in southern China using multi-temporal MODIS images. *Rem. Sens. Enviro.*, 95(4), pp.480-492.
- Xie, L., Zhang, H., Wu, F., Wang, C. and Zhang, B., 2015. Capability of rice mapping using hybrid polarimetric SAR data. *IEEEJ-STARs*, 8(8), pp.3812-3822.
- Yun, S., Cuizhen, W., Xiangtao, F. and Hao, L., 1997, August. Estimation of rice growth status using RADARSAT data. In *Geoscience and Remote Sensing, 1997. IGARSS'97. Remote Sensing-A Scientific Vision for Sustainable Development., 1997 IEEE International* (Vol. 3, 1430-1432). IEEE.
- Yuzugullu, O., Erten, E. and Hajnsek, I., 2015. Rice growth monitoring by means of X-band co-polar SAR: Feature clustering and BBCH scale. *IEEE Geosci. Rem. Sens. Lett.*, 12(6), 1218-1222.
- Zhang, H., Li, Q., Liu, J., Du, X., Dong, T., McNairn, H., Champagne, C., Shang, J. and Liu, M., 2017. Object-based crop classification using multi-temporal SPOT-5 imagery and textural features with a Random Forest classifier. *Geocarto International*, pp.1-40.
- Zhang, Y., Wang, C., Wu, J., Qi, J. and Salas, W.A., 2009. Mapping paddy rice with multitemporal ALOS/PALSAR imagery in southeast China. *Int. J. Rem. sens.*, 30(23), 6301-6315.

Zuhlke, M., Fomferra, N., Brockmann, C., Peters, M., Veci, L., Malik, J. and Regner, P., 2015, December. SNAP (Sentinel Application Platform) and the ESA Sentinel 3 Toolbox. In *Sentinel-3 for Science Workshop* (Vol. 734, p. 21).

## Chapter 3: Satellite data may underestimate rice residue and associated burning emissions in Vietnam<sup>2</sup>

### 3.1 Abstract

In this study, we estimate rice residue, associated burning emissions, and compare results with existing emissions inventories employing a bottom-up approach. We first estimated field-level post-harvest rice residues, including separate fuel-loading factors for rice straw and rice stubble. Results suggested fuel-loading factors of 0.27 kg/m<sup>2</sup> ( $\pm 0.033$ ), 0.61 kg/m<sup>2</sup> ( $\pm 0.076$ ), and 0.88 kg/m<sup>2</sup> ( $\pm 0.083$ ) for rice straw, stubble, and total post-harvest biomass, respectively. Using these factors, we quantified potential emissions from rice residue burning and compared our estimates with other studies. Our results suggest total rice residue burning emissions as 2.24Gg PM<sub>2.5</sub>, 36.54Gg CO and 567.79Gg CO<sub>2</sub> for Hanoi Province, which are significantly higher than earlier studies. We attribute our higher emission estimates to improved fuel-loading factors; moreover, we infer that some earlier studies relying on residue-to-product ratios could be underestimating rice residue emissions by more than a factor of 2.3 for Hanoi, Vietnam. Using the rice planted area data from the Vietnam government, and combining our fuel-loading factors, we also estimated rice residue PM<sub>2.5</sub> emissions for the entire Vietnam and compared these estimates with an existing all-sources emissions inventory, and the Global Fire Emissions Database (GFED). Results suggest 75.98Gg of PM<sub>2.5</sub> released from rice residue burning accounting for 12.8% of total emissions for Vietnam. GFED database suggests 42.56Gg PM<sub>2.5</sub> from biomass burning with 5.62Gg attributed to agricultural waste burning

---

<sup>2</sup> The presented material has been previously published in Lasko K, Vadrevu K P, Tran VT, Ellicott E, Nguyen T T N, Bui H Q, and Justice C 2017. Satellites may underestimate rice residue and associated burning emissions in Vietnam. *Environmental Research Letters* 12(8), 085006.

indicating satellite-based methods may be significantly underestimating emissions. Our results not only provide improved residue and emission estimates, but also highlight the need for emissions mitigation from rice residue burning.

### **3.2 Introduction**

Crop residue burning is an important source of greenhouse gases and aerosols (Streets *et al* 2003; Crutzen and Andreae 1990). The burning of crop residues contributes to at least 34% of global biomass burning emissions (Streets *et al* 2004). While these and other studies provide useful general estimates, analyses need to be region-specific to enable emissions mitigation. Of the different crop residues, rice residues are prevalently burned in South/Southeast Asian countries in addition to forest biomass burning (Streets *et al* 2003; Biswas *et al* 2015).

Rice (*Oryza sativa*) is the staple crop for livelihood in Southeast Asia and more specifically, Vietnam. During 2015, Vietnam produced 45.2 million metric tons of rice with most production in the Mekong River Delta (57%) and the Red River Delta (15%) (Vietnam Govt. Stats 2015). The Red River Delta is home to Hanoi, the capital of Vietnam which outside of the immediate downtown area, exhibits a mosaic landscape dominated by paddy rice, small-holder farms, and plantations, all intermixed amongst a growing peri-urban area (Pham *et al* 2015). Thus, in Hanoi, many residential and commercial areas are not only impacted by urban emissions, but also by smoke from rice residue burning. Studies have attributed crop residue burning to local and regional impacts including long-range transport with effects persisting for weeks or months impacting air quality, atmospheric chemistry, weather, and biogeochemical cycles (Badarinath *et al* 2007; 2009; Vadrevu *et al* 2012; 2014; 2015; Cristofanelli *et al* 2014;

Reddington *et al* 2014; Ponette-Gonzalez *et al* 2016; Yan *et al* 2006; Le *et al.*, 2014). For Hanoi in particular, nocturnal radiation inversions occur during the October rice harvest and burning, greatly enhancing the negative air quality impact of fine-particulate matter emissions (Hien *et al* 2002).

Around Hanoi, the typical paddy rice field size ranges from 150-2,280m<sup>2</sup> (Patanothai 1996) with an average of 790m<sup>2</sup> ( $\sigma = 625\text{m}^2$ ) (this study). Hanoi is located within the heart of the Red River Delta which is Vietnam's 2<sup>nd</sup> largest rice producing hub with over 35% of the land dedicated to rice (Vietnam govt. stats 2015). Rice is routinely irrigated and double-cropped in Hanoi Province with winter rice harvested during June and spring rice harvested during late-September–October. After harvest, a large volume of rice straw is left in rows or piles on the field as well as stubble (figure 3.1). In order to prepare the field for the next harvest, farmers routinely burn the residues. Typical burning of a rice straw pile and post-burned field in Hanoi are shown (figure 3.2). Mostly, the straw is burned or reincorporated into the soil while some is used for cattle feed, cook stoves, composting, and mushroom cultivation (Trach 1998; Hong Van *et al* 2014; Duong and Yoshiro 2015; Nguyen 2012; Oritate *et al* 2015). In comparison to the rural areas, suburban areas such as Hanoi typically burn a higher proportion of rice straw as these areas have less cattle relying on it for food (Duong and Yoshiro 2015). Thus, with a higher proportion of residue burned in Hanoi, there is amplified impact from emissions. Further, post-harvest rice straw is assumed to have moisture content of about 15% or less, however this varies depending on conditions, and residue structure/density can also have an impact on resulting emissions (Korenaga *et al* 2001; Arai *et al* 2015). In order to

estimate emissions impact, accurate bottom-up quantification of residue production and burning is needed.

**Figure 3.1. a) Typical machine-harvested field in Hanoi province with dry straw laid in neat rows; b) typical rice straw pile prior to burning.**

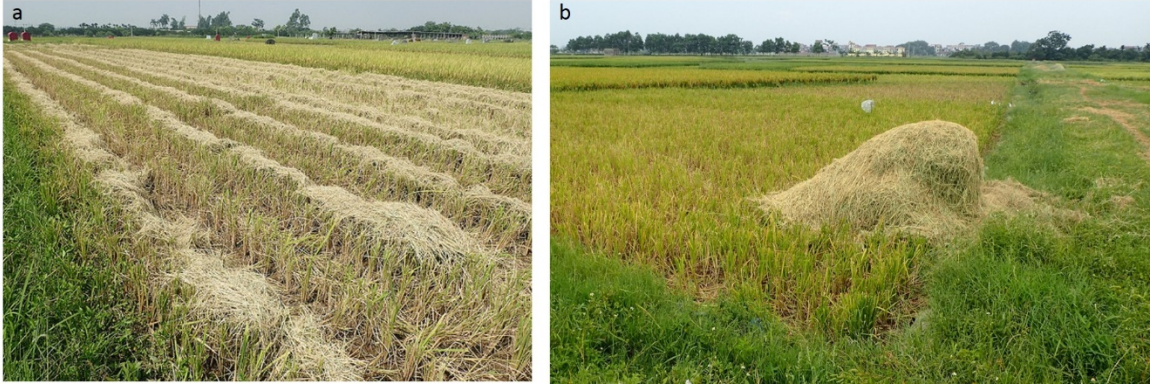
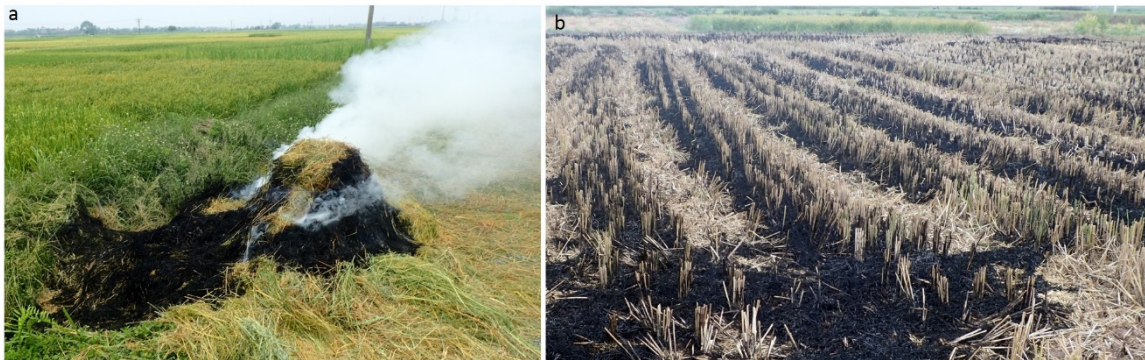


**Figure 3.2. a) Rice straw pile burning; b) Post-burned rice field with most straw burned efficiently, however much stubble is left unburned.**



Earlier studies on estimating emissions from crop residue burning have used agricultural production data, a crop specific residue-to-product ratio, an estimate of the proportion of residue subject to burning, emission factors, and a combustion factor (Streets *et al* 2003; Yevich and Logan 2003; Yan *et al* 2006; Cao *et al* 2008; Gadde *et al* 2009; Kanabkaew and Oanh 2011; Vadrevu and Lasko 2015; Zhang *et al* 2015). While these studies yield insight on emissions estimation, they can be improved by incorporating field-based locally/regionally estimated fuel-loads or emissions factors

established from field measurements (Oanh *et al* 2011; Kanokkanjana *et al* 2011; Rajput *et al* 2014; Hong Van *et al* 2014; Arai *et al* 2015). We note that comprehensive province-level field-estimates of rice straw and rice stubble have yet to be generated for Northern Vietnam.

Field studies estimating rice straw, stubble, and total post-harvest biomass production are labor intensive and costly. Accordingly, remote sensing with its synoptic and consistent coverage can be used for estimating these factors. In Southeast Asia and Vietnam, forecasting of rice yield or biomass has been done using X-band Synthetic Aperture Radar (SAR) (Bouvet *et al* 2014), C-band SAR (Ribbes and Le Toan 1999; Chakraborty *et al* 2005; Lam-Dao *et al* 2009; Inoue *et al* 2014;), and L-band SAR (Torbick *et al* 2011). Further details on these and related mapping applications are available in recent reviews (Mosleh *et al* 2015; Dong and Xiao 2016). Developing a relationship between field-estimated rice biomass and SAR signal is useful for upscaling field studies to broader regions and time periods. Thus, it contributes to systematic and operational monitoring of rice residue production useful for not only estimating emissions from burning, but also emissions mitigation such as bioenergy generation.

In this study, we develop and assess a simple method for efficient and accurate field estimation of rice residue fuel-loading factors for straw, stubble, and total post-harvest biomass. We use these as inputs to calculate resulting potential residue burning emissions for Hanoi, Vietnam and compare results using fuel-loading factors from other studies. Using our fuel-loading factors and those from other studies we upscale our results to the entire Vietnam and compare with an existing emissions inventory to assess rice residue burning contribution to total emissions from all sources. We also compare



our emission estimates with the satellite-derived estimates from the Global Fire Emissions Database (GFED). We then explore the potential forecasting of rice residue using field and SAR data.

We specifically address the following questions: 1) How much rice straw, stubble, and total post-harvest biomass is left in the field, and how does this compare to other regional studies? 2) What are the resulting rice residue burning emissions for major pollutants (PM<sub>2.5</sub>, CO, and CO<sub>2</sub>) in Hanoi Province? 3) What are the resulting rice residue burning emissions for the entire Vietnam and how do they compare to the existing emissions inventories from different sources? 4) How well does SAR data enable forecasting of post-harvest biomass? We addressed these questions using a field and remote sensing based approach representative of typical double-cropped rice region in Hanoi Province, Vietnam.

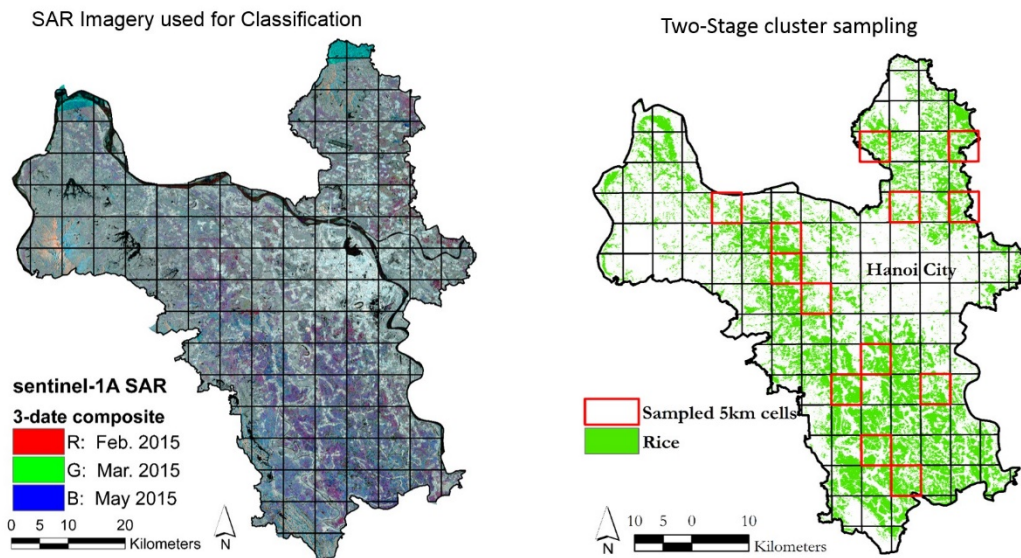
### **3.3. Datasets and methods**

#### *3.3.1 SAR data*

Sentinel-1 carries a 12m long C-Band SAR yielding a unique ability to penetrate most cloud coverage. Sentinel-1 is a constellation of 2 satellites including Sentinel-1A with data since October 2014 and Sentinel-1B launched in spring of 2016. The constellation has a repeat-pass of approximately 6 days for most of the world. From the Alaska Satellite Facility, we obtained a single ground-range detected, interferometric wide-swath (IW), dual-polarized image from Sentinel-1A just prior to harvest for Hanoi Province on September 21, 2016. We processed the imagery following detailed guidelines from European Space Agency using the freely-available S1 toolbox (Zuhlke *et al* 2015) including thermal noise reduction, multi-looking azimuthal compressions to 20m spatial

resolution to reduce noise, terrain correction using the SRTM 30m DEM, speckle filter, and radiometric adjustments to correct for viewing geometry effects (Liang 2005; Torbick *et al* 2011). We first generated a rice map from a full time-series of Sentinel-1A time-series imagery for 2016 using a support vector machine classification method (figure 3.3) and validated it using field data and fine-resolution imagery from Google Earth and field photos; the resulting map had an overall accuracy of 94.3% and approximately 220,000 ha of rice land area (Lasko *et al* 2018). The resulting rice map built upon results from related studies (Torbick *et al* 2017; Nguyen D *et al* 2015) and was used to delineate rice from non-rice for field sampling (figure 3.3).

**Figure 3.3. a) multitemporal SAR composite; b) our classified rice map used to delineate rice areas for field sampling**



The field data for generating the fuel-loading factors were collected from Hanoi Province and include georeferenced photos of rice and non-rice areas used in our rice area mapping classification training or accuracy assessment (Lasko *et al* 2017). For relating our field-level fuel-loading data to SAR, we used the Sentinel-1 VH-polarized

image obtained approximately 1-2 weeks prior to harvest (Sept. 18, 2016). The field data collection is described in the subsequent section.

### 3.3.2 Rice residue and emissions estimation

We developed a field-based approach to estimate total post-harvest rice residues including straw and stubble left in the field for burning. Using a two-stage cluster sampling and the validated rice map generated from Sentinel-1A time-series imagery (figure 3.3) we divided the study area into 5km equal-area grid cells and randomly selected 13 rice-containing cells where 4 randomly selected machine-harvested fields were sampled in each cell for a total of 52 field samples (C.I. = 9.6%, C.L. = 95%) (Sutherland 2006) (figure 3.3). Within each harvested field, we measured the total straw and stubble weight in four randomly selected 0.5m x 0.5m quadrats using a Salter-Brecknell digital scale, bag with known weight, and an Extech MO290 moisture device for relative moisture content. Stubble was cut at the base before weighing, and the weight of the bag was subtracted from the measurements. We also collected ancillary data including field length, width, and number of straw rows. We estimated the amount of straw per square meter for a given field based on the following (equation 3.1):

$$Q_{rs} = \frac{(RS_w \times (1 - RS_m)) \times SR \times R_l}{A}$$

Where  $Q_{rs}$  is the quantity of dry rice straw in kg/m<sup>2</sup> for a given field,  $RS_w$  is the wet rice straw weight per linear meter of a straw row averaged from the quadrat measurements,  $RS_m$  is the average field-measured relative moisture content,  $SR$  is the

number of straw rows in the field,  $R_l$  is the length of the straw rows in meters, and  $A$  is the field area in  $m^2$ .

We estimated the amount of rice stubble for a given field based on a similar (equation 3.2):

$$Q_{sr} = SR_w \times (1 - SR_m) \times A$$

Where  $Q_{sr}$  is the quantity of dry rice stubble in kg for a given field,  $SR_w$  is the average weight of rice stubble per  $m^2$  from the quadrat measurements,  $SR_m$  is the average measured rice stubble relative moisture content,  $A$  is the area of the field measured in  $m^2$ . The resulting  $Q_{sr}$  yields a maximum rice stubble fuel-loading factor in  $kg/m^2$ . We also measured the number of plants in each quadrat for a measure of rice planting density.

Thus, we have three separate fuel-loading factors: straw, stubble, and total post-harvest biomass factors. Using these fuel-loading factors we estimated rice residue burning emissions based on three scenarios 1) All rice straw is burned; 2) all rice straw and stubble are burned; 3) most-likely amount burned based on the previously-mentioned surveys from the literature. We compared these estimates to the typical approach used in most studies which relies on a residue-to-product ratio from government data on crop production. In addition, we also compared maximum potential burning estimates derived using fuel-loading factors from two smaller-scale field studies in villages in Thailand, and factors from another small-scale study in Can Tho, Vietnam located in the Mekong Delta.

We calculated the maximum potential emissions from rice residue burning based on the following (equation 3.3):

$$E_a = A \times FL \times EF_a \times PB \times CF$$

Where  $E_a$  is the maximum potential rice residue burning emissions for a given pollutant in gigagrams,  $A$  is the paddy rice planted area in hectares based on the Vietnam government statistics,  $FL$  is the fuel-loading factor or that estimated from crop production data in kg/ha,  $EF_a$  is the emissions factor for a given pollutant species in g/kg,  $PB$  is the proportion of residue subjected to burning (from 0-100%, i.e. residue left in the field to be burned), and  $CF$  is the combustion factor indicating the burn completeness (from 0-100%) for the residues subjected to burning. For all scenarios estimating emissions in Hanoi Province, we selected a combustion factor of 0.8 (Aalde 2006) as the best available factor representative of croplands in general, the rice area in Hanoi Province based on Vietnam government statistics of 200.8 ha (Vietnam Government 2015), the emission factors for each species: CO 102g/kg ( $\pm 33$ g/kg), CO<sub>2</sub> 1585g/kg ( $\pm 100$ g/kg), and PM<sub>2.5</sub> 6.26 g/kg ( $\pm 2.36$ g/kg) (Akagi 2011), the proportion burned as 100% for the maximum emissions scenario, and 50% straw and 10% stubble for the most-likely scenario based on the literature and our field experience (Tran *et al* 2014; Nguyen 2012; Duong and Yoshiro 2015). To estimate the fuel-loading factor for the production-statistics based scenario, we used a regionally-estimated residue-to-product ratio for rice straw of 0.75 (Menke *et al* 2007) combined with the production data from the government statistics (Vietnam Government 2015) resulting in a fuel-loading factor of 3803kg/ha. For the other smaller-scale studies, we used their fuel-loading factors of 3600kg/ha (Kanokkanjana *et al* 2011), 5800kg/ha (Oanh *et al* 2011), and 3470kg/ha (Hong Van *et al* 2014). The latter factor was derived by averaging the reported seasonal fuel-loading factors of 3500kg/ha (Spring-Summer), 4300kg/ha (Winter-Spring), and

2600kg/ha (Summer-Autumn). For each scenario, all factors were held constant except for the fuel-loading factor and proportion burned.

As our study measurements are representative of a typical double-cropped paddy rice landscape and results from (Hong Van *et al* 2014) cover triple cropping in Mekong Delta Vietnam, we up-scaled the results from both studies to estimate contribution of PM<sub>2.5</sub> emissions from rice residue burning for the entire Vietnam. Rice planted area for year 2008 was obtained from Vietnam Statistics Office (Vietnam 2015). We applied the triple cropping factors to the Mekong Delta rice area, and our study fuel-loading factors to the rest of the rice area in Vietnam. We compared the resulting rice burning emissions estimates with an existing emissions inventory (Regional Emission inventory in ASia (REAS)) for the latest available year, 2008 (Kurokawa *et al* 2013). We calculated Vietnam's total emissions (equation 3.3) for different scenarios including the maximum potential emissions (all residue burned), and the most-likely scenarios of straw and stubble burning based on the literature and our field experience suggesting 50% of straw burned and 10% of stubble burned (Nguyen 2012; Hong Van *et al* 2014; Tran *et al* 2014; Duong and Yoshiro 2015; Oritate *et al* 2015).

While comparison of rice residue burning emissions with REAS yields insight into the relative contribution to total PM<sub>2.5</sub> emissions, this does not address how our field-derived estimates compare with available satellite-derived estimates. The latest available GFED version 4.1s at 0.25 x 0.25 degree was used to derive total biomass burning emissions for Vietnam, GFED also includes the portion contributed from agricultural waste burning (van der Werf *et al* 2010) based on MODIS burned area (Giglio *et al* 2013), and supplemented by small fire burned area (Randerson *et al* 2012). We calculated

the emissions for the same year as REAS using the monthly datasets, and the same emission factors as our field study to maintain consistency. Accordingly, the emissions were derived using the amount of dry matter burned (DM) from GFED and multiplied with the aforementioned emission factors and summed for entire Vietnam.

We also evaluated the accuracy of our field-based straw measurements in eight additional randomly selected fields within Hanoi Province. First, following the same procedure as the initial field data collection we calculated the expected dry straw weight. To calculate the observed dry straw weight, we collected all rice straw within the field and weighed it. After factoring in the weight of the measuring bags and the average moisture content we arrived at an observed dry straw weight. We then compared this to our expected dry rice straw weight ( $\text{kg/m}^2$ ) estimated from our field calculation (equation 3.1). Using these observed and expected rice straw values we calculate an area-weighted root mean square error (RMSE). We also generated a residual plot to check for systematic errors. As the stubble measurement is more straightforward, we assumed the same accuracy as the straw measurement.

In addition to fuel-loading factor error, we also calculated the resulting emissions error rates through the simplified error propagation equations using reported error rates for emission factors, and fuel-loading factors (Harvard 2013).

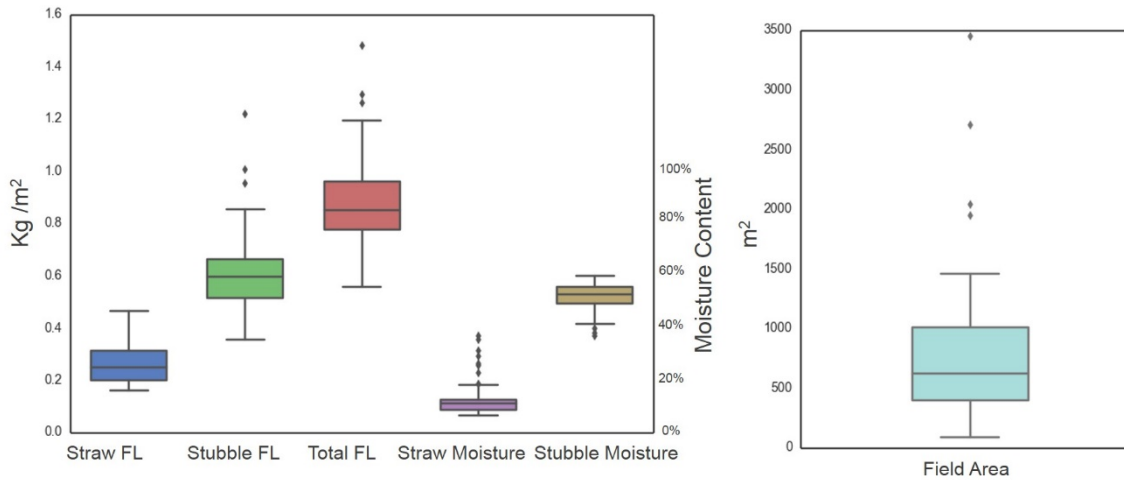
## **3.4 Results**

### *3.4.1 Fuel-loading factors*

Results on field-level distribution of values for rice straw, stubble, total post-harvest biomass, straw moisture content, stubble moisture content, and field area are shown in figure 3.4. The average fuel-loading factors as measured were: rice straw  $0.27 \text{ kg/m}^2$ , rice

stubble 0.61 kg/m<sup>2</sup>, and total post-harvest residue 0.88 kg/m<sup>2</sup>; table 3.1 lists more details

**Figure 3.4. Boxplots highlighting the distribution of field values for field area, straw, stubble, and total post-harvest residue, as well as moisture content.**



including standard deviation and moisture content. The range of standard deviations suggests some spatial variability for the fuel-loading factors and higher ranges for the moisture content attributed to recent rain events. We also found an average field size of 790 m<sup>2</sup> ( $\sigma = 625\text{m}^2$ ), and average number of rice plants 35.1 per m<sup>2</sup> ( $\sigma = 5.2$ ). Based on the Vietnam government’s rice planted area data for 2015 and our fuel-loading factor, we estimated total straw production for Hanoi Province at 433.7Gg of dry rice straw. We also estimated total dry rice stubble as 979.9Gg, and total post-harvest rice biomass as 1413.6Gg of residue.

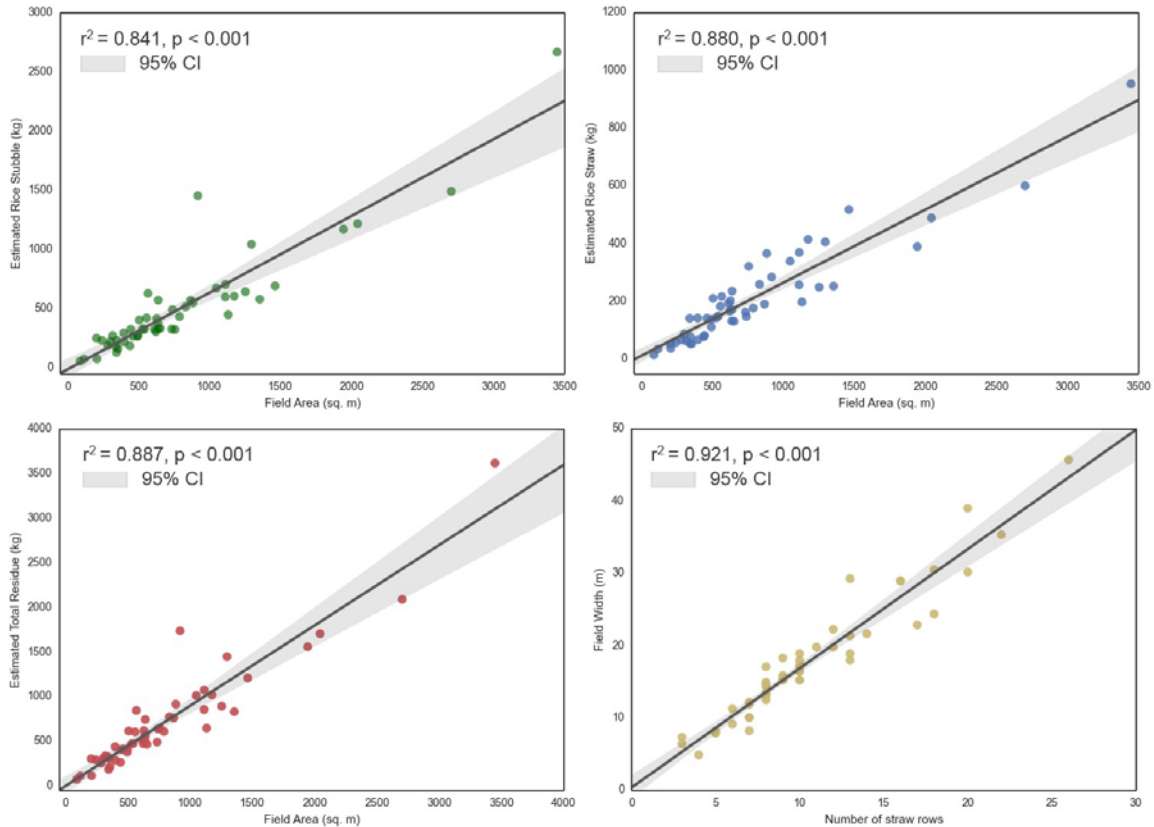
**Table 3.1 Field-based residue estimates.** Uncertainty for rice straw ( $\pm 0.033$ ), Rice Stubble ( $\pm 0.076$ ), Total Residue ( $\pm 0.083$ ) kg/m<sup>2</sup>, Moisture content ( $\pm 3\%$ ).

	Rice Straw	Rice Stubble	Total Residue
Average Dry Fuel Load	0.27 kg/m <sup>2</sup>	0.61 kg/m <sup>2</sup>	0.88 kg/m <sup>2</sup>
St. Dev. Dry Fuel Load	0.08 kg/m <sup>2</sup>	0.16 kg/m <sup>2</sup>	0.19 kg/m <sup>2</sup>
Average Fuel Moisture Content	13.2%	51.5%	32.4%
St. Dev. Fuel Moisture Content	7.3%	5.7%	6.5%



We observed strong correlations between different field parameters (figure 3.5) i.e., field area and estimated rice stubble ( $r^2=0.84$ ), field area and estimated rice straw ( $r^2=0.88$ ), field area and total post-harvest biomass ( $r^2=0.89$ ) and number of straw rows and field width ( $r^2=0.92$ ). We also conducted an accuracy assessment of the field-

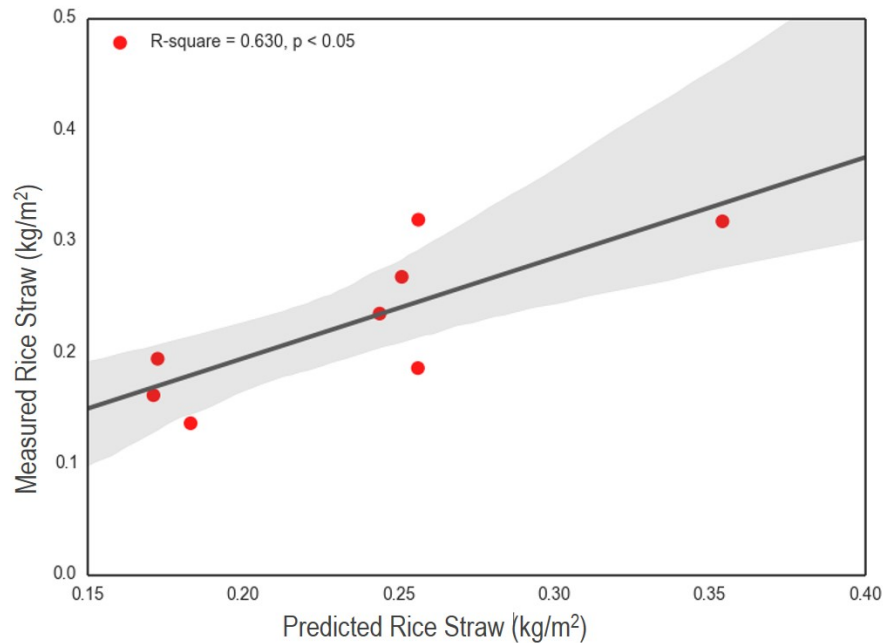
**Figure 3.5. Plots of rice residue parameters measured in the field.**



estimated fuel-loading factors. Based on our field measurements of rice straw, we found an RMSE of  $0.041 \text{ kg/m}^2$  between the observed and expected values (equation 3.1). After also factoring in error propagation from the moisture content device (3% lab-estimated) and scale (0.4%) we arrived at our final fuel-loading factor estimates; dry rice straw is estimated to be  $0.27 \text{ kg/m}^2 (\pm 0.033)$ , dry rice stubble at  $0.61 \text{ kg/m}^2 (\pm 0.076)$ , and total post-harvest biomass at  $0.88 \text{ kg/m}^2 (\pm 0.083)$ . Further, for our fuel-loading factors we observed a moderate relationship between the observed and expected rice straw values ( $r^2$

= 0.63,  $p < 0.05$ ) (figure 3.6) suggesting slight overestimation in our expected rice straw values attributed to field variability including occasional degraded/cut stalk included in measurements.

**Figure 3.6. Relationship between the observed and predicted rice straw values from the accuracy assessment highlighting moderately strong relationship.**



As compared with the rice straw amount derived from the crop production statistics, our rice straw factor is slightly lower (3803kg/ha vs. 2700kg/ha). However, when incorporating stubble, we account for a total biomass estimate which is not calculated in the production statistics method. We note other studies outside Vietnam found higher fuel-loading factors including 3600kg/ha and 5800kg/ha in two separate studies in Thailand (Kanokkanjana *et al* 2011; Oanh *et al* 2011), while the other study in the Mekong Delta, Vietnam had a lower average of 3470kg/ha (Hong Van *et al* 2014). This wide variation suggests region specific fuel-loading factors are an important base for emissions estimates.

### 3.4.2 Emissions estimates

In Hanoi Province, we used our resulting fuel-loading estimates for quantifying rice residue emissions. We used the cropped area data, combustion factor, and emission factors for CO, CO<sub>2</sub>, and PM<sub>2.5</sub> as described above. We present the emissions for each scenario including: maximum emissions from typical production-statistics, maximum emissions using fuel-load factors from field-based study in Can Tho, Vietnam (Hong Van *et al* 2014), and maximum potential and most-likely emissions using our fuel-load factors of rice straw, and total post-harvest biomass. We also estimated maximum potential emissions using fuel-load factors from two village-level studies in Thailand (Kanokkanjana *et al* 2011; Oanh *et al* 2011) using their respective rice straw fuel-loading factors of 3600kg/ha and 5800 kg/ha. Our results suggest maximum emissions ranges for CO (44.24-144.19Gg), CO<sub>2</sub> (687-2240Gg), and PM<sub>2.5</sub> (2.72-8.85Gg) in table 3.2. Based on averaging the residue burning survey data and from our field experience, the most likely proportion burned is 50% straw and 10% stubble. We find the most-likely combined straw and stubble emissions for Hanoi as CO (36.54Gg), CO<sub>2</sub> (567.79Gg), and

**Table 3.2. Potential emissions for Hanoi Province, Vietnam.** Compares different estimates using typical methods employed in the literature, and also shows another Vietnam study. FL (kg/ha), emissions (gigagrams)

Scenario	Fuel load	PM <sub>2.5</sub> Emissions	CO Emissions	CO <sub>2</sub> Emissions
Crop Production Stats-based FL	3803	3.824	62.31	968.30
Can Tho, Vietnam straw FL (Hong Van 2014)	3470 (±830)	3.489 (±7.759)	56.86 (±113.93)	883.51 (±10884)
Can Tho, Vietnam FL (Straw & Stubble)	7330 (±1730)	7.371 (±16.327)	120.10 (±239.53)	1866.32 (±22706)
This study (straw only)	2700 (±330)	2.715 (±5.359)	44.24 (±76.20)	687.46 (±4709)
This study (Straw & Stubble)	8800 (±830)	8.849 (±17.126)	144.19 (±241.99)	2240.61 (±12662)
This study, most-likely emissions (straw)	2700 (±330)	1.629 (±3.215)	26.54 (±45.72)	412.48 (±2825)
This study, most-likely emissions (Stubble)	6100 (±760)	0.613 (±1.219)	10.00 (±17.38)	155.31 (±1126)
This study, most-likely emissions (Straw and Stubble)	-	2.243 (±5.309)	36.54 (±75.02)	567.79 (±3925)

PM<sub>2.5</sub> (2.24Gg). The individual scenario results are presented in table 3.2 including the error rates for each value in parentheses.

We highlight notable variation between the different scenarios. While all rice stubble is not necessarily burned in the study area, in other regions such as India both the straw and stubble are routinely burned (Gadde 2009; Gupta *et al.*, 2014; Vadrevu *et al.*, 2015). However, many studies estimating emissions from rice residue burning rely on residue-to-product ratios. Without accounting for rice stubble that is actually burnt on field, these and other studies may be underestimating emissions by a factor of about 2.3 (table 3.2).

We also estimated total rice residue burning emissions for the entire Vietnam during 2008 and compared with the existing emission inventory (Kurokawa *et al* 2013). Based on the most-likely emissions scenario (10% stubble, 50% straw burned), 75.98Gg of PM<sub>2.5</sub> are emitted from rice residue burning in Vietnam with stubble accounting for 18.36Gg and straw 57.62Gg. The total rice residue burning accounts for 12.8% of Vietnam's total PM<sub>2.5</sub> emissions and is the 2<sup>nd</sup> highest PM<sub>2.5</sub> combustion source after fuelwood burning. However, if all rice residue is burned, rice emissions could result in up to 36.49% of total PM<sub>2.5</sub> emissions. We also add our emissions estimates to the original total from the emissions inventory of 519.81Gg (Kurokawa *et al* 2013) and arrive at new maximum of 818.50Gg and most-likely total PM<sub>2.5</sub> emissions of 595.79Gg for the entire Vietnam. Table 3.3 contains the factors used for estimation, and the individual scenario results including error estimates for residue burning emissions.

**Table 3.3. Potential emissions from rice residue burning for Vietnam.** Comparison with the REAS emission inventory, and contribution of rice residue to total PM<sub>2.5</sub> emissions are also shown. Error estimates for emissions are in parentheses. MRD = Mekong River Delta.

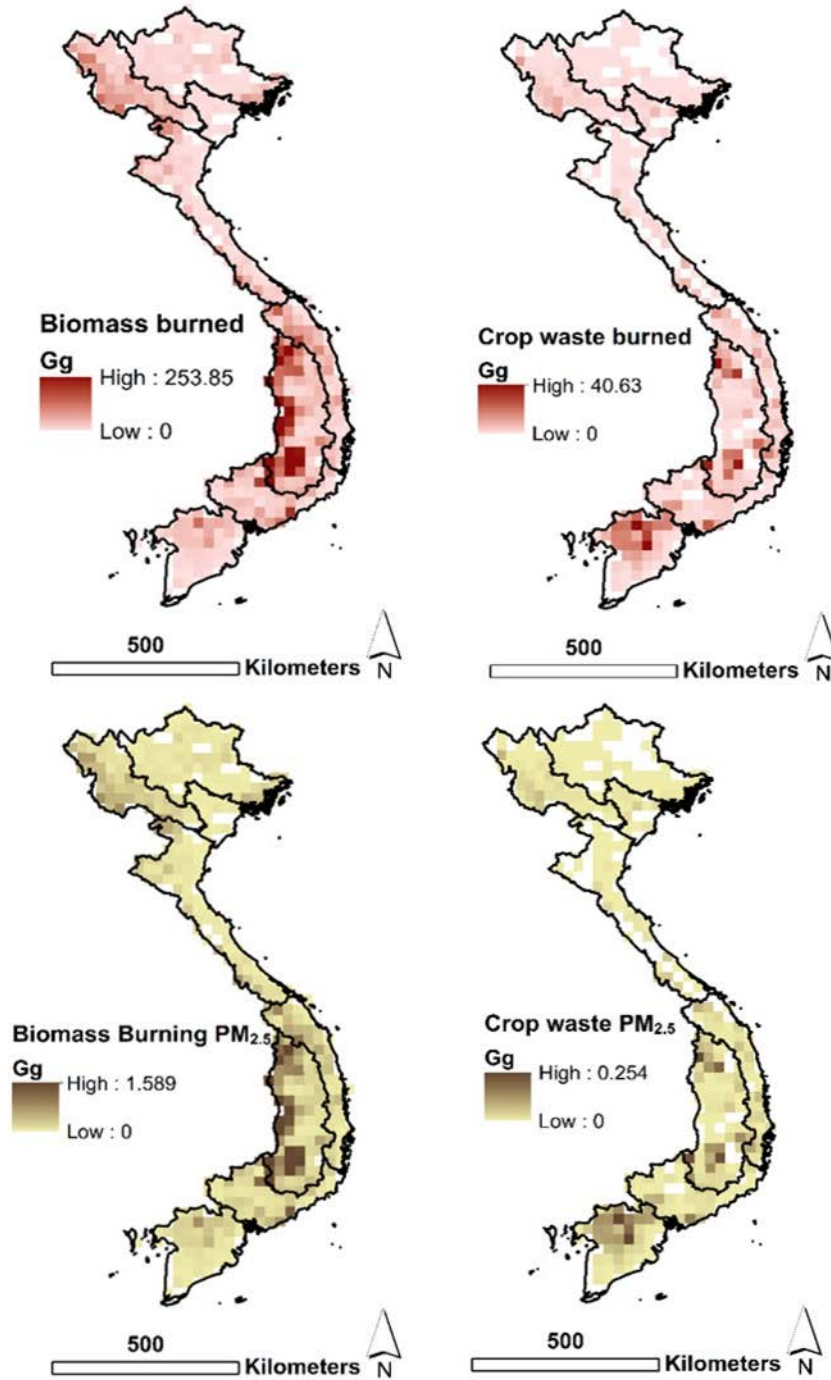
Scenario	Rice area Mekong Delta (ha)	Rice area rest of Vietnam (ha)	Fuel load rest of Vietnam (kg ha <sup>-1</sup> )	Fuel load Mekong Delta (kg ha <sup>-1</sup> )	Combustion factor	Proportion burned	PM <sub>2.5</sub> EF g kg <sup>-1</sup>	Rice burned MRD (Gg)	Rice burned rest of Vietnam (Gg)	Rice residue PM <sub>2.5</sub> (Gg)	Emissions inventory total PM <sub>2.5</sub> (Gg)	New total emissions inventory PM <sub>2.5</sub> (Gg)	Percent of total emissions from rice residue
Entirety of Vietnam: Maximum potential emissions (100% straw and stubble burned)	3858900	3563300	8800	7330	0.8	1	6.26	22628.59	25086.72	298.70 (±87.72)	519.81	818.50	36.49
Entirety of Vietnam: Most likely Scenario (50% straw)	3858900	3563300	2700	3470	0.8	0.5	6.26	5356.15	3848.36	57.62 (±17.76)	519.81	577.43	9.98
Entirety of Vietnam: Most likely Scenario (10% stubble)	3858900	3563300	6100	3867	0.8	0.1	6.26	1193.79	1738.89	18.36 (±5.22)	519.81	538.17	3.41
Entirety of Vietnam: Most likely Scenario (above two combined)	–	–	–	–	–	–	–	6549.94	5587.25	75.98 (±22.97)	519.81	595.79	13.39

GFED-derived PM<sub>2.5</sub> total biomass burning emissions suggested 42.56Gg (±16.0Gg) with 5.62Gg (±2.1Gg) attributed to agricultural waste burning for the entire Vietnam. Accordingly, when agricultural waste burning emissions are compared with our field-derived residue burning emission estimates this suggests GFED underestimation by a factor of 13.5. Even if all biomass burning emissions (42.56Gg) were attributed to residue burning, this would still be less than our field-derived estimates by a factor of 1.8. We also highlight the region-level amount of biomass burning, amount of crop residue burning, and associated emissions in table 3.4 suggesting the highest fraction of crop waste burning to occur in the Mekong River Delta and Red River Delta where rice is the predominant land cover. The spatial variation of biomass burning and emission estimates is highlighted in figure 3.7.

**Table 3.4 GFED-derived regional biomass burned and resulting PM2.5 emissions**

Region	Total biomass burned (Gg)	Total biomass burning PM2.5 (Gg)	Crop waste burned (Gg)	Crop waste burning PM2.5 (Gg)	Contribution from crop waste burning
Central Highlands	3215.18	20.13	258.16	1.62	8.0%
Mekong River Delta	384.43	2.41	277.01	1.73	72.1%
North Central Coast	438.20	2.74	41.54	0.26	9.5%
North East	423.84	2.65	26.60	0.17	6.3%
North West	925.75	5.80	86.21	0.54	9.3%
Red River Delta	29.52	0.18	20.40	0.13	69.1%
South Central Coast	595.82	3.73	91.87	0.57	15.4%
South East	785.76	4.92	96.54	0.60	12.3%
<b>Total</b>	<b>6798.50</b>	<b>42.56</b>	<b>898.33</b>	<b>5.62</b>	<b>13.2%</b>

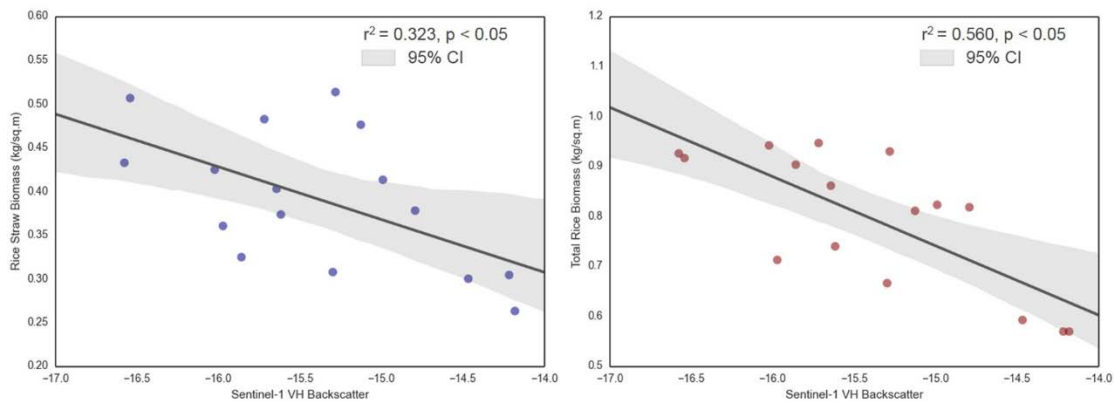
Figure 3.7 GFED spatial variation with region boundaries for total biomass burning and crop waste burning.



### 3.4.3 SAR data and biomass relationship

To evaluate the relationship of SAR backscatter with rice straw and total post-harvest biomass, we selected a single Sentinel-1A image just prior to harvest for the Hanoi Province. We found a moderately-weak relationship between the SAR backscatter and field-measured rice straw ( $r^2 = 0.323$ ,  $p < 0.01$ ), while a moderate relationship was observed with the total rice biomass ( $r^2 = 0.560$ ,  $p < 0.01$ ) (figure 3.8). We observed a negative, linear relationship suggesting fields with lower backscatter values prior to harvest have more post-harvest biomass. The relationship is promising; however, it needs more refinement in order to be useful for estimating rice biomass and rice straw production prior to harvest. Other studies have found good results using SAR to estimate different rice field properties, biomass, or yield (Lam-Dao *et al* 2009; McNairn *et al* 2004; Ribbes and Le Toan 1999; Wiseman *et al* 2014; Paloscia *et al* 1999; Bouvet *et al* 2014; Erten *et al* 2016; Inoue *et al* 2014; Satalino *et al* 2015).

**Figure 3.8 Spatial relationship of Sentinel-1 VH backscatter in dB with a) rice straw biomass; and b) total post-harvest rice biomass**



## 3.5 Discussion

In this study, we focused on measuring residue amounts from machine-harvested fields.

With the increasing urbanization, infrastructure, wealth, and interconnectedness, we



anticipate most fields to switch from hand-harvesting to machine-harvesting (Nguyen et al 2016). Hand-harvested fields are typically cut slightly higher from the ground, thus they have more stubble and less straw to potentially burn. Thus, as machine-harvested fields become increasingly prevalent, residue burning emissions will be exacerbated, as it is more difficult to collect straw after machine harvest (Nguyen et al 2016). Some studies ignore the stubble that is left on the ground, thus underestimating total residue and resulting emissions. However, as undertaken in this study we quantify fuel-loading factors for straw and stubble which provides an improved assessment of rice residue burning emissions, as other studies often ignore the stubble factor. Our estimates incorporating fuel-loading factors for rice straw, rice stubble, and total rice biomass were useful in refining emissions in the Hanoi Province and entire Vietnam. The results can be extended to similar small-holder rice production lands. We note that farmers may burn rice straw either in a pile or in an open-manner including the stubble and straw. Thus, in addition to variable fuel-loads from different harvest methods, the orientation of the rice straw and piling might play a role in the combustion, moisture content, emissions factor, and resulting emissions impact; some of which have been explored, but further quantification is needed (Arai et al 2014; Heinsch et al 2016). Understanding the variation in residue management practices and how they impact emissions, may provide useful additional information on emissions mitigation.

Although the total estimated rice burning emissions may be relatively small as compared to other combustion and non-combustion sources (Kurokawa et al 2013), rice residue burning in Hanoi is practiced two times per year, amplifying and temporally-concentrating the impact from burning. Accordingly, the air quality in Hanoi is frequently

degraded as seen by local haze, and a high air quality index (Nguyen et al 2015). Thus, emissions mitigation from rice residue burning is one critical aspect for improving air quality and human health.

Uncertainty with regard to different aspects of fuel-loading and emissions are important to characterize. Further, due to limited availability of data we highlight some future needs which could improve upon the rice stubble and straw burning emissions estimates. Accordingly, improvements could be made by: using separate combustion factors and emission factors for straw and stubble, deriving improved emissions factors specific to rice in both the Red River Delta and Mekong River Delta, improved mapped rice areal estimates, region/crop specific combustion factors for straw and stubble, and machine versus hand-harvested fuel-loading factor comparisons. We note the government estimates of rice land area for Hanoi are different: government statistics (201,000 ha) versus mapped area (220,000 ha). Accordingly, these variations could have significant impact on resulting emissions estimates, especially once aggregating results to the national scale and accounting for both seasons.

Notably low GFED emission estimates could be attributed to a variety of factors such as prevalent cloud cover impacting satellite observations (Wilson and Walter 2016), small size of agricultural fires in Vietnam, ephemeral agricultural fires, active field management, or burning after MODIS overpass time. All of these factors may lead to satellite-based underestimation of fires and resulting emissions regardless of the fire detection algorithm strength in GFED or any other emission database. We further note that the GFED agricultural waste burning data includes emissions from all agricultural sources, yet the emissions are still notably lower than rice residue burning alone.

However, these results are presented with the caveat that the field-based emission estimates could be improved through refinements mentioned in the limitations section.

### **3.6 Conclusion**

The first part of our study characterized total post-harvest rice residues for the small-holder rice-dominated province of Hanoi, Vietnam. From the field, we developed separate straw, stubble, and total biomass fuel-loading factors representative of a typical double-cropped rice region of Vietnam. Our results on rice residues suggested relatively higher total post-harvest residue factor than the earlier studies. We used Sentinel-1 C-band SAR data for field sampling of residues and to infer the relationship between post-harvest biomass and SAR. We found a moderately weak relationship between the SAR backscatter and field-measured rice straw, while a moderate relationship was observed with the total rice biomass. These results are promising, however, more advanced modelling might be necessary for forecasting the post-harvest biomass using SAR data. Using field data from multiple studies, we then estimate residue burning emissions. We found that rice residue burning accounts for ~13% of total PM<sub>2.5</sub> emissions in Vietnam, and is the 2nd largest PM<sub>2.5</sub> source after fuelwood burning. We compared GFED-derived biomass burning emissions and crop waste burning emissions with our field-derived residue burning emissions. We found a likely notable underestimation by GFED for Vietnam by a factor of over 13. These results suggest a need for improved satellite-derived estimates. Further, emissions mitigation in this sector may be more critical than previously known and is increasingly important for health and air quality concerns in Hanoi, Vietnam.

### 3.7 Acknowledgements

Kristofer Lasko would like to thank his PhD committee members for guidance and support including Ivan Csiszar (NOAA), Matthew Hansen (UMd), and Louis Giglio (UMd). The authors would also like to thank Ha Van Pham (Vietnam National University Hanoi) for field assistance, David Lasko (Integrity Applications Incorporated) for verifying field calculations, as well as Dr. William Salas and Dr. Nathan Torbick from Applied Geosolutions LLC for SAR expertise. This research was funded in part by the Green Fellowship for the Environment, Council on the Environment, University of Maryland. We would also like to thank the anonymous referees for providing feedback which enhanced the quality of the manuscript.

### 3.8 References

- Aalde H *et al* 2006 Generic methodologies applicable to multiple land-use categories. *IPCC guidelines for national greenhouse gas inventories* 4 1-59.
- Akagi S K *et al* 2011 Emission factors for open and domestic biomass burning for use in atmospheric models. *Atmospheric Chemistry and Physics* 11(9) 4039-4072.
- Arai H, Hosen Y, Pham Hong V N, Thi N T, Huu C N, and Inubushi K 2015 Greenhouse gas emissions from rice straw burning and straw-mushroom cultivation in a triple rice cropping system in the Mekong Delta. *Soil Science and Plant Nutrition* 61 4 719-735.
- Badarinath K V S, Kharol S K, & Sharma A R 2009 Long-range transport of aerosols from agriculture crop residue burning in Indo-Gangetic Plains—a study using LIDAR, ground measurements and satellite data *Journal of Atmospheric and Solar-Terrestrial Physics* 71 1 112-120.
- Badarinath K V S *et al* 2007 Multiyear ground-based and satellite observations of aerosol properties over a tropical urban area in India. *Atmospheric Science Letters* 8 1 7-13.
- Badarinath K V S, Sharma A R, Kharol S K, and Prasad V K 2009 Variations in CO, O<sub>3</sub> and black carbon aerosol mass concentrations associated with planetary boundary layer (PBL) over tropical urban environment in India. *Journal of atmospheric chemistry* 62 1 73-86.

- Biswas S, Vadrevu K P, Lwin Z M, Lasko K, and Justice C O 2015. Factors controlling vegetation fires in protected and non-protected areas of Myanmar. *PloS One* 10 4: e0124346.
- Bouvet A *et al* 2014 Estimation of agricultural and biophysical parameters of rice fields in Vietnam using X-band dual-polarization SAR. In *2014 IEEE Geoscience and Remote Sensing Symposium* 1504-1507.
- Cao G, Zhang X, Sunling, and Zheng F 2008. Investigation on emission factors of particulate matter and gaseous pollutants from crop residue burning. *Journal of Environmental Sciences* 20 1 50-55.
- Chakraborty M, Manjunath K R, Panigrahy S, Kundu N, and Parihar J S 2005. Rice crop parameter retrieval using multi-temporal, multi-incidence angle Radarsat SAR data. *ISPRS Journal of Photogrammetry and Remote Sensing* 59 5 310-322.
- Cristofanelli P *et al* 2014 Transport of short-lived climate forcers/pollutants (SLCF/P) to the Himalayas during the South Asian summer monsoon onset. *Environmental Research Letters* 9 8 084005.
- Crutzen P J, and Andreae M O 1990 Biomass burning in the tropics: Impact on atmospheric chemistry and biogeochemical cycles. *Science*, 250 4988 1669-1679.
- Dong J, and Xiao X 2016 Evolution of regional to global paddy rice mapping methods: A review. *ISPRS Journal of Photogrammetry and Remote Sensing* 119 214-227.
- Duong P T, and Yoshiro H 2015 Current Situation and Possibilities of Rice Straw Management in Vietnam. Retrieved from [http://www.jsrsai.jp/Annual\\_Meeting/PROG\\_52/ResumeC/C02-4.pdf](http://www.jsrsai.jp/Annual_Meeting/PROG_52/ResumeC/C02-4.pdf)
- Erten E, Lopez-Sanchez J M, Yuzugullu O, and Hajnsek I 2016 Retrieval of agricultural crop height from space: A comparison of SAR techniques *Remote Sensing of Environment* 187 130-144.
- Gadde B, Bonnet S, Menke C, and Garivait S 2009 Air pollutant emissions from rice straw open field burning in India, Thailand and the Philippines *Environmental Pollution* 157 5 1554-1558.
- Giglio L, Randerson J T, and van der Werf G R 2013 Analysis of daily, monthly, and annual burned area using the fourth-generation global fire emissions database (GFED4) *Journal of Geophysical Research: Biogeosciences* 118 1 317-328.
- Gupta P K *et al* 2001 Study of trace gases and aerosol emissions due to biomass burning at shifting cultivation sites in East Godavari District (Andhra Pradesh) during INDOEX IFP-99. *Curr Sci Ind* 80 186-196.
- Harvard University Department of Physics 2013. A Summary of Error Propagation. Retrieved from [http://ipl.physics.harvard.edu/wp-uploads/2013/03/PS3\\_Error\\_Propagation\\_sp13.pdf](http://ipl.physics.harvard.edu/wp-uploads/2013/03/PS3_Error_Propagation_sp13.pdf) .

Heinsch F A, McHugh C W, and Hardy C C 2016 Fire, Fuel, and Smoke Science Program 2015 Research Accomplishments. Missoula, MT: U.S. Department of Agriculture, Forest Service, Rocky Mountain Research Stations, Missoula Fire Sciences Laboratory.

Hien P D, Bac V T, Tham H C, Nhan D D, and Vinh L D 2002 Influence of meteorological conditions on PM 2.5 and PM 2.5– 10 concentrations during the monsoon season in Hanoi, Vietnam. *Atmospheric Environment* 36 21 3473-3484.

Hong Van N P, Nga T T, Arai H, Hosen Y, Chiem N H, and Inubushi K 2014 Rice Straw Management by Farmers in a Triple Rice Production System in the Mekong Delta, Viet Nam. *Tropical Agriculture and Development* 58 4 155-162.

Inoue Y, Sakaiya E, and Wang C 2014 Capability of C-band backscattering coefficients from high-resolution satellite SAR sensors to assess biophysical variables in paddy rice. *Remote Sensing of Environment* 140 257-266.

Kanabkaew T, and Oanh N T K 2011 Development of spatial and temporal emission inventory for crop residue field burning. *Environmental Modeling & Assessment* 16 5 453-464.

Kanokkanjana K, Cheewaphongphan P, and Garivait S 2011 Black carbon emission from paddy field open burning in Thailand. *IPCBEE Proc.* 6 88-92.

Korenaga T, Liu X, and Huang Z 2001 The influence of moisture content on polycyclic aromatic hydrocarbons emission during rice straw burning. *Chemosphere-Global Change Science* 3 1 117-122.

Kurokawa J *et al* 2013 Emissions of air pollutants and greenhouse gases over Asian regions during 2000–2008: Regional Emission inventory in ASia (REAS) version 2. *Atmospheric Chemistry and Physics* 13 21 11019-11058.

Lam-Dao, N., Le Toan, T., Apan, A., Bouvet, A., Young, F., & Le-Van, T. 2009. Effects of changing rice cultural practices on C-band synthetic aperture radar backscatter using Envisat advanced synthetic aperture radar data in the Mekong River Delta. *Journal of Applied Remote Sensing*, 3(1), 033563-033563.

Le TH, Nguyen TN, Lasko K, Ilavajhala S, Vadrevu KP, and Justice C 2014 Vegetation fires and air pollution in Vietnam. *Environmental Pollution* 195 267-75.

Liang S 2005 *Quantitative remote sensing of land surfaces* (Vol. 30). John Wiley & Sons.

McNairn H, and Brisco B 2004 The application of C-band polarimetric SAR for agriculture: a review. *Canadian Journal of Remote Sensing* 30 3 525-542.

Menke C, Wassmann R, and Gadde B 2009 Possible energy utilization of rice straw in Thailand: seasonal and spatial variations in straw availability as well as potential reduction in greenhouse gas emissions.

- Mosleh M K, Hassan Q K, and Chowdhury E H 2015 Application of remote sensors in mapping rice area and forecasting its production: A review. *Sensors* 15 1 769-791.
- Nguyen M D, 2012 An Estimation of Air Pollutant Emission from Open Rice Straw Burning in Red River Delta, Science and Development Journal (Vietnamese).
- Nguyen D, Wagner W, Naeimi V, and Cao S 2015 Rice-planted area extraction by time series analysis of ENVISAT ASAR WS data using a phenology-based classification approach: A case study for Red River Delta, Vietnam. *International Archives of Photogrammetry* 40 7 77.
- Nguyen T T *et al* 2015 Particulate matter concentration mapping from MODIS satellite data: a Vietnamese case study. *Environmental Research Letters* 10 9 095016.
- Nguyen V H *et al* 2016 Energy efficiency, greenhouse gas emissions, and cost of rice straw collection in the Mekong River Delta of Vietnam. *Field Crops Research* 198 16-22.
- Oanh *et al* 2011 Characterization of particulate matter emission from open burning of rice straw. *Atmospheric Environment* 45 2 493-502.
- Oritate *et al* 2015 Regional Diagnosis of Biomass use in Suburban Village in Southern Vietnam. *Journal of the Japan Institute of Energy*.
- Paloscia S, Macelloni G, Pampaloni P, and Sigismondi S 1999 The potential of C-and L-band SAR in estimating vegetation biomass: the ERS-1 and JERS-1 experiments. *IEEE Transactions on Geoscience and Remote Sensing* 37 4 2107-2110.
- Patanothai A, 1996 *Soils under stress: nutrient recycling and agricultural sustainability in the Red River Delta of Northern Vietnam*. Honolulu: East-West Center.
- Pham V C, Pham T T H, Tong T H A, Nguyen T T H, and Pham N H 2015 The conversion of agricultural land in the peri-urban areas of Hanoi (Vietnam): patterns in space and time. *Journal of Land Use Science* 10 2 224-242.
- Ponette-González A *et al* 2016 Biomass burning drives atmospheric nutrient redistribution within forested peatlands in Borneo. *Environmental Research Letters* 11 8 085003.
- Rajput P, Sarin M, Sharma D, and Singh D 2014 Characteristics and emission budget of carbonaceous species from post-harvest agricultural-waste burning in source region of the Indo-Gangetic Plain. *Tellus B* 66.
- Randerson J T *et al* 2012 Global burned area and biomass burning emissions from small fires. *Journal of Geophysical Research: Biogeosciences* 117 G4.
- Reddington C L *et al* 2014 Contribution of vegetation and peat fires to particulate air pollution in Southeast Asia. *Environmental Research Letters* 9 9 094006.

- Ribbes F, and Le Toan T 1999 Coupling radar data and rice growth model for yield estimation. In *Geoscience and Remote Sensing Symposium. IGARSS'99 Proceedings 4* 2336-2338.
- Satalino G *et al* 2015 Retrieval of wheat biomass from multitemporal dual polarised SAR observations. In *2015 IEEE IGARS* 5194-5197.
- Streets D G *et al* 2004 On the future of carbonaceous aerosol emissions. *Journal of Geophysical Research: Atmospheres* 109 D24.
- Streets D G, Yarber K F, Woo J H, and Carmichael G R 2003 Biomass burning in Asia: Annual and seasonal estimates and atmospheric emissions. *Global Biogeochemical Cycles* 17 4.
- Torbick N *et al* 2011 Integrating SAR and optical imagery for regional mapping of paddy rice attributes in the Poyang Lake Watershed, China *Canadian Journal of Remote Sensing* 37 1 17-26.
- Torbick N, Salas W, Chowdhury D, Ingraham P, and Trinh M 2017 Mapping rice greenhouse gas emissions in the Red River Delta, Vietnam. *Carbon Management* 1-10.
- Trach N X, 1998 The need for improved utilisation of rice straw as feed for ruminants in Vietnam: An overview. *Livestock Research for Rural Development* 10 2 1-14.
- Tran S N, Nguyen T Q N, Nguyen H C, Nguyen V C N, Le H V, and Ingvorsen K 2014 To quantify the seasonal rice straw and its use in different provinces in the Vietnamese Mekong Delta *Can Tho University Science Journal*
- Vadrevu K P, and Lasko K 2015 Satellite-Derived Nitrogen Dioxide Variations from Biomass Burning in a Subtropical Evergreen Forest, Northeast India. In *Remote Sensing of Water Resources, Disasters, and Urban Studies*, CRC Press 545-559
- Vadrevu K P, Ellicott E, Badarinath K V S, and Vermote E 2011 MODIS derived fire characteristics and aerosol optical depth variations during the agricultural residue burning season, north India. *Environmental pollution* 159 6 1560-1569.
- Vadrevu K P *et al* 2012 Vegetation fires in the himalayan region—Aerosol load, black carbon emissions and smoke plume heights. *Atmospheric environment* 47 241-251.
- Vadrevu K P, Lasko K, Giglio L, and Justice C 2014 Analysis of Southeast Asian pollution episode during June 2013 using satellite remote sensing datasets. *Environmental Pollution* 195 245-256.
- Vadrevu K P, Lasko K, Giglio L, and Justice C 2015 Vegetation fires, absorbing aerosols and smoke plume characteristics in diverse biomass burning regions of Asia. *Environmental Research Letters* 10 10 105003.
- Van der Werf G *et al* 2010 Global fire emissions and the contribution of deforestation, savanna, forest, agricultural, and peat fires (1997–2009). *Atmospheric Chemistry and Physics* 10 23 11707-11735.



Vietnam Government, General Statistics Office of Vietnam, 2015. Retrieved from [https://www.gso.gov.vn/default\\_en.aspx](https://www.gso.gov.vn/default_en.aspx)

Wilson A M, and Walter J 2016 Remotely sensed high-resolution global cloud dynamics for predicting ecosystem and biodiversity distributions. *PLoS Biol* 14 3 e1002415.

Wiseman G, McNairn H, Homayouni S, and Shang J 2014 RADARSAT-2 Polarimetric SAR response to crop biomass for agricultural production monitoring. *IEEE Journal of Selected Topics in Applied Earth Observations and Remote Sensing* 7 11 4461-4471.

Yan X, Ohara T, and Akimoto H 2006 Bottom-up estimate of biomass burning in mainland China. *Atmospheric Environment* 40 27 5262-5273.

Yevich R, and Logan J A 2003 An assessment of biofuel use and burning of agricultural waste in the developing world. *Global biogeochemical cycles* 17 4.

Zhang T, Wooster M J, Green D C and Main B 2015 New field-based agricultural biomass burning trace gas, PM 2.5, and black carbon emission ratios and factors measured in situ at crop residue fires in Eastern China. *Atmospheric Environment* 121 22-34.

Zuhlke M *et al* 2015 SNAP (Sentinel Application Platform) and the ESA Sentinel 3 Toolbox *ESA Special Publication* 734 21.

## Chapter 4: Improved rice residue burning emissions estimates: Accounting for practice-specific emission factors in air pollution assessments of Vietnam<sup>3</sup>

### 4.1 Abstract

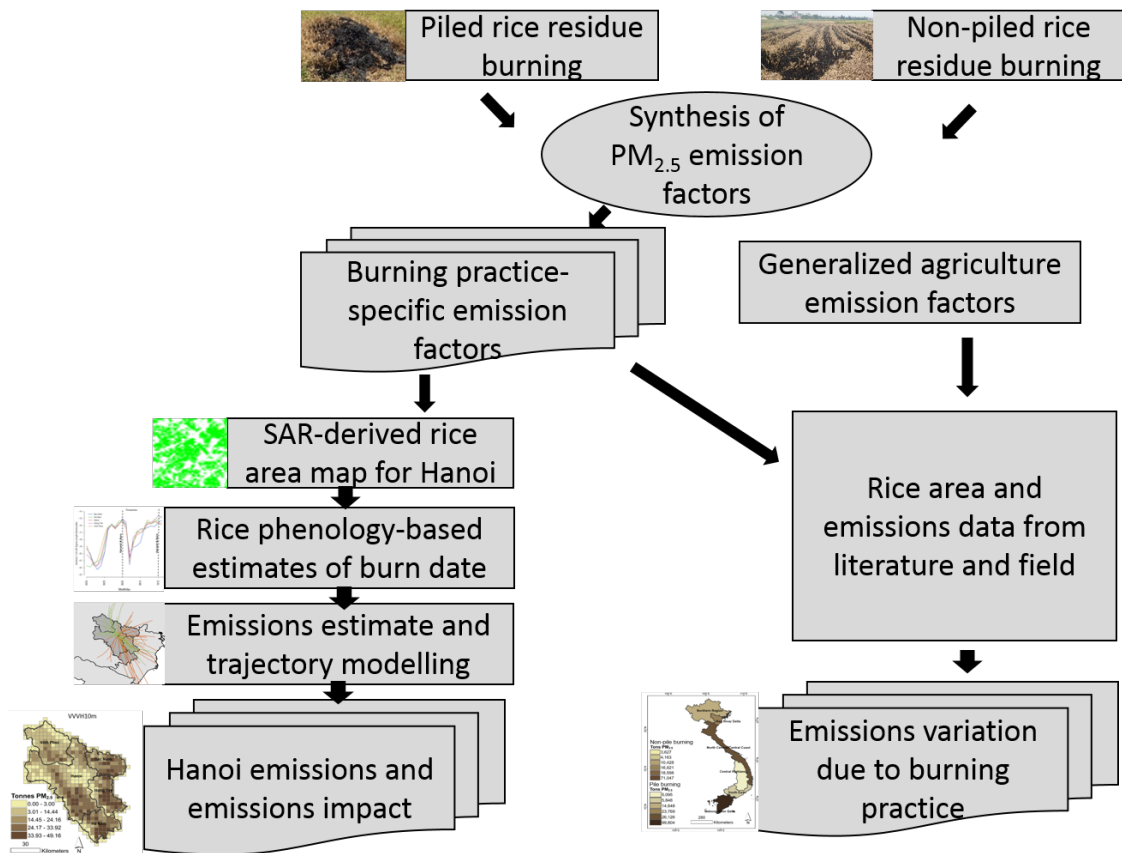
In Southeast Asia and Vietnam, rice residues are routinely burned after the harvest to prepare fields for the next season. Specific to Vietnam, the two prevalent burning practices include: a). piling the residues after hand harvesting; b). burning the residues without piling, after machine harvesting. In this study, we synthesized field and laboratory studies from the literature on rice residue burning emission factors for PM<sub>2.5</sub>. We found significant differences in the resulting burning-practice specific emission factors, with 16.9g kg<sup>-2</sup>(±6.9) for pile burning and 8.8g kg<sup>-2</sup>(±3.5) for non-pile burning. We calculated burning-practice specific emissions based on rice area data, region-specific fuel-loading factors, combined emission factors, and estimates of burning from the literature. Our results for year 2015 estimate 180Gg of PM<sub>2.5</sub> would result from the pile burning method and 130Gg would result from non-pile burning method, with the most-likely current emission scenario of 150Gg PM<sub>2.5</sub> emissions for Vietnam. For comparison purposes, we calculated emissions using generalized agricultural emission factors employed in global biomass burning studies. These results estimate 80Gg PM<sub>2.5</sub>, which is only 44% of the pile burning-based estimates, suggesting underestimation in previous studies. We compare our emissions to an existing all-combustion sources inventory, results show emissions account for 14-18% of Vietnam's total combustion PM<sub>2.5</sub> depending on burning practice. Within the highly-urbanized and cloud-covered Hanoi

---

<sup>3</sup> The presented material has been previously published in: Lasko K, and Vadrevu K P 2018. Improved rice residue burning emissions estimates: Accounting for practice-specific emission factors in air pollution assessments of Vietnam. *Environmental Pollution* 236, 795-806.

Capital region (HCR), we use rice area from Sentinel-1A to derive spatially-explicit emissions and indirectly estimate residue burning dates. Results from HYSPLIT back-trajectory analysis stratified by season show autumn has most emission trajectories originating in the North, while spring has most originating in the South, suggesting the latter may have bigger impact on air quality. From these results, we highlight locations where emission mitigation efforts could be focused and suggest measures for pollutant mitigation. Our study demonstrates the need to account for emissions variation due to different burning practices (figure 4.1).

**Figure 4.1 Flowchart for chapter 4.**



## 4.2 Introduction

Rice (*Oryza sativa*) is one of the prevalent staple crops for the majority of the people in Southeast Asia and Vietnam. Paddy rice production in Vietnam has consistently increased over the past decade, from 32.5 million tons in 2000 to 45.2 million tons in 2015 (Vietnam GSO, 2017). Concurrently, the area under cultivation has negligibly increased with 7.67 million ha in 2000 to 7.83 million ha in 2015 which indicates agricultural intensification.

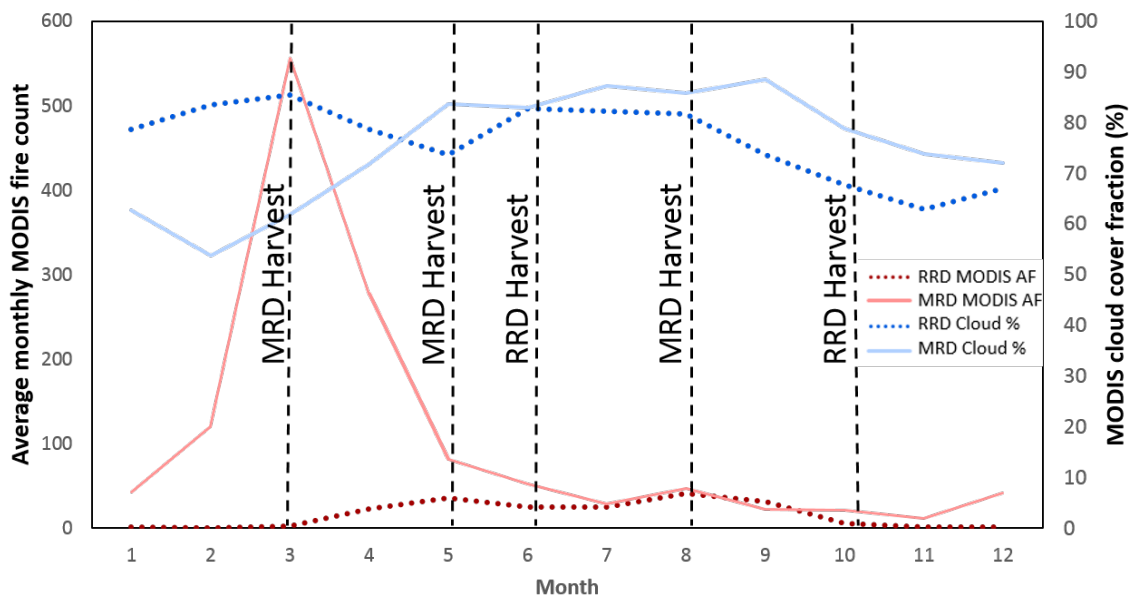
Rice residue (rice straw) is defined as the inedible fibrous plant material left in the field after the harvest. It is routinely burned throughout many rice growing regions such as Philippines, China, India, and Thailand in addition to Vietnam (Badarinath et al. 2006; 2009; Sahai et al. 2007; Zhang et al. 2008; Gadde et al. 2009; Vadrevu et al. 2011; Kharol et al. 2012; Kanokkanjana and Garivait 2013; Hong van 2014; Huang et al. 2016). While other uses for the residue exist such as for animal feed, mushroom cultivation, or bioenergy production, the residue is routinely burned in order to clear the fields for the next crop season. Burning results in emissions of trace gases and aerosols (Streets et al. 2003; Wiedinmyer et al. 2011; Zhang et al. 2017). Unlike most urban or industrial sources, rice burning emissions are focused in a short time period, which has implications for emission inventories, and impacts on local air quality and public health. Studies have suggested significant impact of biomass burning emissions on air quality including rice-wheat residue burning in Punjab, India (Badarinath et al. 2009; Vadrevu et al. 2011; Vadrevu and Lasko 2015); peat and palm plantations in Indonesia (Gaveau et al. 2014; Hayasaka et al. 2014; Vadrevu et al. 2014; Marlier et al. 2015), vegetation fires in southeast Asia (Vadrevu and Justice, 2011; Reddington et al. 2014; Shi et al. 2014; Crippa et al. 2016), agricultural waste burning in China impacting regional and local haze

(Cheng et al. 2014; Zhang and Cao 2015; Liang et al. 2017; Yin et al. 2017). Studies have also shown variation and uncertainty in emissions inventories for biomass burning in agricultural lands (Kurokawa et al. 2013; Saikawa et al. 2017; Shi et al. 2017; Yadav et al. 2017; Lasko and Vadrevu 2018). In addition to local and regional transport, agricultural biomass burning events have been found to transport air pollution such as black carbon through long-range transport, for example with impacts on the Himalayas and across other remote locations (Eckhardt et al. 2007; Ramanathan 2008; Jung and Kim 2011; Vadrevu et al. 2012; Lin et al. 2013; Cayetano et al. 2014; Ikeda and Tanimoto 2015; Yadav et al. 2017). The local and regional effects of biomass burning episodes can persist for weeks to months, impacting atmospheric chemistry, weather, biogeochemical cycles, and animal health (Yan et al. 2006; Badarinath et al. 2009; Cristofanelli et al. 2014; Ponette-Gonzalez et al. 2016; Sanderfoot and Holloway 2017).

High concentrations of fine-particulate matter ( $PM_{2.5}$ ) have been found in urban areas across Southeast Asia including Vietnam, Singapore, Thailand, India, and Indonesia with  $PM_{2.5}$  concentrations averaging 44-168 $\mu\text{g}/\text{m}^3$ , routinely exceeding World Health Organization air quality standards (Oanh et al. 2006). Moreover,  $PM_{2.5}$  can have a high proportion of very fine particles less than 1 $\mu\text{m}$  in diameter with elements such as Pb and Cr, detrimental to human health (Khan et al. 2015; You et al. 2017). These high concentrations in Southeast Asia can be attributed to a variety of sources such as industry, transportation, and biomass burning. Moreover, the detrimental health effects of  $PM_{2.5}$  are even linked to health conditions such as Tuberculosis, as well as premature death (Pope et al. 2007; You et al. 2016).

Use of satellite data for quantifying biomass burning emissions has been demonstrated by earlier studies (van der Werf et al. 2006; Langmann et al. 2009; Mieville et al. 2010; Kaiser et al. 2012; Randerson et al. 2012; Desservettaz et al. 2017; van der Werf et al. 2017). However, monitoring small-holder agricultural fires and resulting emissions is difficult mainly due to the ephemeral nature of agricultural fires, combined with timing of satellite overpass, small flaming fire size, and cloud cover obstructing observations (Justice et al. 2002). For example, in Vietnam, using the MODIS Collection 6 active fires averaged for 2003-2015 and MODIS cloud fraction (Giglio et al. 2016; Platnick et al. 2003), we highlight that relatively low numbers of agricultural fires are detected in regions with known agricultural fires, especially during cloudy months and peak burning times (figure 4.2). While in some other biomass burning regions, significantly more agricultural fires are detected such as in India, China, Myanmar, and

**Figure 4.2 MODIS Collection 6 active fire counts for the Red River Delta and Mekong River Delta averaged with 2003-2015 data. Cloud fraction is over 20% higher during main dry season harvest in RRD (June) than with main harvest in MRD (Feb./March).**



Thailand (Korontzi et al. 2006; Bonnet and Garivait 2011; Giglio et al. 2013; Vadrevu and Lasko 2015; Chen et al. 2017). Thus, because of the difficulty to detect agricultural fires in Vietnam, other approaches may be necessary to indirectly estimate approximate date and location of burning.

In Vietnam, rice is either harvested by machine such as a combine harvester, or by manual cutting (hand-harvest) using sickles or knives to cut the rice crop below the panicle. An example of a hand-harvested field and machine-harvested field with associated pile burning and non-piled burning in Vietnam are shown in figure 4.3. For hand-harvested fields, the rice straw is placed into a pile immediately after it is harvested and threshed, retaining moisture. Whereas in machine-harvested fields the rice is cut and threshed in one collective action, resulting in the rice straw in neat and thin rows within the field leaving the residue more exposed to dry out faster. These harvest practices are important because the resulting residue is burned differently (large, wet piles versus drier and less dense spreading fires). These different burning practices (pile burning versus non-piled burning) result in different combustion behavior such as smoldering or flaming with varied combustion efficiency resulting in different emissions (Korenaga et al. 2001; Christian et al. 2003; Hays et al. 2005; Chen et al. 2010; Akagi et al. 2011; Hayashi et al. 2014; Oanh et al. 2015; Arai et al. 2015; Zhang et al. 2015). Additionally, field studies

**Figure 4.3. Harvested rice fields representative of the two most common burning practice in Southeast Asia and Vietnam. Pictures taken by author in Hanoi Province during June and October 2016.**



have been found to have higher EFs than lab studies, attributed to more realistic field conditions such as residue moisture content (Holder et al. 2017).

Considering the above emissions variations specific to different rice residue burning practices and difficulty in estimating emissions using optical remote sensing data in Vietnam, we specifically addressed the following questions: 1) How do the different emission factors compare between pile burning and non-pile burning? 2). How much do  $PM_{2.5}$  emissions vary for different scenarios based on the different rice straw burning practices; and how do they compare with estimates provided by global studies? 3) How much residue burning emissions are emitted based on synthetic aperture radar (SAR) satellite-based estimates of rice area under cultivation? 4) Considering the limitations of satellite fire detections in this area, are there any indirect approaches useful to estimate



rice residue burning dates? 5) What is the general trajectory of polluted air parcels into Hanoi city during the rice residue burning events, and are there any patterns? We addressed the above questions specific to the Hanoi Capital Region and Vietnam by integrating ground-based measurements, SAR data and combining emission factors for different rice residue burning scenarios.

### **4.3 Study area**

We conducted this study for two focus regions: 1) the entirety of Vietnam to arrive at national-scale rice residue burning emissions; and 2) the rice-dominated provinces of the Hanoi Capital Region (HCR), to highlight spatial location and transport of emissions into this urban area. The HCR includes a large portion of the Red River Delta, Vietnam's oldest and 2<sup>nd</sup> largest rice producing hub after the Mekong River Delta and includes the provinces adjacent to Hanoi. In this study, we included all of the rice-dominated provinces of the HCR with rice area occupying more than 20% of land area according to the Vietnam General Statistics Office: Bac Ninh (44% rice), Hung Yen (43%), Ha Nam (39%), Hanoi (33%), and Vinh Phuc (23%). In the Red River Delta, rice is planted with 2 main seasons: the first in February after the *Tet* holiday and harvested and burned around June, while the second is planted around July and harvested and burned around October. The typical field size in the region is wide ranging, but averages about 800m<sup>2</sup> (Lasko et al. 2017). While rice in the Red River Delta and most of Vietnam is grown in two seasons, in the Mekong River Delta, many farmers practice three rotations of rice resulting in a large amount of rice residues (Kontgis et al. 2015). Much of the rice residues including straw and stubble are subjected to burning to clear the land for the next planting (Pham 2011; Hong Van et al. 2014). Specifically, after the harvest, the rice

residues are either pile burned or non-pile burned (figure 4.3). In addition to rice, the densely populated region is home to over 10 million inhabitants with a vibrant economy including aquaculture, fisheries, mangrove forestry, manufacturing, and construction industries (Devienne 2006).

In this region, local climate conditions of nocturnal radiation inversions during the October burning time, can contribute to an amplified emission effect (Hien et al. 2002). Hanoi, the city with the highest PM<sub>2.5</sub> concentration in Vietnam, has exceedingly high concentrations of PM<sub>2.5</sub> ranging daily from 26-143ug/m<sup>3</sup> with sources especially attributed to secondary pollutant formation, diesel traffic, cookstoves, and industry (Hai and Oanh 2013). Hanoi's monthly PM<sub>2.5</sub> concentrations consistently exceed 35ug/m<sup>3</sup> with the highest during Dec-Mar attributed to drier weather conditions, as well as local traffic and industrial pollution (Oanh et al. 2006; Nguyen et al. 2015).

## **4.4 Methods**

### *4.4.1 Emission factors*

To date, studies have not comprehensively addressed the variation in PM<sub>2.5</sub> emissions from different residue burning practices, a factor which may result in significantly higher emissions than previously thought. Thus, we compiled results from laboratory and field burning emissions estimates of rice straw to address this issue; as these studies have directly or indirectly emulated either pile burning (associated with hand-harvested fields) or non-pile burning (associated with machine-harvested fields). Previous studies typically burn the residues in controlled lab conditions with about 0.1kg to 1kg of rice, whereas field studies are more natural and burn based on actual amount found in the field using in situ devices. With non-pile burning, the residues are mostly dry and burn under flaming

conditions with complete combustion. With pile burning, the residues are usually burned with wetter residue biomass, often resulting in smoldering conditions and incomplete combustion. All selected studies are shown in table 4.1 including a detailed list of emission factors for comparison.

We averaged the emission factors from all selected PM<sub>2.5</sub> studies in table 4.1 to generate the pile burning and non-pile burning emission factors (table 4.2). For pile burning, we selected studies with moisture contents exceeding 20% or if the study mentioned that residues were burned in piles. Whereas for the non-pile burning, we included studies with lower moisture contents (~15% or less) or if pile burning was indicated in the study description. The exact moisture content in the field varies, but averages about 13% in machine-harvested fields with non-pile burning, and about 25% in hand-harvested fields with pile burning as measured from rice residues in Hanoi province prior to burning (Lasko et al. 2017). We note some seasonal variation is also likely. To generate burning-practice specific combustion factors, we averaged combustion factors from three different studies for non-pile burning (Aalde 2006; Sanchis et al. 2014; Romasanta et al. 2017), and 1 study from pile burning (Sanchis et al. 2014). We included fewer studies for combustion factors than emission factors due to lack of availability, or results not interpreted to be representative of the burning practice.

**Table 4.1. List of fine-particulate matter measurements from rice residue burning studies, and their associated burning practice type deduced from interpretation of their study design or as listed in the study. The amount burned per trial indicated residue amount burned in an individual test. We also provide the emission factors and reported error or uncertainty.**

Study	EF (g/kg)	Uncertainty (g/kg)	Burn type	Amount burned per trial	Description
Cao 2008	6.28	1.59	Non-Piled (machine-harvest)	0.5-1.5kg	Air dried residues burned in lab
Oanh 2011	8.3	2.70	Non-Piled (machine-harvest)	entire fields	in situ measurements on machine-harvested fields
Y. Zhang 2013	12.1	4.4	Non-Piled (machine-harvest)	0.3-0.99kg	air dried residues burned in lab; flaming phase EF used
Sanchis 2014	8.66	2.29	Non-Piled (machine-harvest)	3kg	lab measurements with 10% moisture content
Ni 2015	8.5	6.7	Non-Piled (machine-harvest)	0.1-0.2kg	low density, spread fires burned in lab
Christian 2003	4.2	-	Piled (Hand-harvest)	Small piles in field	Spot measurements in selected fields. **They Noted the measurements are likely to be low. Thus, not included in our study
Hays 2005	12.95	2.56	Piled (Hand-harvest)	0.75kg	Piled residues burned in lab
Kanokkanjana 2010	19.21	15.76	Piled (Hand-harvest)	piles in field	Field and outdoor laboratory experiment
Y. Zhang 2013	18.3	13.5	Piled (Hand-harvest)	0.3-0.99kg	Air dried residues burned in lab; smoldering EF used
Sanchis 2014	20.67	3.88	Piled (Hand-harvest)	3kg	Lab measurement with 20% moisture content
T. Zhang 2015	9.6	4.3	Piled (Hand-harvest)	piles in field	In situ measurements on rice residue piles; CO based EF
T. Zhang 2015	20.3	1.5	Piled (Hand-harvest)	piles in field	In situ measurements on rice residue piles; CO <sub>2</sub> based EF
Akagi 2011	6.26	2.36	General agriculture	-	Exhaustive compilation and averaging of global emission factors
Andreae 2001	3.9	-	General agriculture	-	Exhaustive compilation and averaging of global emission factors
Li 2017	14.73	2.42	Unknown	0.01kg	Rice straw burned in small chamber.
Yu 2012	6.28	-	Unknown	N/A (residual mass method)	EF for rice straw PM <sub>10</sub> based on empirical calculation.
Sillapapiromsuk 2013	0.69	-	Unknown	500g	EF for rice straw PM <sub>10</sub> in laboratory chamber experiments

**Table 4.2. Emission Factors (EFs) and Combustion Factors (CFs) used in this study. Factors were obtained from the literature in table 1 and placed into non-pile or pile burning categories based on the moisture content or study design. The EFs and CFs were averaged to obtain burning practice-specific factors.**

<b>Factor</b>	<b>Average and Standard Deviation</b>	<b>EFs/CFs averaged from literature</b>	<b>Notes</b>
Combustion Completeness Factor (non-pile burning)	0.89 ( $\pm 0.08$ )	Aalde 2006 (IPCC); Sanchis 2014; Romasanta 2017	Sanchis et al. 2014 includes ash and burned straw from 10% moisture test
Combustion Completeness Factor (Pile burning)	0.67 ( $\pm 0.07$ )	Sanchis 2014	Factor includes ash and burned straw from 20% moisture test
PM <sub>2.5</sub> emission factor (g/kg) (non-pile burning)	8.8 ( $\pm 1.9$ )	Oanh 2011; Zhang 2013; Cao 2008; Sanchis 2014; Ni 2015	
PM <sub>2.5</sub> emission factor (g/kg) (Pile burning)	16.9 ( $\pm 4.1$ )	Hays 2005; Zhang 2013; Sanchis 2014; Zhang 2015	
PM <sub>2.5</sub> emission factor (g/kg) General agriculture/IPCC	5.1 ( $\pm 1.2$ )	Andreae and Merlet 2001; Akagi 2011	General crop residue burning factors employed by many global studies

#### *4.4.2 Rice area for Hanoi Capital Region*

For the spatially-gridded PM<sub>2.5</sub> emissions in the Hanoi Capital Region (HCR), we derived rice areas from Sentinel-1A C-band SAR imagery for the year 2016 (Lasko et al. 2018). We used a time series of 22 Sentinel-1A IW GRD data obtained from the Alaska Satellite Facility, a direct mirror of ESA's scihub. The Sentinel-1A SAR satellite has a local repeat overpass of approximately 12 days and increasing to 6 days with growing availability of Sentinel-1B imagery. We classified the time series stack of imagery using a random forest classifier with bootstrap aggregated sampling with 1000 trees populated in the forest. Random forest is robust against outliers and over-fitting, nonparametric, has high classification accuracy, and can yield a measure of variable importance (Breiman 2001). In order to highlight spatial variation in emissions resulting from using different SAR datasets for crop area, we processed the SAR imagery into 6 different datasets based on varied SAR polarizations and spatial resolution. They are: Vertical-Vertical (VV) polarized bands at 10m spatial resolution (VV10m), Vertical-Horizontal (VH) polarized bands at 10m spatial resolution (VH10m), and both polarizations at 10m resolution (VVVH10m), as well as the same polarization combinations for 20m imagery (VV20m, VH20m, and VVVH20m). In addition, a robust accuracy assessment following good practices was carried out with overall accuracy exceeding 90% for each dataset (Olofsson et al. 2014) with further details in Lasko et al. 2018.

#### *4.4.3 Rice area for the entirety of Vietnam*

We obtained rice area from the Government of Vietnam for the year 2015 (Vietnam GSO 2017). The dataset is based on a set of surveys conducted by local officials at the

commune-level and has been found to have good overall agreement, and relatively similar results to other rice mapping studies in Vietnam (Kontgis et al. 2015; Nguyen et al. 2015). The data shows a total of 7.8 million ha of rice for Vietnam with 4.3 million ha in the Mekong River Delta and 1.1 million ha in the Red River Delta.

#### 4.4.4 Emissions estimation and scenarios

We calculated the PM<sub>2.5</sub> rice residue burning emissions for both the HCR and entirety of Vietnam based on the following equation 4.1.

$$E_{PM_{2.5}} = A \times FL \times EF \times PB \times CF$$

Where  $E$  is the total PM<sub>2.5</sub> burning emissions for either pile burning or non-pile burning calculated from:  $A$ , the area under cultivation for rice in hectares,  $FL$  is the post-harvest rice residue amount in kg/ha,  $EF$  is the fine-particulate matter emission factor in g kg<sup>-2</sup> averaged from the different studies (table 4.1),  $PB$  is the proportion of rice residue subjected to burning (i.e. not used for cattle feed, cook stoves, etc.), and  $CR$  is the combustion factor indicating the completeness of the combustion (i.e. 0 is failed to burn, and 1 is a complete burn). Combustion factors can be influenced by moisture content, density, and other factors mentioned in the introduction section. For example, a higher combustion factor is seen with non-pile burning found in machine-harvested fields due especially to lower moisture content. We obtained rice area from SAR maps for the HCR and government statistics for the entirety of Vietnam (Vietnam GSO 2017). Following the method in Lasko et al. 2017, we used rice FL of 2700kg/ha (straw), and 6100kg/ha (stubble) and FL of 3470 kg/ha (straw) and 3860kg/ha (stubble) from Hong Van et al.

2014. As the latter FL is representative of triple-cropped fields, it is used for the calculation in the Mekong River Delta. Whereas, the former FL is representative of the common double-cropped rice fields found in the rest of Vietnam. *PB* is assumed as 50% for straw and 10% for stubble gathered from previous field studies in Vietnam (Trach 1998; Nguyen 2012; Hong Van et al. 2014; Duong and Yoshiro 2015; Oritate et al. 2015).

We calculate the emissions for four hypothetical scenarios where: 1) 100% pile burning associated with hand-harvested fields; 2) 100% non-pile burning associated with machine-harvested fields; 3) Approximated current amount based on government data (Vietnam GSO 2017); and 4) Using generalized agriculture emission factors employed in global and regional biomass burning studies. We also calculate emissions uncertainty based on the provided error rates from each study and the approximated error propagation equation for multiplication of quantities where fractional uncertainties add in quadrature (Harvard 2013) as shown in equation (4.2):

$$\delta E_{PM_{2.5}} = |E_{PM_{2.5}}| * \sqrt{\left(\frac{\delta A}{A}\right)^2 + \left(\frac{\delta FL}{FL}\right)^2 + \left(\frac{\delta EF}{EF}\right)^2 + \left(\frac{\delta PB}{PB}\right)^2 + \left(\frac{\delta CR}{CR}\right)^2}$$

Where  $\delta E_{PM_{2.5}}$  is the uncertainty for the  $PM_{2.5}$  emissions equation (1) and the uncertainty ( $\delta$ ) for each variable in equation 1. Proportion burned and crop area data from Vietnam government statistics do not have reported error. Thus, we conservatively assumed twenty percent error in these data.

We also compare our resulting emissions estimates with the Regional Emission inventory in ASia 2.1 (REAS), an all-combustion sources emissions inventory, available

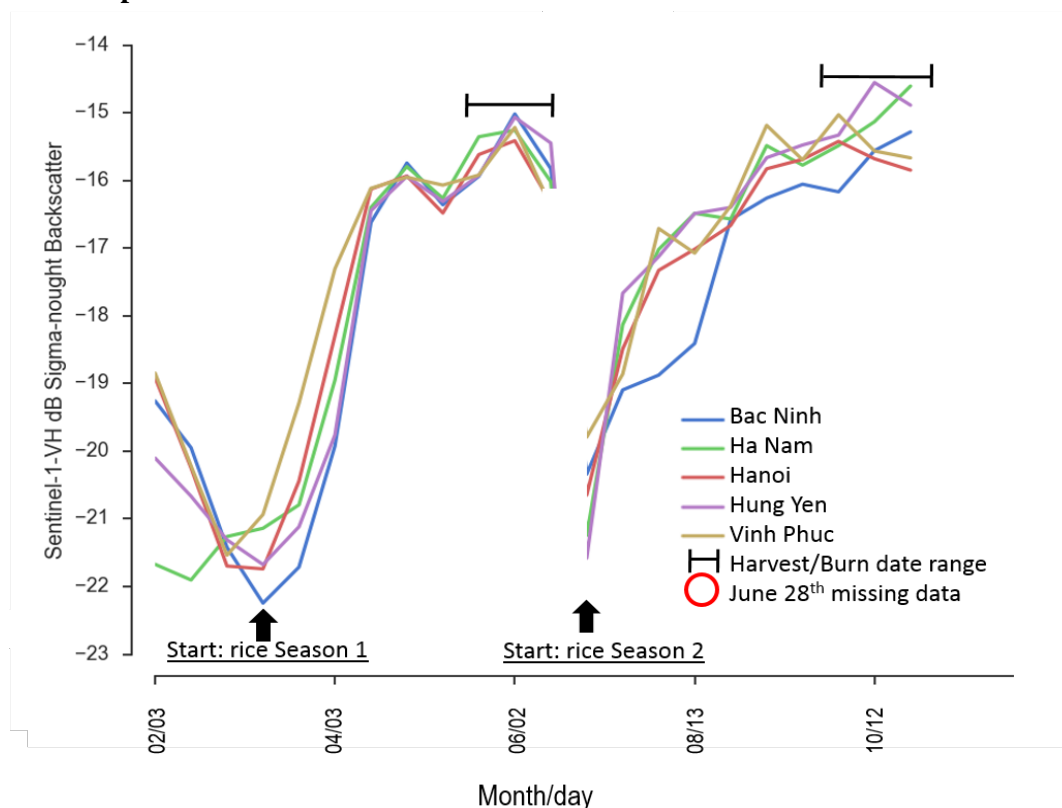


for PM<sub>2.5</sub> for the latest year of 2008 (Kurokawa et al. 2013). The REAS is based on reported industrial activity data and existing survey data as well as other sources. This comparison will yield improved insight into the contribution of rice residue burning to all PM<sub>2.5</sub> emissions.

#### *4.4.5 Date of burning and pollutant transport*

Due to consistent cloud cover and ephemeral agricultural fires in Vietnam, with only an average of about eighty fires detected during the residue burning season within the Red River Delta, other methods are needed to estimate burning (figure 4.2). We employ an indirect approach to estimate date of burning using time series of Sentinel-1A imagery as described in the previous section (figure 4.4). We used a total of 22 VH-polarized images starting on 3<sup>rd</sup> February 2016 and ending on 24<sup>th</sup> October 2016 with images for every 12 days excluding approximately June 28<sup>th</sup> due to no data. The phenology of rice fields has been highlighted in a number of recent studies, where minimum VH-polarized backscatter is observed during sowing because of inundation, and the maximum occurs at or near harvest attributed to removal of water prior to harvest and biomass removal, as well as double-bounce between rice plants and underlying surface and dielectric conditions of the canopy (Inoue et al. 2002; Choudhury and Chakraborty 2006; Bouvet et al. 2009; Lopez-Sanchez et al. 2014; Inoue et al. 2014; de Bernardis et al. 2015; Yuzugullu et al. 2015; Mansaray et al. 2017). We note that incident angle is constant throughout study area and is not a factor on backscatter variation.

**Figure 4.4. Sentinel-1 VH backscatter averaged for each province. For each season, the date where backscatter values reach a maximum, coincides with the rice harvest; then the burning is assumed to occur within 3 days of harvested based on field experience. Note data was unavailable for June 28<sup>th</sup>.**



Within 4km grid cells, we calculate the approximate harvest date based on the date of maximum backscatter within a window of each season based on local growing conditions (i.e. Feb – June for season 1, and Jun – Oct. for season 2). Based on our field experience, we found that rice residues were typically burned within 3 days of harvest (Lasko et al. 2017). Thus, we estimate the burn date by adding three days to the date of maximum backscatter. We then use these dates as the basis for air pollutant transport within the heavily populated study area, where air quality impacts would be strong due to the dense urban population (Hopke et al. 2008).

Back trajectories have been implemented by a number of studies attributing air quality to different biomass burning events in south/southeast Asia and abroad (Reiner et

al. 2001; Eck et al. 2003; Kim et al. 2006; Badarinath et al. 2009; Sharma et al. 2010; Li et al. 2010; Sonkaew and Macatangay 2015; Zhao et al. 2015). For the back-trajectory analysis we use the NOAA Hybrid Single Particle Lagrangian Integrated Trajectory (HYSPLIT) model (Draxler and Hess, 1998; Stein et al. 2015; Rolph et al. 2017) with hourly archived meteorological data from the US National Center for Environmental Prediction (NCEP) Global Data Assimilation System (GDAS). Back-trajectories were calculated during each estimated burn date and 1 day before and after, to account for variation in estimated burn date. The model parameters included: starting a new ground-level (5m), 6 hour back-trajectory every 3 hours with start times selected during the day from 9AM to 6PM within the typical range of burn times and distances (Tipayarom and Oanh 2007; Chen et al. 2017). We ran the HYSPLIT model for a total of 18 different dates.

## **4.5 Results**

### *4.5.1 Rice area estimates*

The rice area maps generated from each of the six datasets had mapped rice areas (in thousand ha) of 214.5 (VVVH10m), 220.3 (VVVH20m), 212.4 (VH10m), 218.8 (VH20m), 208.2 (VV10m), 214.9 (VV20m). Whereas the Vietnam Government data indicated 198.9 ha, showing similar results, with about 7.3% less than our most accurate VVVH10m data. Additional variation due to polarization and spatial resolution is described in Lasko et al. 2018. The rice map together with the field-based fuel-loading factors were used to estimate total rice residue using the factors shown in table 4.2. The resulting rice residue map was the basis for emissions estimation in the Hanoi Capital Region of Vietnam. The total PM<sub>2.5</sub> emissions for the HCR from rice residue burning are

shown in table 4.3 and figure 4.5 including the contribution to total estimated rice residue burning emissions for Vietnam with associated uncertainties in parentheses.

**Figure 4.5. a) PM<sub>2.5</sub> emissions for Vietnam comparing values that would result from Non-Pile Burning (Non-PB), Pile Burning (PB), and most-likely current status (CS) which assumes 50% PB and 50% non-PB based on a report from Vietnam Office of Statistics. B) CS PM<sub>2.5</sub> emissions per 4km gridcell based on the SAR rice map for Hanoi.**

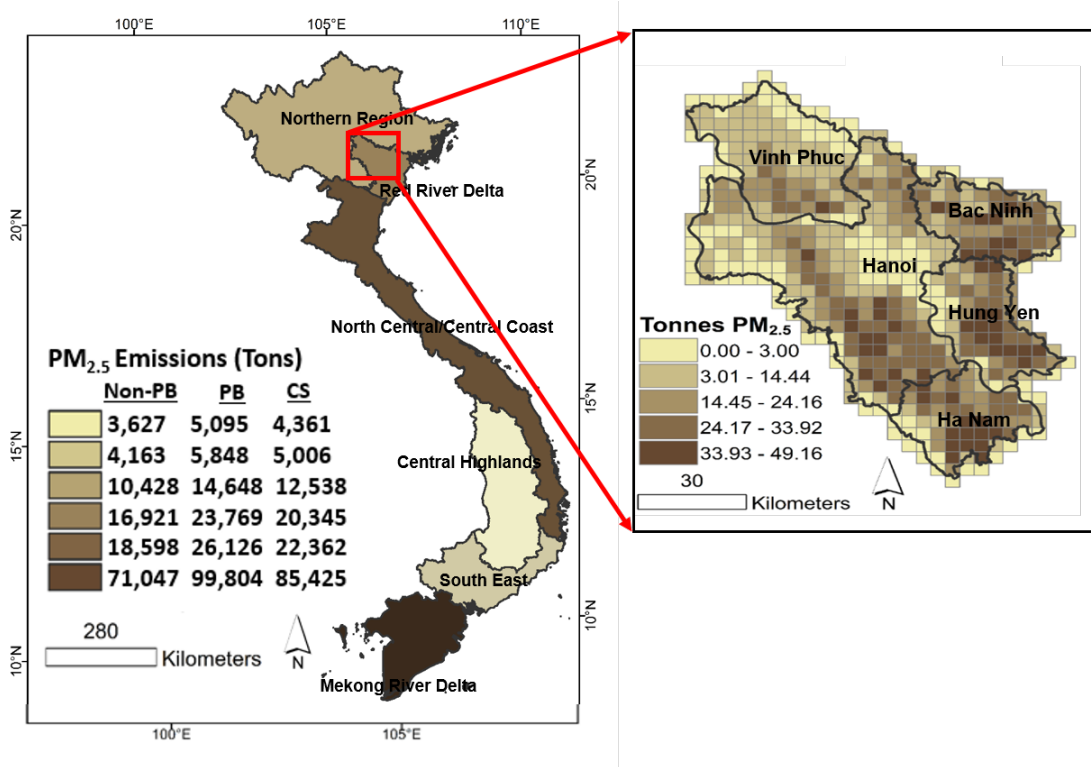


**Table 4.3. Vietnam’s total emissions. PM<sup>2.5</sup> emissions shown in metric tons for the Hanoi Capital Region (HCR) and Vietnam based on the different rice residue burning scenarios. Residue amounts are in terragrams. Note the emissions estimates are shown only to 2 significant digits. Error rates are shown in parentheses for the emissions estimates. The last column shows the total percentage of rice residue burning emissions.**

<b>Rice area dataset</b>	<b>Region</b>	<b>Rice residue amount produced (Tg)</b>	<b>PM<sub>2.5</sub> using general EF/CF</b>	<b>100% pile burning PM<sub>2.5</sub></b>	<b>100% non-pile burning PM<sub>2.5</sub></b>	<b>Most-likely scenario (50/50) PM<sub>2.5</sub></b>	<b>Percent of emissions for entire Vietnam</b>
SAR map	HCR	3.762	3400	9400 (±7,800)	6600 (±4,700)	8000 (±6,200)	5%
Govt. stats	Red River Delta	9.771	11000	24000 (±20,000)	17000 (±15,000)	21000 (±18,000)	14%
Govt. stats	Mekong River Delta	31.58	46000	100000 (±88,000)	72000 (±63,000)	86000 (±76,000)	58%
Govt. stats	Entire Vietnam	62.61	80000	180000 (±150,000)	130000 (±110,000)	150000 (±130,000)	100%

#### *4.5.2 Burning practice specific emission factors*

The PM<sub>2.5</sub> EF's for rice straw burning range from as low as 4.2 g kg<sup>-2</sup> to 20.67 g kg<sup>-2</sup>, whereas the generalized agricultural emission factors used in various global and regional biomass burning studies are 3.9 g kg<sup>-2</sup> and 6.26 g kg<sup>-2</sup>. The pile burning EFs have an average EF of 16.8g kg<sup>-2</sup>(±6.9), as compared to 8.8g kg<sup>-2</sup>(±3.5) from non-pile burning often found in machine-harvested fields, suggesting pile burning emits almost double the PM<sub>2.5</sub> than non-pile burning fire emissions. An even starker contrast is seen between the general agriculture emission factors (i.e. 6.26g kg<sup>-2</sup> in Akagi et al. 2011 and 3.9g kg<sup>-2</sup> in Andreae and Merlet 2001). These results demonstrate a shortcoming and potential underestimation in global studies. While challenging, larger-scale biomass burning studies should employ crop and burning practice specific emission factors in order to best capture biomass burning emissions variation and to avoid significant potential underestimation in the emissions. For example, using the general agriculture emission factor in Akagi et al. 2011 for this study instead of the pile burning emission factor, would yield a 77% difference in the resulting emissions.

The combustion factors ranged from 66.7% to 98.7% with generally lower factors for pile burning. The average for non-pile burning is 89% (±8%), and 67% (±7%) for pile burning. We note that combustion factor measurements are difficult to measure in the laboratory, and thus, may not be completely representative of field conditions with inherent uncertainty. The combustion factor used in general agricultural studies and global studies is 80%, i.e., eighty-percent burned as reported in the IPCC report on greenhouse gas emissions (Aalde et al. 2006).

#### *4.5.3 PM<sub>2.5</sub> emission Scenarios*

The PM<sub>2.5</sub> emissions estimates for non-pile burning and pile burning scenarios are shown for each region of Vietnam (figure 4.5). The majority of emissions are from the Mekong River Delta (72Gg PM<sub>2.5</sub> and 100Gg PM<sub>2.5</sub>) for non-pile burning and pile burning respectively. The lowest emissions are found in the Central Highlands which is characterized by slash and burn agriculture and coffee plantations (Le et al. 2014). In total, for Vietnam 180Gg of PM<sub>2.5</sub> would be emitted if rice residues were burned following the pile burning method with fields harvested by hand, whereas 130Gg would be emitted if rice residues were non-pile burned, a scenario assuming all fields are mechanized and harvested using combine harvesters or similar equipment. The most-likely current emission scenario (50% pile burn, 50% non-pile burning) estimates 150Gg PM<sub>2.5</sub> emissions for the entirety of Vietnam. Overall, there is a 32% difference between pile burning and non-pile burning emission scenarios suggesting that the burning practice plays a very important role in total emissions. The specific emission scenarios with associated uncertainty are shown in table 4.3.

We also compared our emission estimates to an existing all combustion-sources inventory (Kurokawa et al. 2013). The results show rice residue burning contributes to 14%, 18%, and 16% of all combustion sources in Vietnam respectively for non-pile burning, pile burning, and most-likely current situation. This suggests that rice residue burning is one of the major emissions contributors in Vietnam, and is the second largest contributor after fuelwood burning.

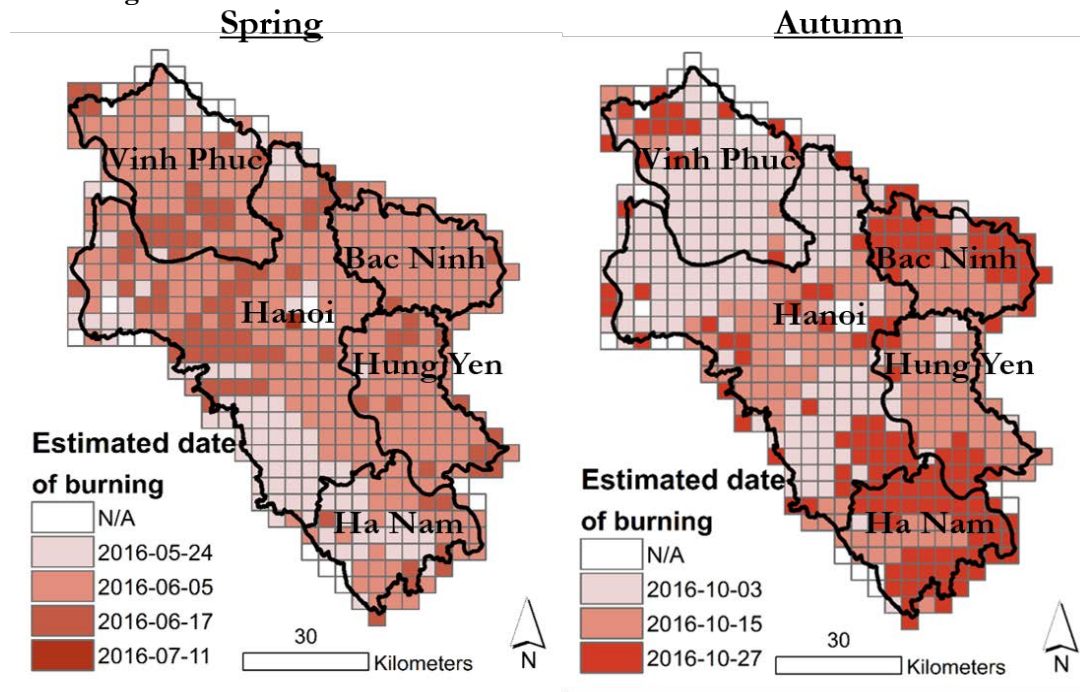
Many large-scale biomass burning studies rely on generalized agriculture emission factors due to currently limited availability of crop, region, or burning-practice specific data (Andreae et al. 2001; Akagi et al. 2011). To estimate emissions for the entirety of Vietnam, we used the 2015 rice area from Vietnam office of statistics and the general agriculture emission factor from Akagi et al. 2011 with general agriculture combustion factor from IPCC (Aalde et al. 2006). The resulting rice residue burning PM<sub>2.5</sub> emissions for Vietnam using these factors would be: 80Gg which is only 44% of pile burning and 62% of non-pile burning. This large difference demonstrates burning practice specific and crop-specific factors are important to improve existing global and regional emission inventories.



#### 4.5.4 Emissions transport

Based on the time-series SAR imagery for 2016, seasonal date of maximum backscatter per grid cell, and 3 day estimate between harvest and burn, we mapped the estimated burn date for each season (figure 4.6). The estimated burn dates were May 24<sup>th</sup>, June 5<sup>th</sup>, and June 17<sup>th</sup> for season one. For season two, the dates of burn were October 3<sup>rd</sup>, October 15<sup>th</sup>, and October 27<sup>th</sup>. These dates are constrained by the 12-day overpass for Sentinel-1 and burn date uncertainty. We subsequently ran the HYSPLIT back-trajectories over Hanoi City, Vietnam on these dates of burning as well as 1 day before and after to account for some variation.

**Figure 4.6. Estimated dates of burning based on the Sentinel-1 SAR maximum backscatter value for each 4km grid cell for Spring and Autumn residue burning seasons.**



Results from the HYSPLIT back-trajectory maps are shown in figure 4.7 and were conducted for the spring and autumn rice burning seasons. Trajectories generally originate from all directions outside of Hanoi City, suggesting potential rice residue

burning impacts. Results stratified by season show that for autumn most trajectories originate from the North while for spring most originate from the South, likely due to synoptic weather patterns. A breakdown for the top 3 wind directions in the spring are: 31% South, 17% southeast, and 17% east; whereas for autumn: 26% North, 24% southeast, and 15% east. The biggest difference was 26% of trajectories originated north of Hanoi in Autumn, but only 6% during Spring as illustrated in the map. Thus, depending on the season, the emissions from different regions and directions will be more impactful in Hanoi City, highlighting the importance of accurate spatial maps of emissions. Overall, the air quality in Hanoi City could be linked with rice residue burning events, but the level of impact will be dependent on seasonal variability and timing and locations of burning. This suggests a need for further research on atmospheric chemical and concentration modelling in Hanoi.

Figure 4.7 (a,b). HYSPLIT back-trajectories stratified by the two burning seasons of Spring (a) and Autumn (b). Trajectory patterns suggested relatively more polluted air parcels moving into Hanoi City originate from the North during Autumn, while more originate the South during Spring.

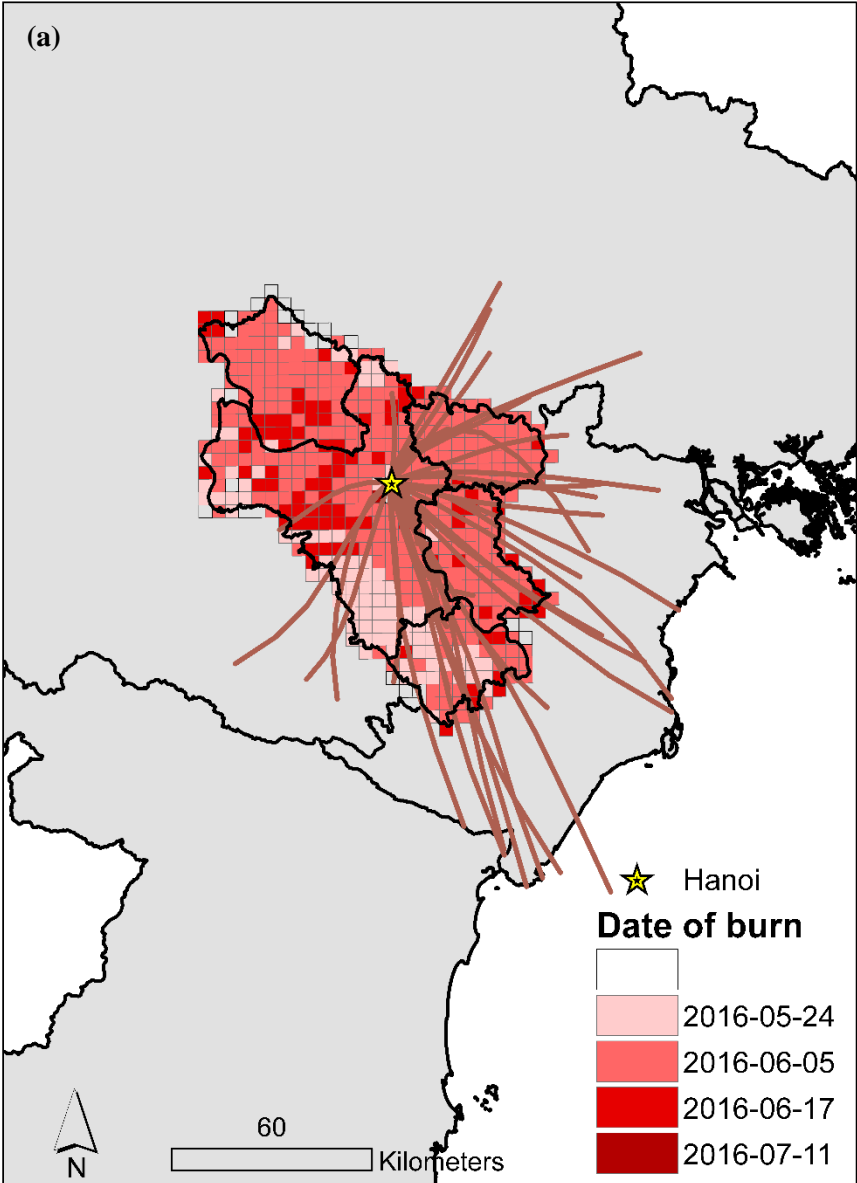
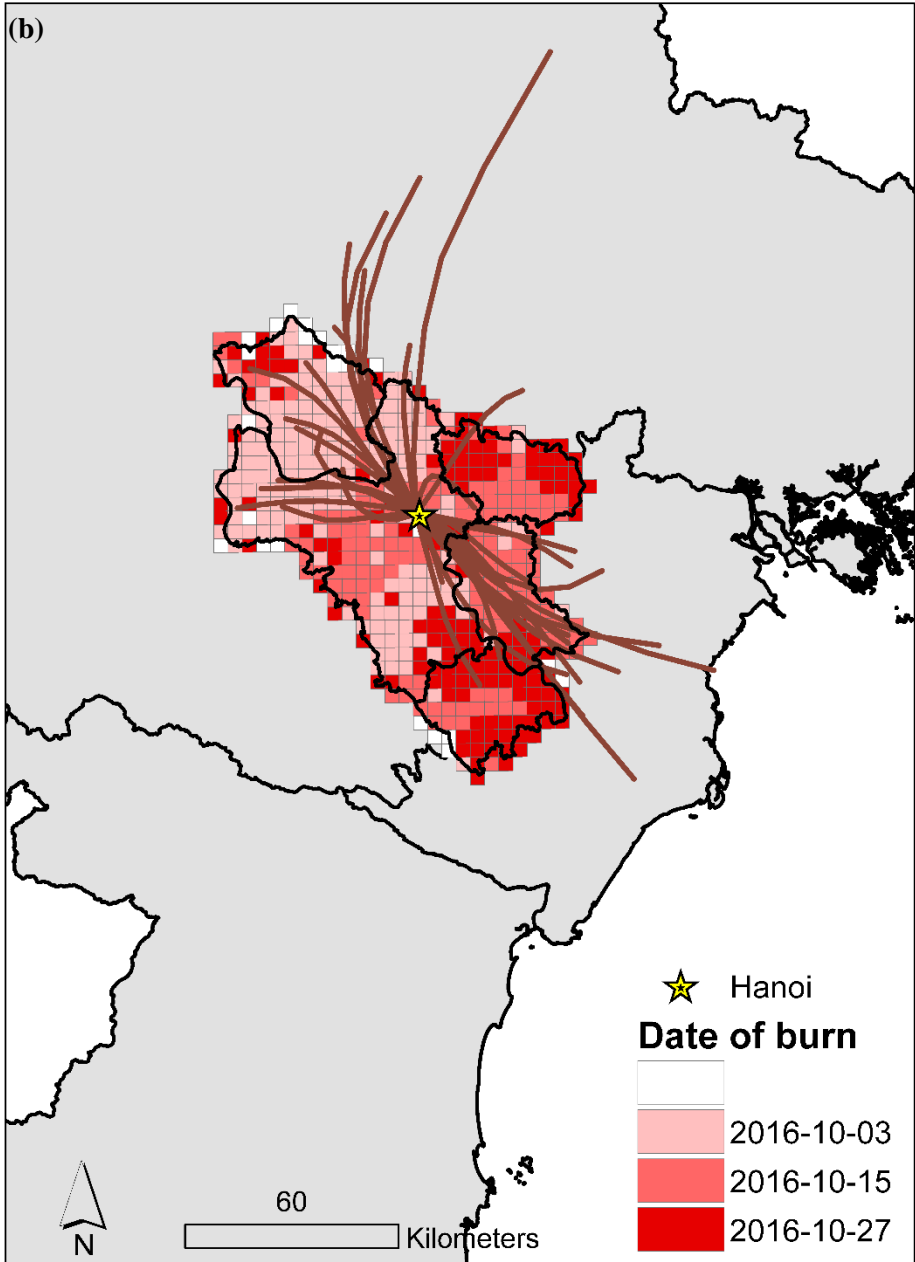


Figure 4.7 (a,b). HYSPLIT back-trajectories stratified by the two burning seasons of Spring (a) and Autumn (b). Trajectory patterns suggested relatively more polluted air parcels moving into Hanoi City originate from the North during Autumn, while more originate the South during Spring.



#### **4.6 Perspectives and conclusions**

Our study illustrates that when burning practice specific emission factors are employed, a large difference is seen between emission estimates. Moreover, our results provide improved estimates of emissions, and also highlight that previous large-scale studies using general emission factors could be significantly underestimating emissions. Our latest estimates for the entirety of Vietnam for year 2015 show that the PM<sub>2.5</sub> emissions likely fall somewhere between 130Gg (100% non-pile burning) and 180Gg (100% pile burned). Our rice residue burning estimates on PM<sub>2.5</sub> thus will add significantly to the overall PM<sub>2.5</sub> emissions such as in the REAS emission inventory (Kurokawa et al. 2013). Our findings also show that rice residue burning contributes to 14% (non-pile burning), 18% (pile burning), and 16% (current situation) of total combustion PM<sub>2.5</sub> emissions in Vietnam in comparison with the REAS. These findings are important for improving upon existing emissions inventories and source apportionment.

These results have an important implication in terms of policy measures and for estimating future emissions. Both our field visit and the literature showed an increasing use of mechanized farming (Oanh et al. 2011; Lasko et al. 2017; Vietnam GSO 2017). As harvesting practices transition from manual to machine-harvesting with non-pile burning, and assuming a constant rate of burning, the emissions could naturally decrease to the non-pile burning level. In addition, it's possible to further mitigate emissions by improving crop residue management practices such as incorporating residues into the field and avoiding GHG emissions from residue burning. Whereas, the pile burning emissions estimates for Vietnam would be representative of historical emissions amounts prior to mechanization of agriculture.

The HYSPLIT trajectory model demonstrates common spatial patterns of rice residue burning emissions transport. With this knowledge, focusing emissions mitigation efforts in areas impacted by rice residue burning could be most beneficial. Some efforts to alleviate emissions impact have included: rice straw mushroom cultivation, enforcement of rice residue burning laws, and education on alternative uses such as for fertilizer, cattle feed, etc.

Our study is limited by several factors. Hanoi experiences higher rainfall during June burning time than during the October burning time. This rainfall could impact the moisture content of the rice residues and resulting emissions. However, with current data limitations we are unable to quantify this effect in a meaningful way. In addition, we found in our field experience that farmers may wait to burn the residues after rain events have cleared and dried up. We also note from our field experience that there may be different amounts subjected to burning based on the harvest and burning practice, however, we are unable to quantify this difference; additional fieldwork is already planned to address this. Another limitation in our study is the combustion factor. Only a few of the compiled studies had combustion factor measurements representative of the different burning practices, and there is a lot of uncertainty in this factor. Future work should explore this factor in more detail to reduce uncertainty. Additionally, the rice area estimates for Vietnam have inherent error, however, there are not any available error rates. Although, recent studies have demonstrated relatively high accuracy with the government rice area estimates in Vietnam (Kontgis et al. 2015; Nguyen et al. 2015; Man et al. 2018). Additionally, we note there is moderate variability and therefore reliability between the different residue burning studies for each burning practice. For example, pile

burning EFs ranged from 9.6g kg<sup>-2</sup> to 20.7g kg<sup>-2</sup>, whereas non-pile burning ranged from 6.3g kg<sup>-2</sup> to 12.1g kg<sup>-2</sup> of PM<sub>2.5</sub>. Future work could improve upon the study reliability and reduce uncertainty. Moreover, future work could improve upon this study by simulating resulting PM<sub>2.5</sub> concentration in Hanoi due to rice residue burning.

Overall our study compiled and combined emissions factors from previous rice residue burning experiments representative of the two common practices of rice straw burning, found especially in Southeast Asia and Vietnam: 1) wet and smoldering conditions found in pile burning associated with hand-harvested fields; and 2) drier and flaming conditions found in non-pile burning associated with machine-harvested fields. We then used these burning practice-specific factors to estimate emissions for Vietnam, and compared emissions based on the general agriculture emission factor relied upon in global or regional studies. Our results showed a 32% difference in emissions between the two different burning practices (pile burning, versus non-pile burning), suggesting burning practice is a major factor for studies to account for in the PM<sub>2.5</sub> emissions equation. We also inferred that when using the global emission factors, PM<sub>2.5</sub> emissions are underestimated by 44% - 77% compared to when using management specific emission factors. In addition, we found seasonal differences in rice residue emissions transport into Hanoi; thus, we believe the emissions impact could be reduced with focused mitigation efforts. Further, we infer that mechanization of agriculture could lead to reduced PM<sub>2.5</sub> emissions from rice residue burning. We also stress on the need to follow crop residue best management practices and alternatives to burning. Overall, our study's novelty demonstrates the importance of burning practices on resulting emissions

estimates, and that burning practice is generally not considered in many existing biomass burning studies.

#### **4.7 Acknowledgements**

The authors give thanks for fieldwork assistance to: Thanh Nhat Thi Nguyen, Hung Quang Bui, Chuc Duc Man, and Ha Van Pham from the Center of Multidisciplinary Integrated Technologies for Field Monitoring at Vietnam National University in Hanoi. Kristofer Lasko acknowledges funding from the American Society for Engineering Education SMART scholarship, and University of Maryland Green Fund Fellowship. Kristofer Lasko thanks his PhD committee members for support: Christopher Justice, Krishna Vadrevu, Ivan Csiszar, Louis Giglio, and Matthew Hansen.

#### **4.8 References**

- Aalde, H., Gonzalez, P., Gytarsky, M., Krug, T., Kurz, W.A., Lasco, R.D., Martino, D.L., McConkey, B.G., Ogle, S., Paustian, K. and Raison, J., 2006. Generic methodologies applicable to multiple land-use categories. IPCC guidelines for national greenhouse gas inventories, 4, p.1-59.
- Akagi, S.K., Yokelson, R.J., Wiedinmyer, C., Alvarado, M.J., Reid, J.S., Karl, T., Crounse, J.D. and Wennberg, P.O., 2011. Emission factors for open and domestic biomass burning for use in atmospheric models. *Atmospheric Chemistry and Physics*, 11(9), p.4039-4072.
- Arai, H., Hosen, Y., Pham Hong, V.N., Thi, N.T., Huu, C.N. and Inubushi, K., 2015. Greenhouse gas emissions from rice straw burning and straw-mushroom cultivation in a triple rice cropping system in the Mekong Delta. *Soil science and plant nutrition*, 61(4), p.719-735.
- Badarinath, K.V.S., Chand, T.K. and Prasad, V.K., 2006. Agriculture crop residue burning in the Indo-Gangetic Plains—a study using IRS-P6 AWiFS satellite data. *Current Science*, p.1085-1089.
- Badarinath, K.V.S., Kharol, S.K. and Sharma, A.R., 2009. Long-range transport of aerosols from agriculture crop residue burning in Indo-Gangetic Plains—a study using



LIDAR, ground measurements and satellite data. *Journal of Atmospheric and Solar-Terrestrial Physics*, 71(1), p.112-120.

Bonnet, S. and Garivait, S., 2011. Seasonal variability of biomass open burning activities in the greater mekong sub-region. *Global Environmental Research*, 15(1), p.31-37.

Boschetti, M., Busetto, L., Manfron, G., Laborte, A., Asilo, S., Pazhanivelan, S. and Nelson, A., 2017. PhenoRice: A method for automatic extraction of spatio-temporal information on rice crops using satellite data time series. *Remote Sensing of Environment*, 194, p.347-365.

Cayetano, M.G., Hopke, P.K., Lee, K.H., Jung, J., Batmunkh, T., Lee, K. and Kim, Y.J., 2014. Investigations of the particle compositions of transported and local emissions in Korea. *Aerosol and Air Quality Research*, 14(3), p.793-805.

Chen, D., Pereira, J.M., Masiero, A. and Pirotti, F., 2017. Mapping fire regimes in China using MODIS active fire and burned area data. *Applied Geography*, 85, p.14-26.

Cheng, Z., Wang, S., Fu, X., Watson, J.G., Jiang, J., Fu, Q., Chen, C., Xu, B., Yu, J., Chow, J.C. and Hao, J., 2014. Impact of biomass burning on haze pollution in the Yangtze River delta, China: a case study in summer 2011. *Atmospheric Chemistry and Physics*, 14(9), p.4573-4585.

Christian, T.J., Kleiss, B., Yokelson, R.J., Holzinger, R., Crutzen, P.J., Hao, W.M., Saharjo, B.H. and Ward, D.E., 2003. Comprehensive laboratory measurements of biomass-burning emissions: 1. Emissions from Indonesian, African, and other fuels. *Journal of Geophysical Research: Atmospheres*, 108(D23).

Crippa, P., Castruccio, S., Archer-Nicholls, S., Lebron, G.B., Kuwata, M., Thota, A., Sumin, S., Butt, E., Wiedinmyer, C. and Spracklen, D.V., 2016. Population exposure to hazardous air quality due to the 2015 fires in Equatorial Asia. *Scientific reports*, 6, p.37074.

Devienne, S., 2006. Red River Delta: fifty years of change. *Moussons. Recherche en sciences humaines sur l'Asie du Sud-Est*, (9-10), p.255-280.

Draxler, R.R. and Hess, G.D., 1998. An overview of the HYSPLIT\_4 modelling system for trajectories. *Australian meteorological magazine*, 47(4), p.295-308.

Duong, P.T. and Yoshiro, H., 2015. Current Situation and Possibilities of Rice Straw Management in Vietnam. University of Tsukuba. Accessed from [http://www.jsrsai.jp/Annual\\_Meeting/PROG\\_52/ResumeC/C02-4.pdf](http://www.jsrsai.jp/Annual_Meeting/PROG_52/ResumeC/C02-4.pdf) .

Eck, T.F., Holben, B.N., Reid, J.S., O'Neill, N.T., Schafer, J.S., Dubovik, O., Smirnov, A., Yamasoe, M.A. and Artaxo, P., 2003. High aerosol optical depth biomass burning events: A comparison of optical properties for different source regions. *Geophysical Research Letters*, 30(20).

- Gadde, B., Bonnet, S., Menke, C. and Garivait, S., 2009. Air pollutant emissions from rice straw open field burning in India, Thailand and the Philippines. *Environmental Pollution*, 157(5), p.1554-1558.
- Gaveau, D.L., Salim, M.A., Hergoualc'h, K., Locatelli, B., Sloan, S., Wooster, M., Marlier, M.E., Molidena, E., Yaen, H., DeFries, R. and Verchot, L., 2014. Major atmospheric emissions from peat fires in Southeast Asia during non-drought years: evidence from the 2013 Sumatran fires. *Scientific reports*, 4.
- Giglio, L., Randerson, J.T. and Werf, G.R., 2013. Analysis of daily, monthly, and annual burned area using the fourth-generation global fire emissions database (GFED4). *Journal of Geophysical Research: Biogeosciences*, 118(1), p.317-328.
- Giglio, L., Schroeder, W. and Justice, C.O., 2016. The collection 6 MODIS active fire detection algorithm and fire products. *Remote Sensing of Environment*, 178, p.31-41.
- Gullett, B. and Touati, A., 2003. PCDD/F emissions from burning wheat and rice field residue. *Atmospheric Environment*, 37(35), p.4893-4899.
- Hai, C.D. and Oanh, N.T.K., 2013. Effects of local, regional meteorology and emission sources on mass and compositions of particulate matter in Hanoi. *Atmospheric environment*, 78, p.105-112.
- Harvard 2013. A summary of error propagation. Accessed from [http://ipl.physics.harvard.edu/wp-uploads/2013/03/PS3\\_Error\\_Propagation\\_sp13.pdf](http://ipl.physics.harvard.edu/wp-uploads/2013/03/PS3_Error_Propagation_sp13.pdf).
- Hayasaka, H., Noguchi, I., Putra, E.I., Yulianti, N. and Vadrevu, K., 2014. Peat-fire-related air pollution in Central Kalimantan, Indonesia. *Environmental Pollution*, 195, p.257-266.
- Holder, A.L., Gullett, B.K., Urbanski, S.P., Elleman, R., O'Neill, S., Tabor, D., Mitchell, W. and Baker, K.R., 2017. Emissions from prescribed burning of agricultural fields in the Pacific Northwest. *Atmospheric Environment*, 166, p.22-33.
- Hong Van, N.P.H., Nga, T.T., Arai, H., Hosen, Y., Chiem, N.H. and Inubushi, K., 2014. Rice Straw Management by Farmers in a Triple Rice Production System in the Mekong Delta, Viet Nam. *Tropical Agriculture and Development*, 58(4), p.155-162.
- Hopke, P.K., Cohen, D.D., Begum, B.A., Biswas, S.K., Ni, B., Pandit, G.G., Santoso, M., Chung, Y.S., Davy, P., Markwitz, A. and Waheed, S., 2008. Urban air quality in the Asian region. *Science of the Total Environment*, 404(1), p.103-112.
- Huang, W.R., Wang, S.H., Yen, M.C., Lin, N.H. and Promchote, P., 2016. Interannual variation of springtime biomass burning in Indochina: Regional differences, associated atmospheric dynamical changes, and downwind impacts. *Journal of Geophysical Research: Atmospheres*, 121(17).
- Ikeda, K. and Tanimoto, H., 2015. Exceedances of air quality standard level of PM<sub>2.5</sub> in Japan caused by Siberian wildfires. *Environmental Research Letters*, 10(10), p.105001.

- Izumi, Y., Demirci, S., bin Baharuddin, M.Z., Watanabe, T. and Sumantyo, J.T.S., 2017. Analysis of Dual-and Full-Circular Polarimetric SAR Modes for Rice Phenology Monitoring: An Experimental Investigation through Ground-Based Measurements. *Applied Sciences*, 7(4), p.368.
- Kaiser, J.W., Heil, A., Andreae, M.O., Benedetti, A., Chubarova, N., Jones, L., Morcrette, J.J., Razinger, M., Schultz, M.G., Suttie, M. and Van Der Werf, G.R., 2012. Biomass burning emissions estimated with a global fire assimilation system based on observed fire radiative power. *Biogeosciences*, 9(1), p. 527.
- Kanokkanjana, K. and Garivait, S., 2013. Alternative rice straw management practices to reduce field open burning in Thailand. *International Journal of Environmental Science and Development*, 4(2), p.119.
- Kanokkanjana, K. Garivait, S., Thongboonchoo, N. et al. 2010. An emission assessment of carbonaceous aerosols from agricultural open burning in Thailand: integrating experimental data and remote sensing. PhD Thesis King Mongkut's University of Technology, Thonburi, Bangkok, Thailand.
- Khan, M.F., Latif, M.T., Saw, W.H., Amil, N., Nadzir, M.S.M., Sahani, M., Tahir, N.M. and Chung, J.X., 2016. Fine particulate matter in the tropical environment: monsoonal effects, source apportionment, and health risk assessment. *Atmospheric Chemistry and Physics*, 16(2), pp.597-617.
- Kharol, S.K., Badarinath, K.V.S., Sharma, A.R., Mahalakshmi, D.V., Singh, D. and Prasad, V.K., 2012. Black carbon aerosol variations over Patiala city, Punjab, India—a study during agriculture crop residue burning period using ground measurements and satellite data. *Journal of Atmospheric and Solar-Terrestrial Physics*, 84, p. 45-51.
- Kim, J., Yoon, S.C., Jefferson, A. and Kim, S.W., 2006. Aerosol hygroscopic properties during Asian dust, pollution, and biomass burning episodes at Gosan, Korea in April 2001. *Atmospheric Environment*, 40(8), p.1550-1560.
- Kontgis, C., Schneider, A. and Ozdogan, M., 2015. Mapping rice paddy extent and intensification in the Vietnamese Mekong River Delta with dense time stacks of Landsat data. *Remote Sensing of Environment*, 169, p.255-269.
- Korenaga, T., Liu, X. and Huang, Z., 2001. The influence of moisture content on polycyclic aromatic hydrocarbons emission during rice straw burning. *Chemosphere-Global Change Science*, 3(1), p.117-122.
- Korontzi, S., McCarty, J., Loboda, T., Kumar, S. and Justice, C., 2006. Global distribution of agricultural fires in croplands from 3 years of Moderate Resolution Imaging Spectroradiometer (MODIS) data. *Global Biogeochemical Cycles*, 20(2).
- Kurokawa, J., Ohara, T., Morikawa, T., Hanayama, S., Janssens-Maenhout, G., Fukui, T., Kawashima, K. and Akimoto, H., 2013. Emissions of air pollutants and greenhouse gases

over Asian regions during 2000–2008: Regional Emission inventory in ASia (REAS) version 2. *Atmospheric Chemistry and Physics*, 13(21), p.11019-11058.

Langmann, B., Duncan, B., Textor, C., Trentmann, J. and van der Werf, G.R., 2009. Vegetation fire emissions and their impact on air pollution and climate. *Atmospheric Environment*, 43(1), p.107-116.

Lasko, K., Vadrevu, K., Tran, V., Ellicott, E., Nguyen, T., Bui, H. and Justice, C., 2017. Satellites may underestimate rice residue and associated burning emissions in Vietnam. *Environmental Research Letters*, 12(8), p.085006.

Lasko K., Vadrevu, K. Tran, V., Justice, C. 2018. Mapping of double and single crop paddy rice using Sentinel-1A imagery at varying spatial scales and polarizations in Hanoi, Vietnam. *IEEE Journal of Selected Topics in Applied Earth Observation and Remote Sensing*, 11(2).

Le, T.H., Nguyen, T.N.T., Lasko, K., Ilavajhala, S., Vadrevu, K.P. and Justice, C., 2014. Vegetation fires and air pollution in Vietnam. *Environmental Pollution*, 195, p.267-275.

Li, C., Hu, Y., Zhang, F., Chen, J., Ma, Z., Ye, X., Yang, X., Wang, L., Tang, X., Zhang, R. and Mu, M., 2017. Multi-pollutant emissions from the burning of major agricultural residues in China and the related health-economic effects. *Atmospheric Chemistry and Physics*, 17(8), p.4957-4988.

Li, H., Han, Z., Cheng, T., Du, H., Kong, L., Chen, J., Zhang, R. and Wang, W., 2010. Agricultural fire impacts on the air quality of Shanghai during summer harvesttime. *Aerosol and Air Quality Research*, 10(2), p.95-101.

Liang, L., Engling, G., Zhang, X., Sun, J., Zhang, Y., Xu, W., Liu, C., Zhang, G., Liu, X. and Ma, Q., 2017. Chemical characteristics of PM<sub>2.5</sub> during summer at a background site of the Yangtze River Delta in China. *Atmospheric Research*, 198, pp.163-172.

Lin, N.H., Tsay, S.C., Maring, H.B., Yen, M.C., Sheu, G.R., Wang, S.H., Chi, K.H., Chuang, M.T., Ou-Yang, C.F., Fu, J.S. and Reid, J.S., 2013. An overview of regional experiments on biomass burning aerosols and related pollutants in Southeast Asia: From BASE-ASIA and the Dongsha Experiment to 7-SEAS. *Atmospheric Environment*, 78, p.1-19.

Lopez-Sanchez, J.M., Vicente-Guijalba, F., Ballester-Berman, J.D. and Cloude, S.R., 2014. Polarimetric response of rice fields at C-band: Analysis and phenology retrieval. *IEEE Transactions on Geoscience and Remote Sensing*, 52(5), p.2977-2993.

Lu, F., Xu, D., Cheng, Y., Dong, S., Guo, C., Jiang, X. and Zheng, X., 2015. Systematic review and meta-analysis of the adverse health effects of ambient PM<sub>2.5</sub> and PM<sub>10</sub> pollution in the Chinese population. *Environmental research*, 136, p.196-204.

Man, C.D., Nguyen, T.T., Bui, H.Q., Lasko, K. and Nguyen, T.N.T., 2018. Improvement of land-cover classification over frequently cloud-covered areas using Landsat 8 time-

series composites and an ensemble of supervised classifiers. *International Journal of Remote Sensing*, 39(4), p.1243-1255.

Mansaray, L.R., Huang, W., Zhang, D., Huang, J. and Li, J., 2017. Mapping Rice Fields in Urban Shanghai, Southeast China, Using Sentinel-1A and Landsat 8 Datasets. *Remote Sensing*, 9(3), p.257.

Mieville, A., Granier, C., Lioussé, C., Guillaume, B., Mouillot, F., Lamarque, J.F., Grégoire, J.M. and Pétron, G., 2010. Emissions of gases and particles from biomass burning during the 20th century using satellite data and an historical reconstruction. *Atmospheric Environment*, 44(11), p.1469-1477.

Nguyen, D., Wagner, W., Naeimi, V. and Cao, S., 2015. Rice-planted area extraction by time series analysis of ENVISAT ASAR WS data using a phenology-based classification approach: A case study for Red River Delta, Vietnam. *The International Archives of Photogrammetry, Remote Sensing and Spatial Information Sciences*, 40(7), p.77.

Nguyen, D.B., Gruber, A. and Wagner, W., 2016. Mapping rice extent and cropping scheme in the Mekong Delta using Sentinel-1A data. *Remote Sensing Letters*, 7(12), p.1209-1218.

Nguyen, T.T., Bui, H.Q., Pham, H.V., Luu, H.V., Man, C.D., Pham, H.N., Le, H.T. and Nguyen, T.T., 2015. Particulate matter concentration mapping from MODIS satellite data: a Vietnamese case study. *Environmental Research Letters*, 10(9), p.095016.

Oanh, N.K., Upadhyay, N., Zhuang, Y.H., Hao, Z.P., Murthy, D.V.S., Lestari, P., Villarin, J.T., Chengchua, K., Co, H.X., Dung, N.T. and Lindgren, E.S., 2006. Particulate air pollution in six Asian cities: Spatial and temporal distributions, and associated sources. *Atmospheric environment*, 40(18), p.3367-3380.

Oanh, N.T.K., Ly, B.T., Tipayarom, D., Manandhar, B.R., Prapat, P., Simpson, C.D. and Liu, L.J.S., 2011. Characterization of particulate matter emission from open burning of rice straw. *Atmospheric Environment*, 45(2), p.493-502.

Oanh, N.T.K., Tipayarom, A., Bich, T.L., Tipayarom, D., Simpson, C.D., Hardie, D. and Liu, L.J.S., 2015. Characterization of gaseous and semi-volatile organic compounds emitted from field burning of rice straw. *Atmospheric Environment*, 119, p.182-191.

Olofsson, P., Foody, G.M., Herold, M., Stehman, S.V., Woodcock, C.E. and Wulder, M.A., 2014. Good practices for estimating area and assessing accuracy of land change. *Remote Sensing of Environment*, 148, p.42-57.

Oritate, F., Yuyama, Y., NAKAMURA, M., YAMAOKA, M., NGUYEN, P.D., DANG, V.B.H., MOCHIDZUKI, K. and SAKODA, A., 2015. Regional diagnosis of biomass use in suburban village in Southern Vietnam. *Journal of the Japan Institute of Energy*, 94(8), p.805-829.

- Pereira, G.M., Alves, N.D.O., Caumo, S.E.S., Soares, S., Teinilä, K., Custódio, D., Hillamo, R., Alves, C. and Vasconcellos, P.C., 2017. Chemical composition of aerosol in São Paulo, Brazil: influence of the transport of pollutants. *Air Quality, Atmosphere & Health*, 10(4), p.457-468.
- Pham, DT., 2011. Mapping paddy cultivation and crop burn areas using MODIS in Mekong Delta, Vietnam (Master's Thesis). Asian Institute of Technology.
- Pham, V.C., Pham, T.T.H., Tong, T.H.A., Nguyen, T.T.H. and Pham, N.H., 2015. The conversion of agricultural land in the peri-urban areas of Hanoi (Vietnam): patterns in space and time. *Journal of Land Use Science*, 10(2), p.224-242.
- Pope III, C.A., 2007. Mortality effects of longer term exposures to fine particulate air pollution: review of recent epidemiological evidence. *Inhalation toxicology*, 19(sup1), p.33-38.
- Randerson, J.T., Chen, Y., Werf, G.R., Rogers, B.M. and Morton, D.C., 2012. Global burned area and biomass burning emissions from small fires. *Journal of Geophysical Research: Biogeosciences*, 117(G4).
- Reiner, T., Sprung, D., Jost, C., Gabriel, R., Mayol-Bracero, O.L., Andreae, M.O., Campos, T.L. and Shelter, R.E., 2001. Chemical characterization of pollution layers over the tropical Indian Ocean: Signatures of emissions from biomass and fossil fuel burning. *Journal of Geophysical Research: Atmospheres*, 106(D22), p.28497-28510.
- Rolph, G., Stein, A. and Stunder, B., 2017. Real-time Environmental Applications and Display sYstem: READY. *Environmental Modelling & Software*, 95, p.210-228.
- Romasanta, R.R., Sander, B.O., Gaihre, Y.K., Alberto, M.C., Gummert, M., Quilty, J., Castalone, A.G., Balingbing, C., Sandro, J., Correa, T. and Wassmann, R., 2017. How does burning of rice straw affect CH<sub>4</sub> and N<sub>2</sub>O emissions? A comparative experiment of different on-field straw management practices. *Agriculture, Ecosystems & Environment*, 239, p.143-153.
- Sahai, S., Sharma, C., Singh, D.P., Dixit, C.K., Singh, N., Sharma, P., Singh, K., Bhatt, S., Ghude, S., Gupta, V. and Gupta, R.K., 2007. A study for development of emission factors for trace gases and carbonaceous particulate species from in situ burning of wheat straw in agricultural fields in India. *Atmospheric Environment*, 41(39), p.9173-9186.
- Sanderfoot, O.V. and Holloway, T., 2017. Air pollution impacts on avian species via inhalation exposure and associated outcomes. *Environmental Research Letters*, 12(8), p.083002.
- Sharma, A.R., Kharol, S.K., Badarinath, K.V.S. and Singh, D., 2010, February. Impact of agriculture crop residue burning on atmospheric aerosol loading—a study over Punjab State, India. In *Annales geophysicae: atmospheres, hydrospheres and space sciences* (Vol. 28, No. 2, p. 367).

- Shi, Y., Sasai, T. and Yamaguchi, Y., 2014. Spatio-temporal evaluation of carbon emissions from biomass burning in Southeast Asia during the period 2001–2010. *Ecological modelling*, 272, p.98-115.
- Son, N.T., Chen, C.F., Chen, C.R. and Minh, V.Q., 2017. Assessment of Sentinel-1A data for rice crop classification using random forests and support vector machines. *Geocarto International*, p.1-15.
- Sonkaew, T. and Macatangay, R., 2015. Determining relationships and mechanisms between tropospheric ozone column concentrations and tropical biomass burning in Thailand and its surrounding regions. *Environmental Research Letters*, 10(6), p.065009.
- Stein, A.F., Draxler, R.R., Rolph, G.D., Stunder, B.J., Cohen, M.D. and Ngan, F., 2015. NOAA's HYSPLIT atmospheric transport and dispersion modeling system. *Bulletin of the American Meteorological Society*, 96(12), p.2059-2077.
- Streets, D.G., Yarber, K.F., Woo, J.H. and Carmichael, G.R., 2003. Biomass burning in Asia: Annual and seasonal estimates and atmospheric emissions. *Global Biogeochemical Cycles*, 17(4).
- Tang, L., Nagashima, T., Hasegawa, K., Ohara, T., Sudo, K. and Itsubo, N., 2015. Development of human health damage factors for PM<sub>2.5</sub> based on a global chemical transport model. *The International Journal of Life Cycle Assessment*, p.1-11.
- Tariq, A., Vu, Q.D., Jensen, L.S., de Tourdonnet, S., Sander, B.O., Wassmann, R., Van Mai, T. and de Neergaard, A., 2017. Mitigating CH<sub>4</sub> and N<sub>2</sub>O emissions from intensive rice production systems in northern Vietnam: Efficiency of drainage patterns in combination with rice residue incorporation. *Agriculture, Ecosystems & Environment*, 249, p.101-111.
- Tipayarom, D. and Oanh, N.K., 2007. Effects from open rice straw burning emission on air quality in the Bangkok Metropolitan Region. *Science Asia*, 33(3), p.339-345.
- Torbick, N., Salas, W., Chowdhury, D., Ingraham, P. and Trinh, M., 2017. Mapping rice greenhouse gas emissions in the Red River Delta, Vietnam. *Carbon Management*, 8(1), p.99-108.
- Vadrevu, K.P. and Justice, C.O., 2011. Vegetation fires in the Asian region: Satellite observational needs and priorities. *Global Environmental Research*, 15(1), p.65-76.
- Vadrevu, K.P., Ellicott, E., Badarinath, K.V.S. and Vermote, E., 2011. MODIS derived fire characteristics and aerosol optical depth variations during the agricultural residue burning season, north India. *Environmental pollution*, 159(6), p.1560-1569.
- Vadrevu, K.P., Ellicott, E., Giglio, L., Badarinath, K.V.S., Vermote, E., Justice, C. and Lau, W.K., 2012. Vegetation fires in the himalayan region—Aerosol load, black carbon emissions and smoke plume heights. *Atmospheric environment*, 47, p.241-251.

- Vadrevu, K.P., Lasko, K., Giglio, L. and Justice, C., 2014. Analysis of Southeast Asian pollution episode during June 2013 using satellite remote sensing datasets. *Environmental Pollution*, 195, p.245-256.
- Vadrevu, K. and Lasko, K., 2015. Fire regimes and potential bioenergy loss from agricultural lands in the Indo-Gangetic Plains. *Journal of environmental management*, 148, p.10-20.
- van der Werf, G.R., Randerson, J.T., Giglio, L., van Leeuwen, T.T., Chen, Y., Rogers, B.M., Mu, M., van Marle, M.J., Morton, D.C., Collatz, G.J. and Yokelson, R.J., 2017. Global fire emissions estimates during 1997–2016. *Earth System Science Data*, 9(2), p.697.
- Vietnam GSO, 2017. General Statistics Office of Vietnam: Agriculture, forestry, and fishery. Accessed from [https://www.gso.gov.vn/default\\_en.aspx?tabid=778](https://www.gso.gov.vn/default_en.aspx?tabid=778) . Note: data from year 2015.
- Wiedinmyer, C., Akagi, S.K., Yokelson, R.J., Emmons, L.K., Al-Saadi, J.A., Orlando, J.J. and Soja, A.J., 2011. The Fire INventory from NCAR (FINN): a high resolution global model to estimate the emissions from open burning. *Geoscientific Model Development*, 4(3), p.625.
- Yadav, I.C., Devi, N.L., Li, J., Syed, J.H., Zhang, G. and Watanabe, H., 2017. Biomass burning in Indo-China peninsula and its impacts on regional air quality and global climate change-a review. *Environmental Pollution*, 227, p.414-427.
- Yang, Z., Shao, Y., Li, K., Liu, Q., Liu, L. and Brisco, B., 2017. An improved scheme for rice phenology estimation based on time-series multispectral HJ-1A/B and polarimetric RADARSAT-2data. *Remote Sensing of Environment*, 195, p.184-201.
- Yin, S., Wang, X., Xiao, Y., Tani, H., Zhong, G. and Sun, Z., 2017. Study on spatial distribution of crop residue burning and PM 2.5 change in China. *Environmental Pollution*, 220, p.204-221.
- You, S., Tong, Y.W., Neoh, K.G., Dai, Y. and Wang, C.H., 2016. On the association between outdoor PM 2.5 concentration and the seasonality of tuberculosis for Beijing and Hong Kong. *Environmental Pollution*, 218, pp.1170-1179.
- You, S., Yao, Z., Dai, Y. and Wang, C.H., 2017. A comparison of PM exposure related to emission hotspots in a hot and humid urban environment: Concentrations, compositions, respiratory deposition, and potential health risks. *Science of The Total Environment*, 599, p.464-473.
- Yu, T.Y., Lin, C.Y. and Chang, L.F.W., 2012. Estimating air pollutant emission factors from open burning of rice straw by the residual mass method. *Atmospheric environment*, 54, p.428-438.



Yuzugullu, O., Marelli, S., Erten, E., Sudret, B. and Hajnsek, I., 2017. Determining Rice Growth Stage with X-Band SAR: A Metamodel Based Inversion. *Remote Sensing*, 9(5), p.460. Zhang, A., Qi, Q., Jiang, L., Zhou, F. and Wang, J., 2013. Population exposure to PM<sub>2.5</sub> in the urban area of Beijing. *PloS one*, 8(5), p.e63486.

Zhang, Y., Shao, M., Lin, Y., Luan, S., Mao, N., Chen, W. and Wang, M., 2013. Emission inventory of carbonaceous pollutants from biomass burning in the Pearl River Delta Region, China. *Atmospheric environment*, 76, pp.189-199.

Zhang, H., Hu, J., Qi, Y., Li, C., Chen, J., Wang, X., He, J., Wang, S., Hao, J., Zhang, L. and Zhang, L., 2017. Emission characterization, environmental impact, and control measure of PM<sub>2.5</sub> emitted from agricultural crop residue burning in China. *Journal of Cleaner Production*, 149, p.629-635.

Zhang, T., Wooster, M.J., Green, D.C. and Main, B., 2015. New field-based agricultural biomass burning trace gas, PM<sub>2.5</sub>, and black carbon emission ratios and factors measured in situ at crop residue fires in Eastern China. *Atmospheric Environment*, 121, p.22-34.

Zhang, Y.L. and Cao, F., 2015. Is it time to tackle PM<sub>2.5</sub> air pollutions in China from biomass-burning emissions?. *Environmental Pollution*, 202, p.217-219.

Zhao, H., Wang, S., Wang, W., Liu, R. and Zhou, B., 2015. Investigation of ground-level ozone and high-pollution episodes in a megacity of Eastern China. *PloS one*, 10(6), p.e0131878.

## Chapter 5: Current status of air pollution over Hanoi, Vietnam using reanalysis data, satellite-based data, and synoptic-scale patterns<sup>4</sup>

### 5.1 Abstract

Air pollution is one of the major environmental concerns in Vietnam. In this study, we assess the current status of air pollution over Hanoi, Vietnam using multiple different satellite datasets and weather information, and assess the potential to capture rice residue burning emissions with satellite data in a cloud-covered region. We used a timeseries of Ozone Monitoring Instrument (OMI) Ultraviolet Aerosol Index (UVAI) satellite data to characterize absorbing aerosols related to biomass burning. We also tested a timeseries of 3-hourly MERRA-2 reanalysis Black Carbon (BC) concentration data for 5 years from 2012-2016 and explored pollution trends over time. We then used MODIS active fires, and synoptic wind patterns to attribute variability in Hanoi pollution to different sources. Because Hanoi is within the Red River Delta where rice residue burning is prominent, we explored trends to see if the residue burning signal is evident in the UVAI or BC data. Further, as the region experiences monsoon-influenced rainfall patterns, we adjusted the BC data based on daily rainfall amounts. Results indicated forest biomass burning from Northwest Vietnam and Laos impacts Hanoi air quality during the peak UVAI months of March and April. Whereas, during local rice residue burning months of June and October, no increase in UVAI is observed, with slight BC increase in October only. During the peak BC months of December and January, wind patterns indicated pollutant transport from southern China megacity areas. Results also suggested severe pollution episodes during December 2013 and January 2014. We observed significantly higher BC concentrations

---

<sup>4</sup> The presented material is under review: Lasko K, Vadrevu K P, and Nguyen T T N 2018 (*in review*). Analysis of air pollution over Hanoi, Vietnam using multi-satellite and MERRA reanalysis datasets. *PLoS One*.

during nighttime than daytime with peaks generally between 2130 and 0030 local time. Our results highlight the need for better air pollution monitoring systems to capture episodic pollution events and their surface-level impacts, such as rice residue burning in cloud-prone regions in general and Hanoi, Vietnam in particular.

## **5.2 Introduction**

Biomass burning, industries, transportation, economic growth, and power production in Southeast Asia have been increasing in recent times, resulting in air pollution and air quality degradation issues throughout Southeast Asia (Streets et al. 2003; Ohara et al. 2007; Kurokawa et al. 2013). Black carbon (BC) is a key short-lived climate pollutant species paramount for air pollution abatement, climate mitigation, and air quality as it can influence regional radiative forcing, precipitation, and monsoon patterns (Ramanathan et al. 2005; Burney and Ramanathan 2014). Moreover, emissions from agricultural rice residue burning, forest biomass burning as well as industrial sources, have all been linked to long and medium range transport of air pollution in different regions of the world. For example, agricultural residue burning in the Indo-Ganges region impacting Himalayas through positive radiative forcing (Ramanathan and Carimichael, 2008; Vadrevu et al., 2014), arctic ice loss attributed to surface albedo change from agricultural fires in Russia (Warneke et al., 2009), air quality degradation in Japan attributed to fires in Russia (Tanimoto et al., 2000), cold season transport of industrial pollutants from China to Korea (Kwon et al., 2002), degraded air quality in Singapore and Malaysia due to peat and palm plantation fires in Indonesia (Hayasaka et al. 2014), as well as biomass burning pollution impacts in Thailand due to local and regional fires from Myanmar, Laos, and Cambodia (Vadrevu et

al. 2014; Marlier et al. 2015; Oh et al. 2015; Biswas et al., 2015; Sonkaew and Macatangay 2015; Chuang et al. 2016).

With the above examples demonstrating complex interplay and interaction of air pollution emissions throughout the world, BC is known to not only absorb visible light, thereby warming the atmosphere, but also contributes to human health problems such as asthma even with short-term exposure (Beverland et al. 2012). BC surface concentration levels are especially influenced by winds, precipitation, planetary boundary layer, as well as atmospheric mixing heights due to sensitivity to wet and dry deposition (Thompson et al. 2001; Dawson et al. 2007; Tai et al. 2010; Jhun et al. 2015). Studies have also demonstrated that the effects from air pollution events can persist on a scale of days to months with impacts on atmospheric chemistry, weather, biogeochemical cycles, and linkage to disease and premature death (Pope and Dockery 2006; Yan et al. 2006; Cristofanelli et al. 2014; Ponette-Gonzalez et al. 2016; You et al. 2016; Sanderfoot and Holloway 2017). However, monitoring pollutant impacts can be limited by uncertainty and discrepancies between air pollution datasets (Saikawa et al. 2017; Shi and Matsunaga 2017).

Of the different countries in Asia, Vietnam emits approximately 83Gg of BC annually, and it is the fifth highest emitter after some of the most populous countries including China, India, Indonesia, and Pakistan (Kurokawa et al. 2013). Much of the BC emissions from Vietnam are concentrated in the capital region of Hanoi, home to over 10 million people (Vietnam office of statistics 2016) with areas of forest biomass burning impacting air pollution in the Northwest, and rice straw burning within the Red River Delta surrounding Hanoi (Le et al. 2014). It's uncertain how much of the air pollution in Hanoi

is due to different sources from the surrounding region. This study explores how and if pollution contribution from other sources impact Hanoi's pollution levels, such as local rice residue burning within the Red River Delta during June and October (Lasko et al. 2017), as well as urban pollution from megacities in Southern China, and absorbing aerosols from forest fires in Laos and Vietnam (Le et al. 2014).

In addition to BC, the Ultra-Violet Aerosol Index (UVAI) can monitor biomass burning events due to their release of absorbing aerosols associated with positive UVAI values (Kaufman et al. 2002; Vadrevu et al. 2015). However, use of this UVAI optical satellite data alone, can be difficult to accurately quantify pollution levels in cloud-covered regions such as Hanoi, Vietnam, as the satellite data can be obscured by cloud cover, although less so than other datasets due to use of UV-spectrum. It may also be difficult to quantify short, but intense biomass burning events such as from rice straw burning in June or October as emission may be focused across several weeks with daily variability and potentially low smoke plume heights. However, reanalysis data which assimilates datasets from a variety of platforms, provides mostly consistent spatiotemporal coverage through time, but with its own limitations.

In this study, we use a time series of reanalysis BC concentration data, as well as satellite-derived UVAI, MODIS active fires, and synoptic meteorology patterns to explore trends in air pollution across Hanoi, Vietnam, and the surrounding region to investigate potential sources of air pollution, as well as to determine if rice residue biomass burning events, which emit a large amount of absorbing aerosols, are captured in the timeseries UVAI or BC data. We also assessed robust 3-hourly datasets of BC using rainfall-adjusted BC analysis based on the meteorology data. In this study, we addressed the following

questions: 1) How does BC concentration in Hanoi vary across different time scales (i.e., hourly, daily and monthly)? 2) What are the major BC influencing factors? 3) How do the BC trends vary after adjusting for atmospheric conditions? 4) How well can rice residue burning emissions from the surrounding areas be linked with air pollution levels in Hanoi? (June and October).

### *5.2.2 Study area*

Hanoi, the cultural center and capital city of Vietnam, is located within the most populous urban area of the country, the Hanoi Capital Region, a substantial portion of the Red River Delta. The landscape includes a wide array of land cover types with the majority allocated to rice, impervious surfaces, and other croplands (Lasko et al. 2018; Man et al. 2018). Hanoi is unique in that it is not only very populous with over 10 million people (Vietnam Office of Statistics 2016), but it exhibits a mosaic landscape covered with small-holder paddy rice, other farms, and plantations all intermixed amongst a growing peri-urban area resulting from ongoing conversion of agricultural lands (Pham et al. 2015). The city has a humid, subtropical monsoonal climate influenced by the northeast monsoon during winter and the southeast monsoon during summer. Hanoi has the highest precipitation during summer (July-Aug) and lowest during winter (Dec-Jan). During many of the drier months, this most polluted city in Vietnam experiences routinely degraded air quality especially from fine particulate matter attributed to a variety of sources such as heavy vehicular traffic in Hanoi, rice residue burning during June and October, as well as regional transport from external sources (Hien et al. 2002; Hien et al. 2004; Oanh et al. 2006; Hai and Oanh 2013; Nguyen et al. 2015).

## 5.3 Data and Methods

### 5.3.1 Merra-2 Reanalysis data

The Modern-Era Retrospective analysis for Research and Applications, Version 2 (MERRA-2) data is an improved, advanced data assimilation system combining hyperspectral radiance and microwave data, GPS-Radio occultation data, ozone profile observations, and several other datasets (Gelaro et al. 2017). It is the first long-term global reanalysis dataset to include satellite-based aerosols and their interactions, with the aerosol data largely based on QFED, GFED, and RETROv2 (Duncan et al. 2003; Randerson et al 2006; Randles et al. 2016; Darmenov and da Silva 2015). The dataset is available at approximately 50km spatial resolution similar to MERRA with a temporal resolution of 1-hour available from 1980-present. The data is freely available from NASA Goddard Earth Sciences (GES) Data and Information Services Center (DISC) in netCDF format. In this study, we obtained the 3-hourly data for 5 years from 2012-2016, and also processed it into corresponding day (9am – 12am), night (12am-9am), daily, monthly, and 3-hourly datasets useful for later comparison. Specifically, we obtained the Black Carbon Surface Mass Concentration (BCSMASS) subset and we processed it into  $\mu\text{g}/\text{m}^3$ . In addition, wind vector data (u and v) were used to derive wind speed and direction using the following equations:

$$ws = \sqrt{u^2 + v^2}$$

Where ws is wind speed in m/s and u and v are the wind vector components in the x and y direction respectively.

$$wd = \text{atan2}(v, u)$$

Where wd is the cardinal wind direction in degrees.

### *5.3.2 Rainfall data*

We obtained 5 years (2012-2016) of daily precipitation from Climate Hazards Group InfraRed Precipitation with Station (CHIRPS), version 2.0 data which combines coarse resolution satellite imagery with in-situ rain station data resulting in gridded rainfall data at approximately 0.05 degree spatial resolution (Funk et al. 2015). We obtained netCDF rainfall data in mm/day and upscaled it to align and match the spatial resolution of MERRA-2 data. The CHIRPS data is freely available from 1981-present.

### *5.3.3 Active Fires data*

For characterizing fire activity, we used the MODIS collection 6 daily active fire hotspot data (MCD14ML) for 2012-2016 (also freely available for years 2000-present). The data comprises of fire locations derived from a contextual algorithm based on the thermal response of fire in the middle-infrared spectrum (Giglio et al. 2003; Giglio et al. 2016). Fire hotspots are detected based on the MODIS instrument onboard the Aqua and Terra satellites with sun-synchronous, polar orbit passing over at approximately 1030am/pm and 130AM/pm local time. The MODIS Advanced Processing System processes the data using the enhanced contextual fire detection algorithm Giglio et al. 2003).

### *5.3.4 Ultraviolet Aerosol Index (UVAI) data*

The daily UVAI data was obtained for 2012-2016 (freely available for years 2004-present). Positive UVAI values indicate the presence of absorbing aerosols such dust, and also black carbon often associated with biomass burning activities. Whereas, negative values indicate non-absorbing aerosols. The OMEAEUV dataset based on the Ozone Monitoring Instrument (OMI) imagery in 354nm – 388nm spectral range produces surface-level UVAI



measurements based on the columnar data and are provided at a spatial resolution of approximately 0.25 degrees (Torres et al. 2007; Torres et al. 2013). Unlike MODIS with a two-satellite constellation, OMI onboard the Aura satellite, operates with a single daily overpass instead of twice daily. Because UVAI values range from negative to positive with low values indicative of cloud cover, we removed all values less than 0.1, in order to better represent pollution values.

#### *5.3.5 Cloud cover data*

Cloud cover data was freely obtained from NASA's Clouds and the Earth's Radiant Energy System (CERES) website. The SSF1deg dataset which contains MODIS cloud area fraction data was obtained for 5 years at a daily temporal resolution and 1 degree spatial resolution (Torres et al. 2007; Torres et al. 2013). This dataset was used to provide ancillary information for the analysis and general cloud cover trends over Hanoi and the rest of the Continental Southeast Asia region.

### **5.4 Methods**

Hanoi, Vietnam has experienced routinely degraded air quality over the past several decades due to urban expansion and development, as well as emissions from rice residue biomass burning typically during June and October (Lasko et al. 2017). While emissions from rice residue burning have been quantified, it's unknown how much impact is measured through the satellite air pollution datasets. We integrated meteorological factors such as wind speed, direction, and precipitation combined with MODIS active fire data to explore BC trends and levels. We also assessed the potential of UVAI for monitoring absorbing aerosols from biomass burning, such as rice residue burning in Hanoi, which is

a heavily cloud-covered region. Moreover, we compare average monthly MODIS cloud fractions over the region, as well as the average monthly number of clear sky observations of OMI UVAI per month.

We employed a timeseries of 3-hourly Merra-2 Reanalysis BC concentration data to explore pollution trends over both Hanoi City as well as the surrounding continental Southeast Asia. We explore the BC concentration and distribution of values throughout the time period using boxplots and timeseries plots, as well as exploring patterns of extreme values through time using the 90<sup>th</sup> and 95<sup>th</sup> percentiles of daily averaged data. We explore the same using 3-hourly data to further explore trends in diurnal variation of BC, and compare day and night values by averaging from 9am – 9PM (Day) and 9PM – 9AM (Night). We further investigate trends in BC concentrations during the rice residue burning months of June and October to determine if BC levels are elevated during these significant biomass burning events which emit a large amount of fine-particulate matter (Lasko et al. 2017). We also investigate pollutant transport and contribution to variability in BC levels from the surrounding region based on synoptic wind direction patterns and biomass burning based on MODIS active fire products averaged on a monthly scale throughout the surrounding continental Southeast Asia region.

To better understand the type of pollutants observed during different months, we compare UVAI values with BC values to infer if the source of pollution can be attributed to biomass burning or not as positive UVAI values can be representative of absorbing aerosols related to biomass burning (Vadrevu et al. 2015).

Lastly, we adjust the BC data based on meteorological parameters such as rain, and compare the original BC with the other ancillary datasets. Rainfall impacts BC levels

significantly due to increased wet deposition. Previous work has adjusted, or detrended, different aerosol species based on meteorological variables and often found non-linear relationship between the pollutant and precipitation (Blanchard et al. 2010; Henneman et al. 2015; Shumway and Stoffer 2015). Rainfall-adjusted values have the most utility for monitoring changes in long-term pollutant trends as well as other long-term studies such as relating to climate, aerosols, and evapotranspiration (Shiogama et al. 2013; Li et al. 2014). A best-fit regression is conducted on the BC and rainfall data resulting in a non-linear power-function fit as,

$$y = a * x^b$$

Where ‘y’ is the daily BC concentration, ‘a’ is a constant and ‘x’ is daily rainfall. The equation can be linearized by taking the base 10 log of both sides of equation to obtain:

$$\log_{10}(y) = \log_{10}(a) + b * \log_{10}(x)$$

Then for each day of BC data we minimize the effects of rainfall by first calculating the residual:

$$residual = y_i - \hat{y}$$

Where  $\hat{y}$  is the predicted BC and  $y_i$  is the observed BC for that day. We then subtracted the residual from our original BC data to get rainfall-adjusted BC concentration useful to compare variation between the biomass burning months and non-biomass burning months and general longer-term trends.

## 5.5 Results

### 5.5.1 *Cloud conditions over Hanoi*

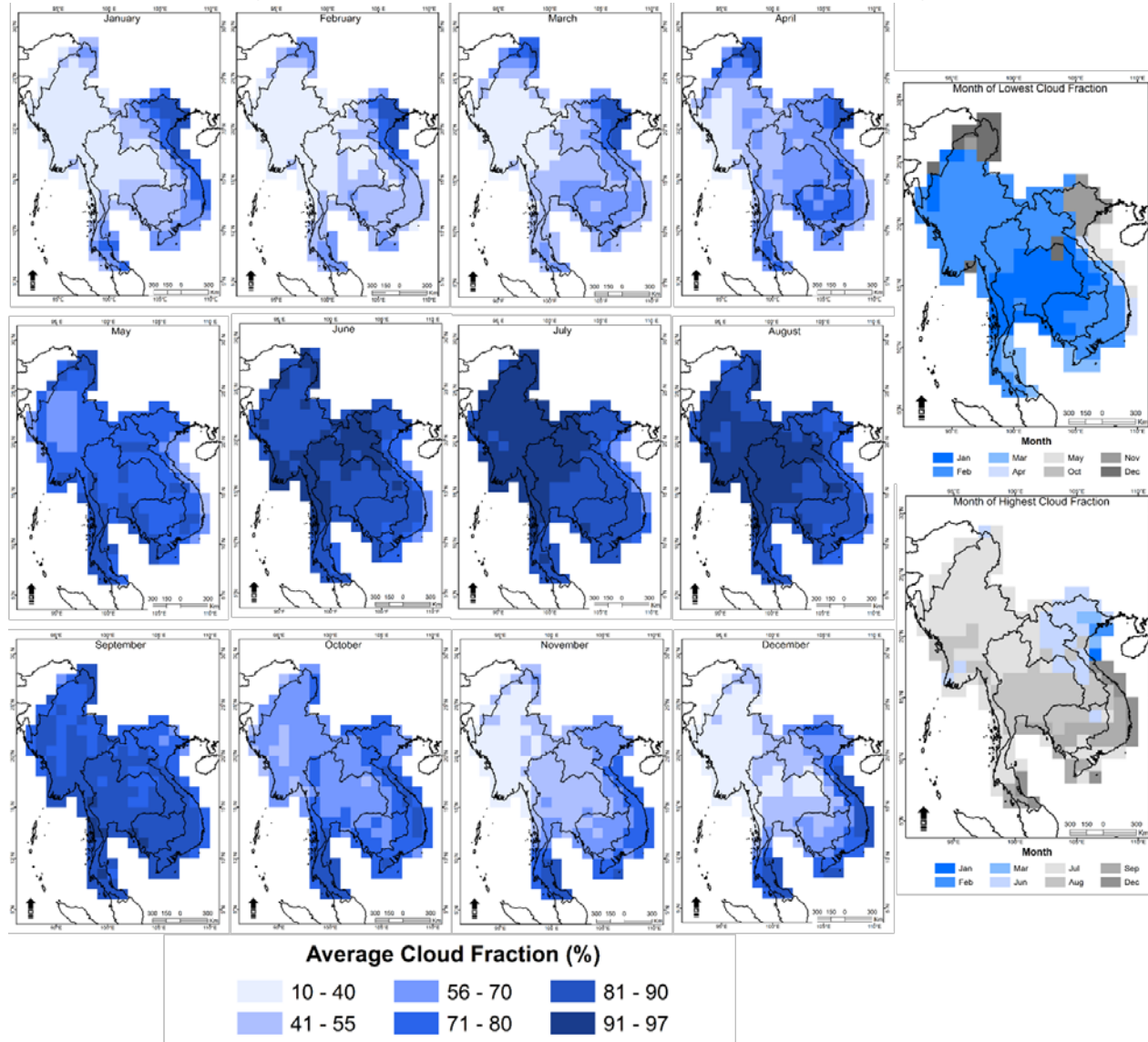
Country-level analysis of cloud cover fraction in continental southeast Asia revealed Vietnam as having the highest monthly average cloud cover (72.4%) followed by Cambodia (69.7%), Laos (67.7%), Thailand (67.6%), and Myanmar (59.9%). Moreover, of these different countries, Vietnam also has the lowest monthly active fire detections with 647 hinting at potential under detections due to cloud cover. Monitoring of active fires from rice residue burning in the Red River Delta is especially difficult. For example, the month of highest cloud cover is during the rainy season of July or August for most of Thailand, Myanmar, Cambodia, and Southern Vietnam. In contrast, Hanoi and the Red River Delta experience highest cloud coverage during the June residue burning time, whereas there are fewer clouds during November and December. In comparing the two rice growing regions of Vietnam, the Red River Delta averages only 25 active fires during the June rice burning time, whereas the Mekong River Delta averages 556 fires during the peak residue burning month of March. This discrepancy can be largely attributed to the higher cloud cover over the Red River Delta during burning months, compounded by relatively smaller field and fire sizes with average field size of about 5000m<sup>2</sup> in the Mekong River Delta compared to about 800m<sup>2</sup> in Hanoi and the Red River Delta (Le et al. 2014; Nguyen et al. 2016; Lasko et al. 2017; Son et al. 2017).

Consistently high cloud coverage over the Red River Delta and Hanoi, has important implications for monitoring air pollution and air quality in these regions. For example, current satellite-based datasets provide daily observations of global air pollution, but cannot provide meaningful local observation if obstructed by cloud.

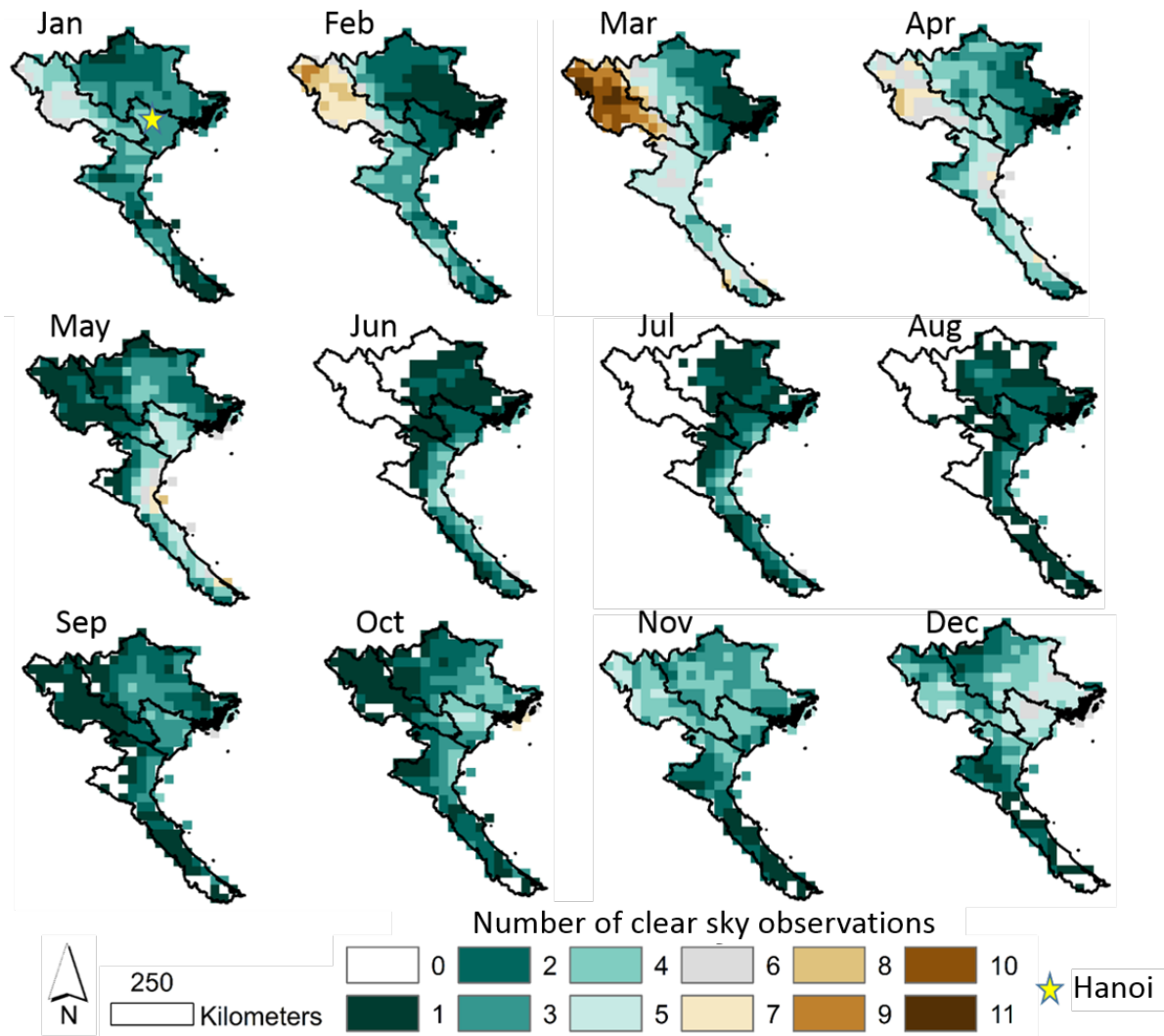
### *5.5.2 UVAI and number of clear observations*

The UVAI is a satellite-derived pollution index sensitive to absorbing aerosols related to biomass burning. The average monthly total number of cloud-free observations for the UVAI (where  $UVAI > 0.1$ ) are shown across Northern Vietnam in figure 5.1. Over Hanoi, the highest number of observations occur during May and December which are generally drier months, still averaging only 5 or 6 clear observations. Whereas, very few observations are recorded especially during rainy months of June-August. The remaining months only experience between 1 and 5 clear observations on average (figure 5.2). This lack of clear observations makes it very difficult to monitor the effects of air pollution with remote sensing. Moreover, because air pollution episodes often occur over rapid time-scales lasting for a few days (Vadrevu et al. 2014; Marlier et al. 2016), severe pollution events could be missed entirely, such as rice residue biomass burning events which occur in June and October.

**Figure 5.1 Cloud cover variation by month averaged for 2003-2014 per 1 degree grid cell; with month of average minimum and maximum cloud fraction shown on the right.**



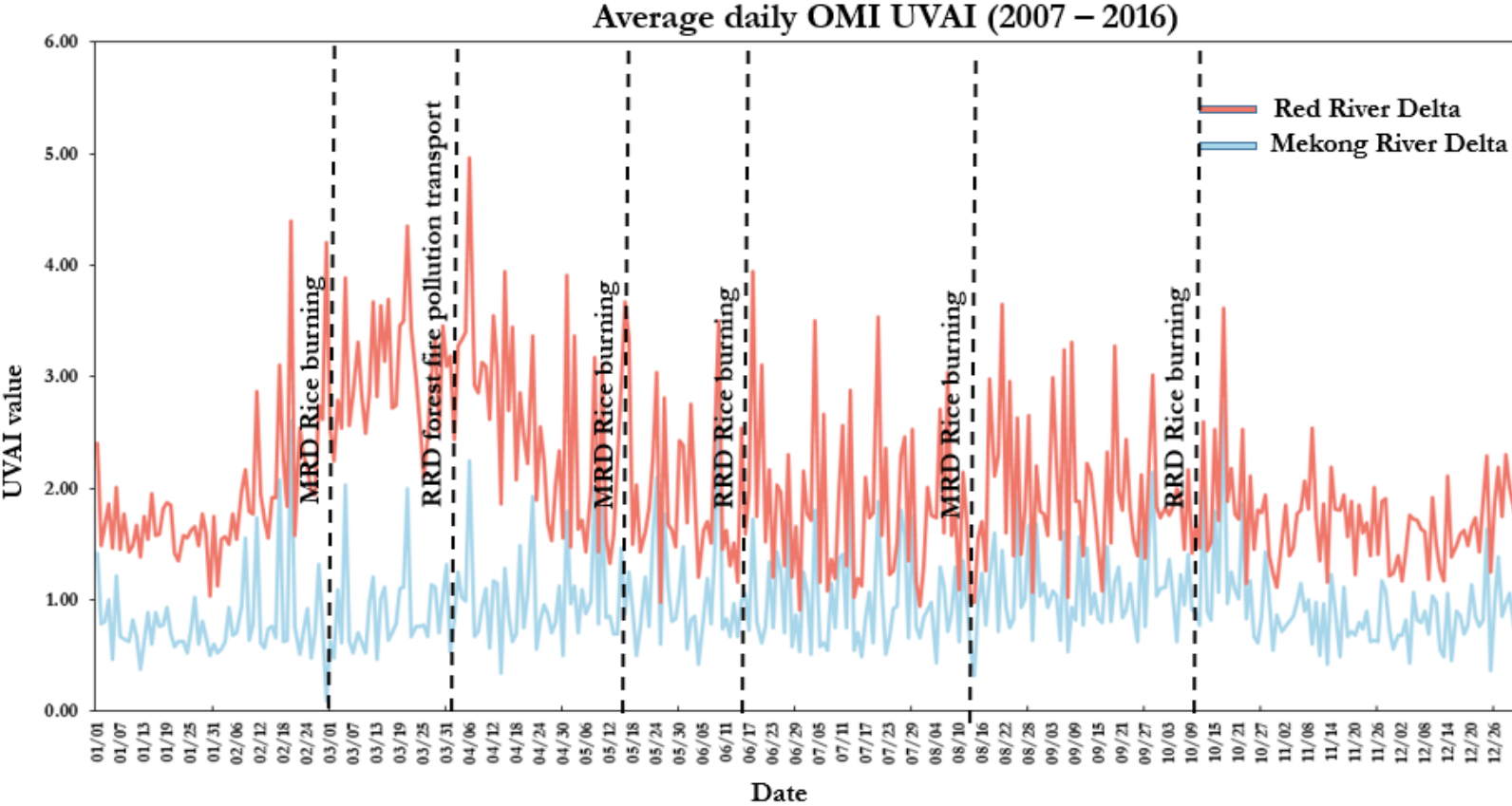
**Figure 5.2 Average monthly number of non-cloudy observations of UVAI over Northern Vietnam.**



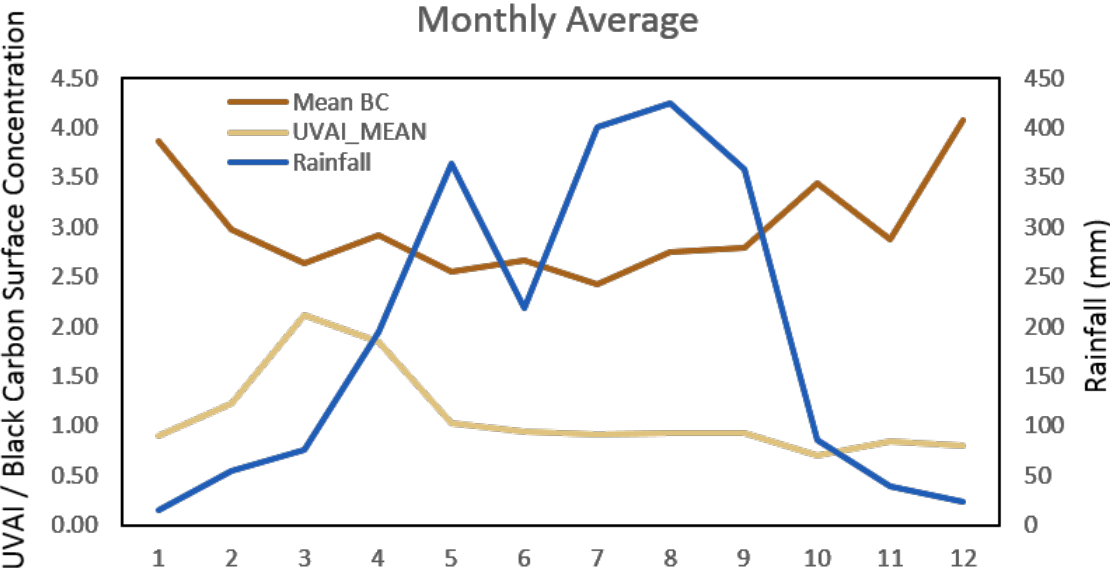
To demonstrate an impact at least partially attributed to clouds or missing data, we show the daily average UVAI values averaged for the Red River Delta in figure 5.3. A peak during March and April is observed where UVAI averages about 3.8 for both months. These are the peak months for air pollution over the region, and it can largely be attributed not only to local sources of pollution, but especially to transport of absorbing aerosols from forest fires in the Northwest of Vietnam and Laos. The latter will be demonstrated in a subsequent section. Aside from the peak during March and April, average monthly values for UVAI only range from 1.2 in December to 1.9 in August showing minimal monthly variation. At a daily-scale, very high values are occasionally observed during the other months such as October when rice residue burning is present (figure 5.3). However, even though a lot of absorbing aerosol pollutants are emitted, monthly average observations do not demonstrate an increase in UVAI during residue burning months of June or October – suggesting the emissions impacts may be almost entirely missed by satellite data (Lasko et al. 2017), as shown in figure 5.4 with rainfall and BC.



Figure 5.3. Average daily OMI UVAI variation shown over the Red River Delta and Mekong River Delta.



**Figure 5.4. Monthly average black carbon concentration ( $\mu\text{g}/\text{m}^3$ ), UVAI, and rainfall (mm) over Hanoi, Vietnam.**



*5.5.3 MERRA-2 BC patterns and de-trending*

Because of the cloud cover issues over Hanoi, we use the MERRA-2 reanalysis BC concentration data which uses a combination of satellite and ground-based datasets with a relatively more complete set of observations. The MERRA-2 BC data at 3-hourly intervals showed more dynamic trends in pollution than those observed through UVAI alone. The 3-hourly data analysis for each month revealed December ( $4.08\mu\text{g}/\text{m}^3$ ), January ( $3.87\mu\text{g}/\text{m}^3$ ), and October ( $3.44\mu\text{g}/\text{m}^3$ ) with the highest median and average monthly values. However, it should be noted that April often experiences the most outlier values suggesting a large amount of pollution episodes (figure 5.5). We also compared the distribution of pollution across day and night (figure 5.5). The results illustrate higher nighttime BC concentrations than daytime values. In addition, the most diurnal variation occurs during rainy season months of June – September. Minimal diurnal variation has been observed during March and April with a difference of about  $0.3\mu\text{g}/\text{m}^3$  between

daytime and nighttime median values for March. Low diurnal variation may be indicative of large-scale persistent biomass burning fires such as from Laos or NW Vietnam where pollutants could be transported through day and night, as compared with urban pollutants such as from traffic, which are more cyclic, exhibiting diurnal variation. Moreover, diurnal variation from rainfall would also have an effect due to wet deposition, however, the rainfall observations are only available once per day.

Analysis of trends using 3-hourly monthly datasets showed the lowest BC values over Hanoi around 3:30am or 6:30am attributed to less vehicular traffic and industrial pollutants (figure 5.5). BC concentration during the evening and nighttime are at least 200% higher than morning concentrations during June, July, August, and September. During the rice residue burning month of June, BC values are not elevated and are relatively similar to neighboring months of May and July. Whereas, during the other rice residue burning month of October, BC concentrations are slightly elevated and about  $0.5\mu\text{g}/\text{m}^3$  higher at each 3-hour period than September –attributed to relatively lower rainfall. BC concentrations are about 19% higher in rice residue burning month of October than in November. Over the 5-year time period on a daily level, the BC concentrations indicated very slight decrease with  $y = -0.003x + 2.7142$  partially attributed to higher rainfall events in 2015 and 2016 (figure 5.6).

Figure 5.5 Distribution of 3-hourly BC surface concentrations: a) per month; and b) stratified by day vs night.

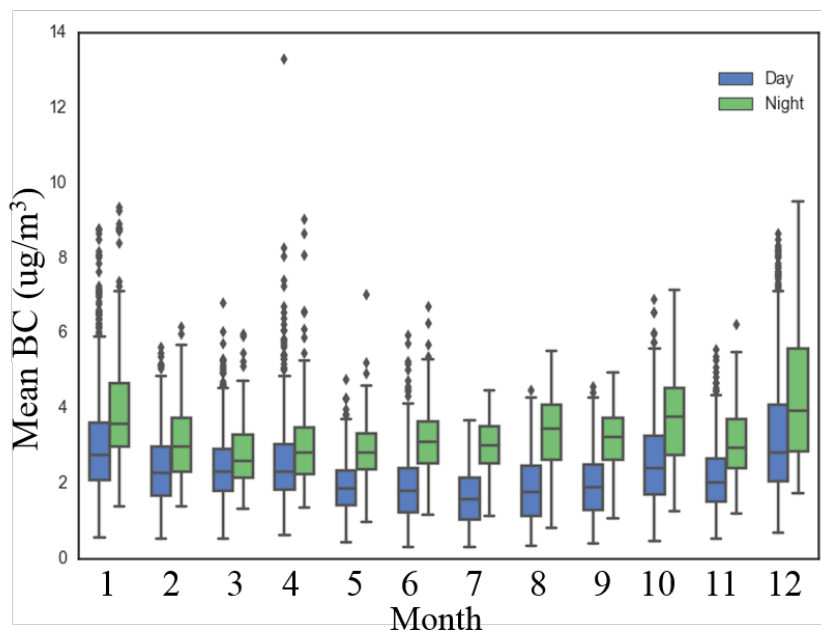
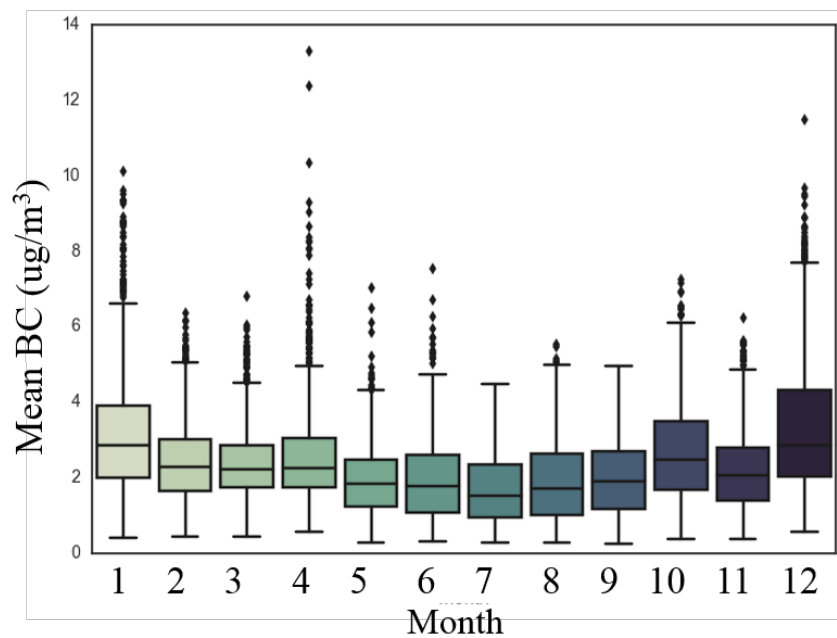
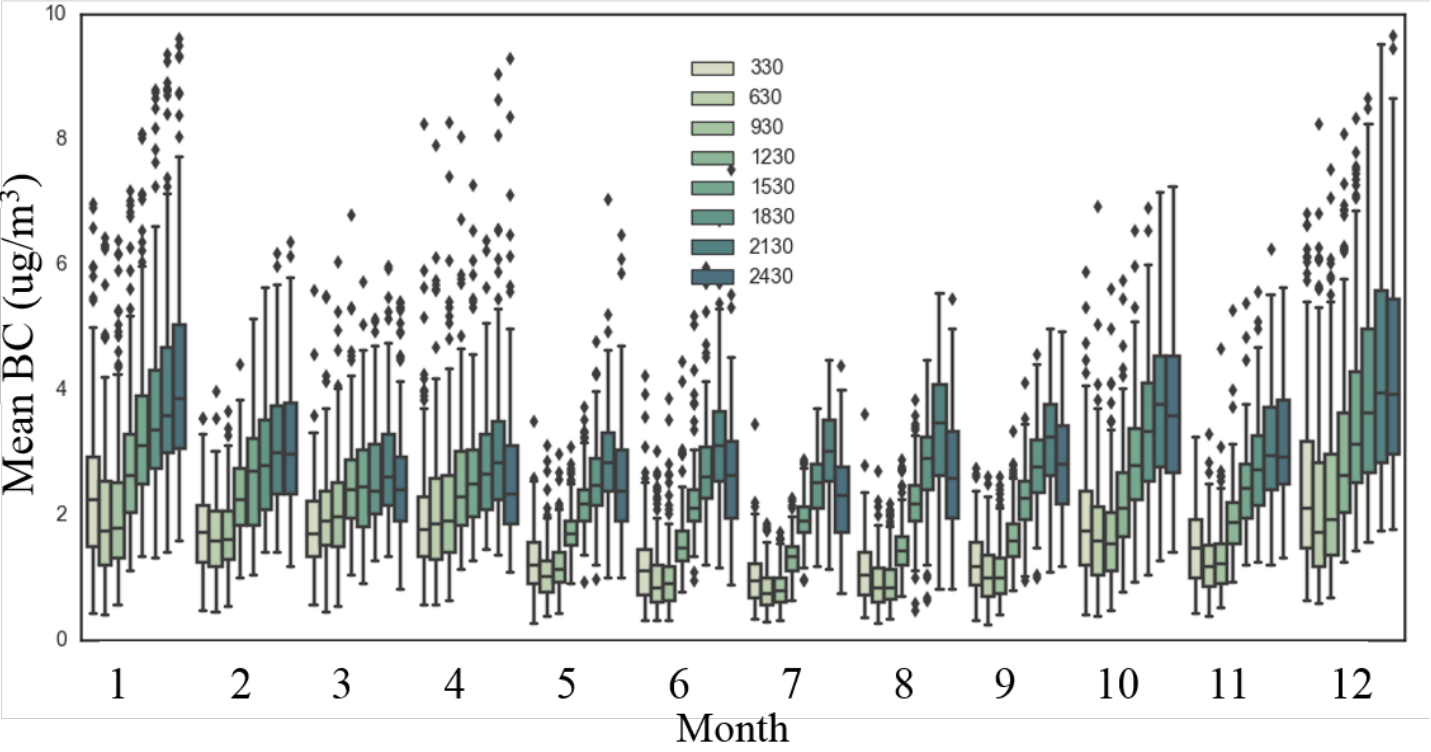
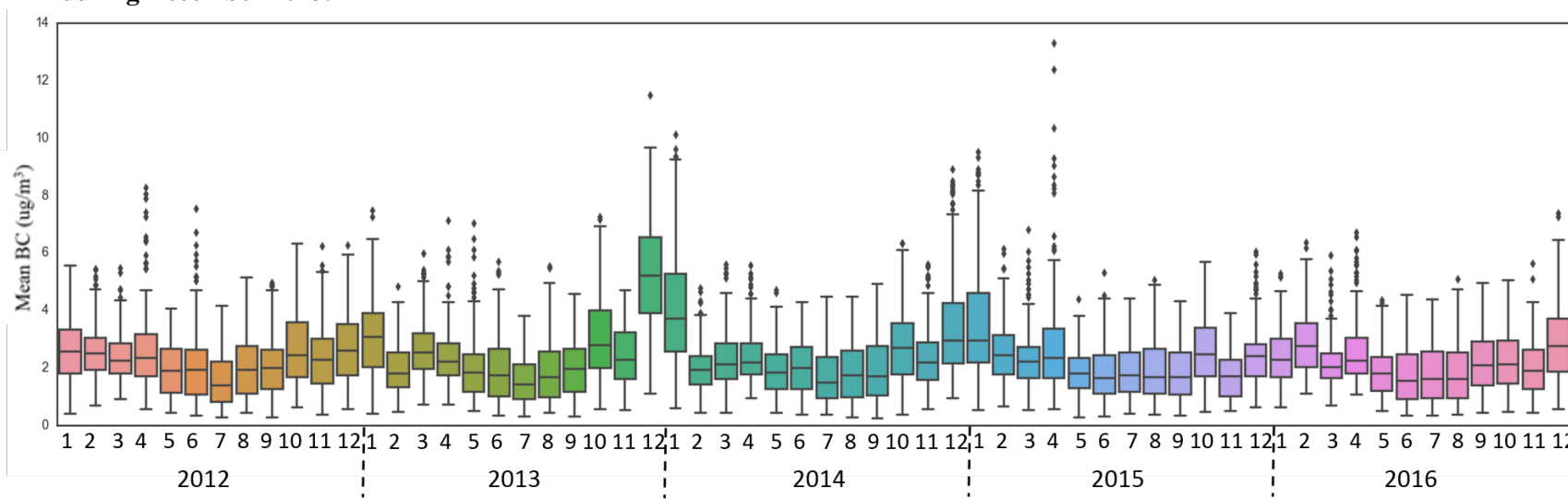


Figure 5.5c: Distribution of 3-hourly BC surface concentrations for each 3-hour time period to highlight diurnal variation.



**Figure 5.6: Monthly distribution of 3-hourly BC surface concentration for the previous 5 years showing a high pollution episode during December 2013.**



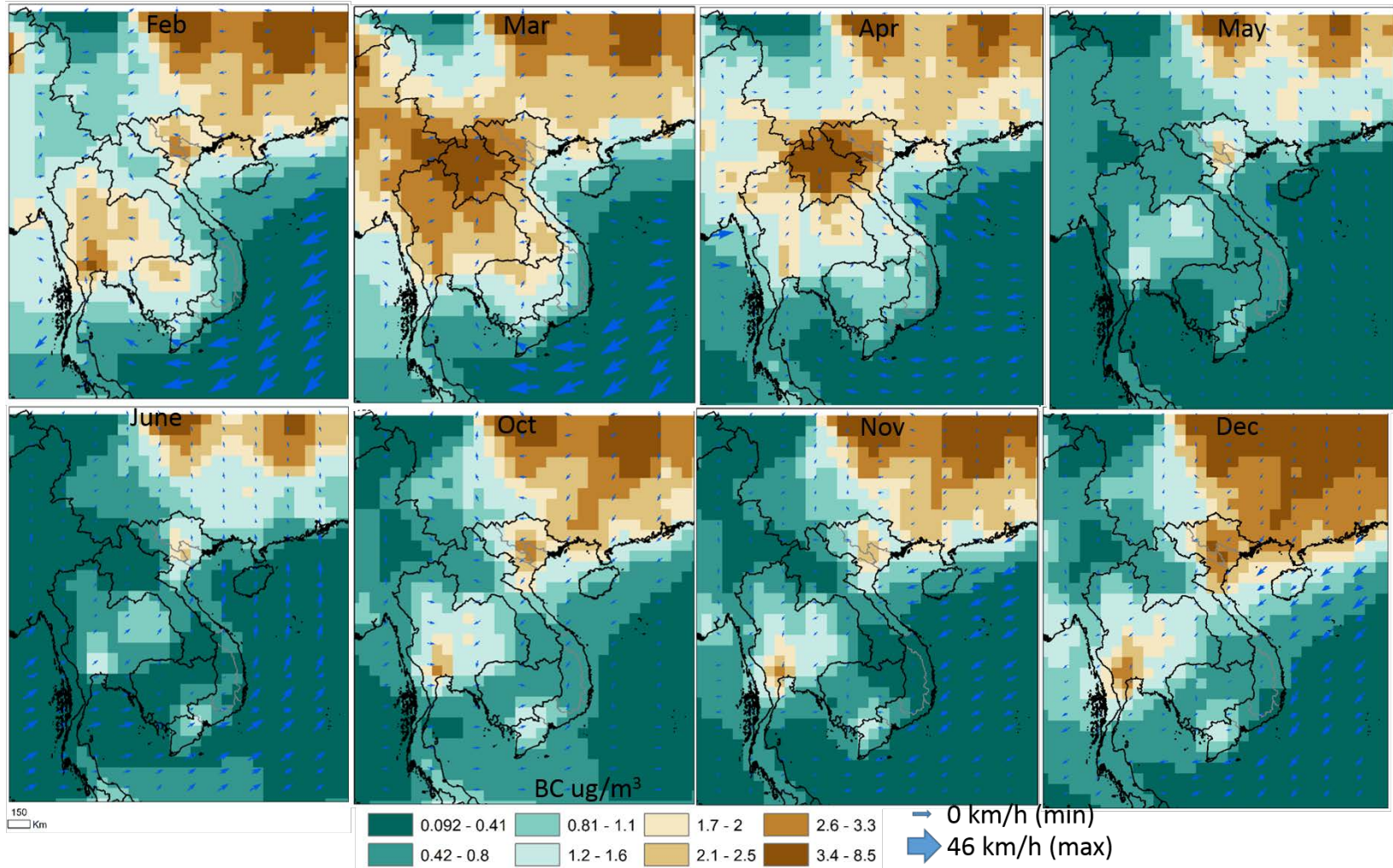
Timeseries distribution of the 3-hourly data for every month shows a cyclical pattern of BC levels aligned with the monsoon and associated rainfall. Abnormally high BC concentrations were observed during December 2013 and January 2014 with median values of  $5.3\mu\text{g}/\text{m}^3$  and  $3.7\mu\text{g}/\text{m}^3$  respectively (figure 5.6). This severe pollution episode may be linked with pollution in South and East China with the pollutants transport from industrial and vehicular sources from mega-urban areas of Chongqing as shown in figure 5.7 (Jiang et al. 2015; Wang et al. 2015). Since, UVAI had a peak only in March and April, we infer that biomass burning impacts over Hanoi are most significant during this time. However, we also know that absorbing aerosols from rice residue burning are emitted in June and October, but no increase in UVAI is observed during these months, suggesting the satellite-based datasets may miss this phenomena over Hanoi. More research with  $\text{PM}_{2.5}$  data may provide insights. In addition, because UVAI is not high during the peak BC months of January and December, we infer that these months may especially be impacted by non-absorbing aerosols from non-biomass burning including transport from other regions (i.e. southern China) and reduced rainfall effects, however the results are inconclusive due to limited UVAI observations in any given month.

While monthly averages and distribution of 3-hourly data provides some insight, they do not highlight temporal characteristics of extreme pollutant events. To better understand extreme pollution events in each month, we explored the exceedance of BC levels above 90<sup>th</sup> and 95<sup>th</sup> percentile (figure 5.8). As expected, results showed most extreme values during December, January, and October followed by April, February, and March. In comparison to the rice residue burning months, June has less than 25 incidences

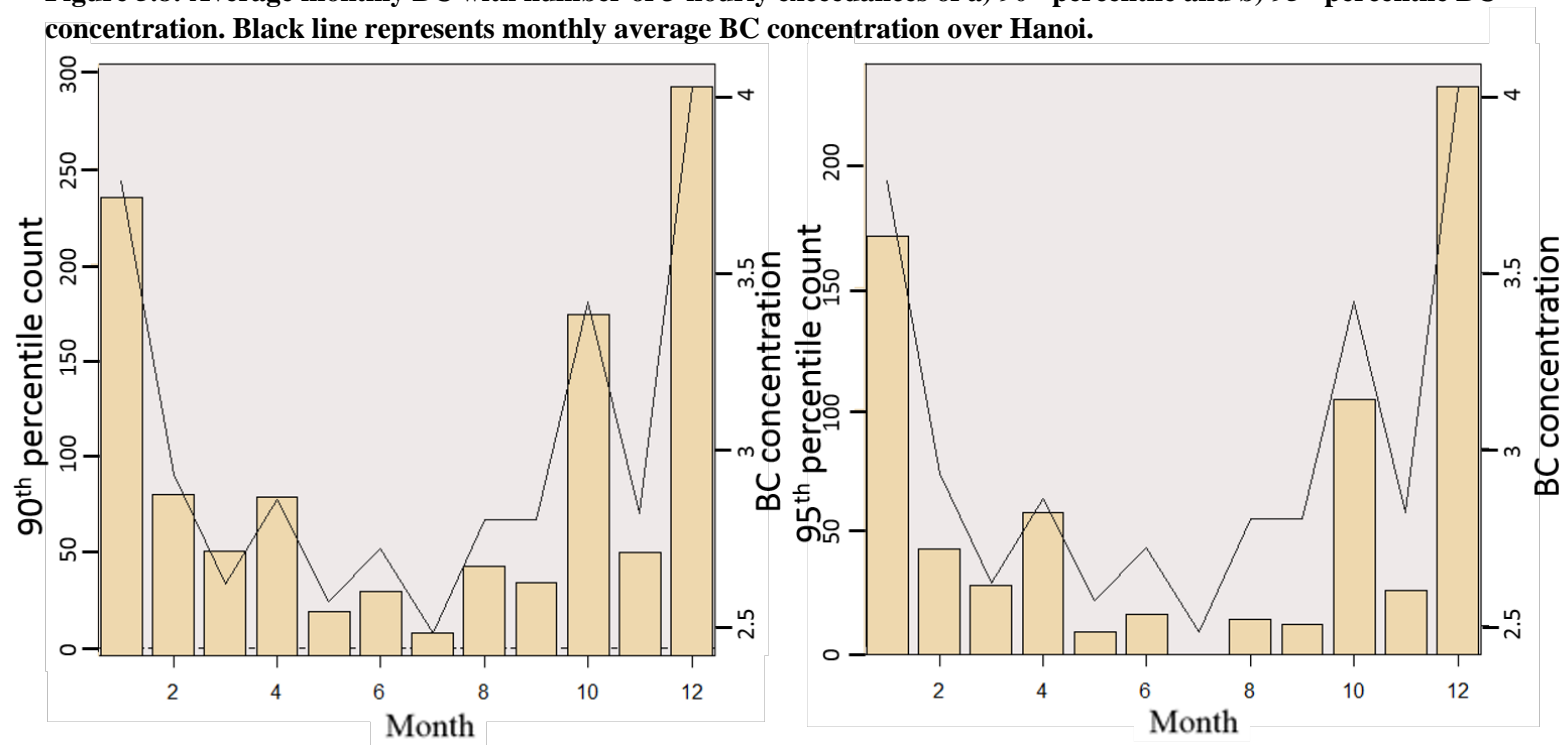
exceeding the 90<sup>th</sup> percentile, whereas October has about 170 suggesting that October may have more residue burning impacts than June.



Figure 5.7. BC concentrations averaged per month with wind direction in blue arrows with sizing based on relative wind speed. Patterns for July-Sept follow similar trend as June. January also omitted for space and shares similar trend to December.



**Figure 5.8: Average monthly BC with number of 3-hourly exceedances of a) 90<sup>th</sup> percentile and b) 95<sup>th</sup> percentile BC concentration. Black line represents monthly average BC concentration over Hanoi.**



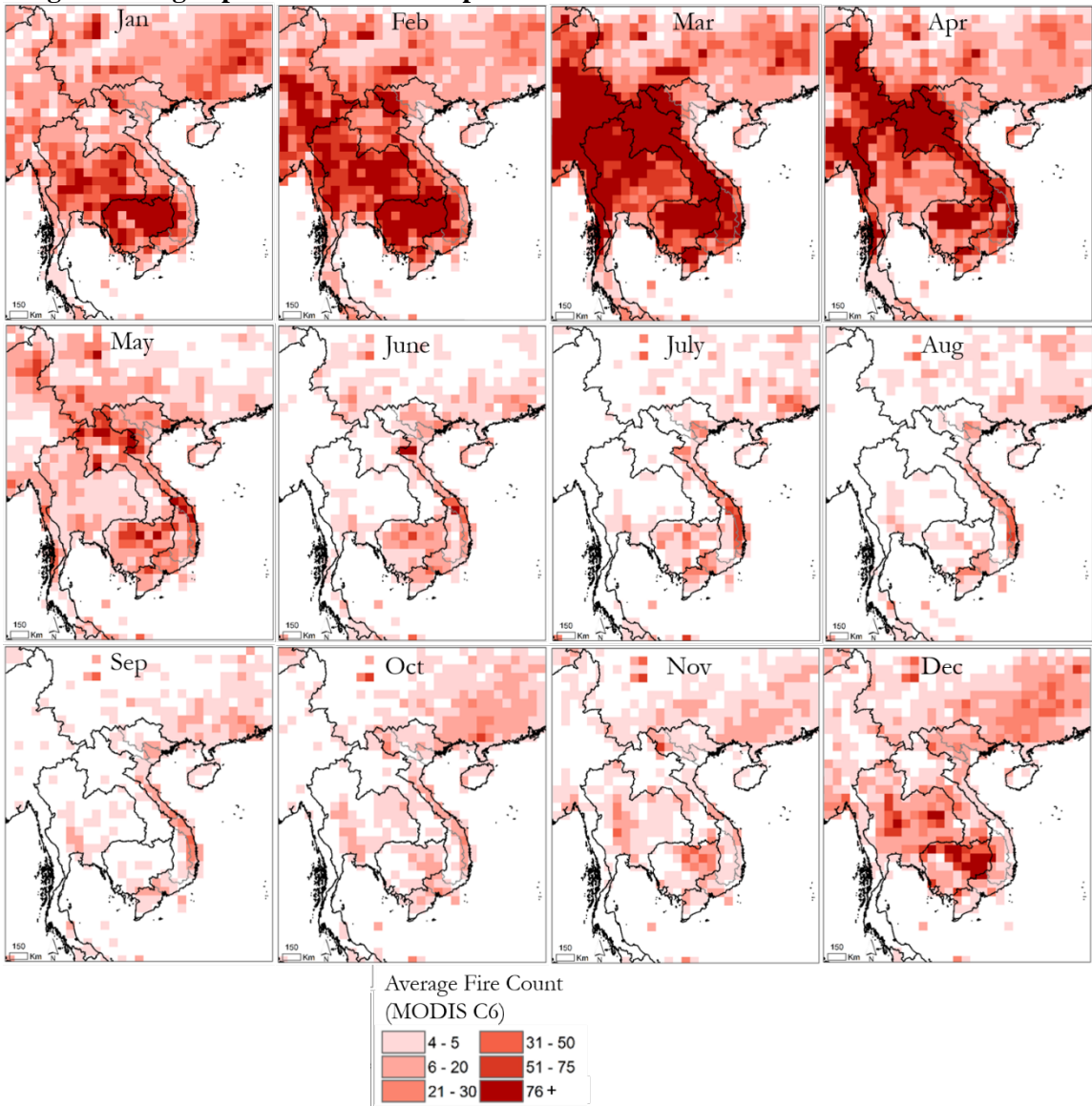
The UVAI values peak during March and April, but are relatively stable in the remaining months. We infer that March and April have the highest air quality impacts due to absorbing aerosols from biomass burning such as those transported from Laos and Northwest Vietnam as described in the subsequent section. Whereas, during the remaining months, low UVAI is observed. This includes peak MERRA-2 BC levels in December and January, however, with relatively low UVAI, we attribute the peak to non-absorbing aerosols from urban sources such as those transported from North of Hanoi and cities in southern China. Elevated UVAI levels are not observed during known rice residue burning months of June and October.

#### *5.5.4 Wind and active fires*

Transport of polluted air into Hanoi becomes apparent from monthly averaged wind direction and speed patterns shown in figure 5.7 along with monthly average BC surface concentrations. General synoptic meteorology patterns indicate northerly winds flowing from South China into Northern Vietnam and Hanoi during October – March, whereas during Apr-Aug more south or southeasterly winds from Laos, Southern Vietnam, and the South China Sea. BC levels in the Southeast Asia region show a peak during March across Thailand and Myanmar attributed to agricultural and small-holder burning (figure 5.9) (Vadrevu et al. 2015). During March and April, high BC values over Laos and Northwest province of Vietnam are attributed especially to forest fires and slash and burn agriculture (Le et al. 2014). Relatively high BC levels throughout all months are consistently observed from Southern China largely originating from the mega-urban Chengdu and Chongqing

cities with biomass burning also as a non-negligible emission source during these months (Wang et al. 2015).

**Figure 5.9. MODIS active fire trends in the surrounding continental Southeast Asia region averaged per month at same spatial scale as MERRA-2.**



Trends in the latest MODIS collection 6 active fire algorithm show peak burning in March and April as well as high levels of burning during Jan-Feb across much of Laos, Myanmar,

Vietnam, Cambodia, and Northern Thailand due to forest and agricultural biomass burning (figure 5.9). Relatively low active fires are detected across the region during June – November, a large portion of which is attributed to the rainy season (table 5.1).

BC concentrations during October reach as much as 45% higher than the following month of November with the largest difference in 2015. On average, BC levels are 19% higher in October than November. These two months are relatively comparable due to synoptic wind patterns, rainfall, and active fires, as well as being adjacent in time.

**Table 5.1 Average monthly MODIS active fire counts within 1000km of Hanoi**

Month	Avg. fire count	Location
Jan	22,795	Thailand, Cambodia
Feb	31,544	Thailand, Cambodia, China, N/E/W of RRD
Mar	68,618	Laos, Thailand, N/China, E China, NW Vietnam
Apr	43,402	Laos (MAX), NW Vietnam (MAX), N China, E China Low,
May	6,777	Laos (medium), N Vietnam (low/med), E China (Low), Thailand (low)
June	1,994	E China (low-Med), NCC Vietnam (med), E of RRD (low/med)
July	1,078	RRD fires, E China
Aug	1157	RRD, E china (low)
Sep	986	RRD, E China (low/low-med)
Oct	1,811	E China: Medium, NW Vietnam (low)
Nov	1,963	N China, E China (low-med), NW Vietnam (low)
Dec	7,598	E China (med-high), N China (med-h9gh), Thailand (med-low), NW Vietnam (med), E of RRD (med-high)

#### 5.5.5 Rain

Monthly rainfall patterns show a peak during July and August averaging 401 and 425mm respectively. Whereas October – March are relatively dry ranging from 84mm in October to 14mm in January (figure 5.4). Over a five year period we observed a slight increasing trend in rainfall. For comparison purposes and to explore rice residue burning impact, we

compare October (84mm rain) and November (39mm rain) due to similar rainfall, wind, active fires, and proximity. We note June (218mm rain) is more difficult to analyze air pollution concentration due to much different rainfall than adjacent months, therefore the pattern may be observed in de-trending. Moreover, the higher rainfall in June may contribute to relatively lower impact from rice residue burning than during October as seen in the BC data.

We adjusted the timeseries BC data based on the rainfall data over Hanoi to yield weather-adjusted BC values. Results show a negative non-linear power function trend where BC decreases as rainfall increases with about 17% of variation in BC attributed to rainfall (figure 5.10). Results show the weather-adjusted values are much less variable through time and that BC values are much lower in many months such as June, July, and August due to rainfall events. However, the de-trending reduced overall monthly variation in the BC dataset with lowest concentration during August at  $2.3\mu\text{g}/\text{m}^3$  and highest in January with  $2.76\mu\text{g}/\text{m}^3$ . The highest standard deviation of the daily BC data is during February, January, and October respectively ranging from  $0.45$  to  $0.40\mu\text{g}/\text{m}^3$  (figure 5.11).

**Figure 5.10 Relationship between daily rainfall and average black carbon over Hanoi, Vietnam for 2012-2016.**

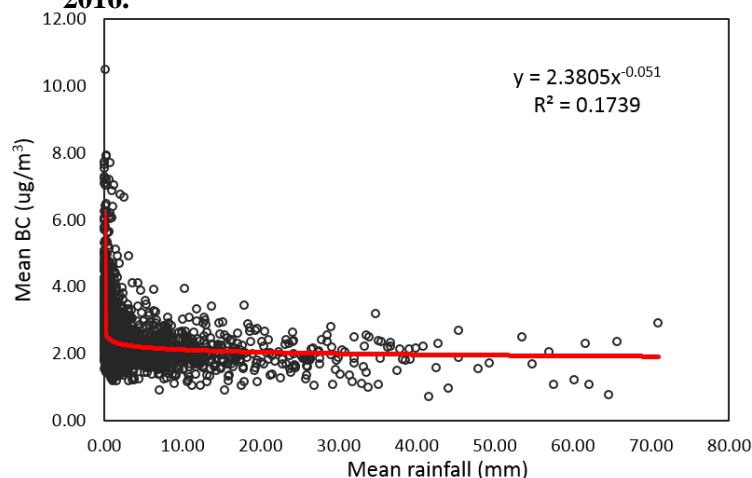
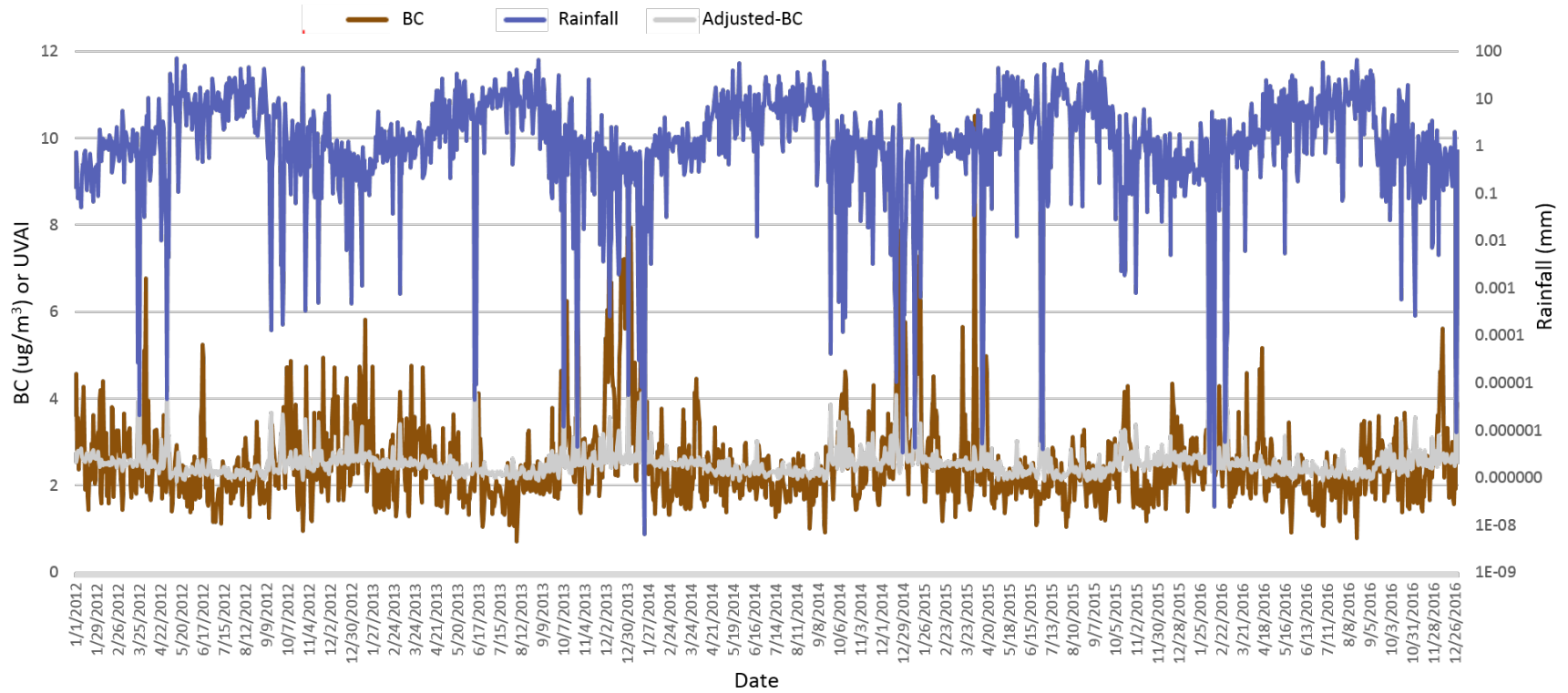




Figure 5.11 Timeseries of black carbon concentration, rainfall, and weather-adjusted black carbon from 2012-2016 over Hanoi



## 5.6 Discussion

Previous studies have demonstrated that even limited duration exposure to polluted air such as PM<sub>2.5</sub> or one of its major constituents of BC, may lead to serious health concerns and even premature death in at-risk populations such as the elderly (Pope et al. 2009). One such example in Beijing estimated 5,100 people died prematurely due to air pollution exposure during 2001-2012 (Zheng et al. 2015). Therefore, it is of significant importance to address and properly quantify some of the air quality issues over Hanoi, such as from rice residue biomass burning events in June and October. However, it is also important to quantify air pollution for much of the Asian region due to long-range transport from different emission sources. While the Hanoi area experiences monsoon-influenced conditions with heavy rains in summer, studies have found that severe and strong fires can result after heavy rain events such as during drier months of fall and winter (Gaveau et al. 2014). These examples highlight the need to mitigate air pollution emissions throughout the Asian region.

This study's results align well with the earlier studies conducted in Southeast Asia on air pollution and air quality trends. For example, one recent study showed Laos, Thailand, Cambodia, and Myanmar emit large amounts of BC emissions from non-agricultural fires (Song et al. 2010). Moreover, previous work has also found biomass burning emissions peak during March and April across continental Southeast Asia attributed to forest and agricultural burning (Huang et al. 2013). A recent study in Thailand demonstrated peak biomass burning in the dry season of April not only due to fires in Northern Thailand, but also due to emissions from surrounding Myanmar, Laos, and India (Sonkaew and Macatangay 2015). Previous studies have also demonstrated difficulty to model and monitor serious air pollution events in the Southeast Asian region (Macatangay



et al. 2017), including those from rice residue biomass burning (Lasko et al. 2017). We found the BC values observed over the Hanoi area as relatively higher through time than other Southeast Asian countries such as Laos, Thailand, and Cambodia. An even greater difference is observed in comparison to European countries where values are much lower averaging between 1.5 and 2.5 $\mu\text{g}/\text{m}^3$  (Randles et al. 2017). Continued monitoring and collaborative efforts are critical to address the ongoing air pollution concerns in the region (Reid et al. 2013). In the study region, capturing pollution trends coinciding with rice residue burning during June and October/early-November is difficult and confounded by smoke injection heights, highly variable rainfall and wet deposition, as well as a current lack of good quality surface concentration datasets.

Previous *in situ* studies in Hanoi have found the most polluted months to be during the December-February dry season, corroborating some of the findings of this study with peaks during January, December, and October (Hai and Oanh 2013). Another study found that nocturnal radiation inversions during October – December and subsidence temperature inversions from January to March help to amplify air pollution and air quality concerns in Hanoi; as well as high pressure systems over Central China during winter leading to southerly air flow, additionally corroborating some of the study findings (Hien et al. 2002). Moreover, work has also demonstrated polluted air parcel movement from southern and Eastern China during months of September – March, and pollutant transport from the Indochina peninsula during rainier months of June – August (Hien et al. 2004). Another study demonstrated Hanoi ozone levels and  $\text{NO}_2$  levels as routinely exceeding WHO standards attributed to high levels of motorcycles and traffic (Sakamoto et al. 2017). However, a clear pattern from both UVAI and BC data relating to the large amount of rice

residue burning practiced during June and October was not clear. Rice residue burning fires are typically small, low temperature fires difficult to monitor by satellite, especially due to varied burning practices (Lasko et al. 2018). Moreover, the UVAI data is a columnar measurement which does not capture surface concentration, while the BC data is similarly limited and often affected by interpolation issues. The MERRA-2 data has some utility for monitoring air pollutant trends over time, but with caveats for rice residue and biomass burning emissions in general.

Our study demonstrated that MERRA-2 BC concentration is useful for capturing variation in air pollution concentration especially attributed to urban sources including transport from southern China especially during the dry season months of December and January. We found that Hanoi suffers elevated UVAI during March and April attributed to forest biomass burning transport from NW Vietnam and Laos, but no increase in the MERRA-2 BC is observed during this time. While we know from previous studies that rice residues are subjected to burning in June and October, emitting a large amount of PM<sub>2.5</sub>, both of these datasets did not detect elevated air pollution levels. It's possible that this can be attributed to coarse spatial resolution datasets, lack of ground observations, as well as cloud cover obstructing satellite measurements. We found an average range of 2-5 clear UVAI observations in any given month making episodic biomass burning difficult to detect.

Although the MERRA-2 data has potential, it is limited by coarse resolution which may impede ability to monitor rice residue burning, confounded by emissions released steadily over the course of 4-6 weeks, diluting the signal. The MERRA-2 data currently, is limited in effectiveness for rice residue burning emissions monitoring. The

BC concentration dataset may not be sensitive to these biomass burning events as they generally emit more organic carbon than black carbon. Some additional limitations of this study include that BC values may be relatively low in absolute terms, but they are representative of a 0.5-degree cell average which spreads across not only the Hanoi urban area, but also much of the rice areas and countryside resulting in slightly low BC values. Moreover, there is a need for ground station datasets for improved air pollution monitoring, which would also be useful for comparison with MERRA-2.

Future work should also be done to simulate air pollutant concentrations resulting from rice residue burning to better understand the land-atmospheric interactions. Another future improvement can be through including PM<sub>2.5</sub> concentration data (not just PM<sub>2.5</sub> dust concentration as currently available) in MERRA-2 as it is more sensitive to rice residue burning due to its absorbing nature (Akagi et al. 2011; Zhang et al. 2015). For example, PM<sub>2.5</sub> concentration increases have been linked to rice residue burning events in China (Yin et al. 2017).

## **5.7 Conclusion**

Our study explored the current status of air pollution and pollution monitoring over Hanoi, Vietnam and the surrounding region, and specifically, to determine if the satellite data can capture the air pollution impact from rice residue biomass burning events documented to occur in the Red River Delta where Hanoi is located. Our results showed the Red River Delta and Hanoi experience the highest cloud coverage of the continental Southeast Asian region, and it was found to hinder optical satellite observations of air pollution, such as from OMI UVAI averaging only a few clear observations per month. Therefore, it is

difficult to monitor air pollution in the study area and we did not find significant air pollution impacts over Hanoi attributable to the known rice residue burning events. Further improved methodologies or higher resolution satellite constellations, and ground-based datasets are needed for improved air pollution assessments. We also used MERRA-2 reanalysis data which found the highest BC levels during December, January, and October during the dry season with some pollution attributed to long range transport from the North during this time. We also found biomass burning emissions impact based on UVAI levels with transport from Laos and NW Vietnam during March and April based on synoptic wind patterns. Results from both UVAI and BC did not indicate elevated pollution levels from rice residue burning during June, however, slightly elevated levels in October were often observed. Findings suggest that improved datasets and observations are necessary for monitoring rice residue burning emissions.

## 5.8 References

- Akagi, S.K., Yokelson, R.J., Wiedinmyer, C., Alvarado, M.J., Reid, J.S., Karl, T., Crounse, J.D. and Wennberg, P.O., 2011. Emission factors for open and domestic biomass burning for use in atmospheric models. *Atmospheric Chemistry and Physics*, 11(9), pp.4039-4072.
- Beverland, I.J., Cohen, G.R., Heal, M.R., Carder, M., Yap, C., Robertson, C., Hart, C.L. and Agius, R.M., 2012. A comparison of short-term and long-term air pollution exposure associations with mortality in two cohorts in Scotland. *Environmental health perspectives*, 120(9), p.1280.
- Biswas, S., Lasko, K. and Vadrevu, K.P. 2015. "Fire Disturbance in Tropical Forests of Myanmar—Analysis Using MODIS Satellite Datasets." *IEEE Journal of Selected Topics in Applied Earth Observations and Remote Sensing* 8(5): 2273-2281.
- Blanchard, C.L., Hidy, G.M. and Tanenbaum, S., 2010. NMOC, ozone, and organic aerosol in the southeastern United States, 1999–2007: 2. Ozone trends and sensitivity to NMOC emissions in Atlanta, Georgia. *Atmospheric Environment*, 44(38), pp.4840-4849.

- Buchard, V., da Silva, A.M., Colarco, P.R., Darmenov, A., Randles, C.A., Govindaraju, R., Torres, O., Campbell, J. and Spurr, R., 2015. Using the OMI aerosol index and absorption aerosol optical depth to evaluate the NASA MERRA Aerosol Reanalysis. *Atmos. Chem. Phys*, 15(10), pp.5743-5760.
- Burney, J. and Ramanathan, V., 2014. Recent climate and air pollution impacts on Indian agriculture. *Proceedings of the National Academy of Sciences*, 111(46), pp.16319-16324.
- Chuang, M.T., Lee, C.T., Chou, C.C.K., Engling, G., Chang, S.Y., Chang, S.C., Sheu, G.R., Lin, N.H., Sopajaree, K., Chang, Y.J. and Hong, G.J., 2016. Aerosol transport from Chiang Mai, Thailand to Mt. Lulin, Taiwan—Implication of aerosol aging during long-range transport. *Atmospheric Environment*, 137, pp.101-112
- Dawson, J.P., Adams, P.J. and Pandis, S.N., 2007. Sensitivity of ozone to summertime climate in the eastern USA: A modeling case study. *Atmospheric environment*, 41(7), pp.1494-1511.
- Duncan, B.N., Martin, R.V., Staudt, A.C., Yevich, R. and Logan, J.A., 2003. Interannual and seasonal variability of biomass burning emissions constrained by satellite observations. *Journal of Geophysical Research: Atmospheres*, 108(D2).
- Feng, N. and Christopher, S.A., 2013. Satellite and surface-based remote sensing of Southeast Asian aerosols and their radiative effects. *Atmospheric research*, 122, pp.544-554.
- Funk, C., Peterson, P., Landsfeld, M., Pedreros, D., Verdin, J., Shukla, S., Husak, G., Rowland, J., Harrison, L., Hoell, A. and Michaelsen, J., 2015. The climate hazards infrared precipitation with stations—a new environmental record for monitoring extremes. *Scientific data*, 2, p.150066.
- Gaveau, D.L., Salim, M.A., Hergoualc'h, K., Locatelli, B., Sloan, S., Wooster, M., Marlier, M.E., Molidena, E., Yaen, H., DeFries, R. and Verchot, L., 2014. Major atmospheric emissions from peat fires in Southeast Asia during non-drought years: evidence from the 2013 Sumatran fires. *Scientific reports*, 4.
- Gelaro, R., McCarty, W., Suárez, M.J., Todling, R., Molod, A., Takacs, L., Randles, C.A., Darmenov, A., Bosilovich, M.G., Reichle, R. and Wargan, K., 2017. The modern-era retrospective analysis for research and applications, version 2 (MERRA-2). *Journal of Climate*, 30(14), pp.5419-5454.
- General Statistics Office of Vietnam, 2016. Agriculture, forestry, and fishery. Accessed from [https://www.gso.gov.vn/Default\\_en.aspx?tabid=766](https://www.gso.gov.vn/Default_en.aspx?tabid=766) .
- Giglio, L., Descloitres, J., Justice, C.O. and Kaufman, Y.J., 2003. An enhanced contextual fire detection algorithm for MODIS. *Remote sensing of environment*, 87(2), pp.273-282.

- Giglio, L., Schroeder, W. and Justice, C.O., 2016. The collection 6 MODIS active fire detection algorithm and fire products. *Remote Sensing of Environment*, 178, pp.31-41.
- Gupta, R., Somanathan, E. and Dey, S., 2017. Global warming and local air pollution have reduced wheat yields in India. *Climatic Change*, 140(3-4), pp.593-604.
- Hai, C.D. and Oanh, N.T.K., 2013. Effects of local, regional meteorology and emission sources on mass and compositions of particulate matter in Hanoi. *Atmospheric environment*, 78, pp.105-112.
- Hayasaka, H., Noguchi, I., Putra, E.I., Yulianti, N. and Vadrevu, K., 2014. Peat-fire-related air pollution in Central Kalimantan, Indonesia. *Environmental Pollution*, 195, pp.257-266.
- Henneman, L.R., Holmes, H.A., Mulholland, J.A. and Russell, A.G., 2015. Meteorological detrending of primary and secondary pollutant concentrations: Method application and evaluation using long-term (2000–2012) data in Atlanta. *Atmospheric Environment*, 119, pp.201-210.
- Hien, P.D., Bac, V.T. and Thinh, N.T.H., 2004. PMF receptor modelling of fine and coarse PM 10 in air masses governing monsoon conditions in Hanoi, northern Vietnam. *Atmospheric Environment*, 38(2), pp.189-201.
- Hien, P.D., Bac, V.T., Tham, H.C., Nhan, D.D. and Vinh, L.D., 2002. Influence of meteorological conditions on PM 2.5 and PM 2.5– 10 concentrations during the monsoon season in Hanoi, Vietnam. *Atmospheric Environment*, 36(21), pp.3473-3484.
- Huang, K., Fu, J.S., Hsu, N.C., Gao, Y., Dong, X., Tsay, S.C. and Lam, Y.F., 2013. Impact assessment of biomass burning on air quality in Southeast and East Asia during BASE-ASIA. *Atmospheric environment*, 78, pp.291-302.
- Jhun, I., Coull, B.A., Zanobetti, A. and Koutrakis, P., 2015. The impact of nitrogen oxides concentration decreases on ozone trends in the USA. *Air Quality, Atmosphere & Health*, 8(3), pp.283-292.
- Jiang, C., Wang, H., Zhao, T., Li, T. and Che, H., 2015. Modeling study of PM 2.5 pollutant transport across cities in China's Jing–Jin–Ji region during a severe haze episode in December 2013. *Atmospheric Chemistry and Physics*, 15(10), pp.5803-5814.
- Kaufman, Y.J., Tanré, D. and Boucher, O., 2002. A satellite view of aerosols in the climate system. *Nature*, 419(6903), pp.215-223.
- Kim, J., Li, S., Kim, K.R., Stohl, A., Mühle, J., Kim, S.K., Park, M.K., Kang, D.J., Lee, G., Harth, C.M. and Salameh, P.K., 2010. Regional atmospheric emissions determined from measurements at Jeju Island, Korea: Halogenated compounds from China. *Geophysical Research Letters*, 37(12).

- Kurokawa, J. et al 2013. Emissions of air pollutants and greenhouse gases over Asian regions during 2000–2008: Regional Emission inventory in ASia (REAS) version 2. *Atmospheric Chemistry and Physics*, 13(21), pp.11019-11058.
- Lasko, K., Vadrevu, K., Tran, V., Ellicott, E., Nguyen, T., Bui, H. and Justice, C., 2017. Satellites may underestimate rice residue and associated burning emissions in Vietnam. *Environmental Research Letters*, 12(8), 085006.
- Lasko, K., Vadrevu, K.P., Tran, V.T., Justice, C. 2018. Mapping double and single crop paddy rice with Sentinel-1A at varying spatial scales and polarizations in Hanoi, Vietnam. *IEEE Journal of Selected Topics in Applied Earth Observation and Remote Sensing*, 11(2), pp. 498-512.
- Latha, R., Murthy, B.S., Lipi, K., Srivastava, M.K. and Kumar, M., 2017. Absorbing Aerosols, Possible Implication to Crop Yield-A Comparison between IGB Stations. *Aerosol and Air Quality Research*, 17(3), pp.693-705.
- Le, T.H., Nguyen, T.N.T., Lasko, K., Ilavajhala, S., Vadrevu, K.P. and Justice, C., 2014. Vegetation fires and air pollution in Vietnam. *Environmental Pollution*, 195, pp.267-275.
- Lin, N.H., Sayer, A.M., Wang, S.H., Loftus, A.M., Hsiao, T.C., Sheu, G.R., Hsu, N.C., Tsay, S.C. and Chantara, S., 2014. Interactions between biomass-burning aerosols and clouds over Southeast Asia: Current status, challenges, and perspectives. *Environmental Pollution*, 195, pp.292-307.
- Macatangay, R., Bagtasa, G. and Sonkaew, T., 2017, September. Non-chemistry coupled PM10 modeling in Chiang Mai City, Northern Thailand: A fast operational approach for aerosol forecasts. In *Journal of Physics: Conference Series*(Vol. 901, No. 1, p. 012037). IOP Publishing.
- Man, C.D., Nguyen, T.T., Bui, H.Q., Lasko, K. and Nguyen, T.N.T., 2018. Improvement of land-cover classification over frequently cloud-covered areas using Landsat 8 time-series composites and an ensemble of supervised classifiers. *International Journal of Remote Sensing*, 39(4), pp.1243-1255.
- Marlier, M.E., Jina, A.S., Kinney, P.L. and DeFries, R.S., 2016. Extreme air pollution in global megacities. *Current Climate Change Reports*, 2(1), pp.15-27.
- Minnis, P., Sun-Mack, S., Trepte, Q.Z., Chang, F.L., Heck, P.W., Chen, Y., Yi, Y., Arduini, R.F., Ayers, K., Bedka, K. and Bedka, S., 2010, June. CERES Edition 3 cloud retrievals. In *AMS 13th conference atmospheric radiation. Portland, OR, June*.
- Nguyen, D.B., Gruber, A. and Wagner, W., 2016. Mapping rice extent and cropping scheme in the Mekong Delta using Sentinel-1A data. *Remote Sensing Letters*, 7(12), pp.1209-1218.

- Nguyen, T.T., Bui, H.Q., Pham, H.V., Luu, H.V., Man, C.D., Pham, H.N., Le, H.T. and Nguyen, T.T., 2015. Particulate matter concentration mapping from MODIS satellite data: a Vietnamese case study. *Environmental Research Letters*, 10(9), p.095016.
- Oanh, N.K., Upadhyay, N., Zhuang, Y.H., Hao, Z.P., Murthy, D.V.S., Lestari, P., Villarin, J.T., Chengchua, K., Co, H.X., Dung, N.T. and Lindgren, E.S., 2006. Particulate air pollution in six Asian cities: Spatial and temporal distributions, and associated sources. *Atmospheric environment*, 40(18), pp.3367-3380.
- Oh, H.R., Ho, C.H., Kim, J., Chen, D., Lee, S., Choi, Y.S., Chang, L.S. and Song, C.K., 2015. Long-range transport of air pollutants originating in China: a possible major cause of multi-day high-PM 10 episodes during cold season in Seoul, Korea. *Atmospheric Environment*, 109, pp.23-30.
- Ohara, T.A.H.K., Akimoto, H., Kurokawa, J.I., Horii, N., Yamaji, K., Yan, X. and Hayasaka, T., 2007. An Asian emission inventory of anthropogenic emission sources for the period 1980–2020. *Atmospheric Chemistry and Physics*, 7(16), pp.4419-4444.
- Pham, V.C., Pham, T.T.H., Tong, T.H.A., Nguyen, T.T.H. and Pham, N.H., 2015. The conversion of agricultural land in the peri-urban areas of Hanoi (Vietnam): patterns in space and time. *Journal of Land Use Science*, 10(2), pp.224-242.
- Platnick, S., King, M.D., Ackerman, S.A., Menzel, W.P., Baum, B.A., Riédi, J.C. and Frey, R.A., 2003. The MODIS cloud products: Algorithms and examples from Terra. *IEEE Transactions on Geoscience and Remote Sensing*, 41(2), pp.459-473.
- Ponette-González, A.G., Curran, L.M., Pittman, A.M., Carlson, K.M., Steele, B.G., Ratnasari, D. and Weathers, K.C., 2016. Biomass burning drives atmospheric nutrient redistribution within forested peatlands in Borneo. *Environmental Research Letters*, 11(8), p.085003.
- Pope III, C.A. and Dockery, D.W., 2006. Health effects of fine particulate air pollution: lines that connect. *Journal of the air & waste management association*, 56(6), pp.709-742.
- Pope III, C.A., Ezzati, M. and Dockery, D.W., 2009. Fine-particulate air pollution and life expectancy in the United States. *N Engl J Med*, 2009(360), pp.376-386.
- Putero, D., Landi, T.C., Cristofanelli, P., Marinoni, A., Laj, P., Duchì, R., Calzolari, F., Verza, G.P. and Bonasoni, P., 2014. Influence of open vegetation fires on black carbon and ozone variability in the southern Himalayas (NCO-P, 5079 m asl). *Environmental Pollution*, 184, pp.597-604.
- Ramanathan, V. and Carmichael, G., 2008. Global and regional climate changes due to black carbon. *Nature geoscience*, 1(4), pp.221-227.
- Randles, C.A., da Silva, A.M., Buchard, V., Colarco, P.R., Darmenov, A., Govindaraju, R., Smirnov, A., Holben, B., Ferrare, R., Hair, J. and Shinozuka, Y., 2017. The MERRA-



2 aerosol reanalysis, 1980 onward. Part I: System description and data assimilation evaluation. *Journal of Climate*, 30(17), pp.6823-6850.

Reid, J.S., Hyer, E.J., Johnson, R.S., Holben, B.N., Yokelson, R.J., Zhang, J., Campbell, J.R., Christopher, S.A., Di Girolamo, L., Giglio, L. and Holz, R.E., 2013. Observing and understanding the Southeast Asian aerosol system by remote sensing: An initial review and analysis for the Seven Southeast Asian Studies (7SEAS) program. *Atmospheric Research*, 122, pp.403-468.

Saikawa, E., Trail, M., Zhong, M., Wu, Q., Young, C.L., Janssens-Maenhout, G., Klimont, Z., Wagner, F., Kurokawa, J.I., Nagpure, A.S. and Gurjar, B.R., 2017. Uncertainties in emissions estimates of greenhouse gases and air pollutants in India and their impacts on regional air quality. *Environmental Research Letters*, 12(6), p.065002.

Sakamoto, Y., Shoji, K., Bui, M.T., Phạm, T.H., Ly, B.T. and Kajii, Y., 2017. Air quality study in Hanoi, Vietnam in 2015–2016 based on a one-year observation of NO<sub>x</sub>, O<sub>3</sub>, CO and a one-week observation of VOCs. *Atmospheric Pollution Research*.

Sanderfoot, O.V. and Holloway, T., 2017. Air pollution impacts on avian species via inhalation exposure and associated outcomes. *Environmental Research Letters*, 12(8), p.083002.

Shi, Y. and Matsunaga, T., 2017. Temporal comparison of global inventories of CO<sub>2</sub> emissions from biomass burning during 2002–2011 derived from remotely sensed data. *Environmental Science and Pollution Research*, pp.1-12

Shiogama, H., Watanabe, M., Imada, Y., Mori, M., Ishii, M. and Kimoto, M., 2013. An event attribution of the 2010 drought in the South Amazon region using the MIROC5 model. *Atmospheric Science Letters*, 14(3), pp.170-175.

Shumway, R.H. and Stoffer, D.S., 2006. *Time series analysis and its applications: with R examples*. Springer Science & Business Media.

Son, N.T., Chen, C.F., Chen, C.R. and Minh, V.Q., 2017. Assessment of Sentinel-1A data for rice crop classification using random forests and support vector machines. *Geocarto International*, pp.1-15.

Song, Y., Chang, D., Liu, B., Miao, W., Zhu, L. and Zhang, Y., 2010. A new emission inventory for nonagricultural open fires in Asia from 2000 to 2009. *Environmental Research Letters*, 5(1), p.014014.

Sonkaew, T. and Macatangay, R., 2015. Determining relationships and mechanisms between tropospheric ozone column concentrations and tropical biomass burning in Thailand and its surrounding regions. *Environmental Research Letters*, 10(6), p.065009.

Streets, D.G., Yarber, K.F., Woo, J.H. and Carmichael, G.R., 2003. Biomass burning in Asia: Annual and seasonal estimates and atmospheric emissions. *Global Biogeochemical Cycles*, 17(4).

- Tadesse, T., Bathke, D., Wall, N., Petr, J. and Haigh, T., 2015. Participatory Research Workshop on Seasonal Prediction of Hydroclimatic Extremes in the Greater Horn of Africa. *Bulletin of the American Meteorological Society*, 96(8), pp.ES139-ES142.
- Tai A P K, Mickley L J and Jacob D J 2010 Correlations between fine particulate matter (PM<sub>2.5</sub>) and meteorological variables in the United States: implications for the sensitivity of PM<sub>2.5</sub> to climate change *Atmos. Environ.* **44** 3976–84
- Tanimoto, H., Kajii, Y., Hirokawa, J., Akimoto, H. and Minko, N.P., 2000. The atmospheric impact of boreal forest fires in far eastern Siberia on the seasonal variation of carbon monoxide: Observations at Rishiri, a northern remote island in Japan. *Geophysical Research Letters*, 27(24), pp.4073-4076.
- Tao, F., Feng, Z., Tang, H., Chen, Y. and Kobayashi, K., 2017. Effects of climate change, CO<sub>2</sub> and O<sub>3</sub> on wheat productivity in Eastern China, singly and in combination. *Atmospheric Environment*, 153, pp.182-193.
- Thompson M L, Reynolds J, Cox L H, Guttorp P and Sampson P D 2001 A review of statistical methods for the meteorological adjustment of tropospheric ozone *Atmos. Environ.* **35** 617–30
- Torres, O., Ahn, C. and Chen, Z., 2013. Improvements to the OMI near-UV aerosol algorithm using A-train CALIOP and AIRS observations. *Atmospheric Measurement Techniques*, 6(11), p.3257.
- Torres, O., Tanskanen, A., Veihelmann, B., Ahn, C., Braak, R., Bhartia, P.K., Veefkind, P. and Levelt, P., 2007. Aerosols and surface UV products from Ozone Monitoring Instrument observations: An overview. *Journal of Geophysical Research: Atmospheres*, 112(D24).
- Tsay, S.C., Hsu, N.C., Lau, W.K.M., Li, C., Gabriel, P.M., Ji, Q., Holben, B.N., Welton, E.J., Nguyen, A.X., Janjai, S. and Lin, N.H., 2013. From BASE-ASIA toward 7-SEAS: A satellite-surface perspective of boreal spring biomass-burning aerosols and clouds in Southeast Asia. *Atmospheric environment*, 78, pp.20-34.
- Vadrevu, K.P., Lasko, K., Giglio, L. and Justice, C., 2014. Analysis of Southeast Asian pollution episode during June 2013 using satellite remote sensing datasets. *Environmental Pollution*, 195, pp.245-256.
- Vadrevu, K.P., Lasko, K., Giglio, L. and Justice, C., 2015. Vegetation fires, absorbing aerosols and smoke plume characteristics in diverse biomass burning regions of Asia. *Environmental Research Letters*, 10(10), p.105003.
- van der Werf, G.R., Randerson, J.T., Giglio, L., Collatz, G.J., Kasibhatla, P.S. and Arellano Jr, A.F., 2006. Interannual variability in global biomass burning emissions from 1997 to 2004. *Atmospheric Chemistry and Physics*, 6(11), pp.3423-3441.

- Wang, M., Cao, C., Li, G. and Singh, R.P., 2015. Analysis of a severe prolonged regional haze episode in the Yangtze River Delta, China. *Atmospheric Environment*, 102, pp.112-121.
- Warneke, C., Froyd, K.D., Brioude, J., Bahreini, R., Brock, C.A., Cozic, J., De Gouw, J.A., Fahey, D.W., Ferrare, R., Holloway, J.S. and Middlebrook, A.M., 2010. An important contribution to springtime Arctic aerosol from biomass burning in Russia. *Geophysical Research Letters*, 37(1), pp.1-5.
- Yan, X., Ohara, T. and Akimoto, H., 2006. Bottom-up estimate of biomass burning in mainland China. *Atmospheric Environment*, 40(27), pp.5262-5273.
- Yin, S., Wang, X., Xiao, Y., Tani, H., Zhong, G. and Sun, Z., 2017. Study on spatial distribution of crop residue burning and PM 2.5 change in China. *Environmental Pollution*, 220, pp.204-221.
- You, S., Tong, Y.W., Neoh, K.G., Dai, Y. and Wang, C.H., 2016. On the association between outdoor PM 2.5 concentration and the seasonality of tuberculosis for Beijing and Hong Kong. *Environmental Pollution*, 218, pp.1170-1179.
- Zhang, T., Wooster, M.J., Green, D.C. and Main, B., 2015. New field-based agricultural biomass burning trace gas, PM 2.5, and black carbon emission ratios and factors measured in situ at crop residue fires in Eastern China. *Atmospheric Environment*, 121, pp.22-34.
- Zheng, S., Pozzer, A., Cao, C.X. and Lelieveld, J., 2015. Long-term (2001–2012) concentrations of fine particulate matter (PM 2.5) and the impact on human health in Beijing, China. *Atmospheric Chemistry and Physics*, 15(10), pp.5715-5725.

## Chapter 6: Summary findings and conclusion

### 6.1 Summary

Air pollution has been recently attributed as a major contributor to premature deaths with a global estimate of seven million people dying annually from pollution exposure, or one-in-eight deaths (WHO 2014). While pollution from a variety of urban sources has been quantified such as vehicle traffic, power plants, and industrial production, emissions from biomass burning are less known and highly variable. Biomass burning emissions are variable due to a wide variety of factors such as land cover type and change (i.e. forest, crop, and savannah), combustion efficiency, amount subjected to burning, and type of burning, among other factors explored in this dissertation. Agricultural biomass burning, specifically from rice, was chosen as a research topic, as it's difficult to monitor and quantify resulting emissions with remote sensing alone. Ephemeral, small, and actively managed rice residue burning fires are difficult to detect using satellite data. Moreover, cloud cover in some agricultural regions, such as the Red River Delta and Hanoi, only exacerbate the difficulty. The Hanoi Capital Region of Vietnam, located within the Red River Delta, was selected as a primary study area, not only because the majority of land cover is occupied by small-holder paddy rice, but also because it is intermixed amongst peri-urban expansion and the very populous capital city of Hanoi. Thus, addressing air quality and resulting public health effects from pollution are very important for this study area.

The three research objectives comprising the dissertation were designed based on extensive field work and through identifying the gaps and limitations found in the agricultural biomass burning emissions literature. Thus, this dissertation employed a

combination of remote sensing, timeseries data, field data, modelling, and literature analysis. Through the three research objectives, this dissertation not only quantified the first bottom-up, burning-practice specific rice residue emissions estimate for Vietnam, but also highlighted the higher than expected contribution to all PM<sub>2.5</sub> combustion sources, and a significant underestimation from the current global studies. Because of persistent cloud cover and difficulties in detecting agricultural fires in the study area, an indirect approach using timeseries SAR imagery and rice phenology was developed to estimate approximate date and location of burning useful for quantifying air pollution and air quality effects in Hanoi (Chapters 4 and 5). Overall, the study highlights variation in residue burning emissions resulting from different burning practices (i.e. pile or non-pile burning in Chapter 4), and variation in rice area based on different datasets, important for resulting emissions estimation (Chapter 2), and improved methods to estimate rice residue (Chapter 3), as well as crop specific versus generalized emission factors (Chapter 4), including the current trends in air pollution and air quality in Hanoi (Chapter 5). The bottom-up estimates in this dissertation are an improvement upon the existing literature because global studies to date have relied upon generalized emission factors, land cover types, and often crop production-based or net primary productivity-based residue estimates. Overall, this research addresses how crop residue burning emissions are underestimated in small-holder croplands.

## **6.2 Key findings and implications from Chapter 2**

Chapter 2 of this dissertation, entitled “Mapping double and single crop paddy rice with Sentinel-1A at varying spatial scales and polarizations in Hanoi, Vietnam” addressed

*Objective 1: Map paddy rice area variation based on different SAR polarizations and spatial resolution, and characterize the paddy rice landscape and phenology.*

It employed a timeseries of Sentinel-1 C-band synthetic aperture radar imagery to map single and double rotated rice lands in the Hanoi Capital Region. The study used six different, commonly used datasets of Sentinel-1 including VV, VH, and both polarizations, each of which was processed into 10m and 20m spatial resolutions. By comparing these six different datasets, classified with a robust random forest classification algorithm, differences and variation in mapped rice land areas were highlighted. The accuracies for each dataset differed by as much as 2.5% for overall accuracy, 6% for double rice producer's accuracy, and 5% for double rice user's accuracy. With regard to land area, the double-rice land area for each of the six datasets ranged from 208 thousand ha to 220 thousand ha, showing a 5.6% difference. This overall difference in rice area is important not only for operational rice monitoring applications, but also critical for addressing biomass burning pollution. These differences in rice area resulting from classification of the six commonly-used datasets, combined with variation from the other inputs such as different burning practices, varying amount subjected to burning, and wide-ranging combustion completeness, together can account for considerable uncertainty. Moreover, double-rice pixel agreement between the six different datasets showed that only 66% of pixels were in agreement, illustrating that 44% of pixels had some uncertainty with regard to land cover type. Thus, while the absolute variation in the study area was low, this spatial variation is important for spatially-explicit applications such as air pollution and air quality modeling. Location of

the biomass burning is important as it can determine the transport, atmospheric effects, and impact of air pollution on air quality.

Another major result from this chapter was the landscape metrics obtained for double-crop paddy rice fields. Using the most accurate VVVH10m double-rice map, combined with mean-shift image segmentation as well as Fragstats software and the average field size from chapter 3, details about rice collectives were uncovered. Rice collectives are groups of fields grown adjacent to each other so as to facilitate irrigation, planting, and harvest activities. Spatial information on the rice collectives in Vietnam has never before been addressed, and the results have suggested about 3-4 fields on an average make-up a rice collective, operationally defined as a patch undergoing similar phenology from the timeseries SAR data. The resulting collective information provides detail useful for economic, agricultural management, and air quality impact studies.

This chapter also measured the importance of the different SAR bands and associated dates of acquisition for the resulting image classification and rice maps. The results showed that imagery from the harvest stages and 2<sup>nd</sup> season planting stage were most important for classification, especially for the most accurate VVVH10m dataset. However, excluding the harvest stage and late vegetative growth stages may reduce the overall accuracy from about 93% to about 85%. While this exclusion would significantly impact accuracy, it still provides an acceptably accurate map useful for operational mapping of paddy rice prior to final harvest. This could be useful to forecast or estimate not only rice production, critically important for the economy, but also for biomass and rice residue production estimates. Moreover, resulting estimates of emissions could also be forecasted based on these estimates.

### **6.3 Findings and implications from Chapter 3**

Chapter 3 of this dissertation, entitled “Satellite data may underestimate rice residue and associated burning emissions in Vietnam”, addressed *Objective 2: Quantify post-harvest rice residue production through a field study and calculate particulate matter emissions from burning using an approach employed in global studies.*

This chapter developed a novel field method to quickly and accurately estimate rice residues, relate the field estimates to SAR data, and subsequently estimate particulate matter emissions from residue burning for Hanoi Province and the entirety of Vietnam, using the same emission factors employed by global biomass burning studies. The field measurements were robust compared with previous studies as they involved quadrat-based measurements and incorporated moisture content measurements which most studies simply infer or assume. The accuracy assessment also highlighted that this method was effective with 91% overall accuracy. The rice residue was estimated for the entirety of Vietnam by using this chapter’s field-based estimate, as its representative of double-cropped rice fields found throughout Central and Northern Vietnam, and using a rice residue estimate from another study conducted in the other remaining rotation type of triple cropping found in the Mekong River Delta (Hong van et al. 2014). SAR data obtained approximately 2 weeks prior to harvest also showed a moderate in strength linear relationship between the field data and SAR data suggesting the potential to predict or model rice residue for Hanoi.

This research was also unique and contributed to the literature, in that it developed not only rice straw residue factors, but also a separate factor for rice stubble, the standing uncut portion of residue, which is rarely accounted for in other research. Moreover, one of the most common techniques for estimating post-harvest rice residues



is based on grain-to-straw ratios obtained from the literature, which are multiplied by rice production data obtained from government agricultural databases. This technique, while easy to use, was compared with the field-based method developed in Chapter 3. The comparison showed that this method underestimated rice residue by more than 100% because it likely does not account for the stubble component of the residue. Thus, other studies across the region could also be underestimating not only rice residue, with implications for applications such as bioenergy, but also underestimating resulting emissions from burning.

The field-based rice residue estimates were used as a basis for estimating the emissions from burning, instead of the typical crop production statistics approach. For comparison purposes, this chapter employed a general agricultural waste burning emission factor (Andreae and Merlet 2001; Akagi et al. 2011) commonly applied to global and regional biomass burning studies (Streets et al. 2003; Lamarque et al. 2010; van der Werf et al. 2010; Wiedinmyer et al. 2010; Kaiser et al. 2012; van der Werf et al. 2017). One of the most widely-used global biomass burning and emissions datasets is GFED (van der Werf et al. 2017). In this chapter, rice residue burning emissions estimates for the entirety of Vietnam were derived based on the field-based, bottom-up approach and compared with the satellite-derived biomass burning estimates from GFED version 4.2s. The findings were notable and suggested that a significant amount of burning may be missed by GFED by a factor of over 13 for rice residue burning. Moreover, this study placed rice residue burning emissions in the context of all-combustion sources of PM<sub>2.5</sub> for Vietnam, adding more value to the emission estimates. The results showed that emissions from rice residue burning alone, accounted for about

13% of PM<sub>2.5</sub> emissions for the country as compared with the REAS dataset (Kurokawa et al. 2013). These findings are important in that they demonstrate emissions from rice residue are a small but significant part of the emissions inventory. However, while the emissions are small, the air quality effects from rice residue burning could potentially be more significant than other industrial or combustion sources. For example, while the emissions from these sources are generally spread throughout an entire year, rice residue burning emissions are focused into two or three brief periods coinciding with the harvest.

#### **6.4. Findings and implications from Chapter 4**

Chapter 4 of this dissertation, entitled “Integrated analysis of rice residue burning emissions in Vietnam based on satellite observations, field burning practices and combined emissions factors”, addressed *Objective 3: Estimate burning practice specific emissions from rice residue burning, and explore resulting air pollution and air quality effects in Hanoi, Vietnam.*

While Chapter 3 provided enhanced, field-based residue and emissions estimates, Chapter 4 further improved existing emissions estimates by incorporating not only crop and region-specific emission factors, but also included development of separate emission factors for the two prominent burning practices found in Vietnam. An in-depth literature review was carried out and region-specific field and lab-based emissions studies across Asia were collected. Based on details provided in each study’s design, they were placed into a ‘pile burning’ or ‘non-pile burning’ group, the two main types of residue burning found in Vietnam. Average values obtained for each of the factors showed about a 32% difference in emission factors based on the two burning practices. The reason for this difference is due to varied combustion efficiency, and combustion completeness found in

these two burning practices - largely attributed to different moisture content, with the fuel in pile burning generally being wetter than that of non-pile burning. In addition to the emission factors, improved combustion factors were also developed with the same approach. Subsequent emission estimates for Vietnam showed an even larger amount of emissions than estimated in Chapter 3 (approximately 150Gg PM<sub>2.5</sub> versus 76Gg PM<sub>2.5</sub>). The results found that depending on the burning practice, PM<sub>2.5</sub> emissions were underestimated by 44-77% when using the general agricultural emission factors instead of burning practice specific factors for rice. Moreover, these further refined emission estimates suggested that PM<sub>2.5</sub> emissions now account for somewhere between 15% and 21% of total PM<sub>2.5</sub> combustion emissions based on the REAS inventory (Kurokawa et al. 2013). This is much more than the previously estimated 13%, which is vastly more than the roughly 2% estimated by agricultural waste burning from GFED as reported in Chapter 3. Thus, emissions from rice residue burning could in fact be a major factor in PM<sub>2.5</sub> emissions and resulting air quality degradation for Vietnam based on this new assessment.

In the consistently cloud covered region of Hanoi, Vietnam, satellite-based monitoring of actively burning fires and burned areas is extremely difficult. SAR offers an alternative approach to indirectly estimate the date of rice residue burning based on the SAR phenology presented in Chapter 2 especially when combined with data collected in the field. The estimated burning dates, as well as a buffer of dates to account for uncertainty, were used in this study as input for an air parcel trajectory model to explore polluted air parcel movement into the highly populous urban area of Hanoi City. The results showed seasonally variable movement of polluted air parcels, as well as distinct

spatial patterns of movement. These results could be useful to focus efforts to alleviate emissions in certain geographic regions, where governments could provide incentives for alternatives to burning such as mushroom straw cultivation, or use for animal feed.

Overall, this chapter demonstrated the manner by which rice residues are harvested and burned, impacting residue moisture content and structure, and thereby altering combustion completeness, efficiency, and the resulting emissions. Moreover, it highlights the need for biomass burning emissions datasets, such as GFED, to consider land cover and crop-specific emission and fuel-loading factors, as well as burning practice-specific factors for improved estimates.

## **6.5 Findings and implications from chapter 5**

Chapter 5 of this dissertation, entitled “Spatiotemporal trends of air pollution over Hanoi, Vietnam using MERRA-2 reanalysis, satellite-based UVAI, and ancillary atmospheric data”, addressed in more detail the 2<sup>nd</sup> part of *Objective 3: Estimate burning practice specific emissions from rice residue burning, and explore resulting air pollution and air quality effects in Hanoi, Vietnam.*

Chapter 5 explored trends in air pollution within Hanoi, as well as different seasonal contributing factors to the pollution levels. In addition, current limitations and difficulties with monitoring air pollution and air quality in this unique densely populated, small-holder agriculturalist, and cloud-covered region were also highlighted. This chapter demonstrated that the Hanoi area has consistently high cloud cover with an average cloud fraction exceeding 55% or more in any given month. Moreover, due to atmospheric effects and cloud cover during the rice residue burning months of June and October, on average only 3 and 5 clear daily OMI UVAI observations are available over Hanoi. This

limitation makes satellite-based monitoring of air pollution and air quality relatively difficult, as the particulate matter released from burning may only last in the region for a few days due to short atmospheric residence times.

Because of the difficulty to monitor air pollution and air quality with satellite data alone, reanalysis data, with its unbroken temporal record, was used to further assess air pollution and air quality trends based on synoptic meteorology patterns in the Hanoi region. The results demonstrated that the peak air pollution months were December, January, and October. The findings based on synoptic meteorology patterns suggested that during winter months pollution from power plants North of Hanoi, including those in mega-urban areas of China contribute to elevated pollution levels during dry months of December and January. In addition, biomass burning from forest fires in Laos and Northwest Vietnam were found to contribute to elevated pollution levels, especially during the months of March and April.

Air pollution during the rice residue burning months of June and October proved more complicated, due to relatively coarse resolution reanalysis data confounded by highly variable seasonal rainfall and temperature patterns which affect air pollution levels. As a result, the air pollution signal from rice residue burning is not clear. This study overall demonstrated that even after de-trending the pollution data for weather patterns, it's still difficult to tease out the air quality effect from rice residue burning. While air pollution generally trended high in October, the same was not evident during June. However, the results do suggest that Hanoi has very degraded air quality, much higher than many adjacent areas, throughout much of the year aside from the rainiest of

months of July and August. Overall, the results demonstrated the need for future improvements to datasets and monitoring capabilities.

## **6.6 Recommendations for future work**

Future work should focus on improving the satellite record of biomass burning emissions. By addressing shortcomings found within the different inputs of the PM<sub>2.5</sub> emissions equation as undertaken in this dissertation, not only can this lead to improved estimates, but also alleviate inherent uncertainty. One such factor which has promise to be improved in the future, is burning practice type (i.e. pile vs non-pile burning). Satellite-based estimates of burning practice type could be inferred from mapping harvest type. Generally, machine-harvested fields are associated with non-pile burning as the residues are drier and left in rows. Whereas, pile burning is found throughout hand-harvested fields as the residue is left in a pile after threshing. Each practice yields a distinct spatial and spectral pattern in the field which could be possible to map with fine temporal and spatial resolution optical satellite or SAR data, but could be limited due to cloud coverage or lack of clear signal. However, with success, this could provide even more refined emissions estimates than relying upon survey data of burning practice type. In addition, fuel-loading factors should be obtained for hand-harvested fields and compared with those of machine harvest conducted in this research, to quantify the variation, as this would be important for resulting emissions variation. It would result in further improvement to existing emission assessments as this dissertation did not address variation from the different harvest practices. Similarly, the amount of residue burned in the field could also be monitored by satellite, reducing the need to rely upon fieldwork and often uncertain survey data. With a constellation of moderate-to-high spatial

resolution satellites with multiple daily observations of a given area, agricultural residue burning could likely be measured and better quantified. Additionally, successful prototyping of combined optical and SAR-based burned area could prove useful in cloud cover regions such as Hanoi. However, these algorithms would also need to be based upon high temporal and high spatial resolution so as to be effective to overcome the problem of small, ephemeral fire size as well as active field management found within agricultural lands. However, research has not yet demonstrated potential for effective SAR-based burned area mapping, which may require more advanced SAR systems with multiple frequencies and polarizations. Additionally, global and regional emissions databases such as GFED could improve existing estimates by integrating crop-specific land cover with corresponding crop-specific emissions factors –an improvement on existing crop/non-crop distinction. This would then pave the way for integrating with regional, burning practice, and crop-specific emission factors.

Improvements to air quality and air pollution data would also prove useful to determine effects from rice residue burning emissions. Currently, the optical satellite data suffers from cloud cover obstruction. The reanalysis data, such as from MERRA-2 is limited by uncertainty in data quality as well as reliance upon disparate datasets, assimilation, and interpolation confounded by a relatively coarse spatial resolution of about 0.5 degrees. The use of ground-based observation stations, which could monitor air pollution even under cloudy conditions, would prove most useful for air quality applications. Moreover, disparate observation stations should be linked together (such as is currently done with AERONET, Holben et al. 1998) and included in the reanalysis datasets for further improvements and could lead to incorporation of PM<sub>2.5</sub> into the

reanalysis data –instead of relying upon black carbon concentrations. My collaborators at Vietnam National University in Hanoi were recently funded to implement several PM<sub>2.5</sub> monitoring stations across the Hanoi area throughout urban and agricultural areas to link residue burning to air quality. Data from these stations could be used to better understand the linkage, transport, and relationship between air pollution concentrations in agricultural areas outside of the city as well as the densely populated urban center. Moreover, as Vietnam National University is local to Hanoi and much of their funding is from the national government, they have improved standing to guide government policy action and disseminate dissertation results. One example finding which may be of interest, is that altered burning practices (i.e. non-pile burning) can result in reduced particulate matter emissions due to more complete combustion. It may also be key to consider incentivizing burning alternatives (such as mushroom straw farming), instead of just an outright ban which already exists.

At a regional and global scale, ground-based research, such as that conducted as part of this dissertation, should continue to inform and improve upon existing remote sensing-based biomass burning and emissions models or databases. Improved assessments are critical because, as this research demonstrated, emissions could be grossly underestimated for certain sectors and require more attention than previously thought. Moreover, these emissions have been found to contribute to not only degraded local and regional air quality through long-range transport of particulate matter emissions, but also to greenhouse gas emissions impacts, such as CO<sub>2</sub>, important for climate.



This research demonstrated the importance of incorporating field data with remote sensing data and empirical methods. Without the field data, details regarding different burning practices, and amount of residue burned would be difficult to accurately quantify. However, without the remote sensing data there would be no system to consistently estimate emissions and quantify differences resulting from different burning practices. This study demonstrated that field data can be used to inform improvements to existing remote sensing datasets such as GFED, and demonstrated previous methodologies underestimated rice straw and rice stubble amounts in the field. This research highlighted the importance of incorporating regional and local level data into agricultural waste burning emissions datasets, important not only for agricultural waste burning, but also critical to apply to other biomass burning types more broadly. In the future, more robust remote sensing methods to monitor agricultural waste burning, rice residue production, emissions from burning, and air quality impacts can be used based on insights resulting from this research.

## **6.7 References**

- Akagi, S.K., Yokelson, R.J., Wiedinmyer, C., Alvarado, M.J., Reid, J.S., Karl, T., Crounse, J.D. and Wennberg, P.O., 2011. Emission factors for open and domestic biomass burning for use in atmospheric models. *Atmospheric Chemistry and Physics*, 11(9), pp.4039-4072.
- Andreae, M.O. and Merlet, P., 2001. Emission of trace gases and aerosols from biomass burning. *Global biogeochemical cycles*, 15(4), pp.955-966.
- Holben, B.N., Eck, T.F., Slutsker, I., Tanre, D., Buis, J.P., Setzer, A., Vermote, E., Reagan, J.A., Kaufman, Y.J., Nakajima, T. and Lavenu, F., 1998. AERONET—A federated instrument network and data archive for aerosol characterization. *Remote sensing of environment*, 66(1), pp.1-16.

- Kaiser, J.W., Heil, A., Andreae, M.O., Benedetti, A., Chubarova, N., Jones, L., Morcrette, J.J., Razinger, M., Schultz, M.G., Suttie, M. and Van Der Werf, G.R., 2012. Biomass burning emissions estimated with a global fire assimilation system based on observed fire radiative power. *Biogeosciences*, 9(1), p.527.
- Kurokawa, J., Ohara, T., Morikawa, T., Hanayama, S., Janssens-Maenhout, G., Fukui, T., Kawashima, K. and Akimoto, H., 2013. Emissions of air pollutants and greenhouse gases over Asian regions during 2000–2008: Regional Emission inventory in ASia (REAS) version 2. *Atmospheric Chemistry and Physics*, 13(21), pp.11019-11058.
- Lamarque, J.F., Bond, T.C., Eyring, V., Granier, C., Heil, A., Klimont, Z., Lee, D., Liousse, C., Mieville, A., Owen, B. and Schultz, M.G., 2010. Historical (1850–2000) gridded anthropogenic and biomass burning emissions of reactive gases and aerosols: methodology and application. *Atmospheric Chemistry and Physics*, 10(15), pp.7017-7039.
- Streets, D.G., Yarber, K.F., Woo, J.H. and Carmichael, G.R., 2003. Biomass burning in Asia: Annual and seasonal estimates and atmospheric emissions. *Global Biogeochemical Cycles*, 17(4), pp.1-20.
- Van der Werf, G.R., Randerson, J.T., Giglio, L., Collatz, G.J., Mu, M., Kasibhatla, P.S., Morton, D.C., DeFries, R.S., Jin, Y.V. and van Leeuwen, T.T., 2010. Global fire emissions and the contribution of deforestation, savanna, forest, agricultural, and peat fires (1997–2009). *Atmospheric Chemistry and Physics*, 10(23), pp.11707-11735.
- Van Der Werf, G.R., Randerson, J.T., Giglio, L., Van Leeuwen, T.T., Chen, Y., Rogers, B.M., Mu, M., Van Marle, M.J., Morton, D.C., Collatz, G.J. and Yokelson, R.J., 2017. Global fire emissions estimates during 1997–2016. *Earth System Science Data*, 9(2), pp.697.
- WHO, 2014. World Health Organization. Accessed from <http://www.who.int/mediacentre/news/releases/2014/air-pollution/en/>.
- Wiedinmyer, C., Akagi, S.K., Yokelson, R.J., Emmons, L.K., Al-Saadi, J.A., Orlando, J.J. and Soja, A.J., 2010. The Fire INventory from NCAR (FINN)—a high resolution global model to estimate the emissions from open burning. *Geoscientific Model Development Discussions*, 3(4), pp.2439-2476.

## Appendix

### Unbiased areal estimates in accuracy assessment

First, the accuracy assessment error matrix which contains associated pixel counts for each class, and the area proportions of each land cover class, is used as a basis to yield improved accuracy metrics. A Robust accuracy assessment requires effective sampling stratification based on areal representation of each land cover class, as was done in chapter 2 with double-cropped paddy rice, single-cropped paddy rice, and non-rice areas. Because of the accuracy assessment stratification, the number of sample units for each stratum is not necessarily proportionate to the area of that stratum (Olofsson et al. 2014). This makes it necessary to approximate each class' area proportion ( $\hat{p}_{ij}$ ) (equation A.1).

$$\hat{p}_{ij} = w_i \frac{n_{ij}}{n_i}$$

Where  $n_{ij}$  is the sample count for reference class i, divided by the total number of pixels in that stratum ( $n_i$ ). A sample error matrix similar to chapter two classification procedure is shown in table A.1. The updated matrix with estimated area proportions is

**Table A.1. Error matrix for a theoretical example based on chapter 2 showing pixel/sample counts from accuracy assessment.**

Class	REFERENCE			Total	Pixels(Map)	$w_i$
	Double rice	Single rice	Non-rice			
Double rice	410	0	13	423	20234726	0.2630
Single rice	0	161	3	164	411310	0.0053
Non-rice	78	5	918	1001	56280930	0.7316
<b>Total</b>	488	166	934	1588	76926966	1.0000

shown in table A.2. The updated error matrix after applying equation a.1 is shown in table A.2.

**Table A.2. Updated error matrix with estimated area proportions for each class.**

Class	REFERENCE			Total	Pixels(Map)	w <sub>i</sub>	Area (ha)
	Double rice	Single rice	Non-rice				
Double rice	0.25495409	0	0.00808391	0.263038	20234726	0.2630	202,347
Single rice	0	0.005249189	9.7811E-05	0.005347	411310	0.0053	4,113
Non-rice	0.057008961	0.003654421	0.670951618	0.731615	56280930	0.7316	562,809
<b>Total</b>	0.311963051	0.00890361	0.67913334	1	76926966	1.0000	769,270
<b>Unbiased Area(pixels)</b>	<b>23,998,371.01</b>	<b>684,927.67</b>	<b>52,243,667</b>				
<b>Unbiased Area(ha)</b>	<b>239,984</b>	<b>6,849</b>	<b>522,437</b>				

The pixel area for each class is calculated simply by multiplying the reference totals by the number of pixels on the map. The pixel counts are converted into hectares based on the size of the pixel, which in this case is about 100m<sup>2</sup>. The table now displays the unbiased area estimates for each class on the bottom, as well as the original area estimates shown on the top right.

Subsequently, standard errors of these unbiased areal estimates are calculated in order to provide more meaning to the data. These are calculated following the below equation A.2.

$$s(\hat{p}_{\circ j}) = \sqrt{\sum_i \frac{w_i \hat{p}_{ij} - \hat{p}_{ij}^2}{n_{i\circ} - 1}}$$

Where  $S(\hat{p}_{\circ j})$  is the standard error for the area proportion for one class. This equation must be used for each of the three classes. The result is pixel count based, we then convert it into area in hectares. Lastly, we apply a 95% confidence interval by multiplying the area in ha by 1.96. The result now shows the class area (unbiased area), standard error (S(area)), and a 95% confidence interval of the standard error (95% CI ha) as shown in table A.3.

**Table A.3. Updated error matrix with standard errors and associated 95% confidence intervals**

Class	REFERENCE			Total	Pixels(Map)	w <sub>i</sub>	Area (ha)
	Double rice	Single rice	Non-rice				
Double rice	0.25495409	0	0.00808391	0.263038	20234726	0.2630	202,347
Single rice	0	0.005249189	9.7811E-05	0.005347	411310	0.0053	4,113
Non-rice	0.057008961	0.003654421	0.670951618	0.731615	56280930	0.7316	562,809
Total	0.311963051	0.00890361	0.67913334	1	76926966	1.0000	769,270
Unbiased Area(pixels)	23,998,371.01	684,927.67	52,243,667				
Unbiased Area(ha)	239,984	6,849	522,437				
S(area)	0.00658350	0.00163200	0.00552555				
S(Area) ha	5,064	1,255	4,251				
95%CI ha	9,926	2,461	8,331				

Lastly, class omission and commission errors are calculated along with overall accuracy using the improved unbiased areal estimates as a basis, instead of typical pixel counts as employed in some studies. The equations for overall accuracy (A), user's accuracy (U), and producer's accuracy (P) are shown in equations A.3, A.4, and A.5.

$$A = \sum_{j=1}^q p_{ij}$$

$$U_i = \frac{p_{ii}}{p_{i^{\circ}}}$$

$$P_j = \frac{p_{jj}}{p_{^{\circ}j}}$$

The overall accuracy is simply the sum of the diagonals in the error matrix, which in this case would be (0.2549 + 0.005 + 0.67095 = 93.1%). The U and P follow the same accuracy assessment standard procedure omission and commission errors. Confidence intervals for each of the accuracy metrics are then derived based on the sample variance for each class with a 95% confidence interval assuming normal distribution. The final

theoretical example error matrix is shown in table A.4. Consult Olofsson et al. 2014 for more details.

**Table A.4. Updated error matrix with user's accuracy (UA), producer's accuracy (PA), and overall accuracy (OA) with associated 95% confidence intervals (CI).**

Class	REFERENCE			Total	Pixels(Map)	w <sub>i</sub>	Area (ha)	UA	UA CI
	Double rice	Single rice	Non-rice						
Double rice	0.25495409	0	0.00808391	0.263038	20234726	0.2630	202,347	96.9%	0.08%
Single rice	0	0.005249189	9.7811E-05	0.005347	411310	0.0053	4,113	98.2%	0.16%
Non-rice	0.057008961	0.003654421	0.670951618	0.731615	56280930	0.7316	562,809	91.7%	0.05%
<b>Total</b>	0.311963051	0.00890361	0.67913334	1	76926966	1.0000	769,270		
Unbiased Area(pixels)	23,998,371.01	684,927.67	52,243,667						
Unbiased Area(ha)	239,984	6,849	522,437						
S(area)	0.00658350	0.00163200	0.00552555		<b>OA</b>	0.931155			
S(Area) ha	5,064	1,255	4,251						
95%CI ha	9,926	2,461	8,331						
<b>PA</b>	<b>81.7%</b>	<b>59.0%</b>	<b>98.8%</b>						
<b>PA 95% CI</b>	0.16%	0.58%	0.02%		<b>OA CI</b>	1.38%			

The unbiased areal estimates and resulting accuracy metrics are an improvement upon relying only on pixel counts for each class. This assessment accounts for the sampling scheme and class proportions on the map. If the unbiased accuracy metrics were not calculated in this theoretical example, OA would be 94.8%, double rice PA would be 84.0%, and single rice PA would be 97.0%.

## Bibliography

Aalde, H., Gonzalez, P., Gytarsky, M., Krug, T., Kurz, W.A., Lasco, R.D., Martino, D.L., McConkey, B.G., Ogle, S., Paustian, K. and Raison, J., 2006. Generic methodologies applicable to multiple land-use categories. IPCC guidelines for national greenhouse gas inventories, 4, p.1-59.

Akagi, S.K., Yokelson, R.J., Wiedinmyer, C., Alvarado, M.J., Reid, J.S., Karl, T., Crounse, J.D. and Wennberg, P.O., 2011. Emission factors for open and domestic biomass burning for use in atmospheric models. *Atmospheric Chemistry and Physics*, 11(9), pp.4039-4072.

Andreae, M.O. and Merlet, P., 2001. Emission of trace gases and aerosols from biomass burning. *Global biogeochemical cycles*, 15(4), pp.955-966.

Apte, J.S., Marshall, J.D., Cohen, A.J. and Brauer, M., 2015. Addressing global mortality from ambient PM<sub>2.5</sub>. *Environmental science & technology*, 49(13), pp.8057-8066.

Arai H, Hosen Y, Pham Hong V N, Thi N T, Huu C N, and Inubushi K 2015 Greenhouse gas emissions from rice straw burning and straw-mushroom cultivation in a triple rice cropping system in the Mekong Delta. *Soil Science and Plant Nutrition* 61 4 719-735.

Aschbacher, J., Pongsrihadulchai, A., Karnchanasutham, S., Rodprom, C., Paudyal, D.R. and Le Toan, T., 1995. Assessment of ERS-1 SAR data for rice crop mapping and monitoring. In *Geoscience and Remote Sensing Symposium, 1995. IGARSS'95. 'Quantitative Remote Sensing for Science and Applications'*, International Vol. 3, 2183-2185.

Asilo, S., de Bie, K., Skidmore, A., Nelson, A., Barbieri, M. and Maunahan, A., 2014. Complementarity of two rice mapping approaches: Characterizing strata mapped by hypertemporal MODIS and rice paddy identification using multitemporal SAR. *Rem. Sens.*, 6(12), 12789-12814.

Badarinath K V S *et al* 2007 Multiyear ground-based and satellite observations of aerosol properties over a tropical urban area in India. *Atmospheric Science Letters* 8 1 7-13.

Badarinath K V S, Kharol S K, & Sharma A R 2009 Long-range transport of aerosols from agriculture crop residue burning in Indo-Gangetic Plains—a study using LIDAR, ground measurements and satellite data *Journal of Atmospheric and Solar-Terrestrial Physics* 71 1 112-120.

Badarinath K V S, Sharma A R, Kharol S K, and Prasad V K 2009 Variations in CO, O<sub>3</sub> and black carbon aerosol mass concentrations associated with planetary boundary layer (PBL) over tropical urban environment in India. *Journal of atmospheric chemistry* 62 1 73-86.

- Badarinath, K.V.S., Chand, T.K. and Prasad, V.K., 2006. Agriculture crop residue burning in the Indo-Gangetic Plains—a study using IRS-P6 AWiFS satellite data. *Current Science*, p.1085-1089.
- Belgiu, M. and Drăguț, L., 2016. Random forest in remote sensing: A review of applications and future directions. *ISPRS J. Photogramm. Remote Sens.*, 114, pp.24-31.
- Beverland, I.J., Cohen, G.R., Heal, M.R., Carder, M., Yap, C., Robertson, C., Hart, C.L. and Agius, R.M., 2012. A comparison of short-term and long-term air pollution exposure associations with mortality in two cohorts in Scotland. *Environmental health perspectives*, 120(9), p.1280.
- Biswas S, Vadrevu K P, Lwin Z M, Lasko K, and Justice C O 2015. Factors controlling vegetation fires in protected and non-protected areas of Myanmar. *PloS One* 10 4: e0124346.
- Biswas, Sumalika, Kristofer D. Lasko, and Krishna Prasad Vadrevu. "Fire Disturbance in Tropical Forests of Myanmar—Analysis Using MODIS Satellite Datasets." *IEEE Journal of Selected Topics in Applied Earth Observations and Remote Sensing* 8, no. 5 (2015): 2273-2281.
- Blanchard, C.L., Hidy, G.M. and Tanenbaum, S., 2010. NMOC, ozone, and organic aerosol in the southeastern United States, 1999–2007: 2. Ozone trends and sensitivity to NMOC emissions in Atlanta, Georgia. *Atmospheric Environment*, 44(38), pp.4840-4849.
- Bonnet, S. and Garivait, S., 2011. Seasonal variability of biomass open burning activities in the greater mekong sub-region. *Global Environmental Research*, 15(1), p.31-37.
- Boschetti, M., Busetto, L., Manfron, G., Laborte, A., Asilo, S., Pazhanivelan, S. and Nelson, A., 2017. PhenoRice: A method for automatic extraction of spatio-temporal information on rice crops using satellite data time series. *Remote Sensing of Environment*, 194, p.347-365.
- Boschetti, M., Nelson, A., Nutini, F., Manfron, G., Busetto, L., Barbieri, M., Laborte, A., Raviz, J., Holecz, F., Mabalay, M.R.O. and Bacong, A.P., 2015. Rapid assessment of crop status: An application of MODIS and SAR data to rice areas in Leyte, Philippines affected by Typhoon Haiyan. *Remote Sensing*, 7(6), pp.6535-6557.
- Bouvet A *et al* 2014 Estimation of agricultural and biophysical parameters of rice fields in Vietnam using X-band dual-polarization SAR. In *2014 IEEE Geoscience and Remote Sensing Symposium* 1504-1507.
- Bouvet, A., Le Toan, T. and Lam-Dao, N., 2009. Monitoring of the rice cropping system in the Mekong Delta using ENVISAT/ASAR dual polarization data. *IEEE Trans. on Geosci. Rem. Sens.*, 47(2), 517-526.
- Breiman, L., 2001. Random forests. *Machine learning*, 45(1), pp.5-32.



- Buchard, V., da Silva, A.M., Colarco, P.R., Darmenov, A., Randles, C.A., Govindaraju, R., Torres, O., Campbell, J. and Spurr, R., 2015. Using the OMI aerosol index and absorption aerosol optical depth to evaluate the NASA MERRA Aerosol Reanalysis. *Atmos. Chem. Phys.*, 15(10), pp.5743-5760.
- Burney, J. and Ramanathan, V., 2014. Recent climate and air pollution impacts on Indian agriculture. *Proceedings of the National Academy of Sciences*, 111(46), pp.16319-16324.
- Cao G, Zhang X, Sunling, and Zheng F 2008. Investigation on emission factors of particulate matter and gaseous pollutants from crop residue burning. *Journal of Environmental Sciences* 20 1 50-55.
- Cayetano, M.G., Hopke, P.K., Lee, K.H., Jung, J., Batmunkh, T., Lee, K. and Kim, Y.J., 2014. Investigations of the particle compositions of transported and local emissions in Korea. *Aerosol and Air Quality Research*, 14(3), p.793-805.
- Chakraborty M, Manjunath K R, Panigrahy S, Kundu N, and Parihar J S 2005. Rice crop parameter retrieval using multi-temporal, multi-incidence angle Radarsat SAR data. *ISPRS Journal of Photogrammetry and Remote Sensing* 59 5 310-322.
- Chakraborty, M., Panigrahy, E.S. and Sharma, S.A., 1997. Discrimination of rice crop grown under different cultural practices using temporal ERS-1 synthetic aperture radar data. *ISPRS J. Photogramm. Remote Sens.*, 52(4), 183-191.
- Chen, C. and McNairn, H., 2006. A neural network integrated approach for rice crop monitoring. *Int. J. Rem. Sens.*, 27(7), pp.1367-1393.
- Chen, C.F., Son, N.T., Chen, C.R., Chang, L.Y. and Chiang, S.H., 2016. Rice crop mapping using Sentinel-1A phenological metrics. *ISPRS-International Archives of the Photogrammetry*,
- Chen, D., Pereira, J.M., Masiero, A. and Pirotti, F., 2017. Mapping fire regimes in China using MODIS active fire and burned area data. *Applied Geography*, 85, p.14-26.
- Cheng, Z., Wang, S., Fu, X., Watson, J.G., Jiang, J., Fu, Q., Chen, C., Xu, B., Yu, J., Chow, J.C. and Hao, J., 2014. Impact of biomass burning on haze pollution in the Yangtze River delta, China: a case study in summer 2011. *Atmospheric Chemistry and Physics*, 14(9), p.4573-4585.
- Choudhury, I. and Chakraborty, M., 2006. SAR signature investigation of rice crop using RADARSAT data. *Int. J. Rem. Sens.*, 27(3), pp.519-534.
- Christian, T.J., Kleiss, B., Yokelson, R.J., Holzinger, R., Crutzen, P.J., Hao, W.M., Saharjo, B.H. and Ward, D.E., 2003. Comprehensive laboratory measurements of biomass-burning emissions: 1. Emissions from Indonesian, African, and other fuels. *Journal of Geophysical Research: Atmospheres*, 108(D23).
- Chuang, M.T., Lee, C.T., Chou, C.C.K., Engling, G., Chang, S.Y., Chang, S.C., Sheu, G.R., Lin, N.H., Sopajaree, K., Chang, Y.J. and Hong, G.J., 2016. Aerosol transport from

- Chiang Mai, Thailand to Mt. Lulin, Taiwan—Implication of aerosol aging during long-range transport. *Atmospheric Environment*, 137, pp.101-112
- Comaniciu, D. and Meer, P., 2002. Mean shift: A robust approach toward feature space analysis. *IEEE Transactions on pattern analysis and machine intelligence*, 24(5), pp.603-619.
- Congalton, R.G. and Green, K., 2008. *Assessing the accuracy of remotely sensed data: principles and practices*. CRC press.
- Crippa, P., Castruccio, S., Archer-Nicholls, S., Lebron, G.B., Kuwata, M., Thota, A., Sumin, S., Butt, E., Wiedinmyer, C. and Spracklen, D.V., 2016. Population exposure to hazardous air quality due to the 2015 fires in Equatorial Asia. *Scientific reports*, 6, p.37074.
- Cristofanelli, P., Putero, D., Adhikary, B., Landi, T.C., Marinoni, A., Duchi, R., Calzolari, F., Laj, P., Stocchi, P., Verza, G. and Vuillermoz, E., 2014. Transport of short-lived climate forcers/pollutants (SLCF/P) to the Himalayas during the South Asian summer monsoon onset. *Environmental Research Letters*, 9(8), p.084005.
- Crutzen P J, and Andreae M O 1990 Biomass burning in the tropics: Impact on atmospheric chemistry and biogeochemical cycles. *Science*, 250 4988 1669-1679.
- Dawson, J.P., Adams, P.J. and Pandis, S.N., 2007. Sensitivity of ozone to summertime climate in the eastern USA: A modeling case study. *Atmospheric environment*, 41(7), pp.1494-1511.
- de Bernardis, C.G., Vicente-Guijalba, F., Martinez-Marin, T. and Lopez-Sanchez, J.M., 2015. Estimation of key dates and stages in rice crops using dual-polarization SAR time series and a particle filtering approach. *IEEE J-STARS*, 8(3), pp.1008-1018.
- Devienne, S., 2006. Red River Delta: fifty years of change. *Moussons. Recherche en sciences humaines sur l'Asie du Sud-Est*, (9-10), p.255-280.
- Dey M.M. and Ahmed, M., 2005. Aquaculture—food and livelihoods for the poor in Asia: a brief overview of the issues. *Aquaculture Economics & Management*, 9(1-2), pp.1-10.
- Dong J, and Xiao X 2016 Evolution of regional to global paddy rice mapping methods: A review. *ISPRS Journal of Photogrammetry and Remote Sensing* 119 214-227.
- Draxler, R.R. and Hess, G.D., 1998. An overview of the HYSPLIT\_4 modelling system for trajectories. *Australian meteorological magazine*, 47(4), p.295-308.
- Duncan, B.N., Martin, R.V., Staudt, A.C., Yevich, R. and Logan, J.A., 2003. Interannual and seasonal variability of biomass burning emissions constrained by satellite observations. *Journal of Geophysical Research: Atmospheres*, 108(D2).

- Duong P T, and Yoshiro H 2015 Current Situation and Possibilities of Rice Straw Management in Vietnam. Retrieved from [http://www.jsrsai.jp/Annual\\_Meeting/PROG\\_52/ResumeC/C02-4.pdf](http://www.jsrsai.jp/Annual_Meeting/PROG_52/ResumeC/C02-4.pdf)
- Eck, T.F., Holben, B.N., Reid, J.S., O'Neill, N.T., Schafer, J.S., Dubovik, O., Smirnov, A., Yamasoe, M.A. and Artaxo, P., 2003. High aerosol optical depth biomass burning events: A comparison of optical properties for different source regions. *Geophysical Research Letters*, 30(20).
- Erten E, Lopez-Sanchez J M, Yuzugullu O, and Hajnsek I 2016 Retrieval of agricultural crop height from space: A comparison of SAR techniques *Remote Sensing of Environment* 187 130-144.
- Erten, E., Rossi, C. and Yüzügüllü, O., 2015. Polarization impact in TanDEM-X data over vertical-oriented vegetation: The paddy-rice case study. *IEEE Geosci. Rem. Sens. Lett.*, 12(7), 1501-1505.
- Erten, E., Rossi, C., Yüzügüllü, O. and Hajnsek, I., 2014, July. Phenological growth stages of paddy rice according to the BBCH scale and SAR images. In *Geosci. and Rem. Sens. Symp. (IGARSS), 2014 IEEE International* (pp. 1017-1020). IEEE.
- Feng, N. and Christopher, S.A., 2013. Satellite and surface-based remote sensing of Southeast Asian aerosols and their radiative effects. *Atmospheric research*, 122, pp.544-554.
- Fukunaga, K. and Hostetler, L., 1975. The estimation of the gradient of a density function, with applications in pattern recognition. *IEEE Transactions on information theory*, 21(1), pp.32-40.
- Funk, C., Peterson, P., Landsfeld, M., Pedreros, D., Verdin, J., Shukla, S., Husak, G., Rowland, J., Harrison, L., Hoell, A. and Michaelsen, J., 2015. The climate hazards infrared precipitation with stations—a new environmental record for monitoring extremes. *Scientific data*, 2, p.150066.
- Gadde B, Bonnet S, Menke C, and Garivait S 2009 Air pollutant emissions from rice straw open field burning in India, Thailand and the Philippines *Environmental Pollution* 157 5 1554-1558.
- Gaveau, D.L., Salim, M.A., Hergoualc'h, K., Locatelli, B., Sloan, S., Wooster, M., Marlier, M.E., Molidena, E., Yaen, H., DeFries, R. and Verchot, L., 2014. Major atmospheric emissions from peat fires in Southeast Asia during non-drought years: evidence from the 2013 Sumatran fires. *Scientific reports*, 4.
- Gebhardt, S., Huth, J., Nguyen, L.D., Roth, A. and Kuenzer, C., 2012. A comparison of TerraSAR-X Quadpol backscattering with RapidEye multispectral vegetation indices over rice fields in the Mekong Delta, Vietnam. *Int. j. rem. sens.*, 33(24), pp.7644-7661.

Gelaro, R., McCarty, W., Suárez, M.J., Todling, R., Molod, A., Takacs, L., Randles, C.A., Darmenov, A., Bosilovich, M.G., Reichle, R. and Wargan, K., 2017. The modern-era retrospective analysis for research and applications, version 2 (MERRA-2). *Journal of Climate*, 30(14), pp.5419-5454.

General Statistics Office of Vietnam, 2016. Agriculture, forestry, and fishery. Accessed from [https://www.gso.gov.vn/Default\\_en.aspx?tabid=766](https://www.gso.gov.vn/Default_en.aspx?tabid=766) .

Giglio, L., Descloitres, J., Justice, C.O. and Kaufman, Y.J., 2003. An enhanced contextual fire detection algorithm for MODIS. *Remote sensing of environment*, 87(2), pp.273-282.

Giglio, L., Randerson, J.T. and Werf, G.R., 2013. Analysis of daily, monthly, and annual burned area using the fourth-generation global fire emissions database (GFED4). *Journal of Geophysical Research: Biogeosciences*, 118(1), pp.317-328.

Giglio, L., Schroeder, W. and Justice, C.O., 2016. The collection 6 MODIS active fire detection algorithm and fire products. *Remote Sensing of Environment*, 178, pp.31-41.

Gullett, B. and Touati, A., 2003. PCDD/F emissions from burning wheat and rice field residue. *Atmospheric Environment*, 37(35), p.4893-4899.

Gupta P K *et al* 2001 Study of trace gases and aerosol emissions due to biomass burning at shifting cultivation sites in East Godavari District (Andhra Pradesh) during INDOEX IFP-99. *Curr Sci Ind* 80 186-196.

Gupta, R., Somanathan, E. and Dey, S., 2017. Global warming and local air pollution have reduced wheat yields in India. *Climatic Change*, 140(3-4), pp.593-604.

Hai, C.D. and Oanh, N.T.K., 2013. Effects of local, regional meteorology and emission sources on mass and compositions of particulate matter in Hanoi. *Atmospheric environment*, 78, pp.105-112.

Harvard University Department of Physics 2013. A Summary of Error Propagation. Retrieved from [http://ipl.physics.harvard.edu/wp-uploads/2013/03/PS3\\_Error\\_Propagation\\_sp13.pdf](http://ipl.physics.harvard.edu/wp-uploads/2013/03/PS3_Error_Propagation_sp13.pdf) .

Hayasaka, H., Noguchi, I., Putra, E.I., Yulianti, N. and Vadrevu, K., 2014. Peat-fire-related air pollution in Central Kalimantan, Indonesia. *Environmental Pollution*, 195, pp.257-266.

Heinsch, F.A., McHugh, C.W. and Hardy, C.C., 2016. Fire, Fuel, and Smoke Science Program 2015 Research Accomplishments. Accessed from [https://198.61.190.25/sites/default/files/images/downloads/FFS\\_AnnualReport\\_FY2015.pdf](https://198.61.190.25/sites/default/files/images/downloads/FFS_AnnualReport_FY2015.pdf) .

Henneman, L.R., Holmes, H.A., Mulholland, J.A. and Russell, A.G., 2015. Meteorological detrending of primary and secondary pollutant concentrations: Method

application and evaluation using long-term (2000–2012) data in Atlanta. *Atmospheric Environment*, 119, pp.201-210.

Hien P D, Bac V T, Tham H C, Nhan D D, and Vinh L D 2002 Influence of meteorological conditions on PM 2.5 and PM 2.5– 10 concentrations during the monsoon season in Hanoi, Vietnam. *Atmospheric Environment* 36 21 3473-3484.

Hien, P.D., Bac, V.T. and Thinh, N.T.H., 2004. PMF receptor modelling of fine and coarse PM 10 in air masses governing monsoon conditions in Hanoi, northern Vietnam. *Atmospheric Environment*, 38(2), pp.189-201.

Hoang, H.K., Bernier, M., Duchesne, S. and Tran, Y.M., 2016. Rice Mapping Using RADARSAT-2 Dual-and Quad-Pol Data in a Complex Land-Use Watershed: Cau River Basin (Vietnam). *IEEE J-STARS*. g, 9(7), 3082-3096.

Hoang, K.H., Bernier, M., Duchesne, S. and Tran, M.Y., 2014, July. Classification of rice fields in a complex land-use watershed in Northern Vietnam using RADARSAT-2 data. In *Geoscience and Remote Sensing Symposium (IGARSS), 2014 IEEE International* (pp. 1501-1503). IEEE.

Holben, B.N., Eck, T.F., Slutsker, I., Tanre, D., Buis, J.P., Setzer, A., Vermote, E., Reagan, J.A., Kaufman, Y.J., Nakajima, T. and Lavenue, F., 1998. AERONET—A federated instrument network and data archive for aerosol characterization. *Remote sensing of environment*, 66(1), pp.1-16.

Holder, A.L., Gullett, B.K., Urbanski, S.P., Elleman, R., O'Neill, S., Tabor, D., Mitchell, W. and Baker, K.R., 2017. Emissions from prescribed burning of agricultural fields in the Pacific Northwest. *Atmospheric Environment*, 166, pp.22-33.

Hong Van N P, Nga T T, Arai H, Hosen Y, Chiem N H, and Inubushi K 2014 Rice Straw Management by Farmers in a Triple Rice Production System in the Mekong Delta, Viet Nam. *Tropical Agriculture and Development* 58 4 155-162.

Hopke, P.K., Cohen, D.D., Begum, B.A., Biswas, S.K., Ni, B., Pandit, G.G., Santoso, M., Chung, Y.S., Davy, P., Markwitz, A. and Waheed, S., 2008. Urban air quality in the Asian region. *Science of the Total Environment*, 404(1), p.103-112.

Huang, K., Fu, J.S., Hsu, N.C., Gao, Y., Dong, X., Tsay, S.C. and Lam, Y.F., 2013. Impact assessment of biomass burning on air quality in Southeast and East Asia during BASE-ASIA. *Atmospheric environment*, 78, pp.291-302.

Huang, W.R., Wang, S.H., Yen, M.C., Lin, N.H. and Promchote, P., 2016. Interannual variation of springtime biomass burning in Indochina: Regional differences, associated atmospheric dynamical changes, and downwind impacts. *Journal of Geophysical Research: Atmospheres*, 121(17).

Ikeda, K. and Tanimoto, H., 2015. Exceedances of air quality standard level of PM<sub>2.5</sub> in Japan caused by Siberian wildfires. *Environmental Research Letters*, 10(10), p.105001.

- Inoue Y, Sakaiya E, and Wang C 2014 Capability of C-band backscattering coefficients from high-resolution satellite SAR sensors to assess biophysical variables in paddy rice. *Remote Sensing of Environment* 140 257-266.
- Inoue, Y., Kurosu, T., Maeno, H., Uratsuka, S., Kozu, T., Dabrowska-Zielinska, K. and Qi, J., 2002. Season-long daily measurements of multifrequency (Ka, Ku, X, C, and L) and full-polarization backscatter signatures over paddy rice field and their relationship with biological variables. *Rem. Sens. of Enviro.*, 81(2), 194-204.
- Izumi, Y., Demirci, S., bin Baharuddin, M.Z., Watanabe, T. and Sumantyo, J.T.S., 2017. Analysis of Dual-and Full-Circular Polarimetric SAR Modes for Rice Phenology Monitoring: An Experimental Investigation through Ground-Based Measurements. *Applied Sciences*, 7(4), p.368.
- Jhun, I., Coull, B.A., Zanobetti, A. and Koutrakis, P., 2015. The impact of nitrogen oxides concentration decreases on ozone trends in the USA. *Air Quality, Atmosphere & Health*, 8(3), pp.283-292.
- Jia, K., Li, Q., Tian, Y., Wu, B., Zhang, F. and Meng, J., 2012. Crop classification using multi-configuration SAR data in the North China Plain. *Int.l J. Rem. Sens.*, 33(1), pp.170-183.
- Jiang, C., Wang, H., Zhao, T., Li, T. and Che, H., 2015. Modeling study of PM 2.5 pollutant transport across cities in China's Jing–Jin–Ji region during a severe haze episode in December 2013. *Atmospheric Chemistry and Physics*, 15(10), pp.5803-5814.
- Jiao, X., Kovacs, J.M., Shang, J., McNairn, H., Walters, D., Ma, B. and Geng, X., 2014. Object-oriented crop mapping and monitoring using multi-temporal polarimetric RADARSAT-2 data. *ISPRS J. Photogram. Rem. Sens.*, 96, pp.38-46.
- Justice, C.O., Giglio, L., Korontzi, S., Owens, J., Morisette, J.T., Roy, D., Descloitres, J., Alleaume, S., Petitcolin, F. and Kaufman, Y., 2002. The MODIS fire products. *Remote Sensing of Environment*, 83(1), pp.244-262.
- Kaiser, J.W., Heil, A., Andreae, M.O., Benedetti, A., Chubarova, N., Jones, L., Morcrette, J.J., Razinger, M., Schultz, M.G., Suttie, M. and Van Der Werf, G.R., 2012. Biomass burning emissions estimated with a global fire assimilation system based on observed fire radiative power. *Biogeosciences*, 9(1), p.527.
- Kanabkaew T, and Oanh N T K 2011 Development of spatial and temporal emission inventory for crop residue field burning. *Environmental Modeling & Assessment* 16 5 453-464.
- Kanokkanjana K, Cheewaphongphan P, and Garivait S 2011 Black carbon emission from paddy field open burning in Thailand. *IPCBE Proc.* 6 88-92.

- Kanokkanjana, K. and Garivait, S., 2013. Alternative rice straw management practices to reduce field open burning in Thailand. *International Journal of Environmental Science and Development*, 4(2), p.119.
- Kanokkanjana, K. Garivait, S., Thongboonchoo, N. et al. 2010. An emission assessment of carbonaceous aerosols from agricultural open burning in Thailand: integrating experimental data and remote sensing. PhD Thesis King Mongkut's University of Technology, Thonburi, Bangkok, Thailand.
- Karila, K., Nevalainen, O., Krooks, A., Karjalainen, M. and Kaasalainen, S., 2014. Monitoring changes in rice cultivated area from SAR and optical satellite images in Ben Tre and Tra Vinh Provinces in Mekong Delta, Vietnam. *Rem. Sens.*, 6(5), pp.4090-4108.
- Kaufman, Y.J., Tanré, D. and Boucher, O., 2002. A satellite view of aerosols in the climate system. *Nature*, 419(6903), pp.215-223.
- Khan, M.F., Latif, M.T., Saw, W.H., Amil, N., Nadzir, M.S.M., Sahani, M., Tahir, N.M. and Chung, J.X., 2016. Fine particulate matter in the tropical environment: monsoonal effects, source apportionment, and health risk assessment. *Atmospheric Chemistry and Physics*, 16(2), pp.597-617.
- Kharol, S.K., Badarinath, K.V.S., Sharma, A.R., Mahalakshmi, D.V., Singh, D. and Prasad, V.K., 2012. Black carbon aerosol variations over Patiala city, Punjab, India—a study during agriculture crop residue burning period using ground measurements and satellite data. *Journal of Atmospheric and Solar-Terrestrial Physics*, 84, p. 45-51.
- Kim, J., Li, S., Kim, K.R., Stohl, A., Mühle, J., Kim, S.K., Park, M.K., Kang, D.J., Lee, G., Harth, C.M. and Salameh, P.K., 2010. Regional atmospheric emissions determined from measurements at Jeju Island, Korea: Halogenated compounds from China. *Geophysical Research Letters*, 37(12).
- Kim, J., Yoon, S.C., Jefferson, A. and Kim, S.W., 2006. Aerosol hygroscopic properties during Asian dust, pollution, and biomass burning episodes at Gosan, Korea in April 2001. *Atmospheric Environment*, 40(8), p.1550-1560.
- Kontgis, C., Schneider, A. and Ozdogan, M., 2015. Mapping rice paddy extent and intensification in the Vietnamese Mekong River Delta with dense time stacks of Landsat data. *Rem. Sens. Enviro.*, 169, 255-269.
- Koppe, W., Gnyp, M.L., Hütt, C., Yao, Y., Miao, Y., Chen, X. and Bareth, G., 2013. Rice monitoring with multi-temporal and dual-polarimetric TerraSAR-X data. *Int. J. Appl. Earth Obs. Geoinfo.*, 21, pp.568-576.
- Korenaga T, Liu X, and Huang Z 2001 The influence of moisture content on polycyclic aromatic hydrocarbons emission during rice straw burning. *Chemosphere-Global Change Science* 3 1 117-122.

- Korontzi, S., McCarty, J., Loboda, T., Kumar, S. and Justice, C., 2006. Global distribution of agricultural fires in croplands from 3 years of Moderate Resolution Imaging Spectroradiometer (MODIS) data. *Global Biogeochemical Cycles*, 20(2).
- Küçük, Ç., Taşkın, G. and Erten, E., 2016. Paddy-rice phenology classification based on machine-learning methods using multitemporal co-polar X-band SAR images. *IEEE J-STARS*, 9(6), pp.2509-2519.
- Kurokawa J *et al* 2013 Emissions of air pollutants and greenhouse gases over Asian regions during 2000–2008: Regional Emission inventory in ASia (REAS) version 2. *Atmospheric Chemistry and Physics* 13 21 11019-11058.
- Lamarque, J.F., Bond, T.C., Eyring, V., Granier, C., Heil, A., Klimont, Z., Lee, D., Liousse, C., Mieville, A., Owen, B. and Schultz, M.G., 2010. Historical (1850–2000) gridded anthropogenic and biomass burning emissions of reactive gases and aerosols: methodology and application. *Atmospheric Chemistry and Physics*, 10(15), pp.7017-7039.
- Lam-Dao, N., Apan, A., Young, F.R., Le-Van, T., Le-Toan, T. and Bouvet, A., 2007, November. Rice monitoring using ENVISAT-ASAR data: preliminary results of a case study in the Mekong River Delta, Vietnam. In *Proceedings of the 28th Asian Conference on Remote Sensing (ACRS 2007)*. Geoinformatics Center (Klong Luang).
- Lam-Dao, N., Le Toan, T., Apan, A., Bouvet, A., Young, F., & Le-Van, T. 2009. Effects of changing rice cultural practices on C-band synthetic aperture radar backscatter using Envisat advanced synthetic aperture radar data in the Mekong River Delta. *Journal of Applied Remote Sensing*, 3(1), 033563-033563.
- Langmann, B., Duncan, B., Textor, C., Trentmann, J. and van der Werf, G.R., 2009. Vegetation fire emissions and their impact on air pollution and climate. *Atmospheric Environment*, 43(1), p.107-116.
- Lasko, K., Vadrevu, K., Tran, V., Ellicott, E., Nguyen, T., Bui, H. and Justice, C., 2017. Satellites may underestimate rice residue and associated burning emissions in Vietnam. *Environmental Research Letters*, 12(8), 085006.
- Lasko, K., Vadrevu, K., Tran, V., Ellicott, E., Nguyen, T., Bui, H. and Justice, C., 2017. Satellites may underestimate rice residue and associated burning emissions in Vietnam. *Environmental Research Letters*, 12(8).
- Lasko, K., Vadrevu, K.P., Tran, V.T., Justice, C. 2018. Mapping double and single crop paddy rice with Sentinel-1A at varying spatial scales and polarizations in Hanoi, Vietnam. *IEEE Journal of Selected Topics in Applied Earth Observation and Remote Sensing*, 11(2).
- Latha, R., Murthy, B.S., Lipi, K., Srivastava, M.K. and Kumar, M., 2017. Absorbing Aerosols, Possible Implication to Crop Yield-A Comparison between IGB Stations. *Aerosol and Air Quality Research*, 17(3), pp.693-705.



- Le Toan, T., Ribbes, F., Wang, L.F., Floury, N., Ding, K.H., Kong, J.A., Fujita, M. and Kurosu, T., 1997. Rice crop mapping and monitoring using ERS-1 data based on experiment and modeling results. *IEEE Transactions on Geoscience and Remote Sensing*, 35(1), 41-56.
- Le, T.H., Nguyen, T.N.T., Lasko, K., Ilavajhala, S., Vadrevu, K.P. and Justice, C., 2014. Vegetation fires and air pollution in Vietnam. *Environmental Pollution*, 195, pp.267-275.
- Lee, K. S., and S. I. Lee. "Assessment of post-flooding conditions of rice fields with multi-temporal satellite SAR data." *Int. j. Rem. sens.* 24, no. 17 (2003): 3457-3465.
- Li, C., Hu, Y., Zhang, F., Chen, J., Ma, Z., Ye, X., Yang, X., Wang, L., Tang, X., Zhang, R. and Mu, M., 2017. Multi-pollutant emissions from the burning of major agricultural residues in China and the related health-economic effects. *Atmospheric Chemistry and Physics*, 17(8), p.4957-4988.
- Li, H., Han, Z., Cheng, T., Du, H., Kong, L., Chen, J., Zhang, R. and Wang, W., 2010. Agricultural fire impacts on the air quality of Shanghai during summer harvesttime. *Aerosol and Air Quality Research*, 10(2), p.95-101.
- Liang S 2005 *Quantitative remote sensing of land surfaces* (Vol. 30). John Wiley & Sons.
- Liang, L., Engling, G., Zhang, X., Sun, J., Zhang, Y., Xu, W., Liu, C., Zhang, G., Liu, X. and Ma, Q., 2017. Chemical characteristics of PM<sub>2.5</sub> during summer at a background site of the Yangtze River Delta in China. *Atmospheric Research*, 198, pp.163-172.
- Liew, S.C., Kam, S.P., Tuong, T.P., Chen, P., Minh, V.Q. and Lim, H., 1998. Application of multitemporal ERS-2 synthetic aperture radar in delineating rice cropping systems in the Mekong River Delta, Vietnam. *IEEE Trans. Geosci. Rem. Sens.*, 36(5), 1412-1420.
- Lin, N.H., Sayer, A.M., Wang, S.H., Loftus, A.M., Hsiao, T.C., Sheu, G.R., Hsu, N.C., Tsay, S.C. and Chantara, S., 2014. Interactions between biomass-burning aerosols and clouds over Southeast Asia: Current status, challenges, and perspectives. *Environmental Pollution*, 195, pp.292-307.
- Lin, N.H., Tsay, S.C., Maring, H.B., Yen, M.C., Sheu, G.R., Wang, S.H., Chi, K.H., Chuang, M.T., Ou-Yang, C.F., Fu, J.S. and Reid, J.S., 2013. An overview of regional experiments on biomass burning aerosols and related pollutants in Southeast Asia: From BASE-ASIA and the Dongsha Experiment to 7-SEAS. *Atmospheric Environment*, 78, p.1-19.
- Loosvelt, L., Peters, J., Skriver, H., De Baets, B. and Verhoest, N.E., 2012. Impact of reducing polarimetric SAR input on the uncertainty of crop classifications based on the random forests algorithm. *IEEE Transactions on Geoscience and Remote Sensing*, 50(10), pp.4185-4200.

Lopez-Sanchez, J.M., Cloude, S.R. and Ballester-Berman, J.D., 2012. Rice phenology monitoring by means of SAR polarimetry at X-band. *IEEE Trans. Geosci. Rem. Sens.*, 50(7), 2695-2709.

Lopez-Sanchez, J.M., Vicente-Guijalba, F., Ballester-Berman, J.D. and Cloude, S.R., 2014. Polarimetric response of rice fields at C-band: Analysis and phenology retrieval. *IEEE Trans. Geosci. Rem. Sens.*, 52(5), pp.2977-2993.

Lu, F., Xu, D., Cheng, Y., Dong, S., Guo, C., Jiang, X. and Zheng, X., 2015. Systematic review and meta-analysis of the adverse health effects of ambient PM 2.5 and PM 10 pollution in the Chinese population. *Environmental research*, 136, p.196-204.

Macatangay, R., Bagtasa, G. and Sonkaew, T., 2017, September. Non-chemistry coupled PM10 modeling in Chiang Mai City, Northern Thailand: A fast operational approach for aerosol forecasts. In *Journal of Physics: Conference Series*(Vol. 901, No. 1, p. 012037). IOP Publishing.

Man, C.D., Nguyen, T.T., Bui, H.Q., Lasko, K. and Nguyen, T.N.T., 2018. Improvement of land-cover classification over frequently cloud-covered areas using Landsat 8 time-series composites and an ensemble of supervised classifiers. *International Journal of Remote Sensing*, 39(4), pp.1243-1255.

revised classifiers. *International Journal of Remote Sensing*, 39(4), p.1243-1255.

Mansaray, L.R., Huang, W., Zhang, D., Huang, J. and Li, J., 2017. Mapping Rice Fields in Urban Shanghai, Southeast China, Using Sentinel-1A and Landsat 8 Datasets. *Remote Sensing*, 9(3), p.257.

Mansaray, L.R., Zhang, D., Zhou, Z. and Huang, J., 2017. Evaluating the potential of temporal Sentinel-1A data for paddy rice discrimination at local scales. *Rem. Sens. Lett.*, 8(10), pp.967-976.

Marlier, M.E., Jina, A.S., Kinney, P.L. and DeFries, R.S., 2016. Extreme air pollution in global megacities. *Current Climate Change Reports*, 2(1), pp.15-27.

McNairn H, and Brisco B 2004 The application of C-band polarimetric SAR for agriculture: a review. *Canadian Journal of Remote Sensing* 30 3 525-542.

Menke C, Wassmann R, and Gadde B 2009 Possible energy utilization of rice straw in Thailand: seasonal and spatial variations in straw availability as well as potential reduction in greenhouse gas emissions.

Mieville, A., Granier, C., Lioussé, C., Guillaume, B., Mouillot, F., Lamarque, J.F., Grégoire, J.M. and Pétron, G., 2010. Emissions of gases and particles from biomass burning during the 20th century using satellite data and an historical reconstruction. *Atmospheric Environment*, 44(11), p.1469-1477.

- Minnis, P., Sun-Mack, S., Trepte, Q.Z., Chang, F.L., Heck, P.W., Chen, Y., Yi, Y., Arduini, R.F., Ayers, K., Bedka, K. and Bedka, S., 2010, June. CERES Edition 3 cloud retrievals. In *AMS 13th conference atmospheric radiation. Portland, OR, June*.
- Mosleh M K, Hassan Q K, and Chowdhury E H 2015 Application of remote sensors in mapping rice area and forecasting its production: A review. *Sensors 15* 1 769-791.
- Nelson, A., Setiyono, T., Rala, A.B., Quicho, E.D., Raviz, J.V., Abonete, P.J., Maunahan, A.A., Garcia, C.A., Bhatti, H.Z.M., Villano, L.S. and Thongbai, P., 2014. Towards an operational SAR-based rice monitoring system in Asia: Examples from 13 demonstration sites across Asia in the RIICE project. *Rem. Sens.*, 6(11), pp.10773-10812.
- Nguyen D, Wagner W, Naeimi V, and Cao S 2015 Rice-planted area extraction by time series analysis of ENVISAT ASAR WS data using a phenology-based classification approach: A case study for Red River Delta, Vietnam. *International Archives of Photogrammetry* 40 7 77.
- Nguyen M D, 2012 An Estimation of Air Pollutant Emission from Open Rice Straw Burning in Red River Delta, *Science and Development Journal* (Vietnamese).
- Nguyen V H *et al* 2016 Energy efficiency, greenhouse gas emissions, and cost of rice straw collection in the Mekong River Delta of Vietnam. *Field Crops Research* 198 16-22.
- Nguyen, D., Wagner, W., Naeimi, V. and Cao, S., 2015. Rice-planted area extraction by time series analysis of ENVISAT ASAR WS data using a phenology-based classification approach: A case study for Red River Delta, Vietnam. *The International Archives of Photogrammetry, Remote Sensing and Spatial Information Sciences*, 40(7), p.77.
- Nguyen, D.B., Clauss, K., Cao, S., Naeimi, V., Kuenzer, C. and Wagner, W., 2015. Mapping rice seasonality in the Mekong Delta with multi-year Envisat ASAR WSM data. *Rem. Sens.*, 7(12), pp.15868-15893.
- Nguyen, D.B., Gruber, A. and Wagner, W., 2016. Mapping rice extent and cropping scheme in the Mekong Delta using Sentinel-1A data. *Remote Sensing Letters*, 7(12), pp.1209-1218.
- Nguyen, T.T., Bui, H.Q., Pham, H.V., Luu, H.V., Man, C.D., Pham, H.N., Le, H.T. and Nguyen, T.T., 2015. Particulate matter concentration mapping from MODIS satellite data: a Vietnamese case study. *Environmental Research Letters*, 10(9), p.095016.
- Oanh, N.K., Upadhyay, N., Zhuang, Y.H., Hao, Z.P., Murthy, D.V.S., Lestari, P., Villarin, J.T., Chengchua, K., Co, H.X., Dung, N.T. and Lindgren, E.S., 2006. Particulate air pollution in six Asian cities: Spatial and temporal distributions, and associated sources. *Atmospheric environment*, 40(18), pp.3367-3380.
- Oanh, N.K., Upadhyay, N., Zhuang, Y.H., Hao, Z.P., Murthy, D.V.S., Lestari, P., Villarin, J.T., Chengchua, K., Co, H.X., Dung, N.T. and Lindgren, E.S., 2006. Particulate

- air pollution in six Asian cities: Spatial and temporal distributions, and associated sources. *Atmospheric environment*, 40(18), p.3367-3380.
- Oanh, N.T.K., Ly, B.T., Tipayarom, D., Manandhar, B.R., Prapat, P., Simpson, C.D. and Liu, L.J.S., 2011. Characterization of particulate matter emission from open burning of rice straw. *Atmospheric Environment*, 45(2), p.493-502.
- Oanh, N.T.K., Tipayarom, A., Bich, T.L., Tipayarom, D., Simpson, C.D., Hardie, D. and Liu, L.J.S., 2015. Characterization of gaseous and semi-volatile organic compounds emitted from field burning of rice straw. *Atmospheric Environment*, 119, p.182-191.
- Oh, H.R., Ho, C.H., Kim, J., Chen, D., Lee, S., Choi, Y.S., Chang, L.S. and Song, C.K., 2015. Long-range transport of air pollutants originating in China: a possible major cause of multi-day high-PM 10 episodes during cold season in Seoul, Korea. *Atmospheric Environment*, 109, pp.23-30.
- Ohara, T.A.H.K., Akimoto, H., Kurokawa, J.I., Horii, N., Yamaji, K., Yan, X. and Hayasaka, T., 2007. An Asian emission inventory of anthropogenic emission sources for the period 1980–2020. *Atmospheric Chemistry and Physics*, 7(16), pp.4419-4444.
- Olofsson, P., Foody, G.M., Herold, M., Stehman, S.V., Woodcock, C.E. and Wulder, M.A., 2014. Good practices for estimating area and assessing accuracy of land change. *Rem. Sens. Environ.*, 148, 42-57
- Oritate, F., Yuyama, Y., Nakamura, M., Yamaoka, M., Nguyen, P.D., Dang, V.B.H., Mochidzuki, K. and Sakoda, A., 2015. Regional diagnosis of biomass use in suburban village in Southern Vietnam. *Journal of the Japan Institute of Energy*, 94(8), pp.805-829.
- Ottinger, M., Clauss, K. and Kuenzer, C., 2017. Large-Scale Assessment of Coastal Aquaculture Ponds with Sentinel-1 Time Series Data. *Rem. Sens.*, 9(5), p.440.
- Oyoshi, K., Tomiyama, N., Okumura, T., Sobue, S. and Sato, J., 2016. Mapping rice-planted areas using time-series synthetic aperture radar data for the Asia-RiCE activity. *Paddy and Water Environment*, 14(4), pp.463-472.
- Paloscia S, Macelloni G, Pampaloni P, and Sigismondi S 1999 The potential of C-and L-band SAR in estimating vegetation biomass: the ERS-1 and JERS-1 experiments. *IEEE Transactions on Geoscience and Remote Sensing* 37 4 2107-2110.
- Panigrahy, S., Manjunath, K.R., Chakraborty, M., Kundu, N. and Parihar, J.S., 1999. Evaluation of RADARSAT standard beam data for identification of potato and rice crops in India. *ISPRS J. Photogramm. Remote Sens.*, 54(4), 254-262.
- Patanothai, A., 1996. *Soils under stress: nutrient recycling and agricultural sustainability in the Red River Delta of Northern Vietnam*. Honolulu: East-West Center.
- Paudyal, D.R. and Aschbacher, J., 1993. Land-cover separability studies of filtered ERS-1 SAR images in the tropics. In *Geoscience and Remote Sensing Symposium, IGARSS'93. Better Understanding of Earth Environment., International* 1216-1218.

- Pei, Z., Zhang, S., Guo, L., McNairn, H., Shang, J. and Jiao, X., 2011. Rice identification and change detection using TerraSAR-X data. *Canadian J. Rem. Sens.*, 37(1), 151-156.
- Pereira, G.M., Alves, N.D.O., Caumo, S.E.S., Soares, S., Teinilä, K., Custódio, D., Hillamo, R., Alves, C. and Vasconcellos, P.C., 2017. Chemical composition of aerosol in São Paulo, Brazil: influence of the transport of pollutants. *Air Quality, Atmosphere & Health*, 10(4), p.457-468.
- Pham V C, Pham T T H, Tong T H A, Nguyen T T H, and Pham N H 2015 The conversion of agricultural land in the peri-urban areas of Hanoi (Vietnam): patterns in space and time. *Journal of Land Use Science* 10 2 224-242.
- Pham, DT., 2011. Mapping paddy cultivation and crop burn areas using MODIS in Mekong Delta, Vietnam (Master's Thesis). Asian Institute of Technology.
- Pham, V.C., Pham, T.T.H., Tong, T.H.A., Nguyen, T.T.H. and Pham, N.H., 2015. The conversion of agricultural land in the peri-urban areas of Hanoi (Vietnam): patterns in space and time. *Journal of Land Use Science*, 10(2), pp.224-242.
- Platnick, S., King, M.D., Ackerman, S.A., Menzel, W.P., Baum, B.A., Riédi, J.C. and Frey, R.A., 2003. The MODIS cloud products: Algorithms and examples from Terra. *IEEE Transactions on Geoscience and Remote Sensing*, 41(2), pp.459-473.
- Ponette-González, A.G., Curran, L.M., Pittman, A.M., Carlson, K.M., Steele, B.G., Ratnasari, D. and Weathers, K.C., 2016. Biomass burning drives atmospheric nutrient redistribution within forested peatlands in Borneo. *Environmental Research Letters*, 11(8), p.085003.
- Pope III, C.A. and Dockery, D.W., 2006. Health effects of fine particulate air pollution: lines that connect. *Journal of the air & waste management association*, 56(6), pp.709-742.
- Pope III, C.A., 2007. Mortality effects of longer term exposures to fine particulate air pollution: review of recent epidemiological evidence. *Inhalation toxicology*, 19(sup1), p.33-38.
- Pope III, C.A., Ezzati, M. and Dockery, D.W., 2009. Fine-particulate air pollution and life expectancy in the United States. *N Engl J Med*, 2009(360), pp.376-386.
- Putero, D., Landi, T.C., Cristofanelli, P., Marinoni, A., Laj, P., Duchì, R., Calzolari, F., Verza, G.P. and Bonasoni, P., 2014. Influence of open vegetation fires on black carbon and ozone variability in the southern Himalayas (NCO-P, 5079 m asl). *Environmental Pollution*, 184, pp.597-604.
- Rajput P, Sarin M, Sharma D, and Singh D 2014 Characteristics and emission budget of carbonaceous species from post-harvest agricultural-waste burning in source region of the Indo-Gangetic Plain. *Tellus B* 66.

- Ramanathan, V. and Carmichael, G., 2008. Global and regional climate changes due to black carbon. *Nature geoscience*, 1(4), pp.221-227.
- Randerson, J.T., Chen, Y., Werf, G.R., Rogers, B.M. and Morton, D.C., 2012. Global burned area and biomass burning emissions from small fires. *Journal of Geophysical Research: Biogeosciences*, 117(G4).
- Randles, C.A., da Silva, A.M., Buchard, V., Colarco, P.R., Darmenov, A., Govindaraju, R., Smirnov, A., Holben, B., Ferrare, R., Hair, J. and Shinozuka, Y., 2017. The MERRA-2 aerosol reanalysis, 1980 onward. Part I: System description and data assimilation evaluation. *Journal of Climate*, 30(17), pp.6823-6850.
- Reddington C L et al 2014 Contribution of vegetation and peat fires to particulate air pollution in Southeast Asia. *Environmental Research Letters* 9 9 094006.
- Reid, J.S., Hyer, E.J., Johnson, R.S., Holben, B.N., Yokelson, R.J., Zhang, J., Campbell, J.R., Christopher, S.A., Di Girolamo, L., Giglio, L. and Holz, R.E., 2013. Observing and understanding the Southeast Asian aerosol system by remote sensing: An initial review and analysis for the Seven Southeast Asian Studies (7SEAS) program. *Atmospheric Research*, 122, pp.403-468.
- Reiner, T., Sprung, D., Jost, C., Gabriel, R., Mayol-Bracero, O.L., Andreae, M.O., Campos, T.L. and Shelter, R.E., 2001. Chemical characterization of pollution layers over the tropical Indian Ocean: Signatures of emissions from biomass and fossil fuel burning. *Journal of Geophysical Research: Atmospheres*, 106(D22), p.28497-28510.
- Ribbes F, and Le Toan T 1999 Coupling radar data and rice growth model for yield estimation. In *Geoscience and Remote Sensing Symposium. IGARSS'99 Proceedings* 4 2336-2338.
- Ribbes, F., 1999. Rice field mapping and monitoring with RADARSAT data. *Int. J. Rem. Sens.*, 20(4), 745-765.
- Rodriguez-Galiano, V.F., Chica-Olmo, M., Abarca-Hernandez, F., Atkinson, P.M. and Jeganathan, C., 2012. Random Forest classification of Mediterranean land cover using multi-seasonal imagery and multi-seasonal texture. *Rem. Sens. Environ.*, 121, pp.93-107.
- Rolph, G., Stein, A. and Stunder, B., 2017. Real-time Environmental Applications and Display sYstem: READY. *Environmental Modelling & Software*, 95, p.210-228.
- Romasanta, R.R., Sander, B.O., Gaihre, Y.K., Alberto, M.C., Gummert, M., Quilty, J., Castalone, A.G., Balingbing, C., Sandro, J., Correa, T. and Wassmann, R., 2017. How does burning of rice straw affect CH<sub>4</sub> and N<sub>2</sub>O emissions? A comparative experiment of different on-field straw management practices. *Agriculture, Ecosystems & Environment*, 239, p.143-153.
- Sahai, S., Sharma, C., Singh, D.P., Dixit, C.K., Singh, N., Sharma, P., Singh, K., Bhatt, S., Ghude, S., Gupta, V. and Gupta, R.K., 2007. A study for development of emission

factors for trace gases and carbonaceous particulate species from in situ burning of wheat straw in agricultural fields in India. *Atmospheric Environment*, 41(39), p.9173-9186.

Saikawa, E., Trail, M., Zhong, M., Wu, Q., Young, C.L., Janssens-Maenhout, G., Klimont, Z., Wagner, F., Kurokawa, J.I., Nagpure, A.S. and Gurjar, B.R., 2017. Uncertainties in emissions estimates of greenhouse gases and air pollutants in India and their impacts on regional air quality. *Environmental Research Letters*, 12(6), p.065002.

Sakamoto, Y., Shoji, K., Bui, M.T., Phạm, T.H., Ly, B.T. and Kajii, Y., 2017. Air quality study in Hanoi, Vietnam in 2015–2016 based on a one-year observation of NO<sub>x</sub>, O<sub>3</sub>, CO and a one-week observation of VOCs. *Atmospheric Pollution Research*.

Salas, W., Boles, S., Li, C., Yeluripati, J.B., Xiao, X., Frohling, S. and Green, P., 2007. Mapping and modelling of greenhouse gas emissions from rice paddies with satellite radar observations and the DNDC biogeochemical model. *Aquatic conservation: Marine and freshwater ecosystems*, 17(3), 319-329.

Sanderfoot, O.V. and Holloway, T., 2017. Air pollution impacts on avian species via inhalation exposure and associated outcomes. *Environmental Research Letters*, 12(8), p.083002.

Satalino G *et al* 2015 Retrieval of wheat biomass from multitemporal dual polarised SAR observations. In *2015 IEEE IGARS* 5194-5197.

Schroeder, W., Csiszar, I. and Morisette, J., 2008. Quantifying the impact of cloud obscuration on remote sensing of active fires in the Brazilian Amazon. *Remote Sensing of Environment*, 112(2), pp.456-470.

Senthilnath, J., Omkar, S.N., Mani, V., Tejovanth, N., Diwakar, P.G. and Shenoy, A.B., 2012. Hierarchical clustering algorithm for land cover mapping using satellite images. *IEEE J-STARS*, 5(3), pp.762-768.

Shao, Y., Fan, X., Liu, H., Xiao, J., Ross, S., Brisco, B., Brown, R. and Staples, G., 2001. Rice monitoring and production estimation using multitemporal RADARSAT. *Rem. Sens. Enviro.*, 76(3), 310-325.

Sharma, A.R., Kharol, S.K., Badarinath, K.V.S. and Singh, D., 2010, February. Impact of agriculture crop residue burning on atmospheric aerosol loading—a study over Punjab State, India. In *Annales geophysicae: atmospheres, hydrospheres and space sciences* (Vol. 28, No. 2, p. 367).

Shi, Y. and Matsunaga, T., 2017. Temporal comparison of global inventories of CO<sub>2</sub> emissions from biomass burning during 2002–2011 derived from remotely sensed data. *Environmental Science and Pollution Research*, pp.1-12

Shiogama, H., Watanabe, M., Imada, Y., Mori, M., Ishii, M. and Kimoto, M., 2013. An event attribution of the 2010 drought in the South Amazon region using the MIROC5 model. *Atmospheric Science Letters*, 14(3), pp.170-175.

- Shiraishi, T., Motohka, T., Thapa, R.B., Watanabe, M. and Shimada, M., 2014. Comparative assessment of supervised classifiers for land use–land cover classification in a tropical region using time-series palsar mosaic data. *IEEE J-STARS*, 7(4), pp.1186-1199.
- Shumway, R.H. and Stoffer, D.S., 2006. *Time series analysis and its applications: with R examples*. Springer Science & Business Media.
- Son, N.T., Chen, C.F., Chen, C.R. and Minh, V.Q., 2017. Assessment of Sentinel-1A data for rice crop classification using random forests and support vector machines. *Geocarto International*, pp.1-15.
- Song, Y., Chang, D., Liu, B., Miao, W., Zhu, L. and Zhang, Y., 2010. A new emission inventory for nonagricultural open fires in Asia from 2000 to2009. *Environmental Research Letters*, 5(1), p.014014.
- Sonkaew, T. and Macatangay, R., 2015. Determining relationships and mechanisms between tropospheric ozone column concentrations and tropical biomass burning in Thailand and its surrounding regions. *Environmental Research Letters*, 10(6), p.065009.
- Sonobe, R., Tani, H., Wang, X., Kobayashi, N. and Shimamura, H., 2014. Random forest classification of crop type using multi-temporal TerraSAR-X dual-polarimetric data. *Rem. Sens. Lett.*, 5(2), 157-164.
- Steele-Dunne, S.C., McNairn, H., Monsivais-Huertero, A., Judge, J., Liu, P.W. and Papatthanassiou, K., 2017. Radar remote sensing of agricultural canopies: A review. *IEEE J-STARS*, 10(5), pp.2249-2273.
- Stein, A.F., Draxler, R.R., Rolph, G.D., Stunder, B.J., Cohen, M.D. and Ngan, F., 2015. NOAA's HYSPLIT atmospheric transport and dispersion modeling system. *Bulletin of the American Meteorological Society*, 96(12), p.2059-2077.
- Streets D G, Yarber K F, Woo J H, and Carmichael G R 2003 Biomass burning in Asia: Annual and seasonal estimates and atmospheric emissions. *Global Biogeochemical Cycles* 17 4.
- Streets, D.G., Bond, T.C., Carmichael, G.R., Fernandes, S.D., Fu, Q., He, D., Klimont, Z., Nelson, S.M., Tsai, N.Y., Wang, M.Q. and Woo, J.H., 2003. An inventory of gaseous and primary aerosol emissions in Asia in the year 2000. *Journal of Geophysical Research: Atmospheres*, 108(D21).
- Streets, D.G., Bond, T.C., Lee, T. and Jang, C., 2004. On the future of carbonaceous aerosol emissions. *Journal of Geophysical Research: Atmospheres*, 109(D24).
- Streets, D.G., Yarber, K.F., Woo, J.H. and Carmichael, G.R., 2003. Biomass burning in Asia: Annual and seasonal estimates and atmospheric emissions. *Global Biogeochemical Cycles*, 17(4).



- Su, T. and Zhang, S., 2017. Local and global evaluation for remote sensing image segmentation. *ISPRS Journal of Photogrammetry and Remote Sensing*, 130, pp.256-276.
- Suga, Y., Takeuchi, S., Oguro, Y. and Konishi, T., 2000. Monitoring of rice-planted areas using space-borne SAR data. *Int. Arch. of PHOTOGRAM. and Rem. Sens.*, 33(B7/4; PART 7), pp.1480-1483.
- Tadesse, T., Bathke, D., Wall, N., Petr, J. and Haigh, T., 2015. Participatory Research Workshop on Seasonal Prediction of Hydroclimatic Extremes in the Greater Horn of Africa. *Bulletin of the American Meteorological Society*, 96(8), pp.ES139-ES142.
- Tai A P K, Mickley L J and Jacob D J 2010 Correlations between fine particulate matter (PM<sub>2.5</sub>) and meteorological variables in the United States: implications for the sensitivity of PM<sub>2.5</sub> to climate change *Atmos. Environ.* **44** 3976–84
- Takeuchi, S. and Suwanwerakamtorn, R., 1996. Monitoring of Land Cover Conditions in Paddy Fields Using Multitemporal SAR Data. *Int. Archives of Photogramm. And Rem. Sens.*, 31, 683-688.
- Tang, L., Nagashima, T., Hasegawa, K., Ohara, T., Sudo, K. and Itsubo, N., 2015. Development of human health damage factors for PM<sub>2.5</sub> based on a global chemical transport model. *The International Journal of Life Cycle Assessment*, p.1-11.
- Tanimoto, H., Kajii, Y., Hirokawa, J., Akimoto, H. and Minko, N.P., 2000. The atmospheric impact of boreal forest fires in far eastern Siberia on the seasonal variation of carbon monoxide: Observations at Rishiri, a northern remote island in Japan. *Geophysical Research Letters*, 27(24), pp.4073-4076.
- Tao, F., Feng, Z., Tang, H., Chen, Y. and Kobayashi, K., 2017. Effects of climate change, CO<sub>2</sub> and O<sub>3</sub> on wheat productivity in Eastern China, singly and in combination. *Atmospheric Environment*, 153, pp.182-193.
- Tariq, A., Vu, Q.D., Jensen, L.S., de Tourdonnet, S., Sander, B.O., Wassmann, R., Van Mai, T. and de Neergaard, A., 2017. Mitigating CH<sub>4</sub> and N<sub>2</sub>O emissions from intensive rice production systems in northern Vietnam: Efficiency of drainage patterns in combination with rice residue incorporation. *Agriculture, Ecosystems & Environment*, 249, p.101-111.
- Thompson M L, Reynolds J, Cox L H, Guttorp P and Sampson P D 2001 A review of statistical methods for the meteorological adjustment of tropospheric ozone *Atmos. Environ.* **35** 617–30
- Tipayarom, D. and Oanh, N.K., 2007. Effects from open rice straw burning emission on air quality in the Bangkok Metropolitan Region. *Science Asia*, 33(3), p.339-345.
- Torbick N *et al* 2011 Integrating SAR and optical imagery for regional mapping of paddy rice attributes in the Poyang Lake Watershed, China *Canadian Journal of Remote Sensing* 37 1 17-26.

- Torbick, N., Chowdhury, D., Salas, W. and Qi, J., 2017. Monitoring Rice Agriculture across Myanmar Using Time Series Sentinel-1 Assisted by Landsat-8 and PALSAR-2. *Rem. Sens.*, 9(2), p.119.
- Torbick, N., Salas, W., Chowdhury, D., Ingraham, P. and Trinh, M., 2017. Mapping rice greenhouse gas emissions in the Red River Delta, Vietnam. *Carbon Management*, 8(1), pp.99-108.
- Torres, O., Ahn, C. and Chen, Z., 2013. Improvements to the OMI near-UV aerosol algorithm using A-train CALIOP and AIRS observations. *Atmospheric Measurement Techniques*, 6(11), p.3257.
- Torres, O., Tanskanen, A., Veihelmann, B., Ahn, C., Braak, R., Bhartia, P.K., Veefkind, P. and Levelt, P., 2007. Aerosols and surface UV products from Ozone Monitoring Instrument observations: An overview. *Journal of Geophysical Research: Atmospheres*, 112(D24).
- Trach, N.X., 1998. The need for improved utilisation of rice straw as feed for ruminants in Vietnam: An overview. *Livestock Research for Rural Development*, 10(2), pp.1-14.
- Tran S N, Nguyen T Q N, Nguyen H C, Nguyen V C N, Le H V, and Ingvorsen K 2014 To quantify the seasonal rice straw and its use in different provinces in the Vietnamese Mekong Delta *Can Tho University Science Journal*
- Tsay, S.C., Hsu, N.C., Lau, W.K.M., Li, C., Gabriel, P.M., Ji, Q., Holben, B.N., Welton, E.J., Nguyen, A.X., Janjai, S. and Lin, N.H., 2013. From BASE-ASIA toward 7-SEAS: A satellite-surface perspective of boreal spring biomass-burning aerosols and clouds in Southeast Asia. *Atmospheric environment*, 78, pp.20-34.
- Uhlmann, S. and Kiranyaz, S., 2014. Integrating color features in polarimetric SAR image classification. *IEEE Transactions on Geoscience and Remote Sensing*, 52(4), pp.2197-2216.
- Uto, K., Seki, H., Saito, G. and Kosugi, Y., 2013. Characterization of rice paddies by a UAV-mounted miniature hyperspectral sensor system. *IEEE J-STARS*, 6(2), pp.851-860.
- Vadrevu K P *et al* 2012 Vegetation fires in the himalayan region–Aerosol load, black carbon emissions and smoke plume heights. *Atmospheric environment* 47 241-251.
- Vadrevu K P, and Lasko K 2015 Satellite-Derived Nitrogen Dioxide Variations from Biomass Burning in a Subtropical Evergreen Forest, Northeast India. In *Remote Sensing of Water Resources, Disasters, and Urban Studies*, CRC Press 545-559
- Vadrevu K P, Ellicott E, Badarinath K V S, and Vermote E 2011 MODIS derived fire characteristics and aerosol optical depth variations during the agricultural residue burning season, north India. *Environmental pollution* 159 6 1560-1569.

- Vadrevu K P, Lasko K, Giglio L, and Justice C 2014 Analysis of Southeast Asian pollution episode during June 2013 using satellite remote sensing datasets. *Environmental Pollution* 195 245-256.
- Vadrevu K P, Lasko K, Giglio L, and Justice C 2015 Vegetation fires, absorbing aerosols and smoke plume characteristics in diverse biomass burning regions of Asia. *Environmental Research Letters* 10 10 105003.
- Vadrevu, K. and Lasko, K., 2015. Fire regimes and potential bioenergy loss from agricultural lands in the Indo-Gangetic Plains. *Journal of environmental management*, 148, p.10-20.
- Vadrevu, K.P. and Justice, C.O., 2011. Vegetation fires in the Asian region: Satellite observational needs and priorities. *Global Environmental Research*, 15(1), p.65-76.
- Vadrevu, K.P., Ellicott, E., Giglio, L., Badarinath, K.V.S., Vermote, E., Justice, C. and Lau, W.K., 2012. Vegetation fires in the himalayan region–Aerosol load, black carbon emissions and smoke plume heights. *Atmospheric Environment*, 47, pp.241-251.
- Vadrevu, K.P., Lasko, K., Giglio, L. and Justice, C., 2015. Vegetation fires, absorbing aerosols and smoke plume characteristics in diverse biomass burning regions of Asia. *Environmental Research Letters*, 10(10), p.105003.
- van der Werf, G.R., Randerson, J.T., Giglio, L., Collatz, G.J., Kasibhatla, P.S. and Arellano Jr, A.F., 2006. Interannual variability in global biomass burning emissions from 1997 to 2004. *Atmospheric Chemistry and Physics*, 6(11), pp.3423-3441.
- Van der Werf, G.R., Randerson, J.T., Giglio, L., Collatz, G.J., Mu, M., Kasibhatla, P.S., Morton, D.C., DeFries, R.S., Jin, Y.V. and van Leeuwen, T.T., 2010. Global fire emissions and the contribution of deforestation, savanna, forest, agricultural, and peat fires (1997–2009). *Atmospheric Chemistry and Physics*, 10(23), pp.11707-11735.
- Van Der Werf, G.R., Randerson, J.T., Giglio, L., Van Leeuwen, T.T., Chen, Y., Rogers, B.M., Mu, M., Van Marle, M.J., Morton, D.C., Collatz, G.J. and Yokelson, R.J., 2017. Global fire emissions estimates during 1997–2016. *Earth System Science Data*, 9(2), p.697.
- Vietnam Government, General Statistics Office of Vietnam, 2015. Retrieved from [https://www.gso.gov.vn/default\\_en.aspx](https://www.gso.gov.vn/default_en.aspx)
- Vietnam GSO, 2017. General Statistics Office of Vietnam: Agriculture, forestry, and fishery. Accessed from [https://www.gso.gov.vn/default\\_en.aspx?tabid=778](https://www.gso.gov.vn/default_en.aspx?tabid=778) . Note: data from year 2015.
- Vietnam Office of Statistics, 2016. Agriculture, forestry, and fishery. Accessed from [http://www.gso.gov.vn/default\\_en.aspx?tabid=467&idmid=3](http://www.gso.gov.vn/default_en.aspx?tabid=467&idmid=3) .

- Wang, M., Cao, C., Li, G. and Singh, R.P., 2015. Analysis of a severe prolonged regional haze episode in the Yangtze River Delta, China. *Atmospheric Environment*, 102, pp.112-121.
- Wang, W., Yang, X., Li, X., Chen, K., Liu, G., Li, Z. and Gade, M., 2017. A Fully Polarimetric SAR Imagery Classification Scheme for Mud and Sand Flats in Intertidal Zones. *IEEE Trans. Geosci. Rem. Sens.*, 55(3), pp.1734-1742.
- Warneke, C., Froyd, K.D., Brioude, J., Bahreini, R., Brock, C.A., Cozic, J., De Gouw, J.A., Fahey, D.W., Ferrare, R., Holloway, J.S. and Middlebrook, A.M., 2010. An important contribution to springtime Arctic aerosol from biomass burning in Russia. *Geophysical Research Letters*, 37(1), pp.1-5.
- Waske, B. and Braun, M., 2009. Classifier ensembles for land cover mapping using multitemporal SAR imagery. *ISPRS Journal of Photogrammetry and Remote Sensing*, 64(5), pp.450-457.
- Whitcomb, J., Moghaddam, M., McDonald, K., Kellndorfer, J. and Podest, E., 2009. Mapping vegetated wetlands of Alaska using L-band radar satellite imagery. *Canadian J. of Rem. Sens.*, 35(1), pp.54-72.
- Whitcraft, A.K., Becker-Reshef, I. and Justice, C.O., 2015. A framework for defining spatially explicit earth observation requirements for a global agricultural monitoring initiative (GEOGLAM). *Remote Sensing*, 7(2), pp.1461-1481.
- Whitcraft, A.K., Vermote, E.F., Becker-Reshef, I. and Justice, C.O., 2015. Cloud cover throughout the agricultural growing season: Impacts on passive optical earth observations. *Rem. Sens. Enviro.*, 156, 438-447.
- White, L., Brisco, B., Daboor, M., Schmitt, A. and Pratt, A., 2015. A collection of SAR methodologies for monitoring wetlands. *Rem. sens.*, 7(6), pp.7615-7645.
- WHO, 2014. World Health Organization. Accessed from <http://www.who.int/mediacentre/news/releases/2014/air-pollution/en/>.
- Wiedinmyer, C., Akagi, S.K., Yokelson, R.J., Emmons, L.K., Al-Saadi, J.A., Orlando, J.J. and Soja, A.J., 2010. The Fire INventory from NCAR (FINN)—a high resolution global model to estimate the emissions from open burning. *Geoscientific Model Development Discussions*, 3(4), pp.2439-2476.
- Wilson A M, and Walter J 2016 Remotely sensed high-resolution global cloud dynamics for predicting ecosystem and biodiversity distributions. *PLoS Biol* 14 3 e1002415.
- Wiseman G, McNairn H, Homayouni S, and Shang J 2014 RADARSAT-2 Polarimetric SAR response to crop biomass for agricultural production monitoring. *IEEE Journal of Selected Topics in Applied Earth Observations and Remote Sensing* 7 11 4461-4471.

- Xiao, X., Boles, S., Liu, J., Zhuang, D., Frohling, S., Li, C., Salas, W. and Moore, B., 2005. Mapping paddy rice agriculture in southern China using multi-temporal MODIS images. *Rem. Sens. Environ.*, 95(4), pp.480-492.
- Xie, L., Zhang, H., Wu, F., Wang, C. and Zhang, B., 2015. Capability of rice mapping using hybrid polarimetric SAR data. *IEEEJ-STARS*, 8(8), pp.3812-3822.
- Yadav, I.C., Devi, N.L., Li, J., Syed, J.H., Zhang, G. and Watanabe, H., 2017. Biomass burning in Indo-China peninsula and its impacts on regional air quality and global climate change-a review. *Environmental Pollution*, 227, p.414-427.
- Yan, X., Ohara, T. and Akimoto, H., 2006. Bottom-up estimate of biomass burning in mainland China. *Atmospheric Environment*, 40(27), pp.5262-5273.
- Yang, Z., Shao, Y., Li, K., Liu, Q., Liu, L. and Brisco, B., 2017. An improved scheme for rice phenology estimation based on time-series multispectral HJ-1A/B and polarimetric RADARSAT-2 data. *Remote Sensing of Environment*, 195, p.184-201.
- Yevich R, and Logan J A 2003 An assessment of biofuel use and burning of agricultural waste in the developing world. *Global biogeochemical cycles* 17 4.
- Yin, S., Wang, X., Xiao, Y., Tani, H., Zhong, G. and Sun, Z., 2017. Study on spatial distribution of crop residue burning and PM 2.5 change in China. *Environmental Pollution*, 220, pp.204-221.
- You, S., Tong, Y.W., Neoh, K.G., Dai, Y. and Wang, C.H., 2016. On the association between outdoor PM 2.5 concentration and the seasonality of tuberculosis for Beijing and Hong Kong. *Environmental Pollution*, 218, pp.1170-1179.
- You, S., Yao, Z., Dai, Y. and Wang, C.H., 2017. A comparison of PM exposure related to emission hotspots in a hot and humid urban environment: Concentrations, compositions, respiratory deposition, and potential health risks. *Science of The Total Environment*, 599, p.464-473.
- Yu, T.Y., Lin, C.Y. and Chang, L.F.W., 2012. Estimating air pollutant emission factors from open burning of rice straw by the residual mass method. *Atmospheric environment*, 54, p.428-438.
- Yun, S., Cuizhen, W., Xiangtao, F. and Hao, L., 1997, August. Estimation of rice growth status using RADARSAT data. In *Geoscience and Remote Sensing, 1997. IGARSS'97. Remote Sensing-A Scientific Vision for Sustainable Development., 1997 IEEE International* (Vol. 3, 1430-1432). IEEE.
- Yuzugullu, O., Erten, E. and Hajnsek, I., 2015. Rice growth monitoring by means of X-band co-polar SAR: Feature clustering and BBCH scale. *IEEE Geosci. Rem. Sens. Lett.*, 12(6), 1218-1222.
- Yuzugullu, O., Marelli, S., Erten, E., Sudret, B. and Hajnsek, I., 2017. Determining Rice Growth Stage with X-Band SAR: A Metamodel Based Inversion. *Remote Sensing*, 9(5),

- p.460.Zhang, A., Qi, Q., Jiang, L., Zhou, F. and Wang, J., 2013. Population exposure to PM<sub>2.5</sub> in the urban area of Beijing. *PloS one*, 8(5), p.e63486.
- Zhang, H., Hu, J., Qi, Y., Li, C., Chen, J., Wang, X., He, J., Wang, S., Hao, J., Zhang, L. and Zhang, L., 2017. Emission characterization, environmental impact, and control measure of PM<sub>2.5</sub> emitted from agricultural crop residue burning in China. *Journal of Cleaner Production*, 149, p.629-635.
- Zhang, H., Li, Q., Liu, J., Du, X., Dong, T., McNairn, H., Champagne, C., Shang, J. and Liu, M., 2017. Object-based crop classification using multi-temporal SPOT-5 imagery and textural features with a Random Forest classifier. *Geocarto International*, pp.1-40.
- Zhang, T., Wooster, M.J., Green, D.C. and Main, B., 2015. New field-based agricultural biomass burning trace gas, PM<sub>2.5</sub>, and black carbon emission ratios and factors measured in situ at crop residue fires in Eastern China. *Atmospheric Environment*, 121, pp.22-34.
- Zhang, Y., Shao, M., Lin, Y., Luan, S., Mao, N., Chen, W. and Wang, M., 2013. Emission inventory of carbonaceous pollutants from biomass burning in the Pearl River Delta Region, China. *Atmospheric environment*, 76, pp.189-199.
- Zhang, Y., Wang, C., Wu, J., Qi, J. and Salas, W.A., 2009. Mapping paddy rice with multitemporal ALOS/PALSAR imagery in southeast China. *Int. J. Rem. sens.*, 30(23), 6301-6315.
- Zhang, Y.L. and Cao, F., 2015. Is it time to tackle PM<sub>2.5</sub> air pollutions in China from biomass-burning emissions?. *Environmental Pollution*, 202, p.217-219.
- Zhao, H., Wang, S., Wang, W., Liu, R. and Zhou, B., 2015. Investigation of ground-level ozone and high-pollution episodes in a megacity of Eastern China. *PloS one*, 10(6), p.e0131878.
- Zheng, S., Pozzer, A., Cao, C.X. and Lelieveld, J., 2015. Long-term (2001–2012) concentrations of fine particulate matter (PM<sub>2.5</sub>) and the impact on human health in Beijing, China. *Atmospheric Chemistry and Physics*, 15(10), pp.5715-5725.
- Zuhlke, M., Fomferra, N., Brockmann, C., Peters, M., Veci, L., Malik, J. and Regner, P., 2015, December. SNAP (Sentinel Application Platform) and the ESA Sentinel 3 Toolbox. In *Sentinel-3 for Science Workshop* (Vol. 734, p. 21).